Reprogramming Borohydride Reactivity by Integrating Titanium and Chromium in Cooperative Catalysis

Dissertation

zur

Erlangung des Doktorgrades (Dr. rer. nat.)

der

Mathematisch-Naturwissenschaftlichen Fakultät

der

Rheinischen Friedrich-Wilhelms-Universität Bonn

vorgelegt von

Gregor Alexander Weiss

aus Bonn

Bonn

2024

Angefertigt mit Genehmigung der Mathematisch-Naturwissenschaftlichen Fakultät der Rheinischen Friedrich-Wilhelms-Universität Bonn.

Gutachter/Betreuer:	Prof. Dr. Andreas Gansäuer
Gutachter:	Prof. Dr. Sigurd Höger
Tag der Promotion:	11.04.2025
Erscheinungsjahr:	2025

Die vorliegende Arbeit wurde in der Zeit von November 2020 bis September 2024 am Kekulé-Institut für Organische Chemie und Biochemie der Mathematisch-Naturwissenschaftlichen Fakultät der Rheinischen Friedrich-Wilhelms-Universität Bonn unter Leitung von Prof. Dr. Andreas Gansäuer angefertigt.

Teile dieser Arbeit wurden bereits veröffentlicht:

Coupling Ti- and Cr-Catalysis in a Reaction Network for the Reprogramming of $[BH_4]^-$ as ET- and HAT-Reagent for Radical Chemistry

M. Heinz, G. Weiss, G. Shizgal, A. Panfilova, A. Gansäuer, *Angew. Chem. Int. Ed.* **2023**, *62*, e202308680; *Angew. Chem.* **2023**, *135*, e202308680.

DOI: 10.1002/anie.202308680

Für meine Eltern.

Table of Contents

1 General Part 1

1.1 Introduction 1

1.2 Cooperative Catalysis 7

1.3 Radicals in Organic Chemistry 13

1.4 Titanocenes in Epoxide Opening Reactions 16

1.5 Hydrogen Atom Donors 28

1.6 Transition Metal Hydrides as Hydrogen Atom Donors 32

1.7 Cooperative Catalysis with Titanium and Chromium 39

2 Discussion 44

2.1 Objective and Motivation 44

2.2 Borohydrides in Radical Chemistry 44

2.3 Mechanistic Considerations 47

2.4 Reaction Condition Optimization 51

2.5 Application in Reductive Epoxide Openings 62

2.6 Carbon-Carbon Bond Forming Cyclization Reactions 65

2.7 Regiodivergent Epoxide Opening by Cooperative Catalysis 73

2.8 Alternative Hydrogen Atom Transfer Catalysts 88

2.9 Synthesis of Catalysts 99

2.10 Synthesis of Substrates 105

2.11 Conclusion 114

3 Experimental Part 118

3.1 General Information 118

3.2 General Procedures 121

3.3 Substrate Synthesis 124

3.4 Synthesis of Catalysts 151

3.5 Experimental Details of Optimizations and Screenings 159

3.6 Catalysis Products 168

4 References 183

5 Appendix 198

5.1 Abbreviations 198

5.2 List of Figures 201

5.3 List of Schemes 202

5.4 List of Tables 206

5.5 Abstract 208

1 General Part

1.1 Introduction

Chemistry contributes significantly to almost every aspect of modern life – from the production of fuels, food, and clean drinking water to medicines, detergents, and a vast range of other goods. The chemical industry plays an instrumental role in enhancing the quality of life by providing fertilizers and agrochemicals for increased food supply as well as better nutrition, hygiene, and various pharmaceuticals. Moreover, the chemical production is a key driver of modern economic growth. As reported by the *ICCA*, the chemical industry touches nearly every other economic sector and contributed 5.7 trillion US dollars to the global GDP in 2017 – about 7% of total global production. It directly or indirectly supports 120 million jobs.[1,2]

However, despite these positive contributions to the quality of life, chemical production processes also have a negative impact on the environment and are partly responsible for the reduction of natural resources on earth. The chemical sector is the largest consumer of oil and gas and the third largest emitter of CO_2 (2 gigatons in 2020),[3,4] not only because of a high demand for raw materials but also due to a high requirement of process-related energy. Another macroeconomic impact arises from globalized supply chains that enable the sourcing of raw materials and precursors from developing countries. This enables low-cost and minimally regulated manufacturing practices, which encourage a 'throwaway' behavior and the disregard of resources with immense social, environmental, and lately economic costs.[1]

Figure 1: The United Nations 17 Sustainable Development Goals.[5]

In 2015, the 17 Sustainable Development Goals (SDGs) were defined by the United Nations (Figure 1). Among these goals, Goal 9 ('Industry, innovation and infrastructure') and especially Goal 12

('Responsible consumption and production') call on the chemical industry to implement 'environmentally sound management of chemicals and all wastes throughout their life cycle […] and significantly reduce their release to air, water and soil in order to minimize their adverse impacts on human health and the environment'.[6]

These goals incorporate and align with another principle developed earlier. The concept of 'Green Chemistry', rooted in the preference of prevention over cure, supports the design of chemical products and production processes that minimize or eliminate the use and generation of hazardous substances. Developed by *Anastas* and *Warner* in the 1990s, Green Chemistry embodies twelve overarching principles, which guide researchers and industry participants towards more sustainable practices (Figure 2).[7,8] These principles encompass a wide range of strategies, including important aspects of synthetic method development in research, such as the minimization of waste generation, the design of less hazardous chemical syntheses, or the use of renewable and earth-abundant feedstocks.

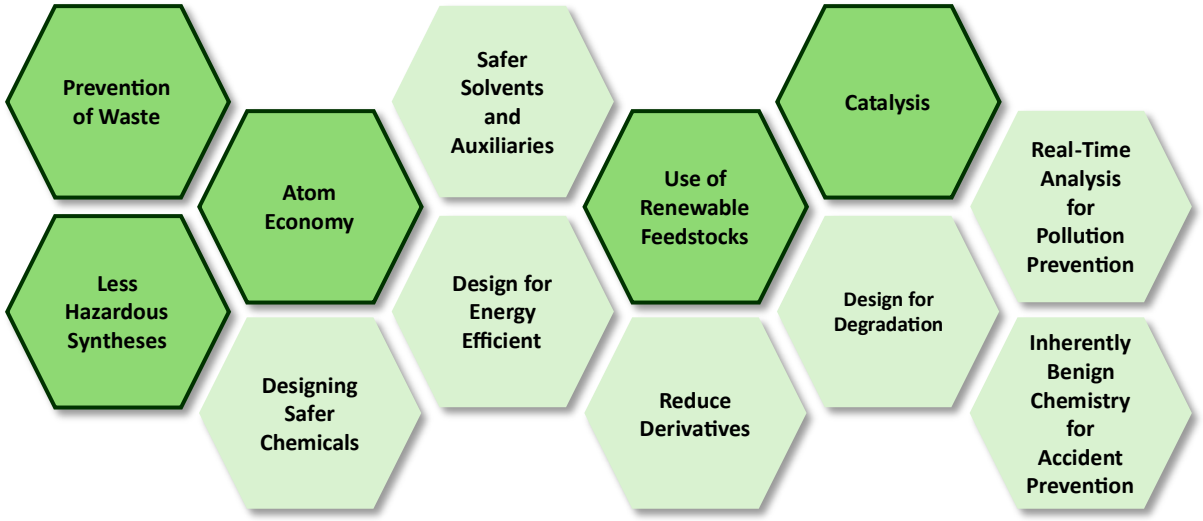

Figure 2: The 12 principles of Green Chemistry.

However, especially the principles of atom economy and catalysis, that are typically closely connected, should be emphasized in this context. Coined by *Trost* in 1991, atom economy quantifies the proportion of atoms in reactants that are incorporated in the desired products of a reaction.[9] It serves as a quantitative metric to evaluate the efficiency of a synthesis by minimizing the generation of waste and maximizing the utilization of atoms, thus aligning well with the principles of Green Chemistry. The pursuit of high atom economy represents a paradigm shift in chemical synthesis, moving away from traditional methodologies that often result in significant waste production. In many conventional processes, the transformation of starting materials into desired products may involve multiple steps, each accompanied by the generation of unwanted by-products and the consumption of additional resources. Such inefficiencies not only contribute to environmental pollution but also entail economic costs associated with waste management and resource consumption.

Undoubtfully, a central strategy to realize higher atom economy, prevent waste, and enhance the energy efficiency of chemical processes is the use of catalytic processes. Catalysts accelerate the rates of chemical reactions by providing alternative reaction pathways with lower activation energies, enabling the conversion of reactants into products with less feedstock or under milder conditions. In contrast to reactants, catalysts pass through multiple reaction cycles unchanged without becoming a by-product or waste.[7] This unique feature has made catalysis indispensable in global manufacturing processes, and literally no chemical or pharmaceutical company could be economically viable without catalytic processes.[8,10] A prime example that shows the indispensability of catalytic techniques is the *Haber-Bosch* process.[11] It generates ammonia that is an essential precursor for the production of fertilizers, from nitrogen and hydrogen heterogeneously catalyzed by an iron-based catalyst. This process alone consumes about 1% of the world's total energy production and accounts for 1.4% of the global CO_2 emissions.[12] Although these numbers are substantial, they would be catastrophic for a hypothetical uncatalyzed process.

Especially pharmaceutical productions can lead to significant waste generation, due to multi-step synthetic processes. However, these processes also offer substantial opportunities for improvement. The industrial synthesis of *ibuprofen* (Scheme 1) serves as an example, highlighting the superiority of catalytic processes over stoichiometric ones.

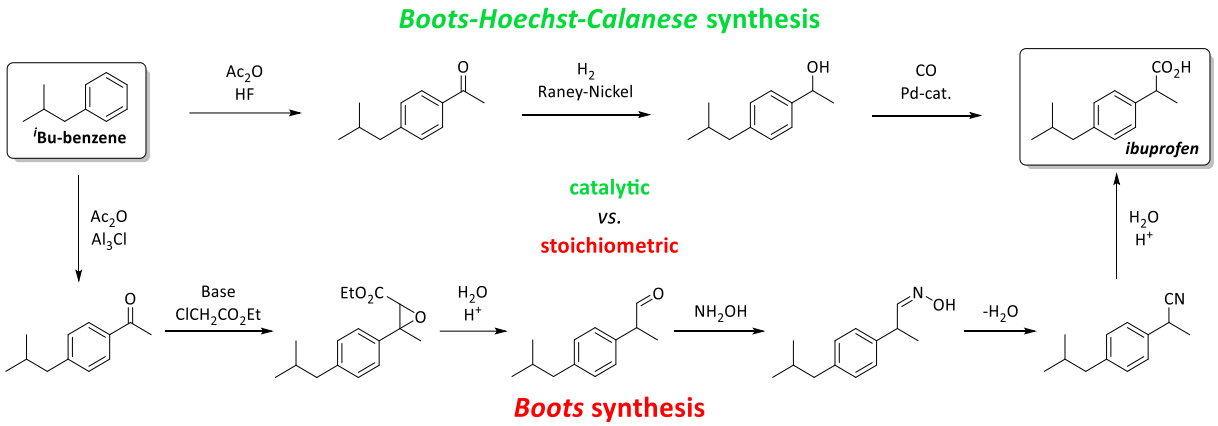

Scheme 1: Industrial synthesis of *ibuprofen* in the original stoichiometric six-step route by *Boots* (bottom) and the improved *Boots-Hoechst-Calanese* three-step synthesis with all three steps being catalytic (top).[13]

The synthesis of the non-steroidal anti-inflammatory drug *ibuprofen* was established and commercialized by the company *Boots* in 1962.[14] The original synthesis involved six stoichiometric synthetic steps and was therefore not very sustainable. For example, the addition of the hydroxylamine NH_2OH leads to the imine, which is then converted to the cyano derivative, which is finally oxidized to the carboxylic acid. This effectively means, the hydroxylamine is added first, only to be cleaved off later, resulting in stoichiometric waste generation and an overall reduction in atom economy. Economic pressure eventually led to the development of a new and more efficient route.[14,15] The

improved synthesis, like the old one, begins with a *Friedel-Crafts* acylation, which is, however, catalyzed by HF and therefore does not require stoichiometric amounts of aluminum chloride. In the subsequent hydrogenation of the ketone, *Raney* nickel is employed as the hydrogenation catalyst, enabling the use of hydrogen as the sole stoichiometric reagent, resulting in excellent atom economy of this step. Also, the final carbonylation of the alcohol proceeds atom economically with utilization of a palladium catalyst and CO pressure. These improvements in the synthesis result in an increase in atom economy from below 40% to about 80%.[16] Moreover, the acetic acid produced in the first acylation step can be regenerated to acetic anhydride industrially to further increase the atom economy.

Although the *ibuprofen* synthesis shown is a great example of the incorporation of catalysis into organic synthesis, it neglects a crucial property of the compound at this point – its chirality. The synthesis does not proceed asymmetrically. In principle, not one but two products are obtained as a racemic mixture of two enantiomers. Enantiomers are chiral molecules, that are mirror images of each other and cannot be transformed into each other by rotation. Enantiomers possess identical physical and chemical properties in achiral environments, but exhibit distinct interactions in chiral environments, such as biological systems or chiral catalysts. This phenomenon plays a critical role in fields ranging from pharmaceuticals and agrochemicals to materials science and flavor chemistry. However, the extent to which two enantiomers can induce different biological effects can vary widely as will be illustrated using three well-known enantiomeric compounds (Figure 3).

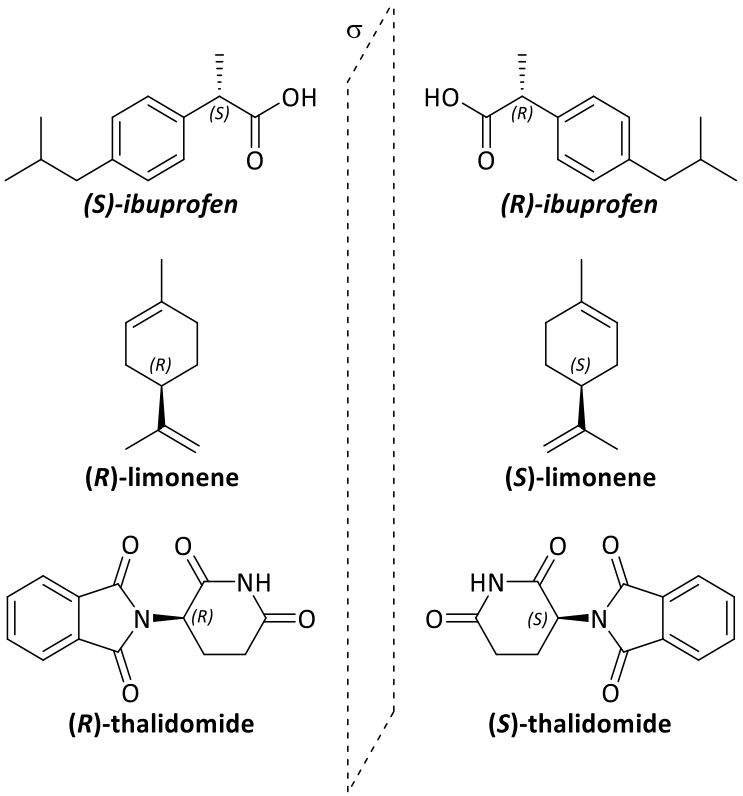

Figure 3: Enantiomers of *ibuprofen*, limonene, and thalidomide.

In pharmaceutical application, *ibuprofen* is usually ingested as racemic mixture of both enantiomers. However, only the (*S*)-*ibuprofen* shows the desired analgesic activity,[17] while the other enantiomer shows no effect, making a more expensive enantioselective synthesis unnecessary. In the case of the naturally occurring terpene limonene, the two enantiomers have a different biological effect which is manifested in the odors. While the (*R*)-limonene has the typical orange or lemon fragrance, the (*S*)-limonene has a pine-like or turpentine-like smell.[17,18] The case is different and less benign for thalidomide, which has formerly been used in the prescription-free sedative *Contergan*. The drug, sold in racemic form in the 1950s and 60s, was later found to be responsible for numerous life-threatening birth defects.[17,19] The (*R*)-thalidomide was identified in kinetic studies with stereochemical stabilization by deuteration to have the sedative effect,[20] while the (*S*)-enantiomer was found to be responsible for the significant teratogenicity.[21] However, a rapid *in vivo* interconversion of the enantiomers into each other, facilitated by the proximity of the stereocenter to the carbonyl group, prohibits an application of the compound even in enantiopure form in this case. These examples and the often significant differences in the activities of the enantiomers illustrate the critical need for the development of not only catalytic but also stereoselective synthetic methods.

Asymmetric induction in metalorganic catalysis to obtain enantiopure products typically relies on the use of enantiopure ligands. These are often 'privileged ligands' including BINOL, BOX, alkaloid- or tartaric acid-derived, or salen ligands (Figure 4).[22]

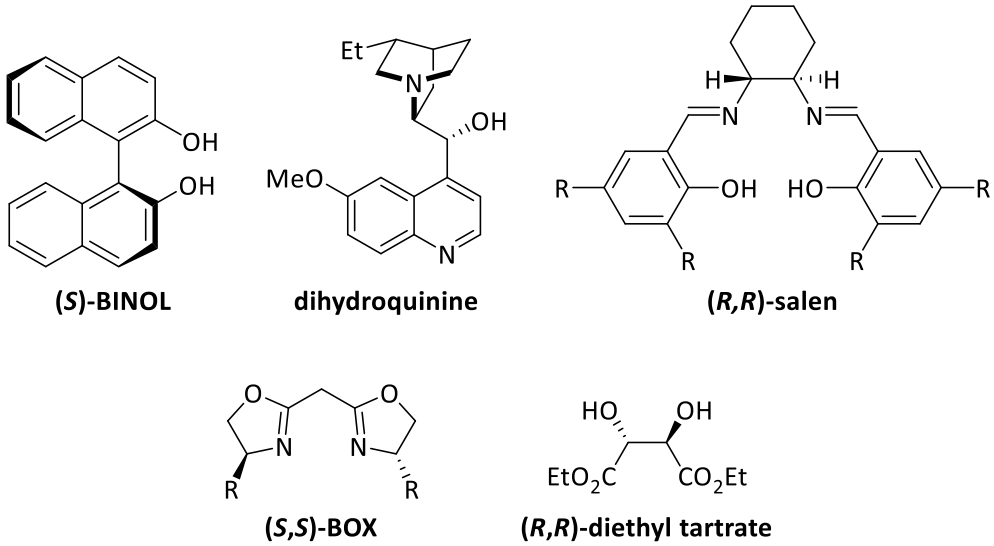

Figure 4: 'Privileged ligands' in asymmetric catalysis.

An early example using an enantiopure chromium salen complex is the asymmetric ring-opening reaction (ARO) of *meso*-epoxides developed by *Jacobsen* (Scheme 3).[22,23]

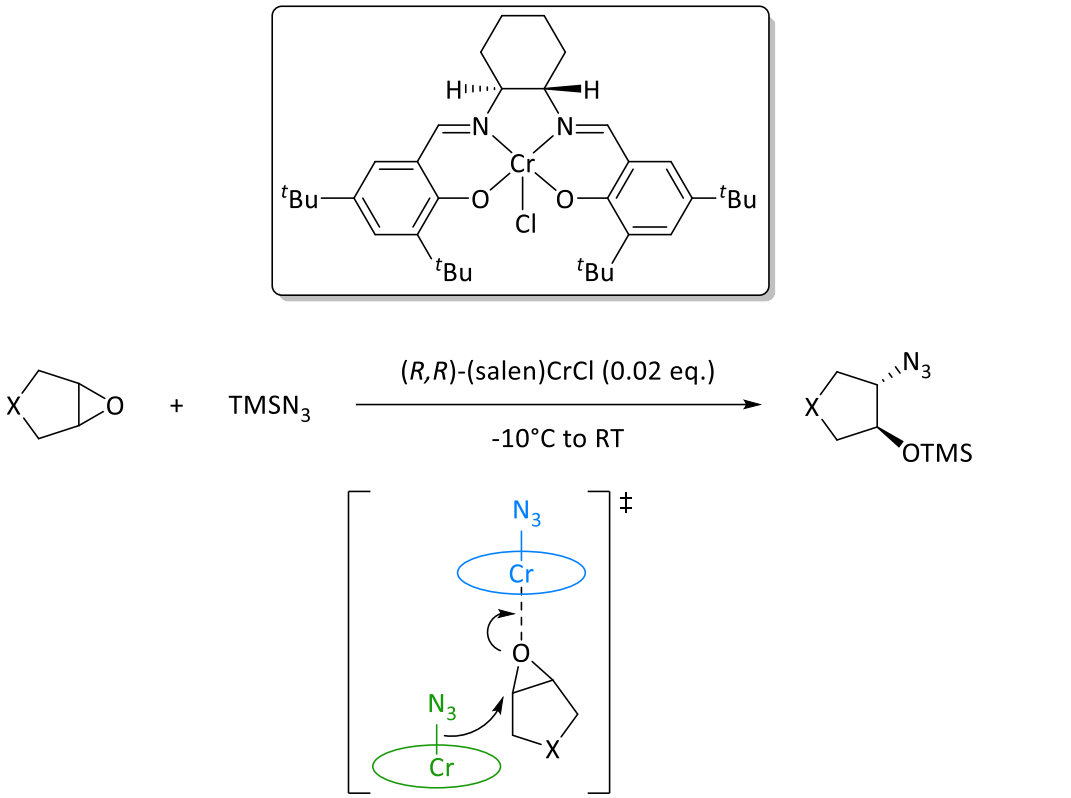

Scheme 2: Asymmetric ring opening (ARO) of *meso*-epoxides using an enantiopure (salen)CrCl complex developed by *Jacobsen*.

After reduction and deprotection of the azido silyl ethers, 1,2-amino alcohols are obtained nearly quantitatively and in good enantiomeric excess (*ee*). The epoxide opening occurs through a bimetallic transition state. In this rate-determining step, one chromium complex delivers the activated azide nucleophile to the epoxide, which is *Lewis* acid activated for nucleophilic attack by the other chromium complex. The highly organized transition state ensures the stereoselectivity of the nucleophilic attack by steric interaction between the two stepped salen ligands. The solvent-free conditions and the possibility of easy catalyst recovery makes the ARO an attractive method, also regarding atom economy and waste reduction. In addition, the differently protected nitrogen and oxygen groups allow for further synthetic manipulations.

The method has been used as a key step in the synthesis of building blocks for pharmaceutically active compounds, including the protein kinase C (PKC) inhibitor balanol and the HIV reverse transcriptase inhibitor (–)-carbovir (Scheme 3).[24,25]

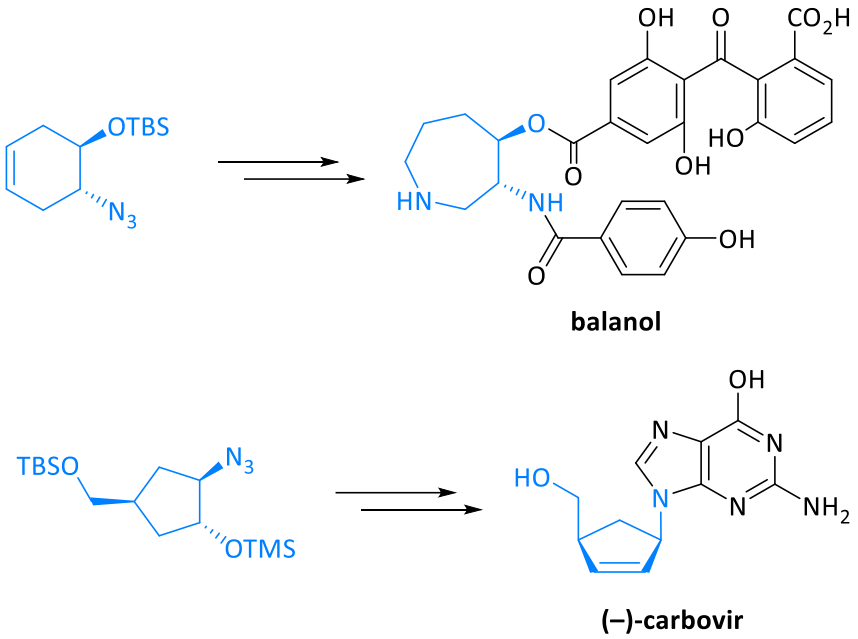

Scheme 3: Synthetic application of protected 1,2-amino alcohols obtained from ARO in the total synthesis of pharmaceutically active balanol and (–)-carbovir.

More than ever the critical demand for energy and raw materials is driving scientists to develop a more sustainable chemical production. Catalysis, especially asymmetric catalysis, is a powerful tool to overcome established and potentially problematic production processes. However, the possibilities may face a limit. One way to overcome established methods and thereby achieving unprecedented reactivity is to exploit new opportunities through cooperative catalysis.

1.2 Cooperative Catalysis

By using two different catalysts simultaneously, cooperative catalysis provides access to reactivity and selectivity that would otherwise not be possible by using a single catalyst alone, and is therefore a promising strategy for the development of sustainable reactions.[26] In designing cooperative catalysis, chemists have the opportunity to combine the different chemistries of the two individual catalyst to achieve 'the best of both worlds'. As a result, great interest has arisen in this field of research in the past years.[27,28] Such powerful catalytic systems provide new routes to highly complex molecules and can outcompete stepwise synthesis also avoiding additional purification steps of intermediates, thereby conserving economic or material resources and maximizing the synthetic efficiency.[27] The potential of tuning the catalytic system is enormous due to the high number of possible catalyst combinations and modifications of each individual catalysts. This holds true also for asymmetric

synthesis. Classic asymmetric catalysis relies on the implementation of enantioselectivity by using a single metal- or organocatalyst. In contrast, cooperative systems are less limited to accomplish enantioselectivity by using one or a combination of two chiral catalysts synergistically. However, in contrast to nature, where enzymes, which are 'tailor-made' and often multi metal center catalysts, mediate all types of transformations with excellent abilities to control reactivity and selectivity, the development of cooperative systems in the laboratory is challenging. For instance, two or more catalysts are free to interact with each other and cause self-inhibition and reactivities of all components must be harmonized.[28]

Cooperative catalysis should not be confused with one-pot catalysis. For clear distinction, cooperative catalysis must be distinguished from sequential catalysis and relay catalysis, which all three form the major field of one-pot catalysis.[26]

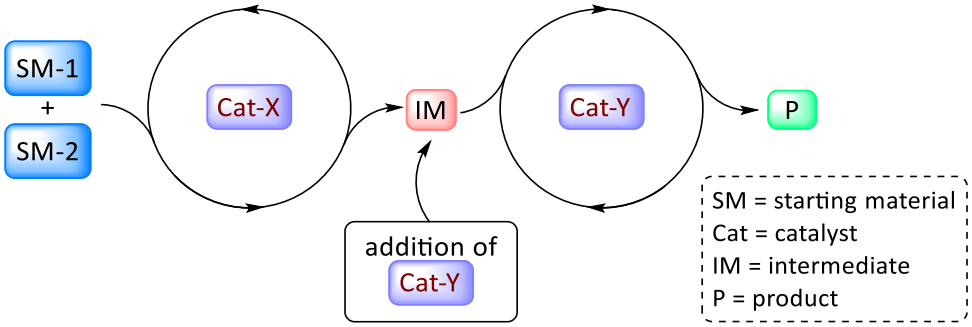

Scheme 4: General representation of sequential catalysis.

Sequential catalysis (Scheme 4) is a set of consecutive catalytic cycles in a one-pot reaction. The substrate reacts with the first catalyst (Cat-X) to form an intermediate that reacts with the second catalyst (Cat-Y). The subsequent addition of the second catalyst (Cat-Y) is crucial because both catalysts are incompatible and self-inhibition or side reactions may occur.

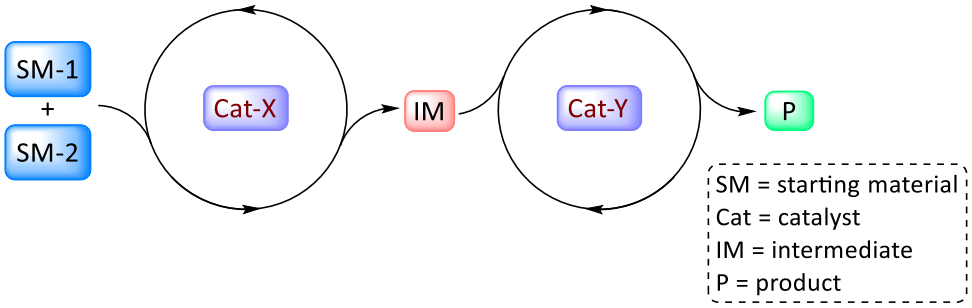

Scheme 5: General representation of relay catalysis.

Similarly, relay catalysis (Scheme 5) has the same consecutive set of catalytic cycles as sequential catalysis. But in contrast to sequential catalysis, both catalysts are present at onset because they are compatible, and Cat-Y does not interrupt the first cycle of Cat-X.[26]

In cooperative catalysis (Scheme 6) both catalysts share the same truly interconnected catalytic cycle. Both catalysts must be present at onset. More than in the sequential or relay catalysis, the two catalysts must be a suitable combination. On the one hand the catalysts must act in concert with each other to not cause self-inhibition, on the other hand both must tolerate all employed reagents and intermediates occurring during the course of the reaction.[26]

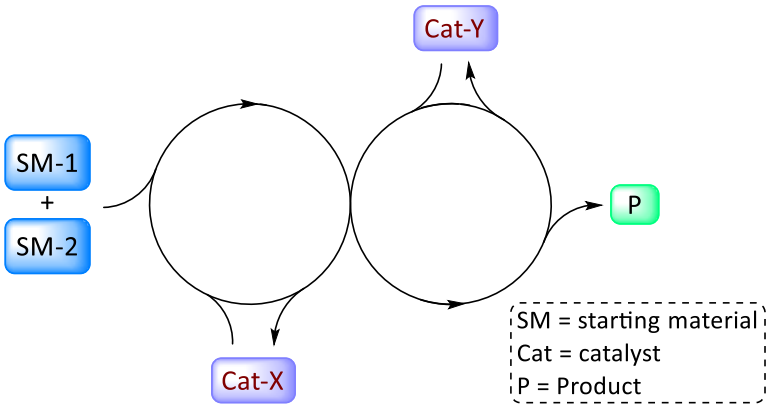

Scheme 6: Schematic representation of cooperative catalysis.

The type of cooperative catalysis can be further specified by subdivision into intramolecular and intermolecular cooperative catalysis. In the intramolecular case (Scheme 7 left) two functional groups of one substrate are mutually activated by two catalysts. In the intermolecular case (Scheme 7 right) two substrates are activated separately by both catalysts followed by a joint transition state. A clear discrimination of both cases is however sometimes difficult and interwoven catalytic cycles with combinations of both are possible.[28]

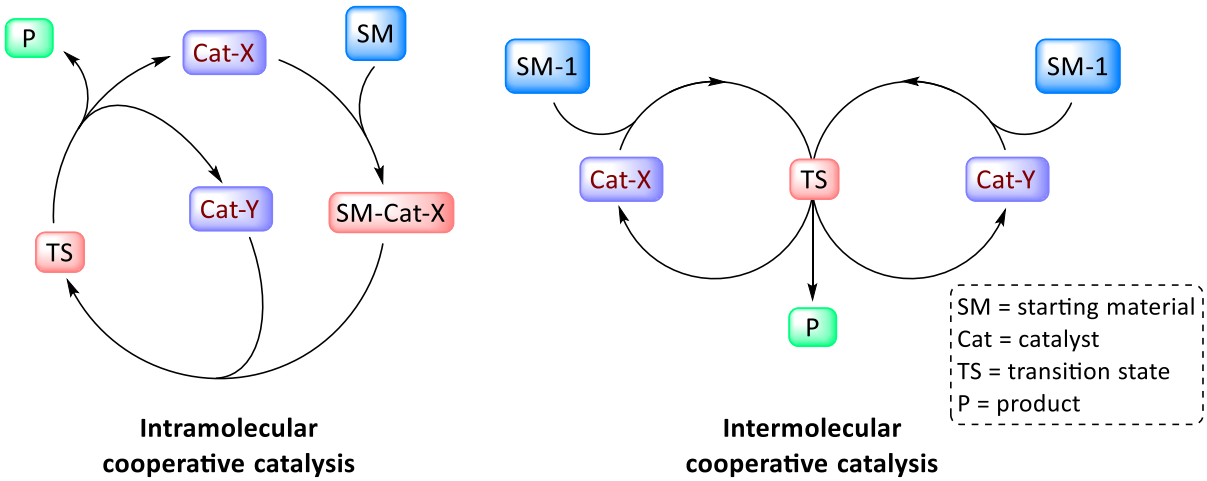

Scheme 7: General representation of intra- and intermolecular cooperative catalysis.

In respect to the nature of the employed catalysts, cooperative catalysis can be classified into three groups:

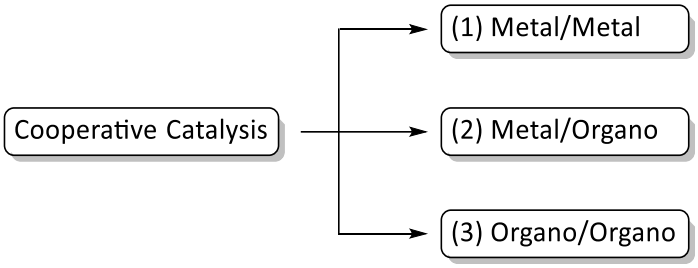

Although major advances have been made in the last year, the area of metal/metal cooperative catalysis is still less developed compared to reactions catalyzed by combinations of metal catalysts and organocatalysts.[29,30] In asymmetric catalysis, this can be attributed to the competing coordination of multiple metal species with the enantiopure ligands used, resulting in an undefined and unpredictable chiral environment. In addition, two metal centered catalysts tend to coordinate to each other and cause self-inhibition.[27] Nevertheless, inspired by biocatalysis, multimetallic catalysis is an emerging field in asymmetric organic synthesis.[31–34,30] As it is closest related to the topic of this work the metal/metal category will be presented here.

An early example of a bimetallic catalytic system is the cross-coupling reaction developed by *Sonogashira* in 1975.[35] Although the term cooperative catalysis was not coined yet at that time, in this reaction a palladium and a copper catalyst work together cooperatively in an intermolecular manner (Scheme 8).

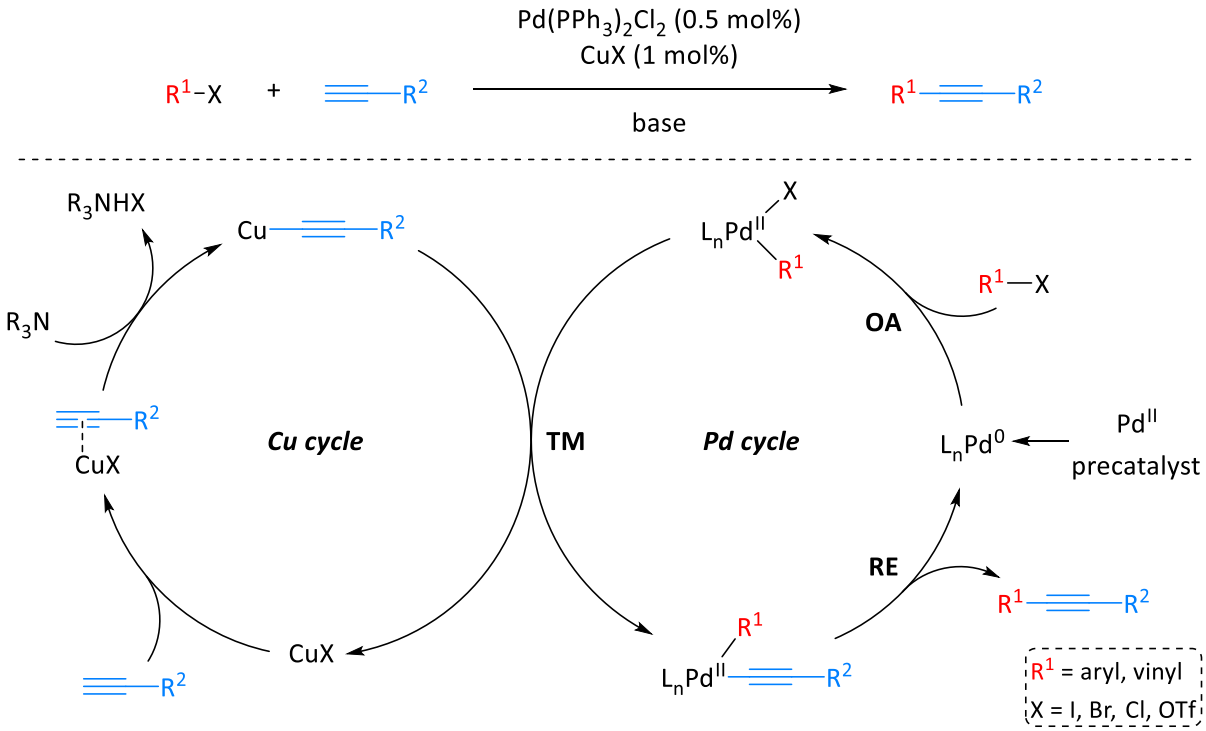

Scheme 8: Mechanism of the *Sonogashira* cross-coupling.

Palladium(0) activates the aryl halide and inserts into the R^1-X bond in an oxidative addition producing a palladium(II) species. The copper catalyst facilitates the deprotonation of the alkyne by π-coordination to the triple bond which leads to the formation of an organocopper species. In the transmetalation step the alkyne substituent is transferred from the organocopper species to palladium releasing an alkynyl palladium(II) species while CuX is regenerated. After a *trans-cis* isomerization and reductive elimination the coupling product is released and the active palladium(0) catalyst is regenerated.[36]

A pioneer example of an enantioselective cooperative catalysis with two separate metal catalyst was reported by *Sawamura, Ito* and co-workers in 1996.[37] Palladium and rhodium catalysis was merged for the enantioselective allylic alkylation of α-cyano esters assisted by the chiral diphosphine ligand AnisTRAP in excellent yields and selectivities (Scheme 9).

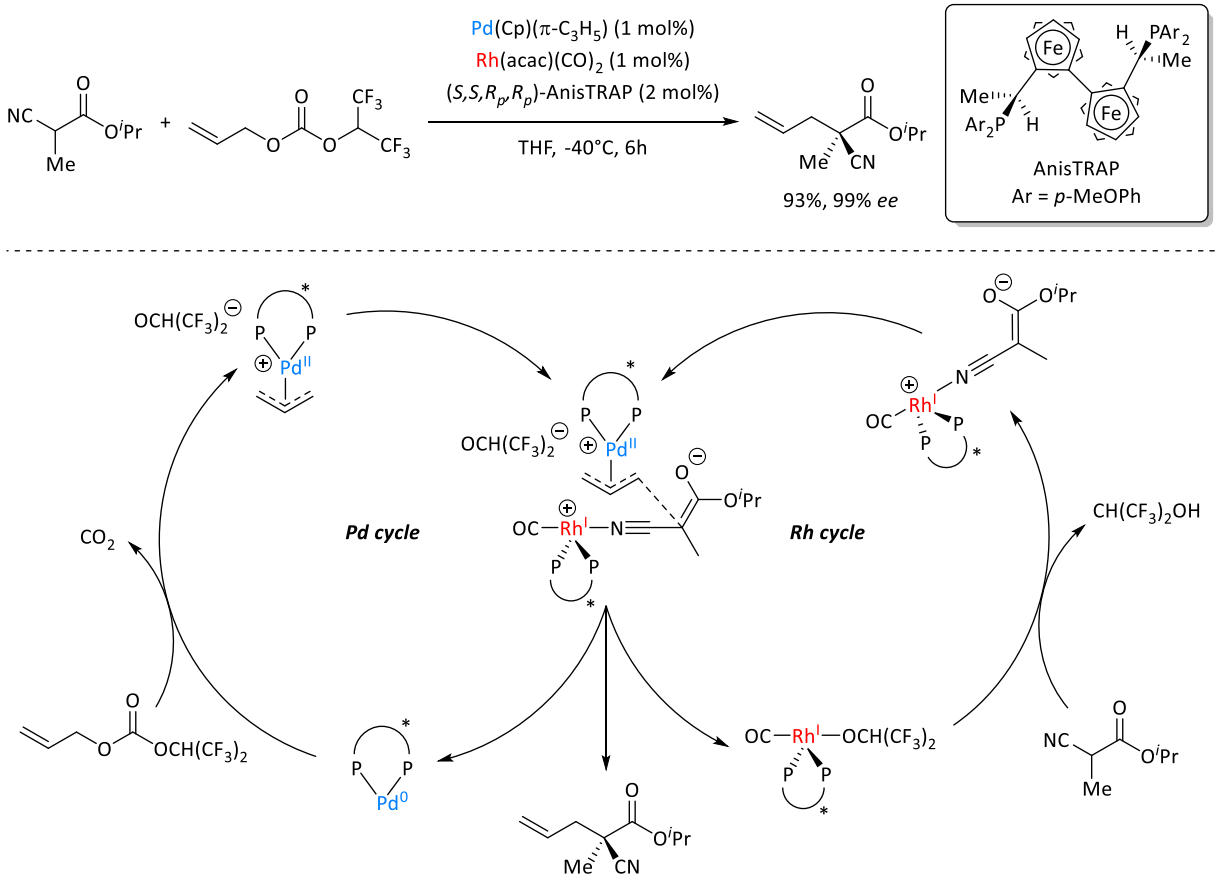

Scheme 9: Enantioselective allylic alkylation of α-cyano esters cooperatively catalyzed by rhodium and palladium.

In the left palladium cycle, in a decarboxylative oxidative addition with the allyl carbonate the π-allylpalladium(II) intermediate is formed from palladium(0). Simultaneously in the right rhodium cycle, the active chiral rhodium(I) complex, that is formed from $Rh(acac)(CO)_2$ and the chiral diphosphine ligand AnisTRAP, coordinates to the nitrile group of the α-cyano ester to form the rhodium(I)-coordinated enolate. This rhodium-bound enolate adds enantioselectively to the

π-allylpalladium electrophile in the central transition state from which the enantiopure α-cyano-α-allyl ester as well as both catalysts are released. The mechanistic studies suggest that although the chiral phosphine ligand binds to both catalysts, the enantioselectivity of the reaction only depends on the ligand bound to the rhodium. While the reaction shows no conversion when only the rhodium catalyst is used, the reaction has a comparable yield but no enantioselectivity when only palladium is employed. The ligand at the palladium center is simply too far away from both the formed stereocenter and the nucleophile to have and influence. Therefore, no competition between the chiral catalysts is observed resulting in the excellent selectivity of this reaction.[37]

A more sophisticated and elegant example of bimetallic catalysis was developed by *Zhang* and coworkers in 2016.[38] They applied the system, which is catalytic in iridium and zinc, to the enantio- and diastereodivergent allylation of unprotected α-hydroxyketones (Scheme 10). The zinc catalyst is combined with the ProPhenol ligand developed by *Trost,*[39] while the iridium complex is merged with a phosphoramidite ligand developed by *Teichert* and *Feringa*.[40] By changing the configuration of one or both ligands, the formation of both stereocenters is controlled and all four diastereoisomers can be synthesized in excellent yield and stereoselectivity from the same starting materials.

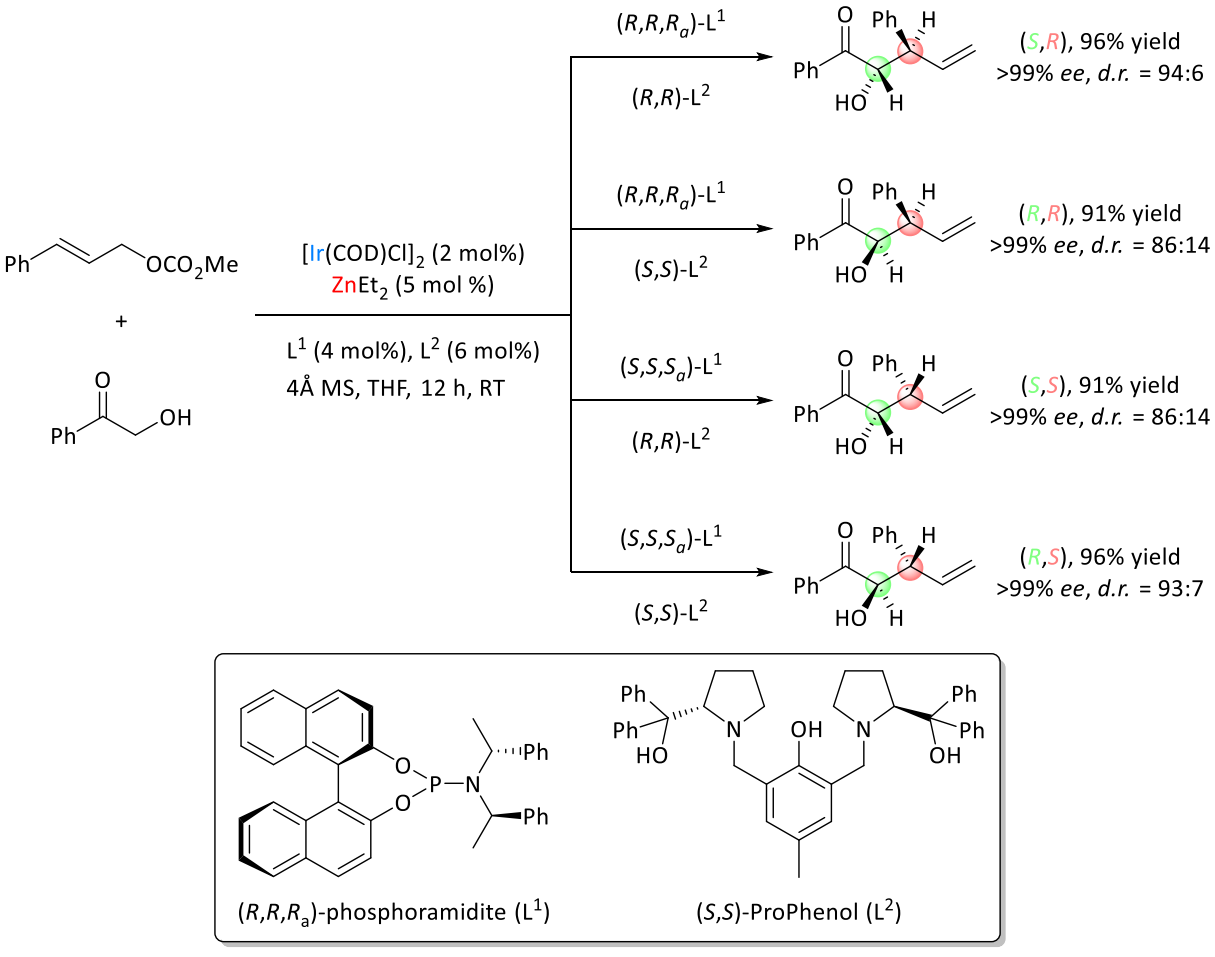

Scheme 10: Iridium and zinc catalyzed enantio- and diastereodivergent allylation of α-hydroxyketones by *Zhang et al*.

Although the mechanism of this reaction is not fully described, its excellent selectivity is explained by the cooperative interaction of the depicted electrophilic iridium complex with the nucleophilic zinc complex (Figure 5).[41]

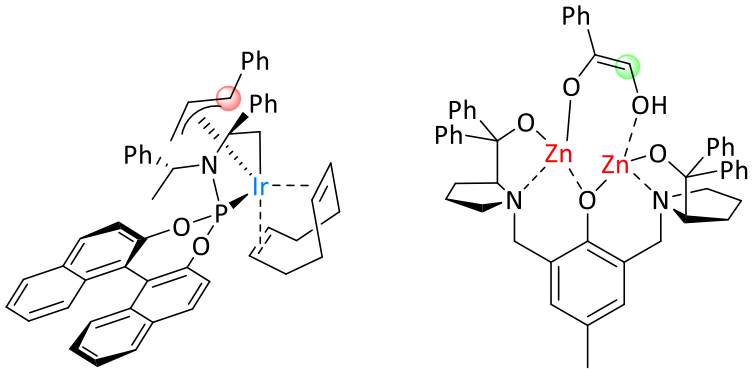

(R,R,R_a)-phosphoramidite-Ir-(π-allyl) (S,S)-ProPhenol-Zn-enolate

Figure 5: Iridium bound prochiral electrophile and zinc bound prochiral nucleophile.

Both zinc centers can coordinate to the oxygen atoms of the hydroxy ketone, thereby controlling the orientation of the nucleophilic site and defining the (*Z*)-configuration of the enolate. The iridium catalyst activates the allylic substrate by forming an electrophilic Ir-π-allyl intermediate. The respective chiral ligands bound in both complexes ensure a stereoselective interaction of the two prochiral intermediates. The choice of both ligands and their specific binding affinity to the metal centers precludes ligand exchange and ensures the high and defined stereoselectivity.[42]

The last example shows the opportunities in the development of cooperative catalysis based on combining established catalyst knowledge systematically. To successfully operate a cooperative system, it is crucial to understand the chemistry of the catalyst involved at first on their own. Therefore, the following chapters will present the fundamentals for the cooperative catalysis investigated in this work, starting with the radical chemistry of titanocenes, before proceeding to hydrogen atom transfer processes, which finally lead to the radical chemistry of chromium complexes.

1.3 Radicals in Organic Chemistry

Before diving into transition metal catalyzed radical chemistry, the general foundations of radical reactions should be introduced. Radicals are defined as atoms, molecules, or ions that have at least one unpaired valence electron. For a long time, radicals were considered too reactive and unpredictable for application in organic synthesis. Their use was mostly limited to industrial polymerization processes. It was the development of tin-based radical chemistry by *Kerk*[43] and the alcohol deoxygenation established by *Barton* and *McCombie*[44] that marked the beginning of the widespread interest in radical chemistry. The advantages of radical transformations have been increasingly appreciated. They typically include a high functional group tolerance and mild reaction

conditions, making them particularly interesting for late-stage synthesis. Also, as neutral particles, the reactivity of radicals is less influenced by solvent effects, and counterion effects are absent in contrast to ionic intermediates.[45–50]

Classically, radical reactions start with the generation of radicals by homolytic bond cleavage. The weak covalent bonds are mostly cleaved by thermally or photochemically induced homolysis to generate initiator radicals. Such bonds can be C–X or X–X bonds (X = N, O, S, Br, I) which are typically substantially weaker than C–H or C–C bonds and can be found in peroxides, disulfides or azo compounds.[45] For comparison some bond dissociation energies (BDE) of common single bonds are given in Table 1.[51]

Table 1: Comparison of bond dissociation energies of several single bonds.

Single bond	**BDE [kcal·mol^{-1}]**
H_3**C–H**	105.0
Ph(O)**C–O**CH_3	97.9
H_3**C–C**H_3	90.2
$(CH_3)_2$H**C–I**	56.1
Ph**S–S**Ph	51.2
CF_3**O–O**CF_3	47.5
^{t}Bu**O–O**^{t}Bu	38.2

An initiator molecule with weak bonds commonly used in organic chemistry is azobisisobutyronitrile (AIBN). It already decomposes at moderate temperatures or irradiation into two initiator radicals In• (Scheme 11).[52] The simultaneous formation of a stable N≡N triple bond additionally favors the radical formation. That manifests in the half-life of AIBN which is around 10 h at a temperature of 65°C, 20 min at 95°C, and even drops to a few seconds at 110°C.[53,45]

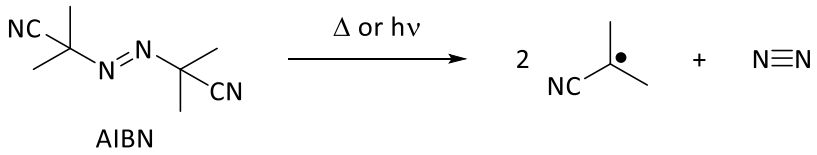

Scheme 11: Thermal or photochemical decomposition of radical initiator azobisisobutyronitrile (AIBN).

As all reactions of a radical with a closed-shell molecule result in the formation of a new radical, the result is a radical chain mechanism. The general radical chain mechanism is depicted in Scheme 12. Once an initiator radical is formed, it can initially react with a substrate molecule, abstracting and atom and generating a new radical R•. The chain is kept alive by certain fundamental transformations that R• can undergo, the propagation steps. These include S_H2 substitutions (bimolecular homolytic substitution), additions to multiple bonds or β-eliminations. All these propagation steps result in the formation of new radicals which themselves can undergo another propagation step. Driving forces is

often the formation of a more stable C–C or C–H bond and cleavage of another weaker bond. The chain reaction ends with a termination when two radicals combine to form again a closed-shell molecule.[46]

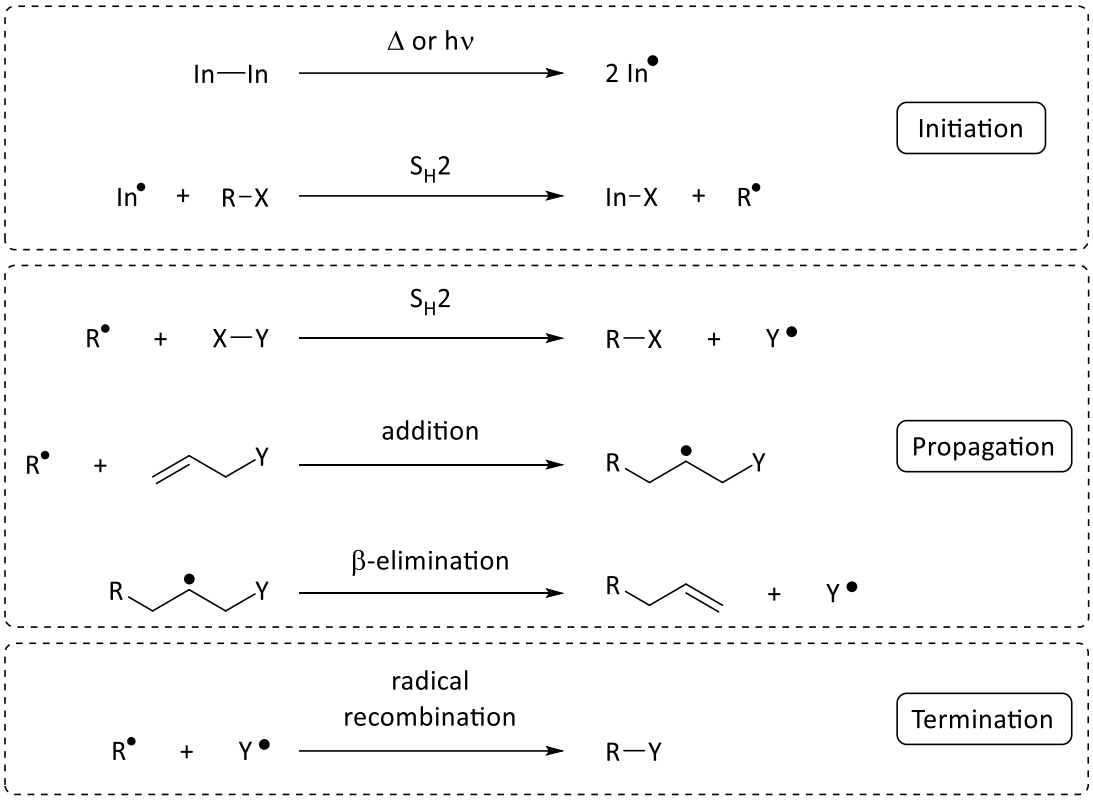

Scheme 12: General representation of radical chain reactions. In = initiator.

However, if a chain reaction or polymerization is not desired, it is necessary to trap the formed radicals before further propagation. Hydrogen atom donors are suitable for this purpose, with the most prominent example in radical chemistry being $^{n}Bu_3SnH$. The tin hydride can react in presence of a carbon-centered radical R• in a hydrogen atom transfer (HAT) to form a R–H bond and a tin-centered radical. The resulting tin radical can then recombine with a second tin radical to form a closed-shell dimer, which terminates the radical sequence.[52] The advantages and problems associated with different hydrogen atom donors will be discussed in more detail later.

Besides thermal or radiation initiated radical generation an alternative is the generation by oxidative or reductive processes. By a single electron reduction of a transition metal complex a metal center radical is obtained which can initially generate an organic radical species by reduction of an electron poor organic molecule. Besides halogenated alkanes, carbonyl compounds, aryl diazonium salts, sulfones and imines, epoxides are particularly suitable as such precursor molecules for radical generation, which explains the great synthetic potential. As reducing agents to mention here are low-valent transition metal complexes and salts containing Co(I), Fe(II),[54] Cr(II), Ru(II), Cu(I), Sm(II),[55] Ti(III).[46] In particular transformations mediated by the earth abundant metal titanium are emphasized here and will be a topic of the following chapters.

1.4 Titanocenes in Epoxide Opening Reactions

Epoxides are versatile substrates and intermediates in organic synthesis. They are easily prepared from carbonyl compounds[56–58] and olefins.[59,60] Besides racemic epoxidations, several methods are known for their enantioselective synthesis. Well-known asymmetric methods are the alkene epoxidations by *Jacobsen*[61] and by *Shi*.[62] The former uses an enantiomerically pure manganese(III)salen complex as catalyst, while the latter uses a fructose-derived organocatalyst. Furthermore, enantiomerically pure epoxides can be obtained from inexpensive racemic mixtures via a kinetic resolution such as the hydrolytic kinetic resolution (HKR) developed by *Jacobsen*.[63,64] By using an enantiomerically pure Co(III)salen catalyst, the undesired epoxide enantiomer is efficiently converted to the diol in a nucleophilic ring opening, allowing for its separation from the racemic mixture. The retained desired epoxide enantiomer is obtained in an excellent enantiomeric ratio (*e.r.)*, but only with a maximum yield of 50% when starting from a racemic mixture. Particularly noteworthy is the Nobel Prize awarded asymmetric epoxidation by *Sharpless*, in which allylic alcohols are enantioselectively oxidized to epoxy alcohols (Scheme 13).[65]

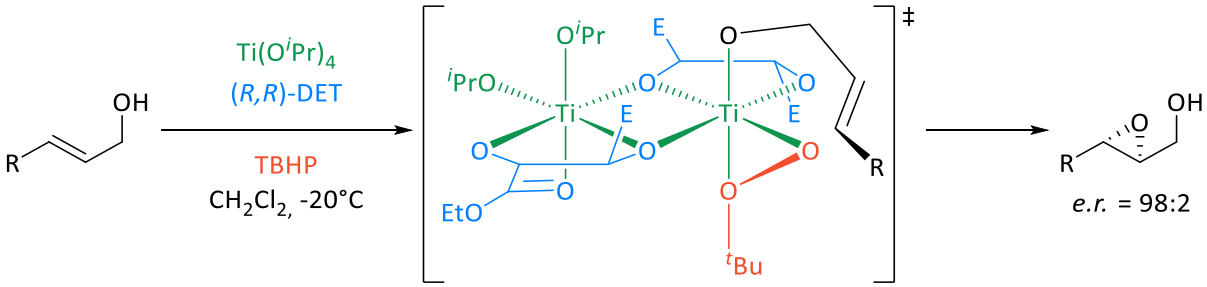

Scheme 13: *Sharpless* epoxidation of allylic alcohols. E = CO_2Et.

The absolute configuration of the product epoxide can be easily controlled by choosing one enantiomer of the diethyl tartrate (DET). The selectivity is based on a dinuclear enantiomerically pure titanium complex formed *in situ* from titanium isopropoxide and (*R,R*)- or (*S,S*)-diethyl tartrate. In the transition state formed by addition of the allylic alcohol substrate and the oxidant *tert*-butyl hydroperoxide (TBHP) to the catalyst complex, oxygen is selectively added from one side to the double bond.[66] Besides its chemoselectivity for allylic alcohols and its excellent stereoselectivity the *Sharpless* epoxidation requires only reagents that are inexpensive and readily available.

The high inherent ring strain of 23 kcal·mol^{-1} present in the three-membered ring of epoxides,[67] makes them spring loaded compounds suitable for multiple types of ring-opening reactions.[68] Well known and commonly used in organic synthesis are nucleophilic epoxide opening reactions (Scheme 14 (a)). The nucleophilic attack occurs in an S_N2-like fashion at the less hindered carbon and is determined by the nucleophile's nature and the epoxide's substitution pattern thus making the regio- and

stereoselectivity predictable.[69,70] The steric demand of the nucleophile and the substituents on the epoxide also influence the reaction rate substantially.

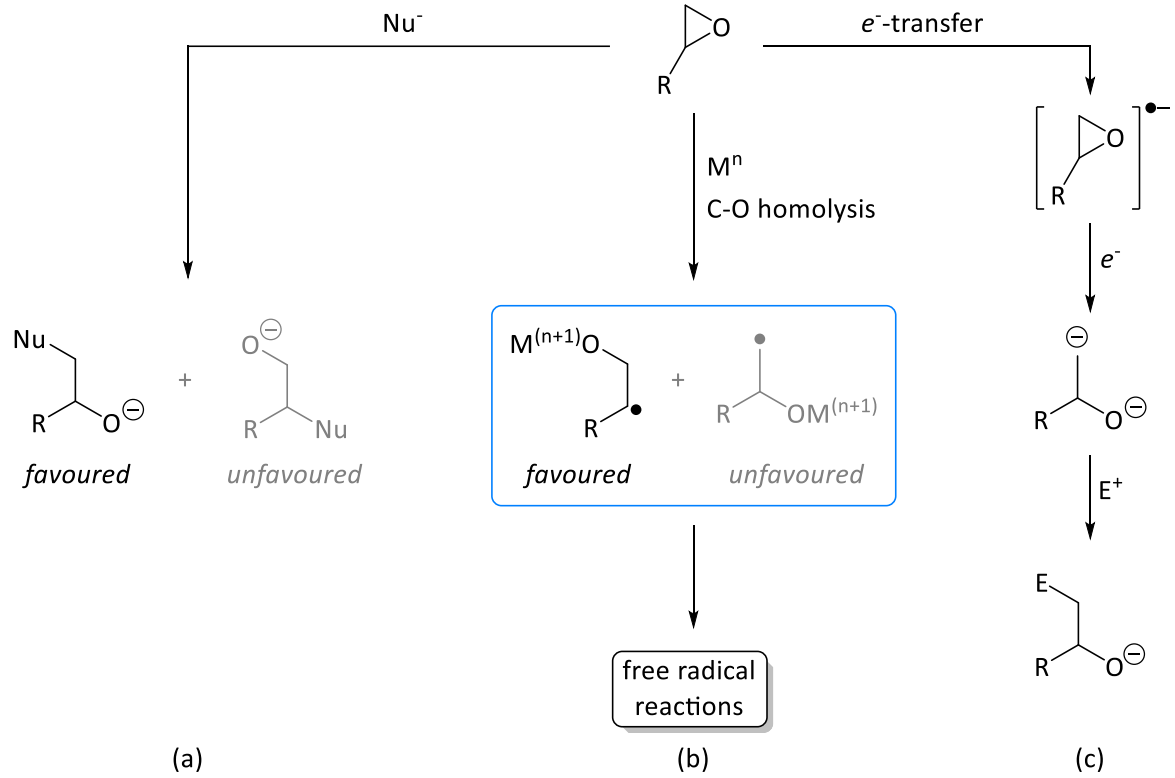

Scheme 14: Epoxide ring-opening reactions via (a) nucleophilic attack, (b) one-electron reductive C–O bond homolysis and (c) two-electron reduction.

Another possible way of epoxide opening via C-O bond homolysis is shown in Scheme 14 (b). As mentioned previously, epoxides can be opened by a transition metal complex in a single electron reduction generating a β-metaloxy radical. The formed radical is stabilized due to the transition metal complexation and therefore less reactive than an uncomplexed free radical. Usually, the regioselectivity of the ring opening is opposite to the nucleophilic opening and the precursor of the *anti-Markovnikov* product is obtained. This is caused by formation of the higher substituted, more stable radical, leading to the alkoxide being at the less substituted carbon. The homolytic epoxide opening occurs under mild conditions and offers access to broad range of functionalized radicals for further modifications.[68,71–74]

For completeness the two-electron reduction of epoxides to form carbanion is also to mentioned here (Scheme 14 (c)). In principle, this umpolung of the epoxide reactivity allows the reaction with electrophiles. However, the harsh reductive conditions required, an associated low functional group tolerance, the low stability of the carbanions towards eliminations and the limited range of employable electrophiles strongly restricts this approach, and thus it will not be discussed further here.

The subsequent discussion will focus on pathway (b) as illustrated in Scheme 14. *Nugent* and *RajanBabu* first identified titanocene(III) chloride (Cp_2TiCl) as a suitable single electron transfer (SET) reagent for the homolytic C–O bond cleavage of epoxides in 1988.[71] They describe a Cp_2TiCl-mediated rearrangement of an epoxide in analogy to the rearrangement of a cyclopropyl methyl radical to a homoallyl radical (Scheme 15). The σ-complexation of the epoxide by the *Lewis* acidic Cp_2TiCl leads to C–O bond cleavage and formation of a β-titanoxy radical. The stoichiometric titanocene(III) chloride is easily obtained by beforehand or *in situ* reduction of titanocene(IV) chloride with a base metal such as zinc or manganese. Driving force of the epoxide opening is the release of the ring strain as well as the formation of a stable Ti-O bond.

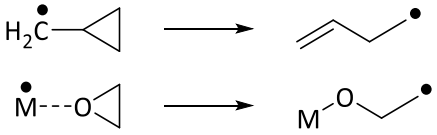

Scheme 15: Analogy between the cyclopropyl methyl radical and the σ-complex of an epoxide with a paramagnetic transition metal.

The β-titanoxy radical obtained by complexation and single electron transfer can undergo several general follow-up reactions, including reductions, additions, and eliminations (Scheme 16).[75]

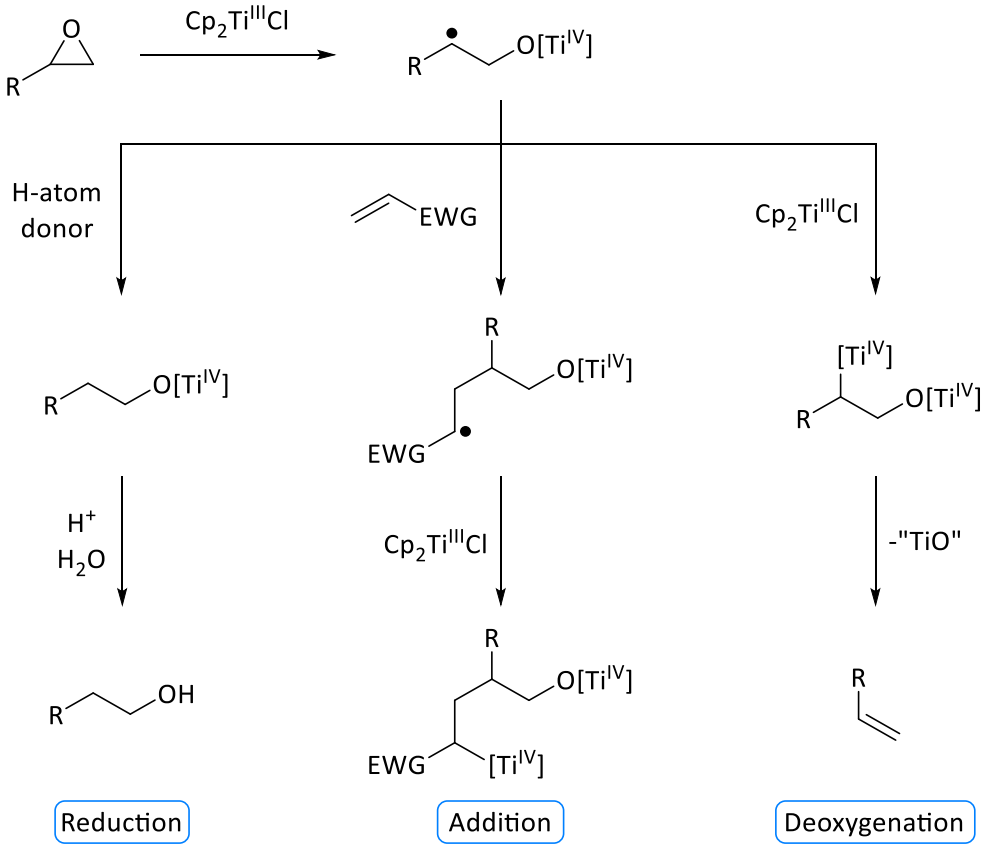

Scheme 16: Follow-up reactions of the β-titanoxy radical. [Ti] = Cp_2TiCl.

The β-titanoxy radical can be reduced by reaction with a hydrogen atom donor, such as 1,4-cyclohexadiene (1,4-CHD), or metal hydrides especially $^{n}Bu_3SnH$.[68,73] Subsequent protonation of the

titanocene-bound alcoholate liberates the *anti-Markovnikov* alcohol. The β-titanoxy radical can also undergo C–C bond forming inter- or intramolecular addition reactions.[68,71] The radical can add in an intramolecular cyclization to double and triple bonds and carbonyl functions or intermolecular to *Michael* acceptors. In the absence of a suitable hydrogen atom donor or radical acceptor, the β-titanoxy radical is trapped by another $Cp_2Ti^{III}Cl$ molecule.[71] Depending on the structure of the substrate, elimination and deoxygenation to the olefin occurs, or, in the case of tertiary radicals, β-hydrogen elimination under formation of $Cp_2Ti(H)Cl$ leads to an allylic alcoholate. The latter process will be discussed in detail in chapter 2.4.

Thus, by using stoichiometric amounts of titanocene(III) and an H-atom donor, preparations of *anti-Markovnikov* alcohols were performed as shown in Scheme 17.[73] The regioselectivity of the ring opening is substrate dependent, as for an S_N2-type reductive pathway, however, opposite for the radical pathway. A major drawback remains the need for stoichiometric or over-stoichiometric amounts of air-sensitive titanocene(III) chloride. Especially for potential application of enantiopure titanocenes and large-scale synthesis, this is a critical limitation, making a catalytic variant desirable.

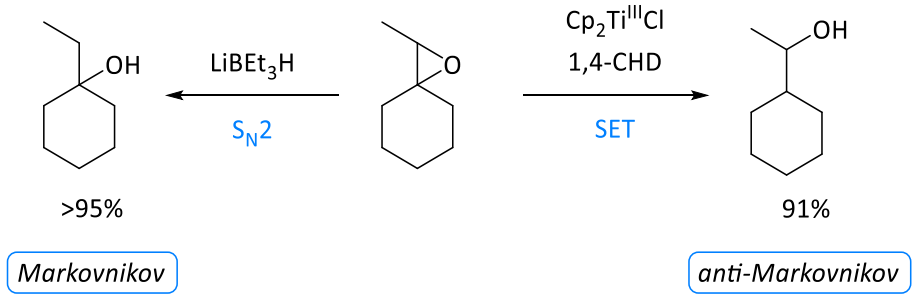

Scheme 17: Regioselectivity of the S_N2 vs. SET reductive epoxide opening.

The first titanocene-catalyzed variant of a homolytic epoxide opening, based on the work of *Nugent* and *RajanBabu*,[68,71] was developed by *Gansäuer* in 1998.[74] The critical step is the Ti–O bond cleavage and recovery of the $Cp_2Ti^{IV}Cl_2$ precatalyst from the alkoxide. This was achieved by choice of a suitable *Brønsted* acid, that must fulfill certain criteria:

1. The acid must be strong enough to cleave the Ti–O bond of the alkoxide while at the same time weak enough not to open the epoxide independently. That manifests in a range of pK_a values between 5.25 and 12.5.
2. The acid must neither oxidize the metal which is used to reduce the titanocene(IV) precatalyst nor any titanocene(III) species.
3. The base resulting from the protonation step must not inhibit any catalytically active species.

These requirements are met by alkyl substituted pyridinium salts (Figure 6), in particular 2,6-lutidine hydrochloride (Lut·HCl) and 2,4,6-collidine hydrochloride (Coll·HCl), with the latter showing the best experimental results.[74,76]

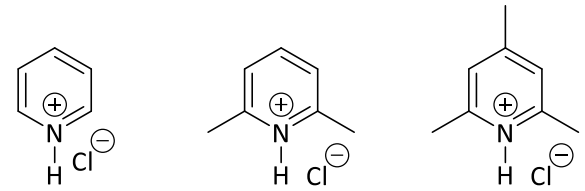

Figure 6: Acidity of pyridine hydrochloride, 2,6-lutidine hydrochloride, and 2,4,6-collidine hydrochloride in water.

Another concern is the choice of the metal that serves as the reductant for the precatalyst. As mentioned above, the active $Cp_2Ti^{III}Cl$ can be efficiently generated *in situ* by reduction of air-stable $Cp_2Ti^{IV}Cl_2$ with zinc or manganese powder. It is important to consider the *Lewis* acidic salt resulting from the reduction, with $MnCl_2$ being less *Lewis* acidic, leading to less interaction with the catalyst and therefore less side reactions. The resulting catalytic cycle of the titanocene-catalyzed reductive epoxide opening by *Gansäuer* is shown in Scheme 18.[77]

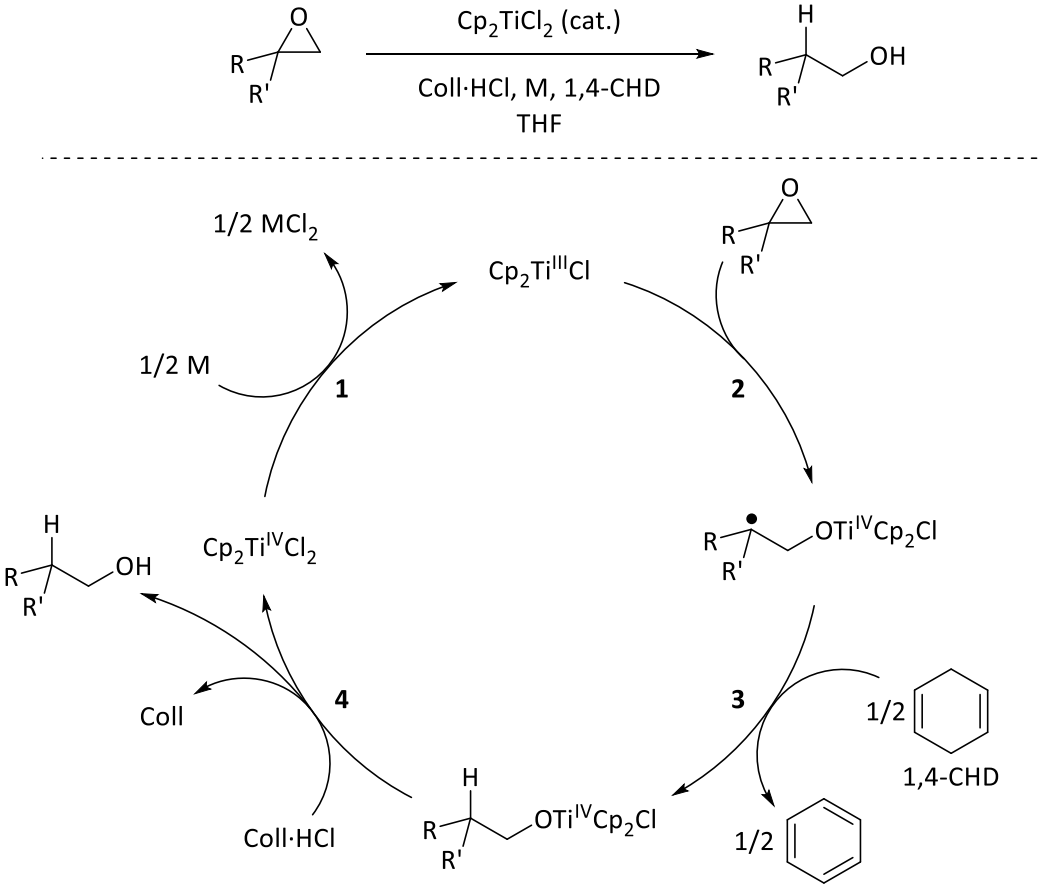

Scheme 18: Mechanism of the titanocene-catalyzed epoxide opening by *Gansäuer*. Reaction conditions: 0.05 eq. Cp_2TiCl_2, 1.5 eq. Coll·HCl, 1.5 eq. Mn, 4.3 eq. 1,4-CHD.[74,77]

The mechanism starts with the activation of the precatalyst $Cp_2Ti^{IV}Cl_2$ by reduction with manganese powder to form the active catalyst $Cp_2Ti^{III}Cl$. In the second step, the epoxide is opened by the titanium centered radical in a single electron oxidative addition to form the β-titanoxy radical. This carbon centered radical undergoes a HAT in the third step with the H-atom donor 1,4-CHD, resulting in the saturated titanocene alkoxide. In the fourth step, the Ti–O bond is cleaved by protonation with the acid Coll·HCl to release the product alcohol as well as the $Cp_2Ti^{IV}Cl_2$ precatalyst. The catalytic cycle is closed by another reduction of titanocene(IV) to titanocene(III) with the metal powder.[74] It is this radical mechanism under very mild reaction conditions which leads to the high functional group tolerance. The tolerated functional groups include esters, chlorides, ketones, and protecting groups like the pivaloyl group, silyl groups, and tosylates.[78]

The described titanocene-catalyzed epoxide opening reaction provides a broad range of *anti-Markovnikov* alcohols. Assuming a previous epoxidation of an olefin, both steps together formally constitute an *anti-Markovnikov* addition of water to a double bond. Classically, this formal addition of water has been achieved by *Brown* hydroboration and subsequent oxidation (Scheme 19).[79–81]

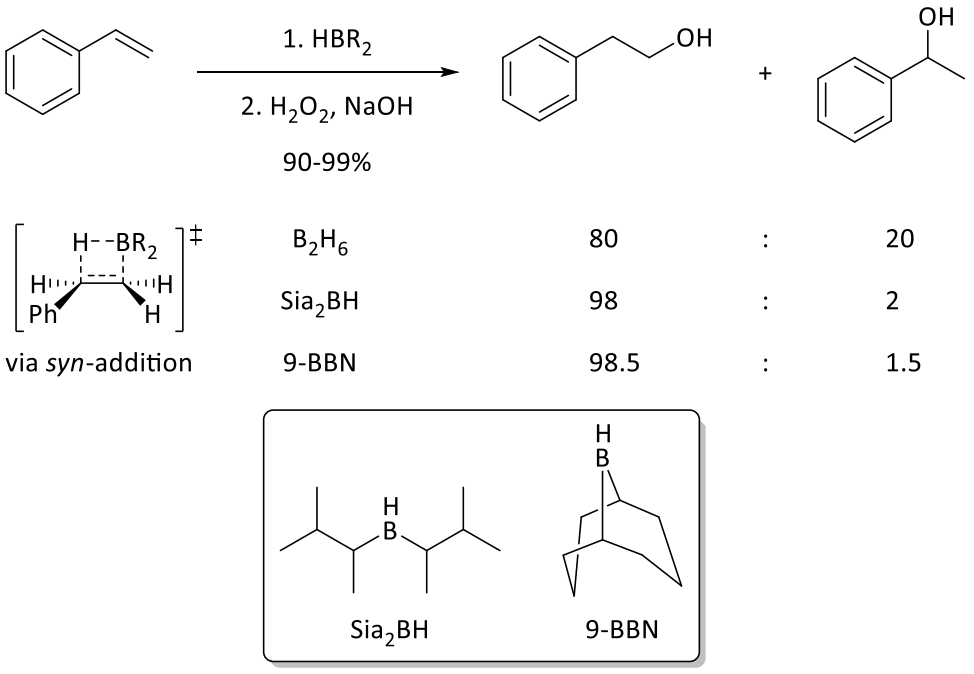

Scheme 19: *Brown* hydroboration and oxidation of styrene.

The regioselectivity of the addition step is based on a *syn*-addition of the B–H bond to the double bond. The hydrogen adds to the higher substituted carbon while the boron atom adds to the less substituted one. Dialkyl boranes such as disiamylborane (Sia_2BH) or 9-BBN increase the selectivity compared to simple B_2H_6 by increasing the steric bulk. To obtain the *anti-Markovnikov* alcohol the organoborane compound must then be oxidized with H_2O_2 in a second step. It is this requirement for oxidizing and basic conditions that reduces the functional group tolerance. In addition, the stoichiometric use of

toxic boranes and the waste production associated with the use of bulky alkyl substituted boranes, which only transfer one equivalent of hydride, is undesirable. Thus, the titanocene catalyzed epoxide opening with its milder conditions and regioselectivity under reagent control is an attractive alternative and holds great potential for further development compared to the hydroboration.

The development of the mild and functional group tolerant titanocene-catalyzed epoxide opening has paved the way for a wide range of applications (Scheme 20). These include catalytic C–C bond forming cyclizations and intermolecular additions,[74,82] radical aromatic substitutions,[83] and regiodivergent epoxide opening reactions.[84] In particular, the latter reaction, which yields enantiopure products, also requires enantiopure titanocenes and is therefore hardly conceivable without a catalytic reaction pathway. The following section will introduce some of the mentioned methods and applications.

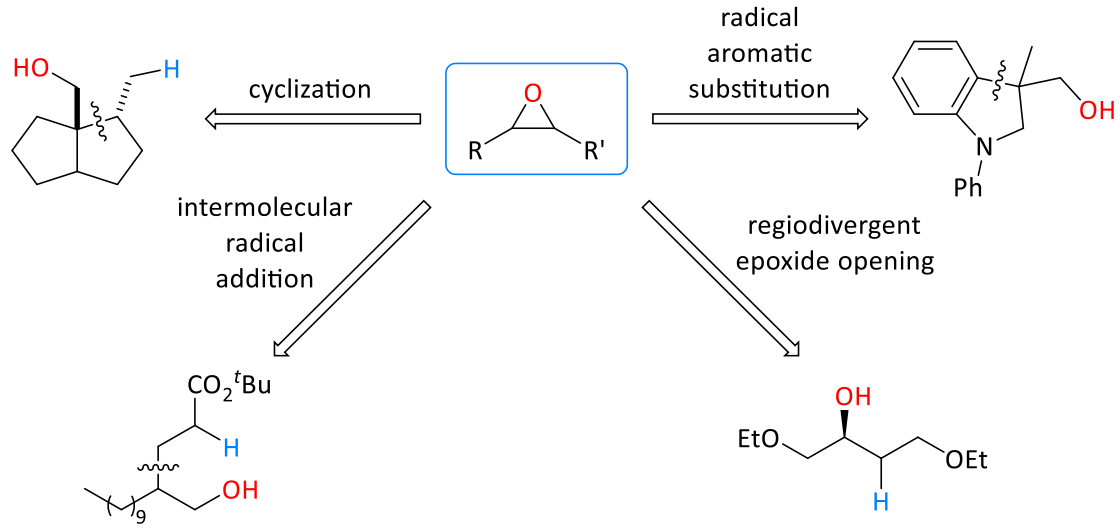

Scheme 20: Various applications of the titanocene-catalyzed reductive epoxide opening.

Titanocene-catalyzed epoxide openings have gained a significant role in natural product and terpene synthesis for example in the total synthesis of furanospongian diterpenes originally occurring in marine sponges. A considerable improvement and reduction of the required synthetic steps was achieved by including a titanocene-catalyzed radical cascade cyclization in the total synthesis of the depicted furanoditerpenoid (Scheme 21), which is found in the sponge *Spongia officinalis,* and shows cytotoxic effects on tumor cells and antiviral activity.[85] TMSCl is added here to facilitate the cleavage of the alkoxide and regeneration of Cp_2TiCl_2.

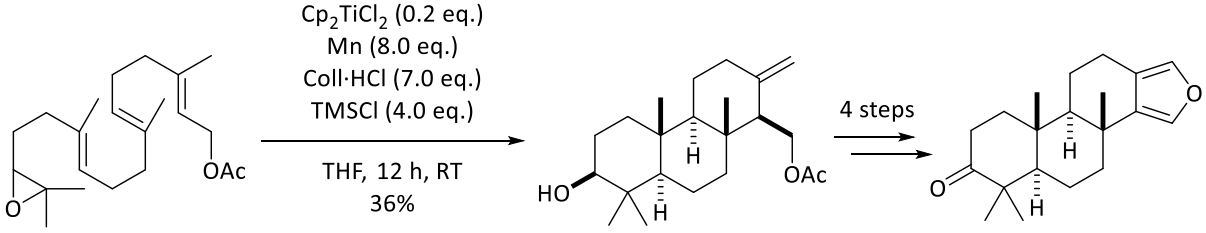

Scheme 21: Titanocene-catalyzed cyclization in the total synthesis of a furanoditerpenoid naturally occurring in *Spongia officinalis.*

A titanocene-mediated intermolecular addition to an acrylate with subsequent lactonization was successfully applied in the total synthesis of maoecrystal Z (Scheme 22), which occurs in the plant *Isodon eriocalyx*. The compound is structurally related to other 6,7-*seco*-*ent*-kauranoid natural products, including trichorabdals A and B, which show *in vivo* anti-tumor activity. The use of catalytic amounts of titanocene in this synthetic step yielded the same product, albeit with a diminished yield.[86]

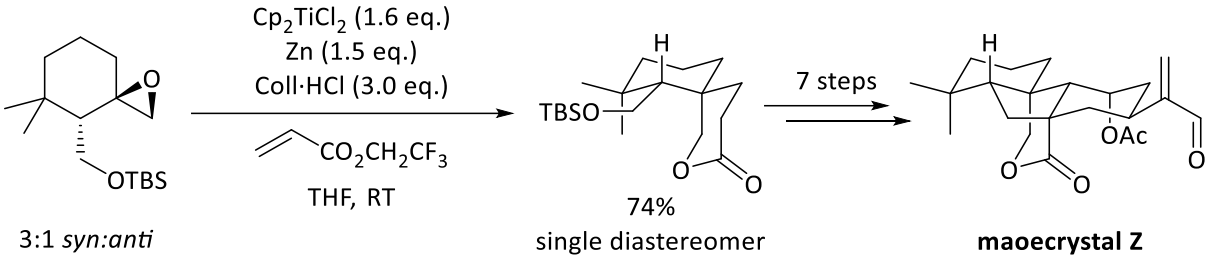

Scheme 22: Titanocene-mediated radical acrylate addition and lactonization in the total synthesis of maoecrystal Z.

The given reagent control together with the possibility of modifying the ligands sphere of titanocenes led to the first enantioselective formation of radicals by epoxide opening described by *Gansäuer* in 1999.[87] The method makes use of enantiopure titanocenes in the desymmetrization of *meso*-epoxides. The chiral titanocenes investigated are, among others, complexes developed by *Kagan* (Figure 7).[88] Chirality is introduced by substituting the cyclopentadienyl ligands with terpene-derived substituents, in this case menthol. The use of naturally occurring menthol, which is available in both enantiomers, makes the synthesis simple, cost efficient, and both catalyst enantiomers accessible.

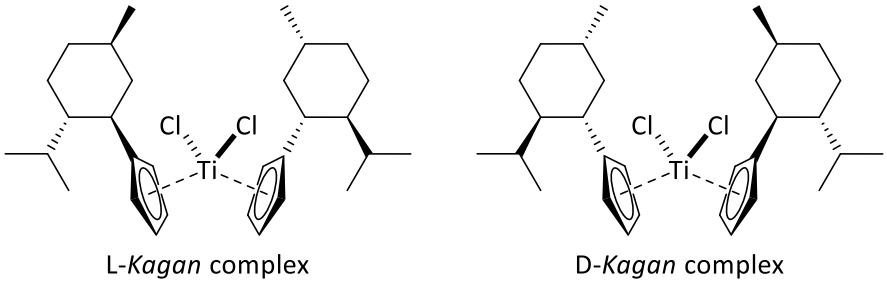

Figure 7: Enantiomers of the menthol-derived *Kagan* complex.

In general, both C–O bonds in *meso*-epoxides share the same electronic and steric properties. Although both enantiomers of a *meso*-epoxide are identical, when the epoxide is opened, it is desymmetrized and in principle two enantiomers are formed. In the opening with the enantiopure *Kagan* titanocene, one of the two alcohol enantiomers can be selectively synthesized (Table 2).[84,87] The *Kagan* complex showed superior results in terms of yield and enantioselectivity compared to the also investigated well-known chiral *Brintzinger* catalyst.

Table 2: Enantioselective reduction of *meso*-epoxides catalyzed by the *Kagan* complex.

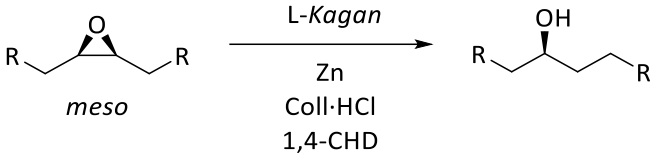

R	yield [%], *ee* [%]
OEt	76, 94
O^{n}Pr	70, 91
O^{t}Bu	66, 86

Reaction conditions: 0.1 eq. L-*Kagan*, 2.0 eq. Zn, 2.5 eq. Coll·HCl, 1.0 eq. 1,4-CHD, THF, 22 h, RT.

The regioselectivity of the ring opening is induced in the coordination of the *Lewis* acidic titanocene(III) to the oxygen atom, leading to the subsequent SET oxidative addition. DFT calculations of the transition state revealed the unequal steric interactions of the *Kagan* complex ligands with the epoxide's substituents (Figure 8).[67] In the given example, the reaction with the L-*Kagan* weakens the C^3–O bond more compared to C^2–O. As a result, the C^3–O bond is preferentially cleaved, forming the alkoxide at C^2 and the radical at C^3.

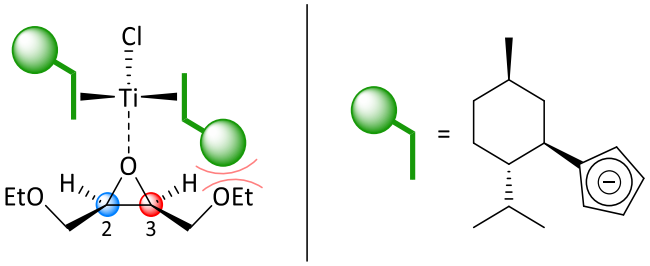

Figure 8: Interactions between the reduced *Kagan* complex and *meso*-epoxides. Different degrees of steric interactions between the epoxide sides cause a regioselective opening of the epoxide.[89]

Since the concept generally works well for *meso*-epoxides, an extension to *pseudo-meso*-epoxides is the continuative step. Indeed, 1,2-disubstituted epoxides with sterically and electronically similar substituents show analogous reactivity with enantiomerically pure titanocenes. In principle, one enantiomer of a non-symmetric 1,2-disubstituted epoxide, when reacted with the L- or D-*Kagan* complex, is opened selectively to one regioisomer and a single enantiomer – a concept described as regiodivergent epoxide opening (REO).[67,90] Both substrate enantiomers must be opened efficiently and with opposite regioselectivity. It is therefore essential that a comparable binding of both substrate enantiomers to the chiral catalyst is achieved. Otherwise, if the two diastereomeric complexes are too energetically different, a kinetic resolution would be the outcome.

These requirements are met for the reduced *Kagan* complex. The results of the regiodivergent epoxide opening of an unsymmetric 1,2-disubsitituted epoxide in racemic and enantioenriched form with the L- and D-*Kagan* are shown in Table 3. Racemic substrates lead to a parallel resolution by formation of two regioisomers. Enantiomerically enriched epoxides, however, undergo a double asymmetric process, resulting in a higher enantiomeric excess in the products than in the substrates.[67,90]

Table 3: Regiodivergent epoxide opening of racemic and enantioenriched epoxides with different *Kagan* enantiomers.

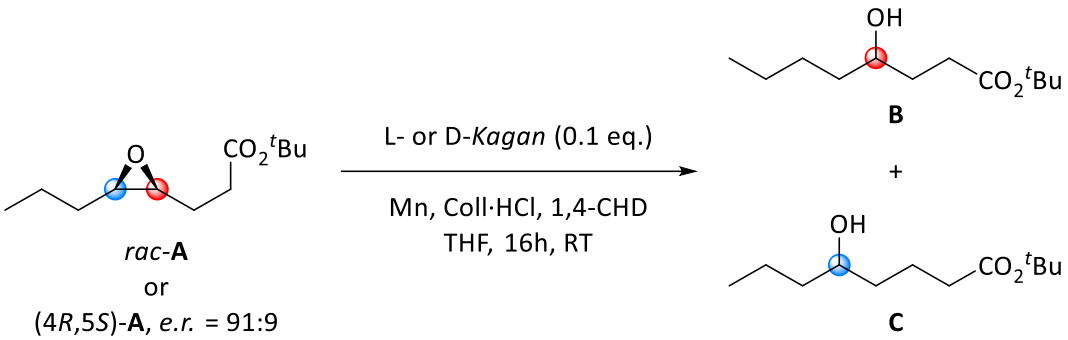

rac-**A**
or
(4*R*,5*S*)-**A**, *e.r.* = 91:9

Substrate	Catalyst	Yield B, C [%]	*e.r.* B	*e.r.* C
rac-**A**	L-*Kagan*	51, 44	88.5:11.5	5:95
rac-**A**	D-*Kagan*	45, 42	9.5:90.5	96.5:3.5
(4*R*,5*S*)-**A**	L-*Kagan*	17, 71	46:54	99.5:0.5
(4*R*,5*S*)-**A**	D-*Kagan*	76, 10	97:3	25:75

Reaction conditions: 0.1 eq. L- or D-*Kagan*, 1.5 eq. Mn, 1.5 eq. Coll·HCl, 4.5 eq. 1,4-CHD, THF, 16 h, RT.

The reaction of the racemic substrate *rac*-**A** with both catalyst enantiomers gives a mixture of the regioisomers **B** and **C** in a similar ratio. The rather small deviation from the ideal 1:1 ratio is due to small differences in the steric and electronic properties of the *pseudo-meso*-epoxide. As the regioselectivity of the ring opening is determined by the configuration of the catalyst, the products are formed with inverse enantioselectivity each. This shows that the reaction rate is similar for both enantiomers. Surprisingly at first glance, in the case of the enantioenriched epoxide (4*R*,5*S*)-**A**, the enantiomeric ratio increases in the product. In the reaction with the L-*Kagan*, starting from an *e.r.* of 91:9 in the substrate, **C** is obtained in 71% yield but with an *e.r.* of 99.5:0.5. The minor product **B** is isolated in 17% yield with a poor *e.r.* (46:54). In the reverse case, using the D-*Kagan*, the major product **B** is obtained in 76% yield and increased *e.r.* (97:3), while the minor product **C** is isolated in 10% yield and an *e.r.* of 25:75. This observation is caused by a double asymmetric process (Scheme 23).[67]

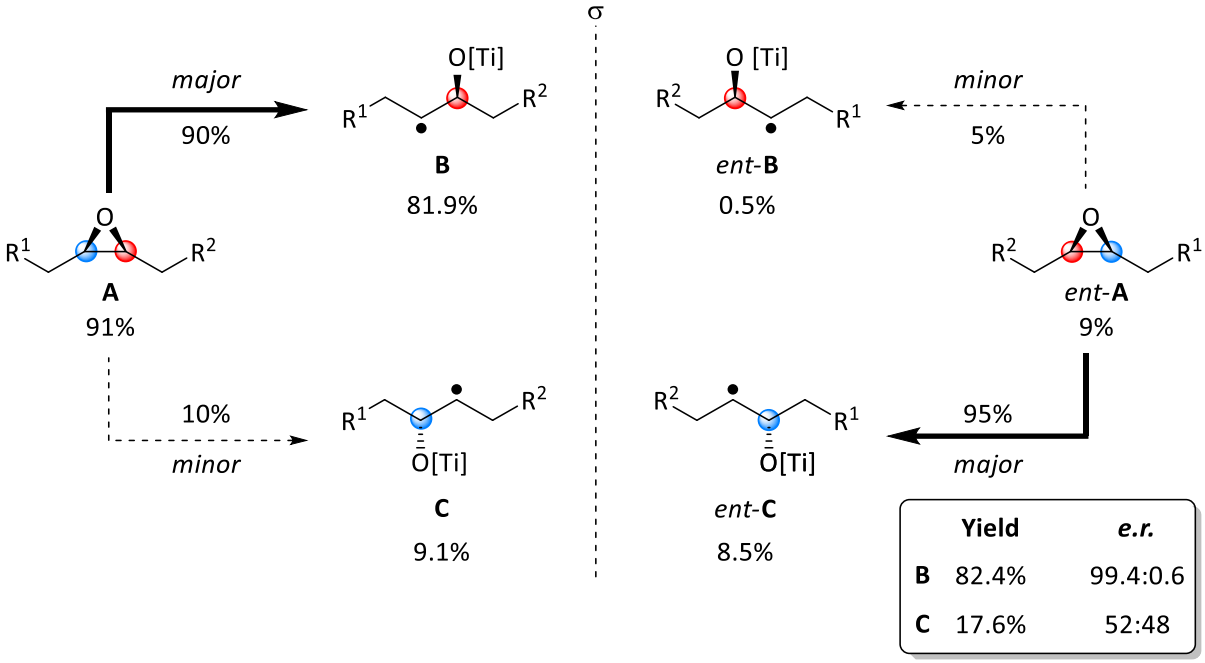

Scheme 23: Exemplary calculation of the enantiomeric enrichment during the REO of enantioenriched epoxides via a double asymmetric process.

The increased enantioselectivity of the major product regioisomer (**B**, *ent*-**B**) is caused by formation via a predominant pathway from the major substrate **A** and a subordinate pathway from the minor substrate *ent*-**A**. Thus, the regiodivergent epoxide opening combines the advantages of radical chemistry with the high selectivity of the ring opening, allowing the synthesis of enantiomerically pure alcohols. The method has been successfully extended to the synthesis of valuable enantiopure 1,3- or 1,4-diols.[91] The 1,3- or 1,4-diol motif is often found in nature and pharmaceutically active compounds, such as the amphotericin B, depicted in Figure 9.[92]

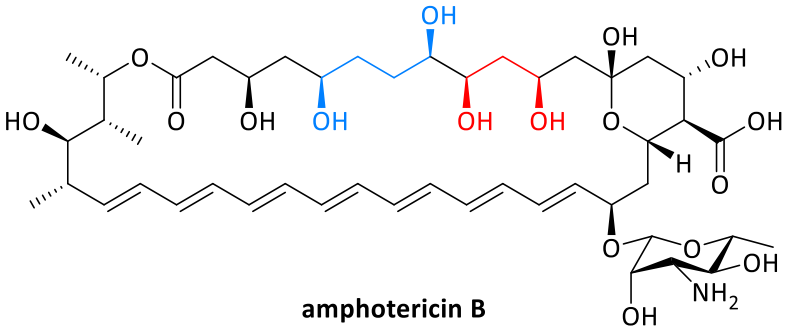

Figure 9: The antifungal drug amphotericin B, which contains multiple diol units. Exemplary, one 1,3- and 1,4-diol unit are marked.

By choice of the catalyst, the 1,3- or 1,4-diol unit is accessible via REO from the same β-hydroxy epoxide starting material. Presuming the *syn*- and *anti*-diastereomers of the β-hydroxy epoxide are available in enantiomerically pure form, all four possible configurations of the *syn* and *anti* 1,3- and 1,4-diol are accessible (Scheme 24).[91]

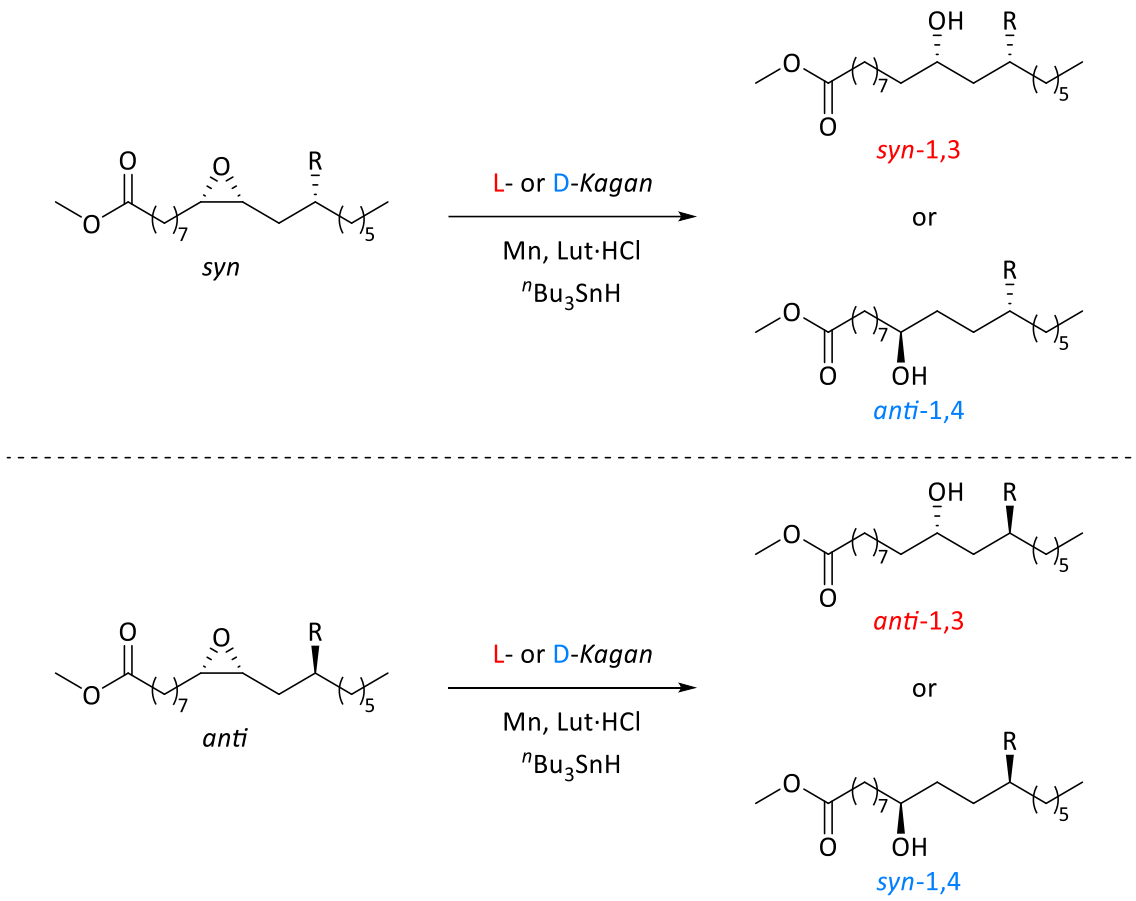

Scheme 24: General scheme of selectivity in the REO.

Moreover, by preceding β-functionalization of the β-hydroxy epoxide, not only diols but also 1,3- or 1,4-difunctionalized molecules are obtained (Table 4).[91]

Table 4: Synthesis of *syn* and *anti* 1,3- and 1,4-difunctionalized molecules via REO.

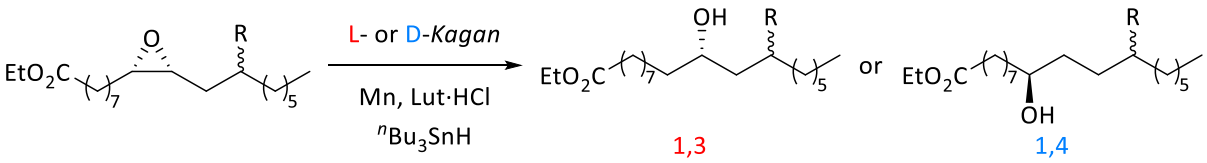

Substrate	Catalyst	Product	Yield [%]	*r.r.* (1,3:1,4)
syn, R = OH[a]	L-*Kagan*	*syn*-1,3	91	99:1
syn, R = OH[a]	D-*Kagan*	*anti*-1,4	88	1:99
anti, R = OH[b]	L-*Kagan*	*anti*-1,3	86	99:1
anti, R = OH[b]	D-*Kagan*	*syn*-1,4	85	1:99
anti, R = F[b]	L-*Kagan*	*anti*-1,3	80	99:1
anti, R = F[b]	D-*Kagan*	*syn*-1,4	88	1:99

Reaction conditions: 0.07 eq. *Kagan*, 1.5 eq. Mn, 1.5 eq. Lut·HCl, 2.2 eq. $^{n}Bu_3SnH$, THF, 72 h, RT;
[a] *e.r* = >99:<1, *d.r.* = 97:3; [b] *e.r.* = >99:<1, *d.r.* = 99:1.

It should be noted that enantioselective methods involving an opening of epoxides typically rely on S_N2-like reactions. However, selectivity in the opening of *meso* and especially unbiased 1,2-disubstituted epoxides remains challenging, as differentiation between the sides of the nucleophilic approach is difficult and depends on the substituents of the substrate in combination with the steric bulk of the nucleophile.[93–95] In contrast the regiodivergent epoxide opening is clearly superior as the reaction proceeds essentially under catalyst control.[89]

1.5 Hydrogen Atom Donors

Although the titanocene-catalyzed methods presented above offer access to a broad range of *anti-Markovnikov* alcohols, cyclization and addition products, as well as 1,3- and 1,4 diol building blocks, they all still leave space for improvement. Common to all methods is a need for optimization due to the use of over-stoichiometric amounts of reagents, which is problematic in terms of waste generation and high resource consumption. In particular, the use of over-stoichiometric hydrogen atom donors is a significant disadvantage. This challenge is largely rooted in the properties of hydrogen atom donors, which, although effective in mediating these reactions, pose significant issues that will be discussed in the following section.

Hydrogen atom donors all share the characteristics of weak C–H or heteroatom X–H bonds with low bond dissociation energies (BDE), making them suitable for reducing radicals to hydrocarbons.[96] Trialkyl stannanes have long been considered the best synthetic equivalent of a hydrogen atom. The well-known $^{n}Bu_3SnH$ has been used in various reaction including dehalogenations and other defunctionalizations or C–C bond forming reactions (radical additions, radical cyclizations).[97–101] The reasonably weak Sn–H bond (78 kcal·mol^{-1})[51] compared to typical hydrocarbon C–H bonds (99 kcal·mol^{-1})[51] allows a rapid hydrogen atom transfer to carbon-centered radicals. Although $^{n}Bu_3SnH$ is a potent hydrogen atom donor, tolerates many functional groups, and is relatively inexpensive, the use of stannanes is now avoided whenever possible. A considerable neurotoxicity of the tin hydrides and the tin by-products limits their applications, especially on an industrial scale.[102] In addition, there are considerable problems with the complete removal of the toxic tin residues following the reaction, which makes pharmaceutical applications particularly unattractive. Thus, development of alternative hydrogen atom donors became crucial to overcome the prevailing ‘tyranny of tin’.[101] As useful alternatives to tin hydrides, silanes, thiols, proaromatic compounds, and metal hydrides have been investigated.[101,103,104] Some BDE values for typical compounds are listed in Table 5. As shown, the bond dissociation energy significantly correlates with the rate of hydrogen atom abstraction by primary alkyl radicals, although it is not the sole factor.

Table 5: BDE values of several hydrogen atom donors and rate constants for the hydrogen atom abstraction by primary alkyl radicals.[51,105–107]

Donor	BDE (X–H) [kcal·mol^{-1}]	k_H [M^{-1}·s^{-1}] (T [°C])
$^{n}Bu_3Sn$–H	78	$2.4 \cdot 10^6$ (25)
$^{n}Bu_3Ge$–H	89	$1.0 \cdot 10^5$ (25)
Et_3Si–H	95	$7.0 \cdot 10^2$ (25)
Ph_3Si–H	89	$3.0 \cdot 10^4$ (50)
$(TMS)_3Si$–H	84	$3.8 \cdot 10^5$ (25)
^{t}BuS–H	87	$8.0 \cdot 10^6$ (25)
1,4-CHD	76	$2.0 \cdot 10^5$ (50)

Replacements for tin have been searched ascending group 14, leading to organogermanium hydrides and organosilanes. Germanium, although considered less toxic than tin, is usually not a sufficient replacement as shown by the kinetic data. Additionally, besides the high costs, the problems associated with its complete removal remain the same as for the tin hydrides.[104,106]

Silanes have been widely used in organic chemistry as nontoxic and inexpensive replacement for tin hydrides. However, the hydrogen atom donor ability of simple silanes is often lacking in potency. Nevertheless, tris(trimethylsilyl)silane ($(TMS)_3SiH$) introduced by *Chatgilialoglu* is only slightly inferior to $^{n}Bu_3SnH$ and could be used as replacement in several studies.[108,109] Here, the relatively high costs limit its application.

Thiols show high rates of hydrogen atom transfer to alkyl radicals, however, they are not suitable for many reactions as the formed thiyl radicals are prone to side reactions and often lead to additional functionalization of the molecule by addition to unsaturated bonds. Also, halogen abstraction by the thiyl radical proceed at low rates, preventing chain reactions. However, as catalyst in combination with silanes, these problems could be overcome for some applications. Nevertheless, the potential toxicity of thiols and the strong odor are downsides as well.[103,104]

The proaromatic 1,4-cyclohexadiene (1,4-CHD) and its derivatives are useful alternatives to tin hydrides. The C–H bond is weakened due to the resonance stabilization of the resulting cyclohexadienyl radical and aromatic benzene, respectively, resulting in sufficient hydrogen atom donor abilities. However, the same stability of the cyclohexadienyl radical makes it unsuitable for chain propagation reactions.[103,110] Their synthesis under *Birch*-like conditions and the regulatory issues associated with the resulting benzene or aromatic compounds limit their applications to laboratory scales.

Despite the applicability of the abovementioned hydrogen atom donors, their significant drawbacks drive ongoing research for more sustainable alternatives, fueled by continued interest in radical

chemistry. In the context of atom economy, H_2 and H_2O are of particular interest. In 2002, *Oltra* and *Rosales* challenged the predominant assumption of the innocence of water in free radical reactions and presented water as a hydrogen atom donor in in the titanocene-mediated epoxide opening (Scheme 25).[111] The use of THF containing a high amount of water led to the saturated alcohol as the major product. Instead, anhydrous THF gave the expected exocyclic alkene. Experiments with D_2O confirm the origin of the hydrogen/deuterium atom from water.

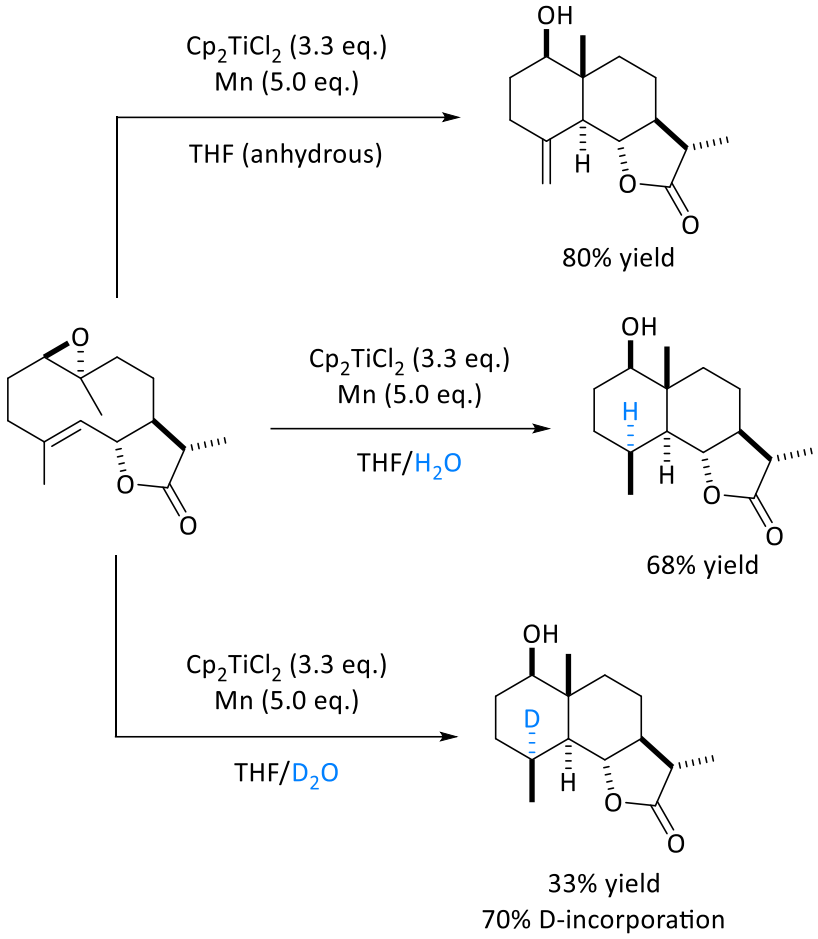

Scheme 25: Water as hydrogen atom donor in the titanocene-mediated epoxide opening.

Water is usually not activated in free radical reactions due to its strong O–H bonds (119 kcal·mol^{-1}).[51] However, DFT calculations later showed that coordination of water to titanocene(III) significantly reduces the BDE by about 65 kcal·mol^{-1}, enabling the hydrogen atom transfer (Scheme 26), and the shown cationic titanocene species was determined by EPR and CV spectroscopy to be the active catalyst responsible for the HAT.[112]

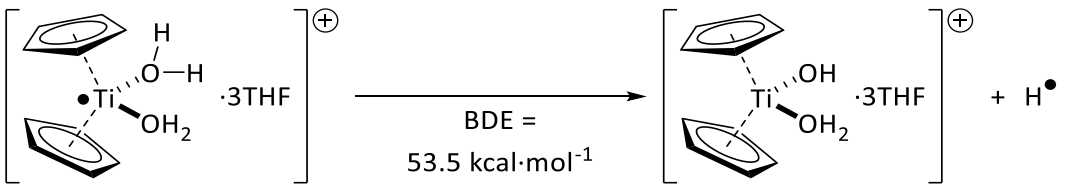

Scheme 26: Catalytically active titanocene species of water activation in the hydrogen atom transfer and the DFT-calculated BDE.

In 2008, *Gansäuer* introduced H_2 as hydrogen atom source in the titanocene-catalyzed epoxide opening in a bimetallic catalytic system based on titanium and rhodium (Scheme 27).[113] The rhodium-containing *Wilkinson* catalyst, which is well-known for its application in alkene and alkyne hydrogenations, was chosen in combination with the titanocene catalyst.

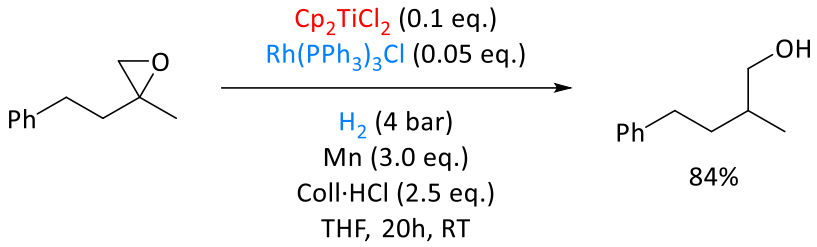

Scheme 27: H_2 as terminal hydrogen atom source in the titanocene-catalyzed epoxide reduction with the *Wilkinson* catalyst.

The proposed catalytic cycle is shown in Scheme 28.[113] The $[Rh]H_2$ complex, formed by oxidative addition of the *Wilkinson* complex to H_2, successively transfers two equivalents of hydrogen atoms to the β-titanoxy radical. For this catalytic system to operate two critical aspects are essential.[113,114] First, the two catalytic systems must be compatible. The hydrogenation catalyst must be stable under the acidic and *Lewis* acidic conditions of the titanocene-catalyzed system. Additionally, the hydrogen atom abstraction by the β-titanoxy radical from $[Rh]H_2$ must be faster than the reaction of the β-titanoxy radical with another molecule of Cp_2TiCl. Both requirements are met for the *Wilkinson* complex.

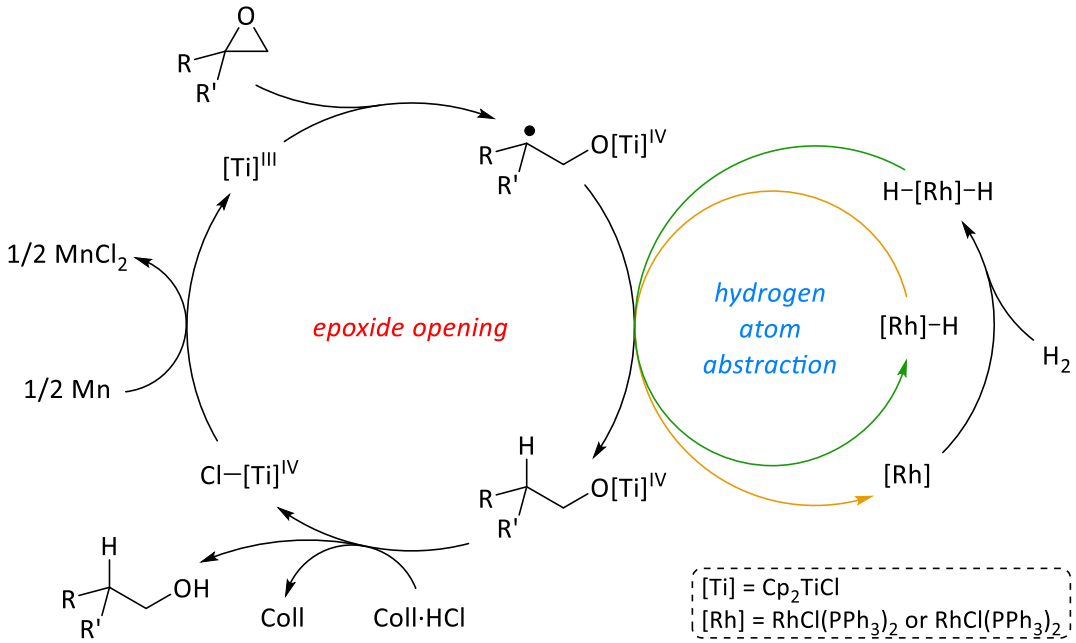

Scheme 28: Mechanism of the titanocene-catalyzed epoxide opening coupled with rhodium-catalyzed HAT.

The reduction of epoxides to the *anti-Markovnikov* alcohols proceeds in similar yields, compared to the previously used 1,4-CHD. However, the presence of the *Wilkinson* hydrogenation catalyst does not

allow cyclization reactions as alkynes and terminal alkenes are not tolerated. The given example marks the beginning of cooperative catalysis in titanocene-catalyzed epoxide openings. Moreover, it indicates the potential of transition metal hydrides to serve as hydrogen atom transfer reagents. Therefore, the following chapter is dedicated to this remarkable class of compounds.

1.6 Transition Metal Hydrides as Hydrogen Atom Donors

The strong H–H bond in molecular hydrogen (BDE = 104 kcal·mol^{-1})[51] prohibits direct reaction of H_2 with unsaturated compounds and therefore requires additional activation. Transition metals are widely used to mediate and catalyze heterogeneous and homogeneous hydrogenations.[115] While heterogeneous catalysts are typically solid and are in a distinct phase, homogeneous catalyst are in the same phase (usually solution) as the reactants. Many well-known homogenous hydrogenation catalysts contain noble metals such as rhodium, iridium, and ruthenium. Among others, the *Wilkinson* complex ($RhCl(PPh_3)_3$), the *Vaska* complex ($IrCl(CO)(PPh_3)_2$), the *Crabtree* complex ($[Ir(COD)(Py)(PCy_3)]PF_6$), or $RuCl_2(PPh_3)_3$ have gained significant importance in synthetic applications.[116,117] Their ability to react with molecular hydrogen forming metal hydrides is essential to enable homogeneous hydrogenations. More important, the combination with asymmetric ligands has led to synthetically important asymmetric hydrogenations.[118–121] To mention just one example, an industrially important process is the asymmetric synthesis of L-DOPA at *Monsanto*, used to treat Parkinson's disease, which was developed by *Knowles* (Scheme 29).[122] Both *Knowles* and *Noyori* were later awarded with the 2001 Nobel Prize for their work in this area.[123]

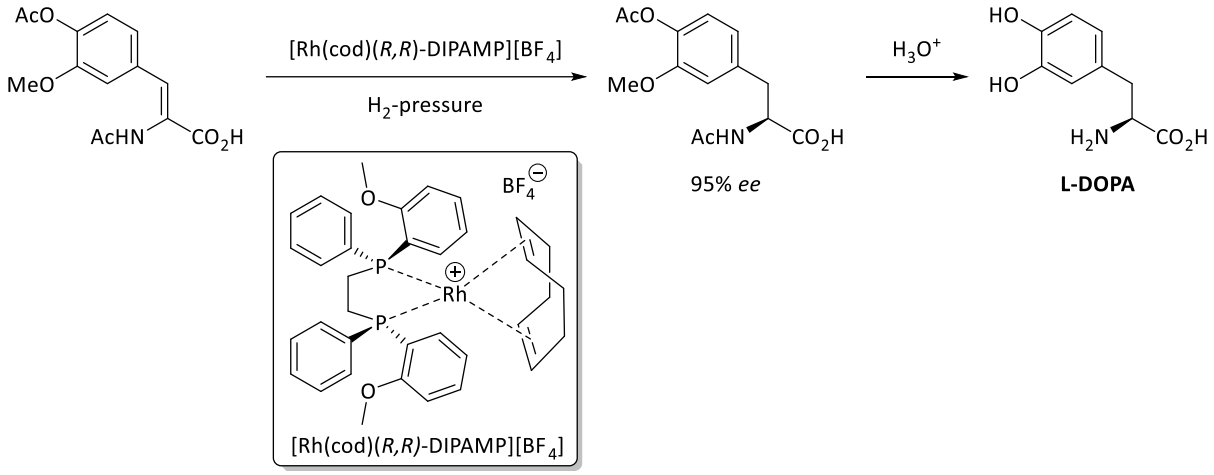

Scheme 29: Asymmetric hydrogenation in the synthesis of L-DOPA by *Knowles*.

Although the widespread application of these catalysts using elemental hydrogen as the terminal reductant, is considered atom-economic, the high price and the ecologic aspects associated with the mining and refining process of these scarce metals draw the attention to the more prevalent first-row transition metals. However, the 3d metals exhibit chemical properties, that are different from their 4d and 5d congeners.

The weak M–H bonds in first-row and early transition metal hydrides, typically between 60 and 65 kcal·mol^{-1},[124] make them interesting candidates as hydrogen atom transfer (HAT) reagents. However, before discussing radical hydrogenation reactions catalyzed by transition metals, the processes mediated by organometallic hydrides should be mentioned first to understand the elementary steps. The reduction of double bonds in acrylates, styrenes, 1,3-dienes, and allenes mediated by transition metal mono hydrides have been demonstrated.[125–133] In 1977 *Sweany* and *Halpern* reported the reduction of α-methyl styrene with $HMn(CO)_5$ that proceeds in two consecutive HAT steps (Scheme 30).[134] In a first HAT step a hydrogen atom is transferred reversibly from the M–H to the C–C double bond, forming a caged radical pair. After cage escape, a second equivalent of the metal hydride reagent reduces the carbon-centered radical in a second fast HAT to form the saturated hydrocarbon. The two resulting metal centered radicals form a dimer species.

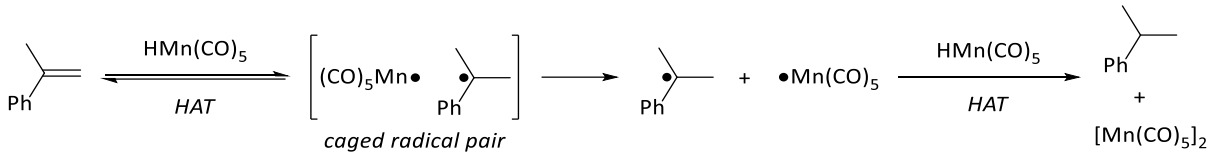

Scheme 30: Radical olefin hydrogenation mediated by transition metal hydrides via two sequential hydrogen atom transfers.

As shown, transition metals hydrides form metal centered radicals during HAT and, therefore, they should be able to also act in radical chain reactions. The *Oshima* group reported a radical chain cyclization mediated by the *Schwartz* reagent (Cp_2ZrHCl) as replacement for $^nBu_3SnH$ (Scheme 31).[135] After initial generation via hydrogen atom abstraction by an ethyl radical, Cp_2ZrCl abstracts a bromine atom from the substrate under formation of the carbon-centered radical and a new stable Zr–Br bond. After the cyclization Cp_2ZrHCl undergoes HAT to form the desired product, also generating the next equivalent of Cp_2ZrCl.

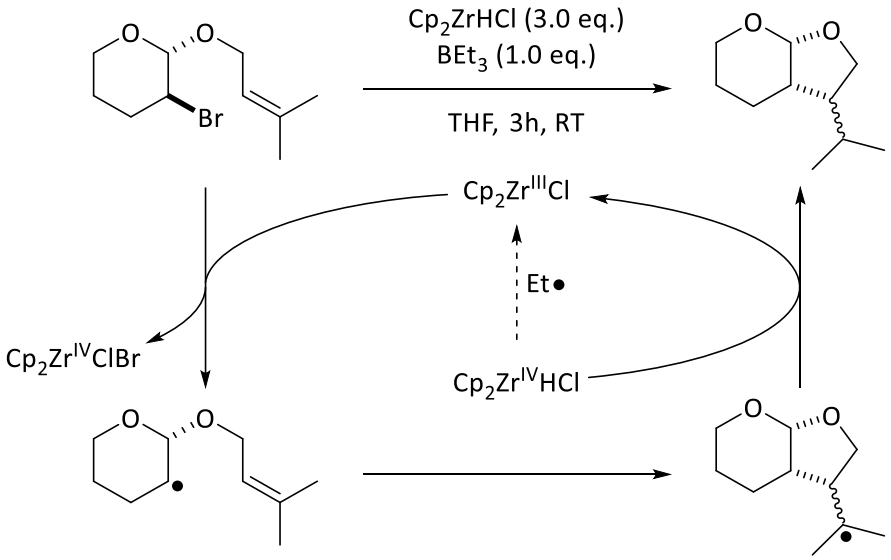

Scheme 31: Radical cyclization mediated by the *Schwartz* reagent.

By using Red-Al as terminal reductant, the process could be conducted with catalytic amounts of the *Schwartz* reagent. The aluminum hydride reagent can reduce Cp_2ZrCl_2 and $Cp_2ZrClBr$ to Cp_2ZrHCl *in situ* and close the catalytic cycle (Scheme 32). However, the use of the strong reducing agent decreases the functional group tolerance and moreover results in significant amounts of waste.

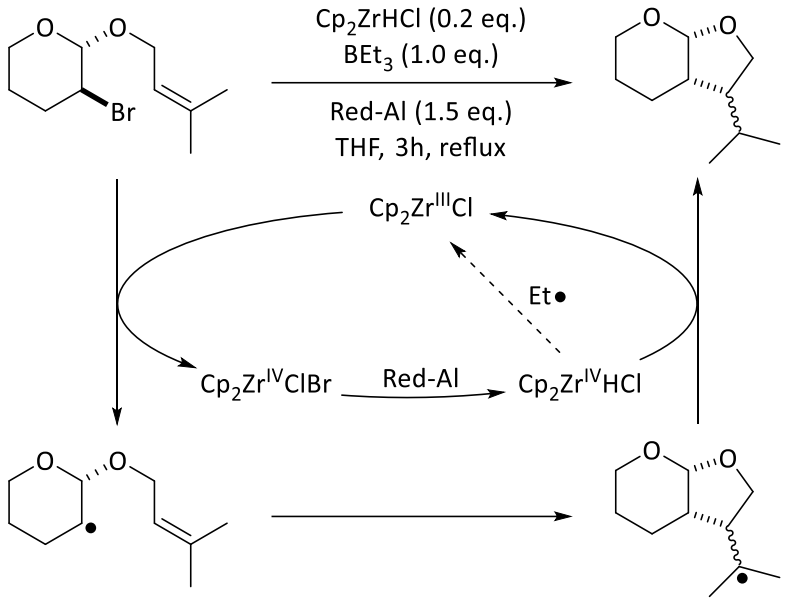

Scheme 32: Radical cyclization catalyzed by *Schwartz* reagent with Red-Al.

To achieve more sustainable and atom economic catalytic hydrogenations using H_2 as terminal reductant, the metal-centered radical must be able to activate H_2 to be regenerated to the HAT reagent. The *Norton* group has successfully applied $CpCr(CO)_3H$ as hydrogenation catalyst in a radical cyclization under H_2 pressure (Scheme 33).[136,137]

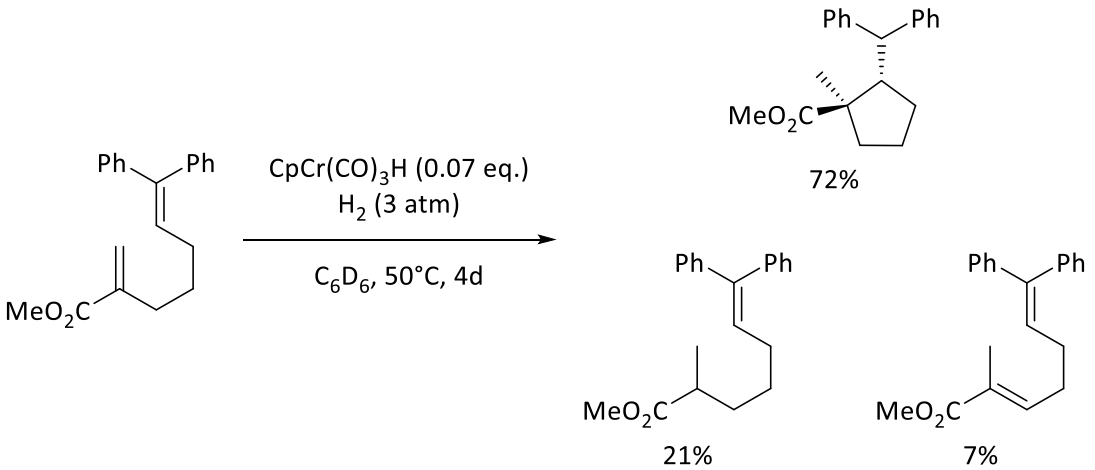

Scheme 33: Radical cyclization catalyzed by $CpCr(CO)_3H$.

The major product is the 5-*exo* cyclization/hydrogenation product. However, the hydrogenation and the isomerization product are obtained as well. The overall mechanistic picture of formation of the major and the side products is shown in Scheme 34.[137]

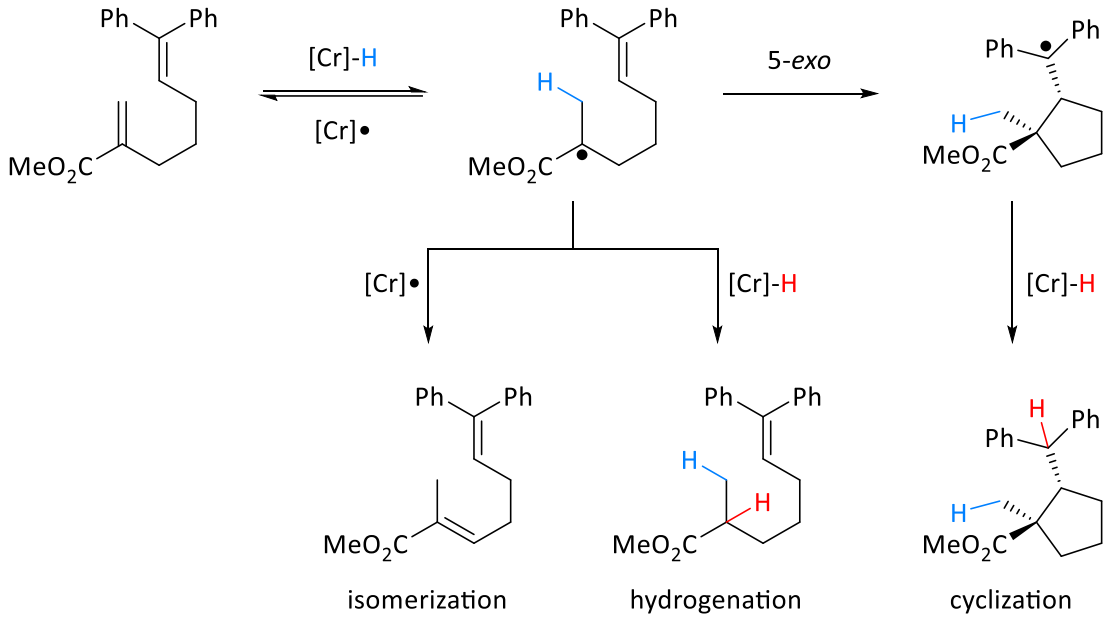

Scheme 34: Formation of the cyclization major product and the isomerization and hydrogenation by-products during the catalytic radical cyclization. [Cr] = $CpCr(CO)_3$.

The product mixture obtained with the cyclization product being the major product, indicates that the rate constants of the cyclization is higher than of the second HAT. Additionally, the cyclization must be faster than hydrogen atom abstraction. Thus, the cyclization outruns the hydrogenation, isomerization, or back reaction to the starting material. To ensure a sufficiently high rate constant of cyclization the radical acceptor olefin should be activated. Indeed, introduction of two ester groups significantly enhances the yield (Scheme 35). However, the acceptor olefin should be trisubstituted to ensure the chemoselectivity of the first radical generating HAT.[137] The 6-*endo* cyclizations are generally not observed as the 5-*exo* is preferred for radical cyclization according the *Beckwith* rules.[138,139]

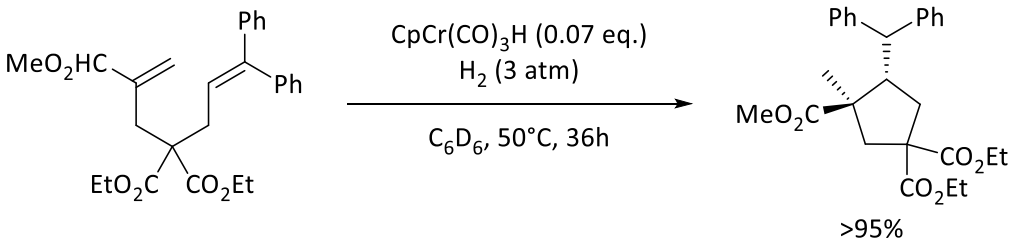

Scheme 35: Activated radical acceptor olefins promote the desired cyclization pathway.

The crucial point for the reaction to proceed catalytically is the ability of $CpCr(CO)_3$• to activate H_2 to be regenerated to the hydrogen atom transfer catalyst $CpCr(CO)_3H$. The analogous cyclization reaction using $HV(CO)_4$dppe could only be conducted stoichiometrically, because •$V(CO)_4$dppe is unable to activate hydrogen. The ability to activate molecular hydrogen under pressure to form monohydrides from the corresponding metal radical has been reported for several transition metal complexes

including $CpCr(CO)_3\bullet$,[140] $Cp^*Cr(CO)_3\bullet$,[141] $[Co(CN)_5]^{3-}$,[142,143] $Co(dmgBF_2)_2L_2$ (L = H_2O, THF, MeCN),[144,145] and (TMP)Rh•.[146]

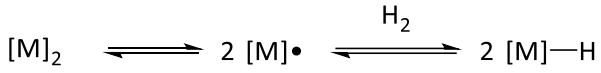

Scheme 36: Equilibrium of metal radicals with hydrogen.

The position of the equilibrium between the metal radical with H_2 and the metal hydride (Scheme 36) correlates with the BDE of the M–H bond. Consequently, the ability of the metal hydride to act as hydrogen atom donor is related to the BDE as well. Complexes with weak M–H bonds are in principle potent H-atom donors. However, a too weak M–H bond slows down or inhibits H_2 activation. *Hoff* estimated a BDE of 56 kcal·mol^{-1} at room temperature as the limit of thermoneutrality under consideration of entropic effects.[147] Complexes weaker than this are thermodynamically unstable towards the loss of H_2. For an overview, the BDE values of various metal hydrides are given in Table 6.

Table 6: Bond dissociation energies of various transition metal hydrides.[124,136,148–150]

Metal hydride	**BDE (M–H) [kcal·mol^{-1}]**
$Co(dmgBF_2)_2(H_2O)H$	55
$CpFe(CO)_2H$	57
$V(CO)_4(dppe)H$	58
$CpCr(CO)_3H$	62
$Cp^*Cr(CO)_3H$	62
$Co(CO)_4H$	66
$Mn(CO)_5H$	68
$CpMo(CO)_3H$	69
$CpW(CO)_3H$	72
$^nBu_3SnH$	78

The V–H bond in $HV(CO)_4L$ complexes are close to the estimated limit. Therefore, they should be prone to loss of hydrogen. However, the hydride complexes are stable at room temperature due to a kinetic barrier leading to a small rate constant for hydrogen release and an even smaller rate constant for the back reaction. Therefore, the complexes are potential potent HAT reagents, but not suitable for catalysis, as activation of H_2 is not possible.[148] The Co–H bond in the $HCo(dmgBF_2)_2(H_2O)$ complex is even weaker, making the complex unstable towards hydrogen loss. The complex does not exhibit the same kinetic barrier as the vanadium hydrides, and with a hydrogen pressure of 5 atm, a useful concentration of the cobalt hydride could be generated, making them interesting candidates as potent hydrogen atom donors.[145,149]

As shown in Scheme 36, many metal radicals are in equilibrium with their metal-metal bound dimer species. The position of this 'pre-equilibrium' also influences the ability of hydrogen activation, as it is the monomer that reacts with hydrogen. The metalloradicals •$Mn(CO)_5$ and •$Co(CO)_4$ form stable dimers, shifting the equilibrium to the left side. Thus, the reactions to the respective manganese or cobalt hydride takes place only under harsh conditions (200-235°C, 200 atm H_2).[151,152] A significant influence on the dimerization equilibrium is the steric hindrance of the metalloradical. For example, dimerization is less favored for $Cp^*Cr(CO)_3$• ($Cp^* = C_5Me_5$) compared to $CpCr(CO)_3$•, which shows a larger rate of dimerization.[153,154] Therefore, sterically demanding complexes generally favor hydrogen activation by disfavor dimerization, shifting the equilibrium more to the monomer.

Table 7: Comparison of BDE values of transition metal hydrides to the rate constants k_H of the HAT to the tris(*p-tert*-butylphenyl) methyl radical at 25°C in toluene.[155]

Metal hydride	BDE (M–H) [kcal·mol^{-1}]	k_H [M^{-1}·s^{-1}]
$CpCr(CO)_3H$	62	335
$Cp^*Mo(CO)_3H$	69	14
$CpMo(CO)_3H$	70	514
$CpW(CO)_3H$	73	91

However, the steric demand not only influences the equilibrium between monomer and dimer but also has a critical effect on the hydrogen atom donor abilities. Some rates of HAT by metal hydrides to the tris(*p-tert*-butylphenyl) methyl radical compared to their BDE are shown in Table 7. Comparison of the rate constants k_H for HAT with BDE values indicates that the BDE has a major influence on this rate, but steric effects also play a significant role. In the case of $CpMo(CO)_3H$ and $CpW(CO)_3H$ with only minimal steric difference, a difference in BDE of 3 kcal·mol^{-1} results in a reduction of the rate constant from 514 to 91 M^{-1}·s^{-1}. The M–H bond strength in $Cp^*Mo(CO)_3H$ and $CpMo(CO)_3H$ differs just by 1 kcal·mol^{-1}. Here the sterically less demanding $CpMo(CO)_3H$ transfers hydrogen 37 times faster. The chromium hydride has a significantly weaker bond (62 kcal·mol^{-1}) than the molybdenum (70 kcal·mol^{-1}) or the tungsten hydride (72 kcal·mol^{-1}). However, k_H of the $CpCr(CO)_3H$ is in between these two. This was assigned to a 0.2 Å shorter M–H bond in the chromium complex (1.30 Å vs. 1.50 Å and 1.51 Å). The shorter bond increases steric congestion and slows down the HAT despite the low BDE.[155]

Taking all the above considerations into account, a complex is needed that balances rate of HAT with sufficient hydrogen activation for catalyst regeneration, while maintaining stability towards loss of hydrogen and stability of the corresponding metalloradical. The $CpCr(CO)_3H$ complex appears to achieve this balance effectively. Therefore, the reactivity of this complex will be discussed further.

As shown, $CpCr(CO)_3$• is able to act as a hydrogenation catalyst and to activate hydrogen, but the mechanism of the activation is not entirely understood. The mode of hydrogen activation by

$Cp^*Cr(CO)_3\bullet$ has been studied by *Hoff*.[141] $[Cp^*Cr(CO)_3]_2$ dissociates to a large extend and is almost exclusively present as monomer in solution. However, in the case of $CpCr(CO)_3\bullet$ an equilibrium with its dimer $[CpCr(CO)_3]_2$ in solution complicates the mechanistic investigation.[153,154,156] Kinetic studies of the hydrogen activation from the $CpCr(CO)_3\bullet/[CpCr(CO)_3]_2$ equilibrium have been performed by the *Norton* group. A second order dependence in chromium was found, indicating a bimolecular mechanism. Subsequently, two plausible mechanisms were proposed in accordance with DFT calculations, via a homolytic and a heterolytic pathway of H_2 cleavage (Scheme 37).[140]

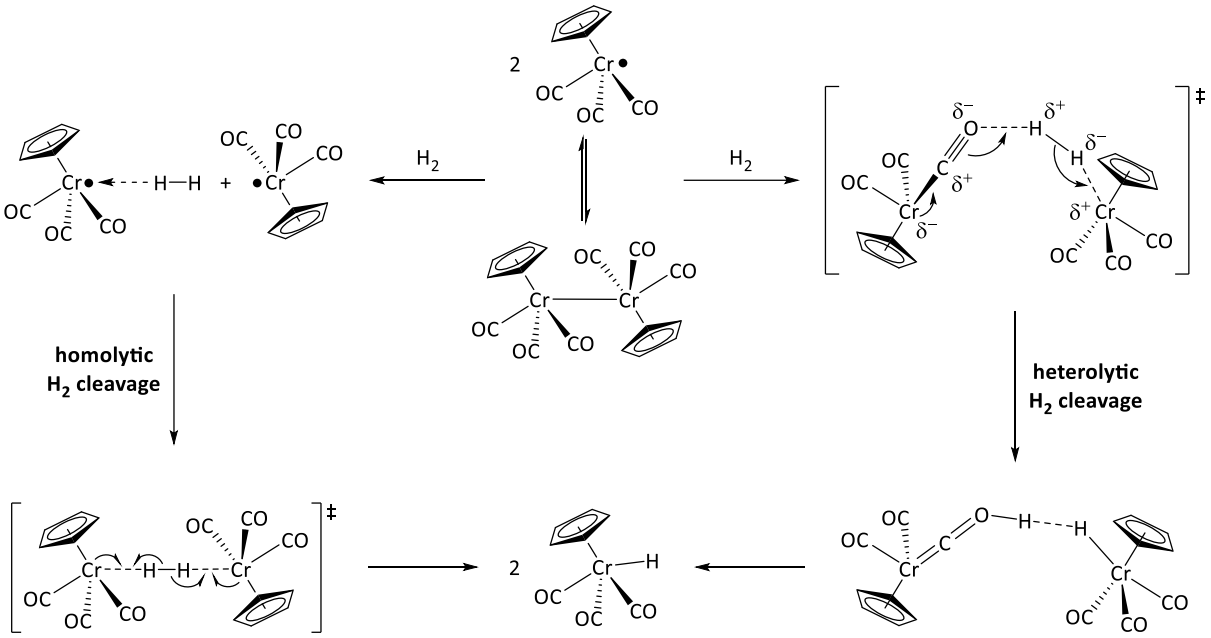

Scheme 37: Two possible mechanisms of hydrogen activation via homolytic and heterolytic H_2 bond cleavage.

For the homolytic pathway, the first step is an *end-on* coordination of H_2 to the first chromium radical. The typically expected *side-on* coordination was excluded for this step by DFT calculations. Subsequently, the second metalloradical abstracts a hydrogen atom in a colinear transition state, releasing two chromium hydride molecules. The heterolytic pathway starts with a charge transfer from the chromium to the carbonyl oxygen. This oxygen then coordinates to a hydrogen molecule that itself is *end-on* coordinated to the second chromium center, leading to heterolytic bond cleavage. The resulting proton on the carbonyl oxygen serves as hydrogen bond donor to the hydride on the other chromium. This mechanism resembles an activation by 'frustrated' *Lewis* acid and base pairs,[157,158] where the hydrogen is held in a reactive cavity between the oxygen and the chromium atom. Although the calculated electronic barrier is almost 12 $kcal \cdot mol^{-1}$ higher for the heterolytic pathway, both mechanisms are plausible, and it is not yet possible to definitively say which mechanism is favored.

The M–H bonds in transition metal hydrides can not only be cleaved in the above shown homolytic way during HAT. There are three possible ways for cleavage of this bond in total (Scheme 38).[159]

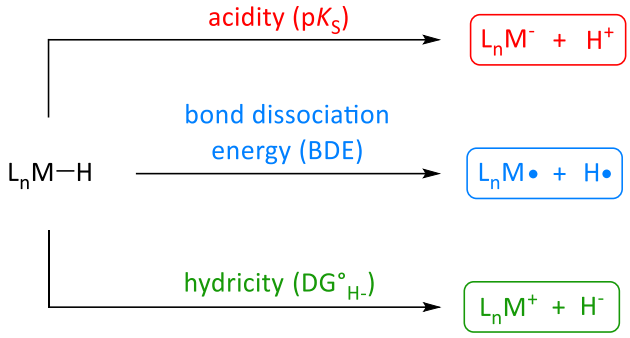

Scheme 38: Possible modes of M–H bond cleavage in transition metal hydrides.

A heterolytic bond cleavage can result either in release of a proton or a hydride. These elementary steps are characterized by the physical properties of acidity and hydricity. While the acidity is quantified by the pK_s value, the hydricity is measured as the free energy required to remove a hydride ($\Delta G°_{H^-}$). The homolysis of the M–H bond releasing a hydrogen atom is, as already mentioned, characterized by the bond dissociation energy (BDE). This versatile reactivity of transition metal hydrides makes them not only strong HAT reagents and catalyst but also promising multifunctional compounds for cooperative catalysis, as the following chapter will show.

1.7 Cooperative Catalysis with Titanium and Chromium

The $CpCr(CO)_3H$ complex achieves a balance in terms of metalloradical stability, M–H bond strength and steric demand and has been shown to be an ideal candidate for catalytic hydrogen atom transfer in radical reactions. First successful attempts to use $CpCr(CO)_3H$ as HAT catalyst to replace the stoichiometric hydrogen atom donors in the titanocene-catalyzed epoxide opening were published by *Gansäuer* in 2009 (Scheme 39).[114]

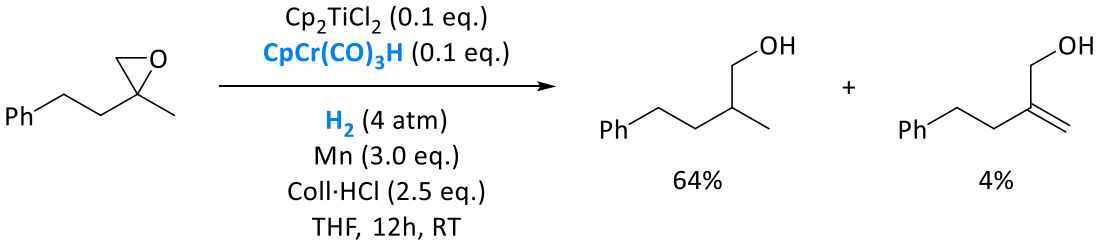

Scheme 39: $CpCr(CO)_3H$ as HAT catalyst with H_2 as terminal reductant in the titanocene-catalyzed epoxide opening.

Under a hydrogen atmosphere of 4 atm, $CpCr(CO)_3H$ is capable of activating H_2 and catalyzing the desired HAT. The *anti-Markovnikov* alcohol is obtained in acceptable yield along with a small amount of the allylic alcohol by-product. The mechanism is analogous to the reaction using the *Wilkinson*

catalyst described in chapter 1.5 (Scheme 28). However, the results were not satisfactory and $CpCr(CO)_3H$ was considered at that time to be inferior to the rhodium-containing *Wilkinson* catalyst.

The results were later improved by *Shizgal* and *Panfilova*.[160] The optimized conditions resulted in a more efficient epoxide reduction with formation of the desired alcohols in good yields, generally with no detectable amounts of by-products. In this way, a range of epoxides was hydrogenated to the corresponding *anti-Markovnikov* alcohols (Table 8).

Table 8: Conditions and scope of the titanocene-catalyzed epoxide opening with $CpCr(CO)_3H$ as HAT catalyst and H_2 as terminal reductant improved by *Panfilova*.

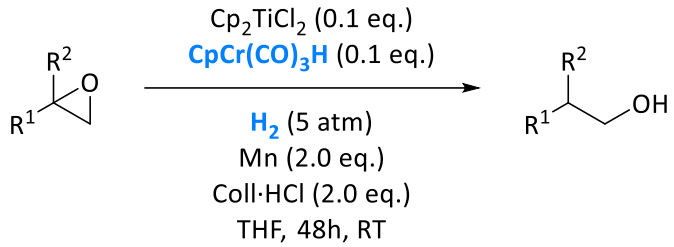

product	yield [%]	product	yield [%]
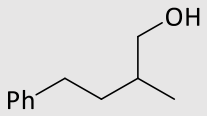	89	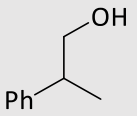	90
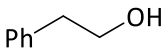	78	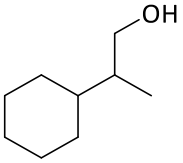	70
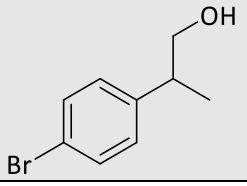	78	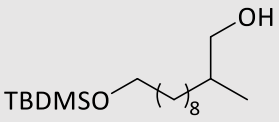	98

Gansäuer and *Norton* further investigated the system by making use of the multifunctionality of $CpCr(CO)_3H$. Besides its function as hydrogen atom donor, it should be possible to catalyze additional steps and replace the other stoichiometric reagents used so far (Coll·HCl, Mn). In 2019, a novel system was presented in which the chromium complex fulfills a triple role. Namely, activation of hydrogen and transfer of a hydrogen atom, protonation of the Ti–O bond of the titanocene-bound alkoxide, and reduction of the titanocene(IV) catalyst.[161]

As shown in Scheme 38, transition metal hydrides are in general not only able to act as hydrogen atom donor but also as *Brønsted* acid. $CpCr(CO)_3H$ has a acidity (pK_a = 13.3 in MeCN),[162] that is close to the value of the collidinium ion (pK_a = 15.0 in MeCN).[163] Thus, the chromium hydride should be capable to protonate the Ti–O bond of the titanocene-bound alkoxide intermediate instead of Coll·HCl.

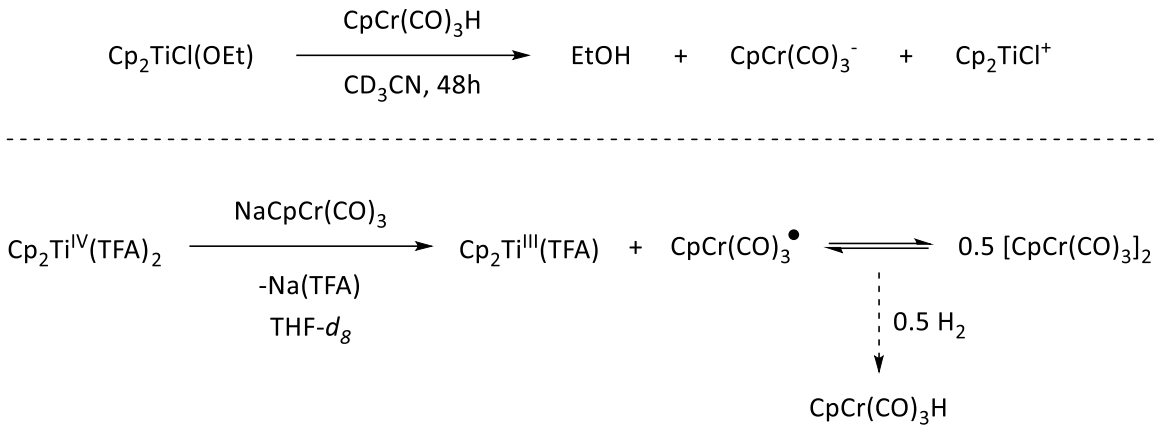

Scheme 40: Protonation of a titanocene alkoxide by $CpCr(CO)_3H$ (top) and reduction of $Cp_2Ti^{IV}(TFA)_2$ by $CpCr(CO)_3^-$ with possible subsequent regeneration of $CpCr(CO)_3H$ (bottom).

This was confirmed experimentally by addition of $CpCr(CO)_3H$ to a $Cp_2TiCl(OEt)$ solution in CD_3CN (Scheme 40 top).[161] The formation of ethanol was detected by ^{1}H-NMR. The resulting corresponding base $CpCr(CO)_3^-$ does not need to be regenerated to the hydride directly, but is instead the key to the third catalytic step. The redox potential of $CpCr(CO)_3^-$ is known to be (E_{ox} = -0.67 V, Fc/Fc^+, MeCN),[164] close to the one of Cp_2TiCl_2.[165,166] Thus, one-electron reduction of titanocenes seems feasible. Indeed, adding $NaCpCr(CO)_3$ to $Cp_2Ti^{IV}(TFA)_2$ in THF-d_8 generated $Cp_2Ti^{III}(TFA)$ along with $CpCr(CO)_3$• in a mixture with its $[CpCr(CO)_3]_2$ dimer (Scheme 40 bottom).[161] Finally, $CpCr(CO)_3$• and pressurized H_2 regenerate $CpCr(CO)_3H$ and complete the puzzle. In light of these findings, a cooperative catalytic system was designed that combines $Cp_2Ti(OMs)_2$ and $NaCpCr(CO)_3$ as catalysts for the activation of H_2 and selective reduction of epoxides to the *anti-Markovnikov* alcohols, resulting in a fully atom-economic reaction (Scheme 41). $CpCr(CO)_3H$ is added to accelerate the reaction although in principle it is not required to initiate the catalytic cycle as it is formed during the course of the reaction. Instead of Cp_2TiCl_2, $Cp_2Ti(OMs)_2$ is required for the catalytic cycle to operate because of its matching redox potential.

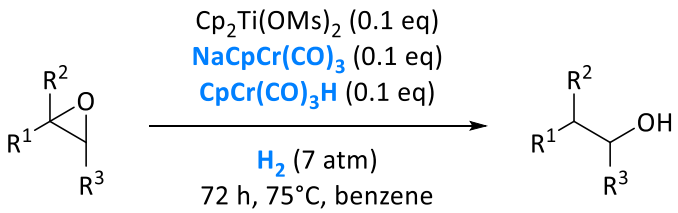

Scheme 41: Cooperative catalysis between chromium and titanium for the activation of H_2 in the selective reduction of epoxides yielding *anti-Markovnikov* alcohols.

Based on the mechanistic insights, a catalytic cycle was proposed, that incorporates the triple role of the chromium catalyst (Scheme 42).[161]

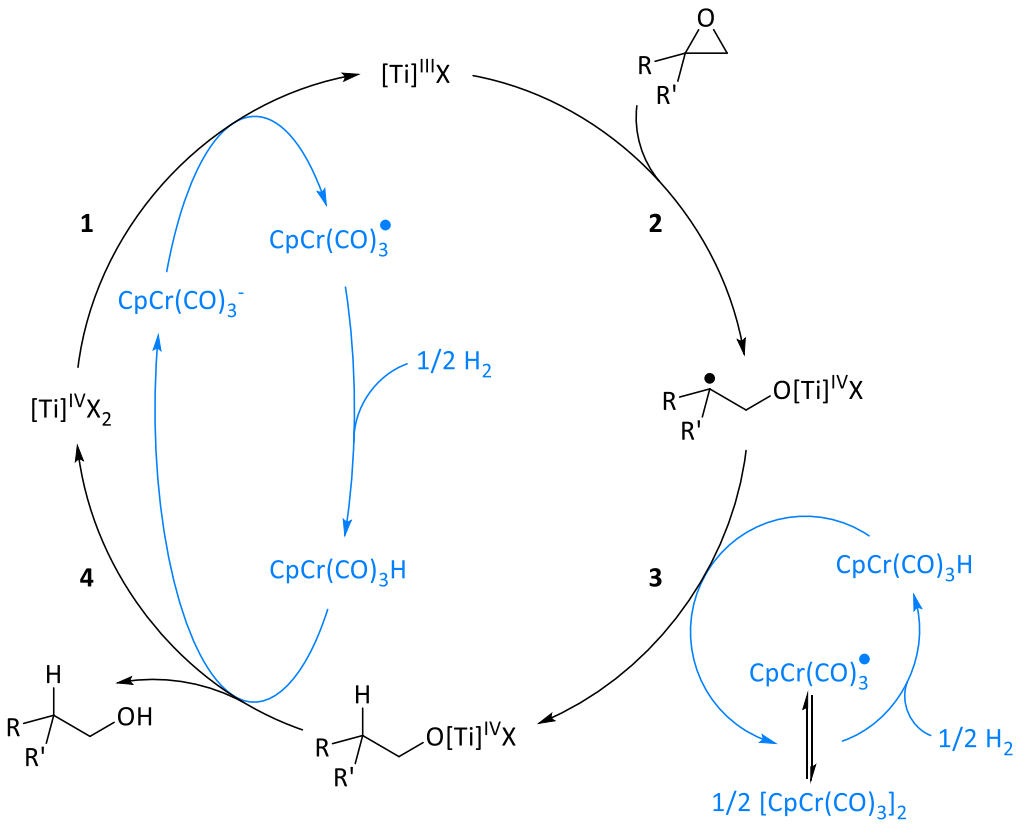

Scheme 42: Proposed catalytic cycle of the titanoce-catalyzed epoxide opening with $CpCr(CO)_3H$/$NaCpCr(CO)_3$. H_2 is transferred sequentially as hydrogen atom, proton, and electron. [Ti] = Cp_2Ti, X = OMs.

In the first step, the precatalyst $Cp_2Ti^{IV}(OMs)_2$ is reduced by the $CpCr(CO)_3^-$ to give the active $Cp_2Ti^{III}(OMs)$ species under formation of $CpCr(CO)_3$• (step 1). The active catalyst opens the epoxide in a single electron oxidative addition giving the β-titanoxy radical (step 2). The β-titanoxy radical is trapped by the HAT catalyst $CpCr(CO)_3H$ to give the titanocene alkoxide and a $CpCr(CO)_3$• radical (step 3). In the last step the alkoxide Ti–O bond is protonated by $CpCr(CO)_3H$ under liberation of the *anti-Markovnikov* alcohol and regeneration of $Cp_2Ti^{IV}(OMs)_2$ and the corresponding base $CpCr(CO)_3^-$ (step 4). The $CpCr(CO)_3$• radicals, which are formed during step 1 and step 3, are in equilibrium with their dimer and activate hydrogen under 7 atm pressure to regenerate $CpCr(CO)_3H$. Overall, hydrogen is formally transferred as electron, hydrogen atom, and proton by cooperative catalysis.

In contrast to the titanocene-catalyzed epoxide opening reactions discussed earlier, in this variant all stoichiometric reagents such as hydrogen atom donors, reducing agents, and acids are replaced by combination of chromium and titanium catalysis. The sole stoichiometric reagent needed is H_2, resulting in full atom economy. In this way, an interesting scope of *anti-Markovnikov* alcohols was

synthesized from mono-substituted, 1,1- and 1,2-disubstituted epoxides in acceptable to good yields (Table 9).[161]

Table 9: Scope of the $CpCr(CO)_3H/NaCpCr(CO)_3$ and H_2 cooperative system. Yield of the inseparable allylic alcohol by-product is shown in parentheses.

product	yield [%]	product	yield [%]
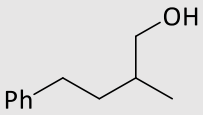	70	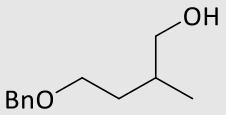	81
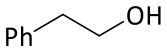	51	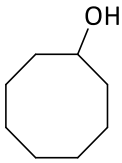	52 (33)
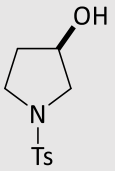	49	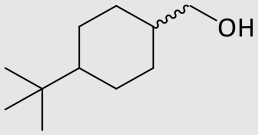 *trans/cis* = 54/46	48 (10)

However, the formation of the inseparable allylic alcohol by-product, resulting from a hydrogen atom abstraction, is observed for several substrates. In addition, epoxide openings with subsequent cyclizations or regiodivergent epoxide openings remain inaccessible here.

The insights about the versatility of transition metal hydrides and especially $CpCr(CO)_3H$ to serve as hydrogen atom transfer catalyst and the unique single-electron reactivities of titanocenes in epoxide opening reactions are the key finding that this work is based upon.

2 Discussion

2.1 Objective and Motivation

The cooperative catalysis between titanium complexes and transition metal hydride complexes, which combines single-electron step catalysis and efficient hydrogen atom transfer (HAT), is currently subject of research in the *Gansäuer* group. The first objective of this work is to investigate alternatives to established yet harmful hydrogen atom donor reagents by activation and reprogramming of established reagents in novel ways through cooperative catalysis. Priority will be given to metal borohydrides that are readily accessible, easy to handle, and less hazardous, thereby enhancing environmental compatibility. This work seeks to develop synthetic methodologies that circumvent the need for reactions using pressurized and highly flammable gas, facilitating safer and more manageable experimental procedures in research laboratories. A central objective of this work is to expand the scope of existing titanium and chromium cooperative catalysis to enable C–C bond forming reactions and formation of enantiopure 1,3- and 1,4-building units, addressing the current limitations in the applicability of cooperative catalysis and unlock its full potential. These desired molecular structures are envisioned to be interesting intermediates in the synthesis of complex natural molecules and pharmaceutically active compounds. Lastly, this work aims to evaluate substitutes for the efficient yet challenging to handle chromium hydride catalyst, ultimately advancing the practicality and accessibility of cooperative catalytic processes in organic synthesis.

2.2 Borohydrides in Radical Chemistry

The utilization of borohydrides in radical chemistry has garnered considerable attention in recent years due to their unique reactivity profiles and versatile synthetic applications.[167] Borohydrides are well-known as mild reducing agents in traditional organic chemistry, often employed for the reduction of carbonyl compounds to their respective alcohols.[168–170] However, their potential in radical chemistry ranges beyond their classic role as reducing agents. A less known feature of borohydrides is their capability to serve as hydrogen atom donors in radical chemistry, thereby participating in radical chain reactions (Scheme 43).[167]

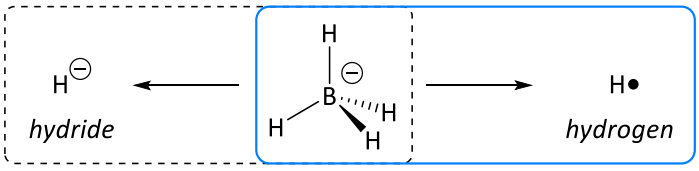

Scheme 43: Two functions of borohydride reagents.

An initiator radical like the *tert*-butoxy radical can efficiently abstract a hydrogen atom from a borohydride or cyanoborohydride to form a borane radical anion (Scheme 44).[171] The formed $BH_3^{-\bullet}$ can undergo rapid halogen atom abstraction from an alkyl halide (Cl, Br, I). The milder $BH_2CN^{-\bullet}$ was generated the same way and reacts with alkyl halides however can only abstract bromine and iodide. These radical initiation steps give access to radical chain reactions.

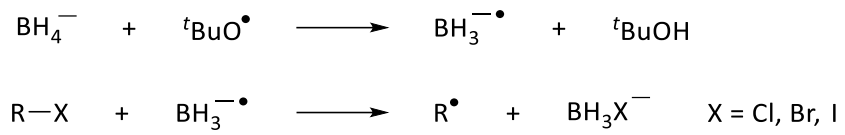

Scheme 44: Generation of the borane radical anion via hydrogen atom abstraction and subsequent halogen atom abstraction.

Kinetic experiments using free-radical clock methodology have been conducted to determine rate constants for the HAT by boranes to carbon centered radicals (Scheme 45). *Beckwith* investigated the kinetics of aryl radical reductions with borohydrides, determining the rate constant for this HAT (k_H = 2.1·10^8 M^{-1}·s^{-1}), which is competitive to the one of ^{n}Bu$_3$SnH (k_H = 7.9·10^8 M^{-1}·s^{-1}).[172] Additionally, the reaction of primary alkyl radicals with (Bu$_4$N)BH$_3$CN was studied by *Ryu*, showing a lower rate constant for the HAT compared to other hydride sources like tributyltin hydride (2.3·10^6 M^{-1}·s^{-1}) or tris(trimethylsilyl)silane (3.8·10^5 M^{-1}·s^{-1}).[173]

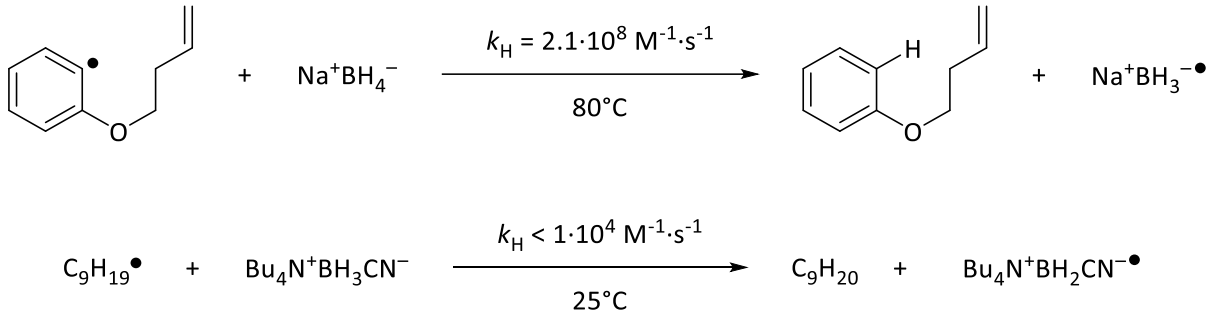

Scheme 45: Rate constants for HAT by the borohydride and cyanoborohydride anion to aryl and alkyl radicals, determined via radical clock experiments.

In an early example, *Barltrop* successfully used sodium borohydride in the photo-induced dehalogenation of halobenzenes (Scheme 46).[174] The proposed mechanism starts with photo-induced cleavage of the halobenzene and generation of the aryl radical. The subsequent hydrogen abstraction from BH_4^- gives benzene and a borane radical anion, which can abstract a halogen atom from another halobenzene to propagate the chain reaction.

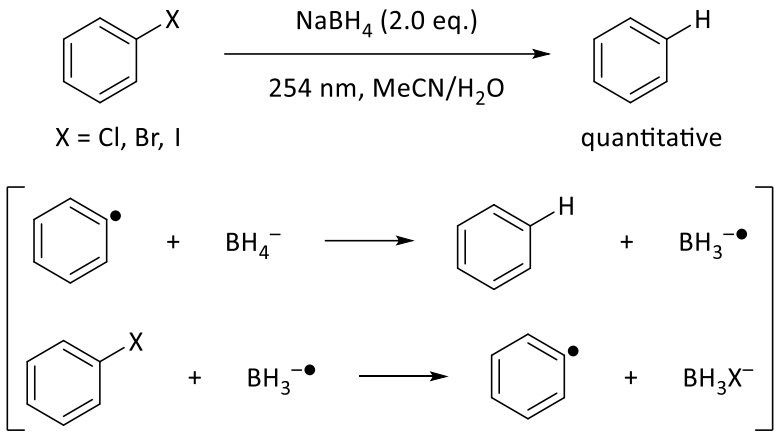

Scheme 46: Photo-induced reduction of halobenzenes using $NaBH_4$ as hydrogen atom source.

The reduction of 7,7-dibromonorcarane by sodium borohydride, reported by *Groves*, proceeds mechanistically similarly (Scheme 47).[175] The bromocyclopropyl radical, formed under heat and oxygen involving conditions, abstracts hydrogen from the borohydride giving the reduced product. The borane radical anion abstracts bromine from another dibromocyclopropane ring, maintaining the radical chain. In the reaction the singly reduces product is obtained as a diastereomeric mixture.

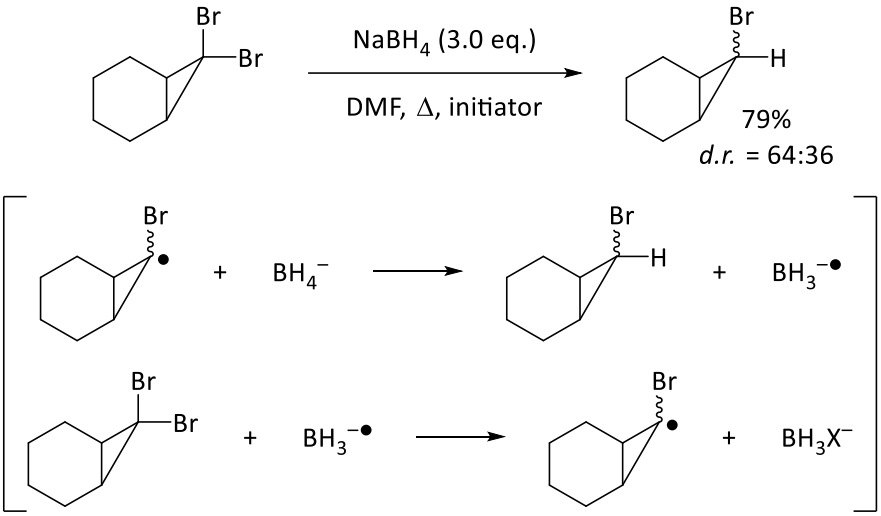

Scheme 47: Radical reduction of 7,7-dibromonorcarane using $NaBH_4$.

The capability of hydrogen atom transfer to organic radicals by borohydrides and cyanoborohydrides was shown. However, this process is typically too slow to be preparatively useful. The B–H bond dissociation energies in borohydrides, which can be generally expected to be higher than BDEs in other hydrogen atom donors,[176,177] make additional activation by a hydrogen atom transfer catalyst necessary. These findings about the multifunctionality of borohydrides to act as both hydride and hydrogen atom donors led to envision of a hydrogen atom donor system for the titanocene catalyzed epoxide opening using borohydrides activated by cooperative catalysis as more sustainable alternative to tin hydrides. Moreover, the mild reaction conditions associated with borohydride-mediated processes promise advantages in terms of functional group tolerance and substrate compatibility,

2.3 Mechanistic Considerations

The ability of borohydrides to function as hydrogen atom donors in organic chemistry, has inspired their potential application in combination with transition metal HAT catalyst. The cooperative catalysis between titanocenes and the chromium hydride $CpCr(CO)_3H$ **1** for the activation of borohydrides as terminal hydrogen source for the synthesis of *anti-Markovnikov* alcohols is currently subject of investigations in the *Gansäuer* group. For a targeted optimization, it is important to elucidate the underlying mechanism of the reaction. The proposed mechanism of the cooperative catalysis is shown in Scheme 48.

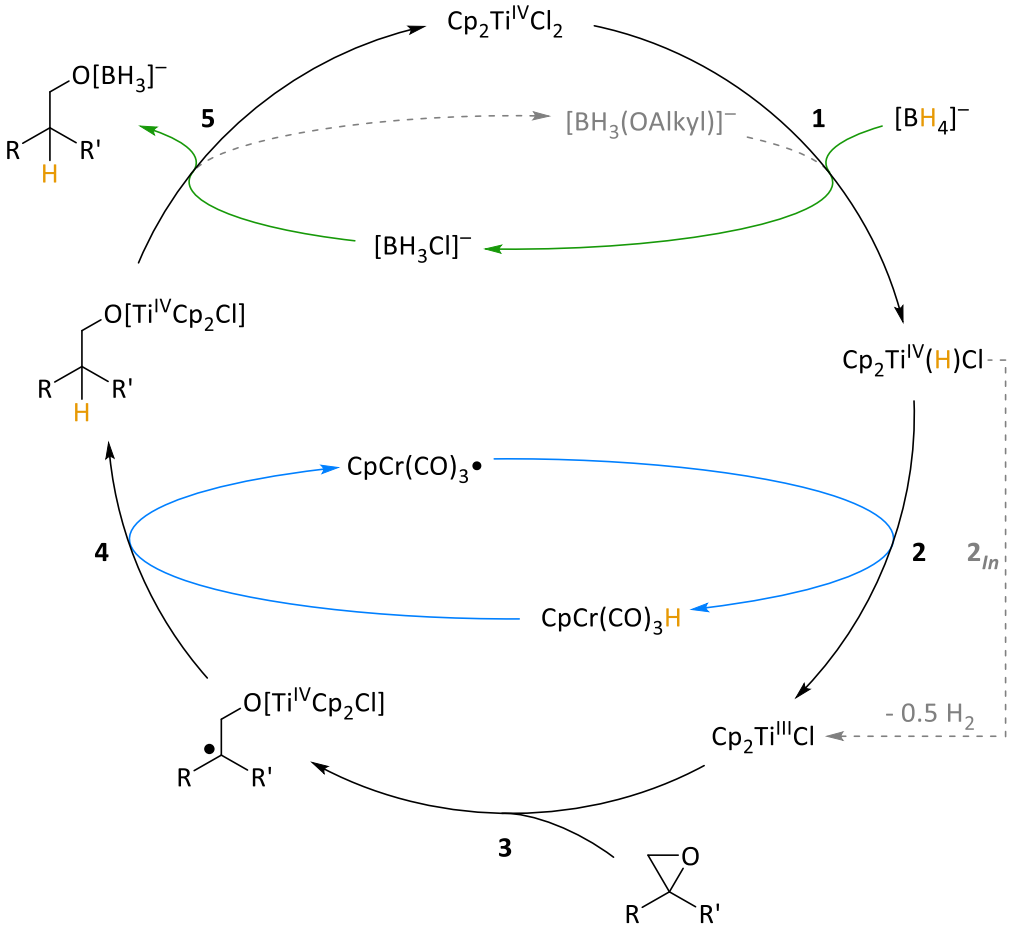

Scheme 48: Proposed cooperative catalytic 'globe' of the titanocene and chromium hydride catalyzed epoxide opening with borohydrides.

In this catalytic 'globe', BH_4^- fulfills a dual role for the generation of both active catalysts, the single-electron transfer catalyst $Cp_2Ti^{III}Cl$ and the hydrogen atom transfer catalyst $CpCr(CO)_3H$. The first step is a σ-bond metathesis reaction with a ligand exchange between BH_4^- and the $Cp_2Ti^{IV}Cl_2$ precatalyst, transferring the hydride ligand to the titanocene and forming BH_3Cl^- and the unstable and reactive $Cp_2Ti^{IV}(H)Cl$ (step 1). In the second step, $Cp_2Ti^{IV}(H)Cl$ undergoes HAT to $CpCr(CO)_3$•, generating both $Cp_2Ti^{III}Cl$ and $CpCr(CO)_3H$ in a single step and in equimolar amounts (step 2). The $Cp_2Ti^{III}Cl$ opens the

epoxide in a single-electron oxidative addition to form a β-titanoxy radical (step 3). A hydrogen atom is then transferred to the carbon-centered radical by the HAT catalyst $CpCr(CO)_3H$ to give the titanocene alkoxide and a $CpCr(CO)_3\bullet$ radical (step 4). The final step is another metathesis between the titanocene alkoxide and the previously formed BH_3Cl^-, which regenerates the $Cp_2Ti^{IV}Cl_2$ precatalyst and an alkoxy hydroborate (step 5). The alkoxy hydroborate can react in two ways. It can reenter the catalytic cycle to transfer another hydride up to the hypothetical maximum of four hydrides (comment in chapter 2.4). Alternatively, upon reaction termination, the B–O bond can be cleaved during the aqueous work-up to release the desired *anti-Markovnikov* alcohol product. Additionally, if not cleaved, the alkoxy hydroborate *in situ* masks the free alcohol, which may otherwise deactivate the active titanocene species.[74] Both, the titanocene cycle and the $CpCr(CO)_3H$ cycle are truly interwoven in this intramolecular cooperative catalytic cycle and achieve in such ways a novel use of the borohydride anion.

The key role of the $Cp_2Ti^{IV}(H)Cl$ species in the catalytic system for the initial and subsequent formation of the active catalyst needs to be discussed in detail. $Cp_2Ti(H)Cl$ is the titanium analog of the *Schwartz* reagent $Cp_2Zr(H)Cl$. However, while the *Schwartz* reagent is a stable compound that is used in organic synthesis[178,179] (see also chapter 1.6), $Cp_2Ti(H)Cl$ is a thermally unstable compound, that has not yet been isolated or observed *in situ*.[180] While the more stable analogue $Cp^*_2Ti(H)Cl$ can be isolated,[181] the sterically less encumbered and therefore labile complex undergoes a rapid decomposition under generation of $Cp_2Ti^{III}Cl$ and liberation of H_2 (Scheme 49, left).[180] This decomposition, however, is crucial for initiating the proposed catalytic cycle, as it allows the initial generation of active $Cp_2Ti^{III}Cl$ when $CpCr(CO)_3\bullet$ is not yet formed (Scheme 48, step 2_{in}). This also allows the use of $CpCr(CO)_3H$ as (pre)catalyst instead of $CpCr(CO)_3\bullet$.

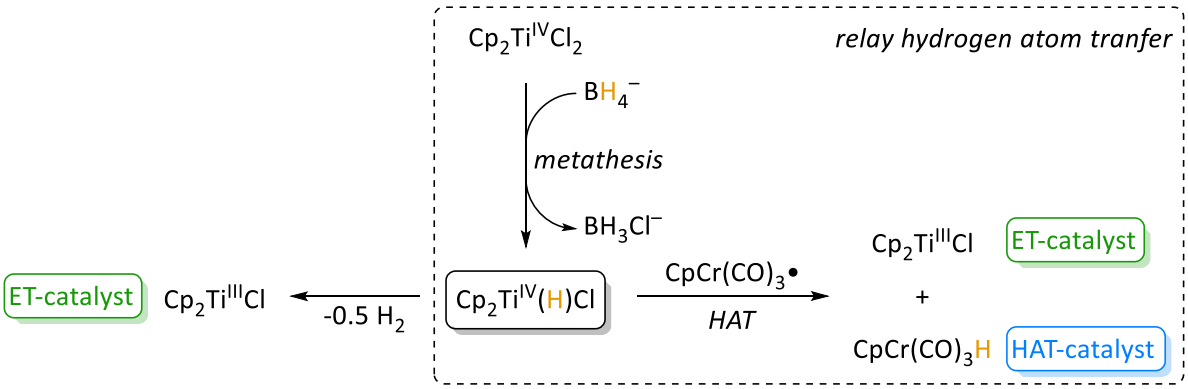

Scheme 49: Two competing processes: Decomposition of $Cp_2Ti(H)Cl$ under formation of H_2 (left) and HAT from $Cp_2Ti(H)Cl$ to $CpCr(CO)_3\bullet$ as part of the relay hydrogen atom transfer from BH_4^-, generating both active catalysts (right).

However, $Cp_2Ti(H)Cl$ is even more essential in a second function for the catalytic cycle to operate. Generation of the electron-transfer catalyst $Cp_2Ti^{III}Cl$ and the HAT catalyst $CpCr(CO)_3H$ is accomplished with BH_4^-. This activation proceeds via an unprecedented relay hydrogen atom transfer from BH_4^- via

$Cp_2Ti(H)Cl$ to $CpCr(CO)_3\bullet$ (Scheme 49, right). The $Cp_2Ti(H)Cl$ formed from the σ-bond metathesis with the borohydride is also able to act as HAT reagent.[180,182] The hydrogen atom is transferred from $Cp_2Ti(H)Cl$ to the $CpCr(CO)_3\bullet$ radical, releasing $Cp_2Ti^{III}Cl$ and $CpCr(CO)_3H$. Thereby both active catalysts are generated simultaneously in equimolar amounts. For this HAT to occur, the Ti–H bond must be weaker than the Cr–H bond and the titanocene hydride chloride must be the better hydrogen atom donor. This can be assumed since $Cp_2Ti(H)Cl$ is thermally unstable in solution and evolves hydrogen and has not been isolated, while $CpCr(CO)_3H$ is semi-stable in compound at room temperature and stable solutions can be prepared. In addition, the DFT-calculated Ti–H bond strength in $Cp_2Ti^{IV}H^+$ (BDE = 43 kcal·mol^{-1}),[183] which neglects the chloride ligand, is significantly lower than the Cr–H bond strength in $CpCr(CO)_3H$ (BDE = 62 kcal·mol^{-1}).[148] This difference can be considered as an indication of the feasibility of the required HAT.

The two possible reactions of $Cp_2Ti(H)Cl$ shown in Scheme 49, the decomposition, releasing H_2 and the HAT to $CpCr(CO)_3\bullet$, are competing processes. The decomposition pathway is only required for the initial catalytic turnover, as it circumvents the generation of $CpCr(CO)_3H$. Therefore, it is important to outcompete the decomposition pathway during the reaction. DFT calculations of both pathways predict a slightly more exergonic process for the desired HAT considering a THF solvation (-11.6 kcal·mol^{-1} vs. -12.6 kcal·mol^{-1}).[180,184] Visible gas evolution immediately after setup of the catalytic reactions indicates the formation of H_2 and supports the presence and partial decomposition of $Cp_2Ti(H)Cl$ at the beginning.

The proposed mechanism was supported by experimental and theoretical experiments. The mechanism as shown in Scheme 48, suggests that the cleavage of the B–O bond and resulting liberation of the product alcohol does not occur during the course of the reaction, but during the aqueous work-up. To test this hypothesis, *Shizgal* performed *in situ* FT-IR experiments (Figure 10).[185]

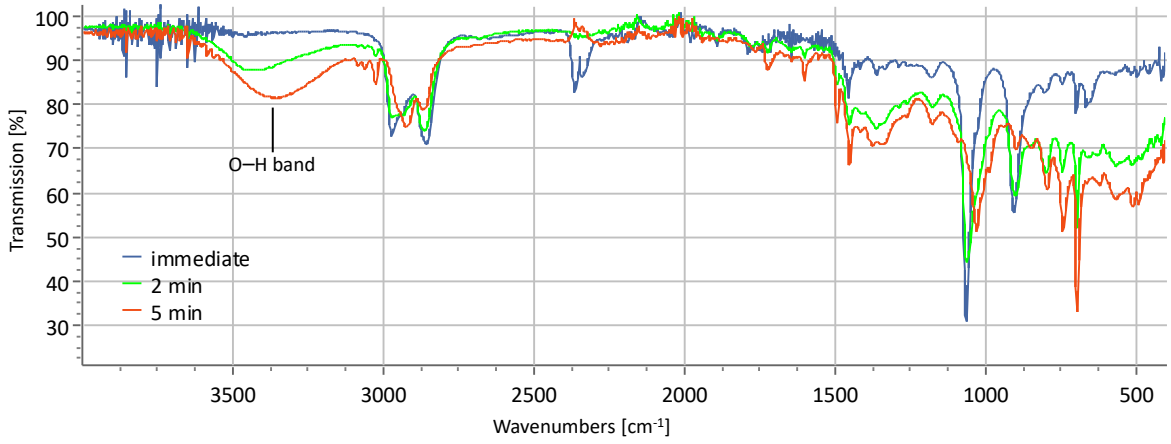

Figure 10: Changing FT-IR spectra of a crude reaction mixture before work-up, recorded immediately and after short exposure to air. Reaction conditions: 1.0 eq. epoxide **2**, 0.1 eq. Cp_2TiCl_2, 0.1 eq. $CpCr(CO)_3H$, 0.5 eq. KBH_4, 0.05 eq. LiCl, THF, RT, 48h (performed by *Shizgal)*.[185]

The IR spectra of a sample taken immediately from the reaction mixture prior to the work-up, shows the absence of a broad band in the area 3650–3200 cm^{-1},[186] which is the expected range for O–H bonds. When the sample is exposed to air and moisture for several minutes, the expected O–H band becomes visible, indicating a cleavage of the alkoxy-substituted boronic ester and liberation of the free alcohol.

Quantum chemical calculations were performed by *Hilche* in collaboration with *Schmitz* from the *Grimme* group.[184] The activation of $Cp_2Ti^{III}Cl$ and $CpCr(CO)_3H$ with BH_4^- was calculated using the DFTB method (Scheme 50). The initial ligand exchange forming $Cp_2Ti^{IV}(H)Cl$ and BH_3Cl^- is only slightly endergonic (+4.3 kcal·mol^{-1}). The subsequent HAT from $Cp_2Ti^{IV}(H)Cl$ to $CpCr(CO)_3$• is exergonic (-12.3 kcal·mol^{-1}), resulting also in an overall exergonic process (-8.3 kcal·mol^{-1}). The hypothetical direct reduction of Cp_2TiCl_2 with BH_4^- and formation of $CpCr(CO)_3H$ via initial formation of $Cp_2TiCl_2^-$ and BH_4• is unlikely, although overall exergonic, due to a highly endergonic first step (+52.4 kcal·mol^{-1} and -60.8 kcal·mol^{-1}).

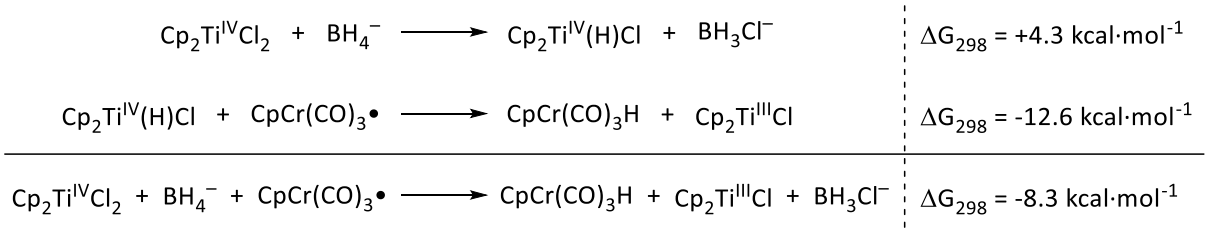

Scheme 50: DFTB calculated free enthalpy for the plausible activation of $Cp_2Ti^{III}Cl$ and $CpCr(CO)_3H$ with BH_4^- through relay hydride transfer via $Cp_2Ti^{IV}(H)Cl$. Geometry optimization: PBE0-D4[CPCM-(THF)]/def2-TZVP; single-point energies: PWPB95-D4/def2-QZVP; solvation free energies: COSMO-RS; thermostatistical correction: GFN2-xTB[GBSA].[184]

Free enthalpies for the opening of a model epoxide **2** by Cp_2TiCl, the HAT from $CpCr(CO)_3H$ to the resulting β-titanoxy radical, and the final ligand metathesis with the titanocene alkoxide under Ti–O bond cleavage to give Cp_2TiCl_2 and BH_3Cl^- were calculated using the same DFTB method and considered as well. Fortunately, the simple Cp_2TiCl_2 precatalyst shows the best overall calculated results of all investigated precatalyst in terms of free enthalpy. The analogously investigated $(C_5H_4Cl)_2TiCl_2$ shows comparable results, while $Cp_2Ti(OMs)_2$ is predicted to perform inferior due to a significantly higher calculated free enthalpy in the epoxide opening step.[184] It must be noted that the metal cation of the borohydride is neglected in these calculations. The cation has a significant influence on the reactivity and especially on the ligand exchange process, as it will be discussed in the next chapter. However, the calculations performed provide indications supporting the plausibility of the proposed mechanism and provide valuable insights for the performance of the subsequent optimization.

2.4 Reaction Condition Optimization

To achieve a novel and efficient use of the borohydride anion in the titanocene-catalyzed epoxide opening, at first optimal reaction conditions needed to be found. As stated above, the formation of $Cp_2Ti(H)Cl$ is crucial for catalyst activation and reaction success. However, besides the σ-bond metathesis between Cp_2TiCl_2 and BH_4^- mentioned before, which yields $Cp_2Ti(H)Cl$, borohydrides are also known to reduce Cp_2TiCl_2 to $Cp_2Ti(BH_4)$ (Scheme 51). By reacting Cp_2TiCl_2 and $LiBH_4$ in Et_2O or $NaBH_4$ in 1,2-dimethoxyethane, dark violet $Cp_2Ti(BH_4)$ is obtained.[187–190] This titanocene borohydride species is not suitable for catalytic epoxide opening, so this deactivation of the titanocene as $Cp_2Ti(BH_4)$ must be avoided.

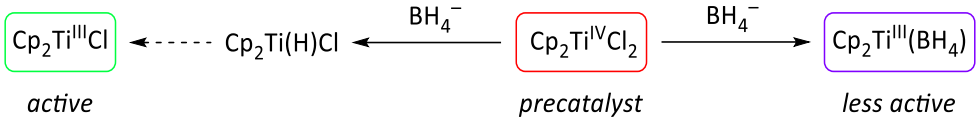

Scheme 51: Competing possible reactions of titanocene dichloride with borohydrides.

Both pathways of reduction of the titanocene dichloride must be considered and the activation must be controlled to achieve a productive reprogramming of the borohydride anion.

Thus, finding the right borohydride complex was a major task of this project. In the preliminary stages of this work, a primal functional system was already established in collaboration with *Panfilova*. The initial investigations started with the commonly used sodium borohydride $NaBH_4$. The main results of this previous optimization using **2** as a benchmark substrate are summarized in Table 10.

Table 10: Previous reaction condition development.[191]

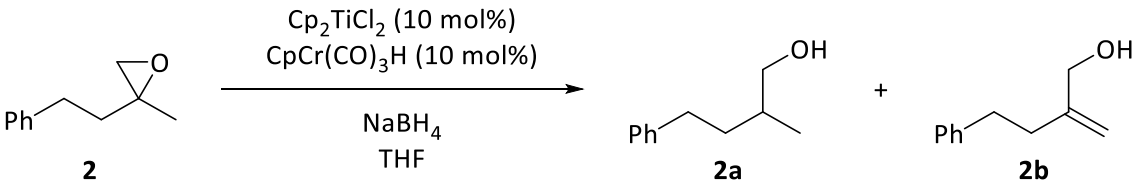

2 **2a** **2b**

entry	$NaBH_4$ [mol%]	T [°C]	t [h]	conversion[a] [%]	ratio[a]	
					2a [%]	2b [%]
1	200	40	48	65	92	8
2	100	40	48	75	93	7
3	50	40	48	100[b]	93	7
4	50	25	48	81	96	4

[a] determined by ^{1}H-NMR of crude reaction mixture. [b] isolated yield: 73% as a 93:7 mixture with **2b**.

Without the addition of any external acid (such as Coll·HCl) or additional reductant (like Mn or Zn), significant conversions of the model epoxide **2** to the *anti-Markovnikov* alcohol **2a** are observed.

Surprisingly at first glance, the conversion of the reaction increases when the amount of the borohydride is decreased from 200 mol% to 50 mol% (entries 1–3). With 50 mol% $NaBH_4$ at 40°C after 48 h, full conversion is obtained. This finding could be assigned to an increased formation of the inactive $Cp_2Ti(BH_4)$ when higher amounts of the borohydride are used. Thus, 50 mol% of borohydride seems to be optimal, which also results in a better resource consumption of the reaction. However, although full conversion is achieved, the formation of **2a** is accompanied by the formation of 7% allylic alcohol **2b** (entry 3). An inseparable mixture of **2a** and **2b** (73%, 93:7) was obtained when this reaction was purified, since the retardation factors in column chromatography of these compounds are essentially the same. Unfortunately, reducing the temperature to room temperature (entry 4) did not prevent formation of **2b** and also decreases the conversion to 81%.

Therefore, the challenge is to find catalytic conditions that are selective for **2a** while avoiding the formation of by-products. In addition, these conditions should operate at room temperature to be suited for a later extension to regiodivergent epoxide opening reactions to ensure selectivity in the formation of enantiopure products.

The cation of the borohydride complex and its *Lewis* acidity has a significant influence on its reactivity. In the context of titanocene-catalyzed epoxide opening, the *Lewis* acid plays a role in facilitating the ligand exchange necessary for the formation of $Cp_2Ti(H)Cl$ and thus generation of the active titanocene catalyst as shown in Figure 11.

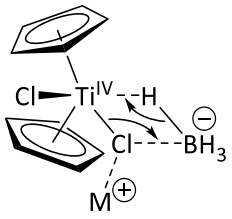

Figure 11: Ligand metathesis between Cp_2TiCl_2 and BH_4^- facilitated by a *Lewis* acidic metal cation in the formation of $Cp_2Ti(H)Cl$.

Therefore, to increase the reactivity, the use of a more reducing borohydride salt seems to be a reasonable choice. $LiBH_4$ is known to be a better reducing agent for functional groups than $NaBH_4$, coupled with Li^+ being a stronger *Lewis* acid than Na^+.[192,193] So, the use of $LiBH_4$ instead of $NaBH_4$ was investigated (Table 11).

Table 11: $LiBH_4$ as sole reductant and as additive together with $NaBH_4$ in THF.[194]

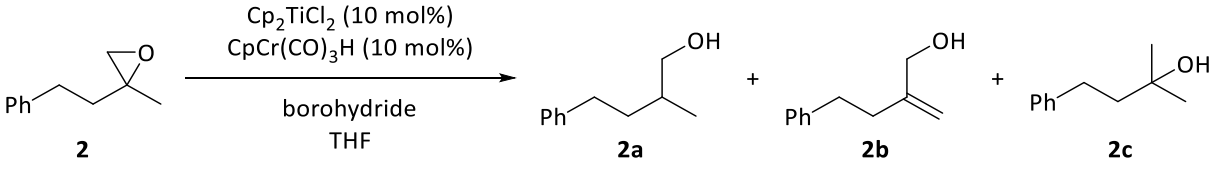

entry	$NaBH_4$ [mol%]	$LiBH_4$ [mol%]	$(^nBu_4N)BH_4$ [mol%]	T [°C]	t [h]	conversion[a] [%]	ratio[a] 2a [%]	2b [%]	2c [%]
1[b]	–	50	–	40	48	100	4	30	66
2[b]	50	1	–	25	72	73	95	5	–
3	50	2	–	25	72	98	88	12	–
4	–	–	50	25	24	75	59	8	33

[a] determined by ^{1}H-NMR of crude reaction mixture. [b] performed by *Shizgal*.

However, besides the formation of the desired *anti-Markovnikov* alcohol **2a** and the allylic alcohol side product **2b**, furthermore, the generation of the *Markovnikov* alcohol **2c** is observed when $LiBH_4$ is used. With 50 mol% $LiBH_4$ in THF (entry 1), mainly **2c** is formed. Also, the addition of $LiBH_4$ in small amounts as additive to the reaction with $NaBH_4$ did not lead to the desired outcome. The addition of 2 mol% $LiBH_4$ results in an improved conversion as expected, but also to a significant amount of **2b**. With a lower loading of 1 mol% $LiBH_4$, the ratio is improved, but at the same time the conversion decreases. Also, using the slightly less reducing but well soluble tetrabutylammonium borohydride $(^nBu_4N)BH_4$, instead of $LiBH_4$ resulted in a significant amount of **2c** (entry 4).

At this point, it is important to understand the formation of the possible side products for a better interpretation and analysis of the reaction outcome and to facilitate further optimization. The often-observed formation of the allylic alcohol **2b** results from a β-hydrogen abstraction from the β-titanoxy radical intermediate, forming an allylic alcoholate (Scheme 52). This β-hydrogen abstraction can occur with another equivalent of the active $Cp_2Ti^{III}Cl$,[114] but presumably also with $CpCr(CO)_3\bullet$. As the first pathway requires a second equivalents of the active titanocene $Cp_2Ti^{III}Cl$ after the epoxide opening, it becomes clear that at a too high concentration, the $Cp_2Ti^{III}Cl$ radical promotes the formation of the allylic alcohol.

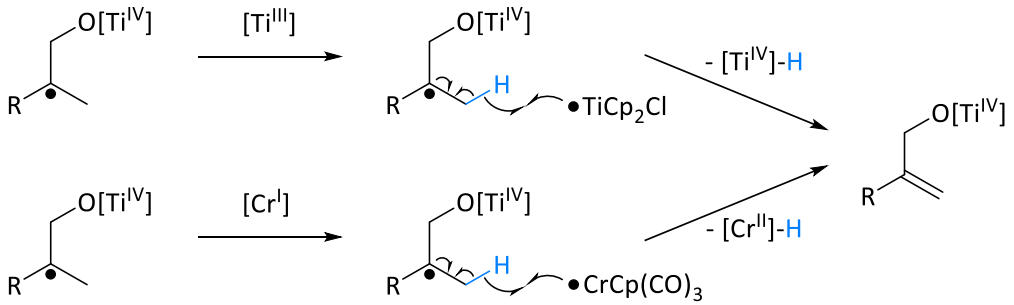

Scheme 52: Formation of the allylic alcohol side product by β-hydrogen abstraction either by $Cp_2TiCl\bullet$ (top) or $CpCr(CO)_3\bullet$ (bottom).

The *Markovnikov* alcohol **2c** forms via a nucleophilic ring-opening of the epoxide. After activation of the epoxide by a *Lewis* acid, the epoxide can be opened in an S_N2-like reaction by hydride-donating reducing agents (Scheme 53). $LiBH_4$ in THF is known to reduce epoxides in this way, also because of the Li^+ cation acting as *Lewis* acid.[193]

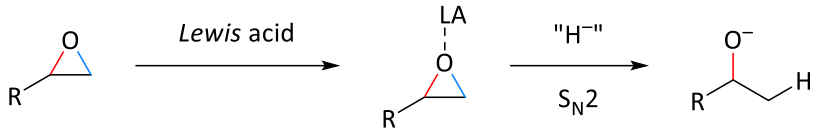

Scheme 53: *Lewis* acid assisted reduction of epoxides to the *Markovnikov* alcohol side product via a S_N2-like reaction by hydride donating reducing agents.

This reactivity was observed also experimentally in the reaction of **2** with $LiBH_4$ in THF (Scheme 54). However, not only Li^+ but also $Cp_2Ti(BH_4)$, formed by reduction of Cp_2TiCl_2 with $LiBH_4$, can be considered as *Lewis* acid capable of activating the epoxide for the nucleophilic ring-opening.

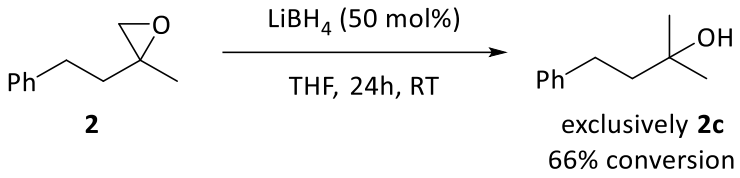

Scheme 54: Formation of the *Markovnikov* alcohol **2c** by reaction of **2** with $LiBH_4$ in THF.

It becomes apparent that $LiBH_4$ in THF exhibits a reactivity that is too strong to fit into the gears of the cooperative catalytic system. While the presence of the *Lewis* acid Li^+ accelerates the desired Ti–Cl bond cleavage and the ligand exchange from Cp_2TiCl_2 leading to the required $Cp_2Ti(H)Cl$, it also facilitates the undesired reduction of Cp_2TiCl_2 to $Cp_2Ti(BH_4)$. Thus, a high concentration of $LiBH_4$ and Li^+, respectively, not only accelerates the activation of the titanocene, but also promote the named side reactions by increasing the concentrations of $Cp_2Ti^{III}Cl$, $Cp_2Ti(BH_4)$, and Li^+ itself. Therefore, $LiBH_4$ has to be used carefully.

Instead of directly using strongly reducing $LiBH_4$, including an equal amount of the *Lewis* acid Li^+, it might be beneficial to add only a certain amount of the *Lewis* acid and to regulate the amount of $LiBH_4$ *in situ*. A procedure reported in the literature to prepare $LiBH_4$ is the metathesis reaction of $NaBH_4$ or KBH_4 with LiCl in THF (Scheme 55).[195]

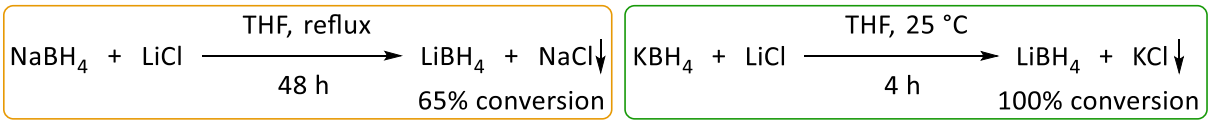

Scheme 55: Synthesis of $LiBH_4$ from $NaBH_4$ and KBH_4 by metathesis with LiCl.

The reaction with $NaBH_4$ proceeds incompletely even after two days in refluxing THF. In contrast, the reaction with KBH_4 is complete already after 4 h at room temperature. The difference in reaction rates

can be attributed to a significant difference in the solubilities of the precipitating alkali metal chlorides in THF, which is lower for KCl than for NaCl.[196] This causes a shift in the equilibria according to the *Le Chatelier* principle. Since the reaction with KBH_4 is faster and takes place at room temperature, the combination of KBH_4 and LiCl as an additive for *in situ* generation of $LiBH_4$ was investigated first. The most important results of these experiments are shown in Table 12.

Table 12: LiCl as additive in the reaction with KBH_4 and $NaBH_4$.[194]

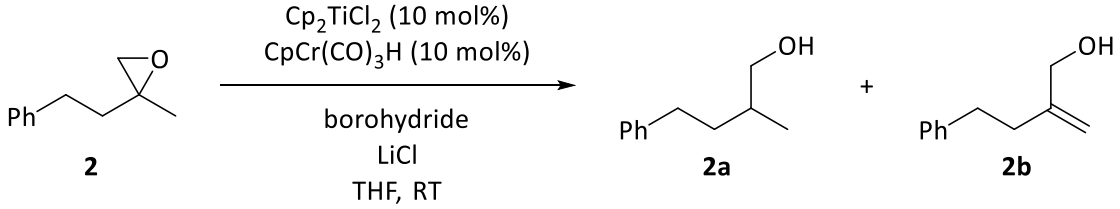

2 **2a** **2b**

entry	borohydride, [mol%]	LiCl [mol%]	t [h]	conversion[a] [%]	ratio[a] 2a [%]	ratio[a] 2b [%]
1[b]	KBH_4, 50	–	48	100	87	13
2	KBH_4, 50	2.5	48	98	88	12
3	KBH_4, 50	5.0	48	97	93	7
4	KBH_4, 50	7.5	48	93	93	7
5[b]	KBH_4, 50	10.0	48	80	97	3
6	$NaBH_4$, 50	5.0	72	86	94	6
7	$NaBH_4$, 50	10.0	72	94	95	5

[a] determined by ^{1}H-NMR of crude reaction mixture. [b] performed by *Shizgal*.

It was observed that the formation of tertiary alcohol **2c** did not occur in any of the reactions. Depending on the amount of LiCl added, two effects were observed. First, as the amount of LiCl is increased from 0 up to 10 mol% (entries 1–5), there is a significant decrease in the conversion of the reaction from 100% to 80%. However, an opposite effect on the product ratio is observed. Unexpectedly, the portion of the desired *anti-Markovnikov* **2a** product is raised from 87% to 97% with increasing amount of LiCl. The visualization of these two opposite effects is shown in Figure 12. A decent optimum, combining a high conversion and an acceptable product ratio, was identified to be at 5 mol% LiCl (entry 3). The combination of $NaBH_4$ and LiCl (entries 6 and 7) generally required longer reaction times, possibly due to the slower metathesis and $LiBH_4$ formation. As no benefit in terms of conversion or product ratio was observed compared to the case of KBH_4, this system was not investigated further.

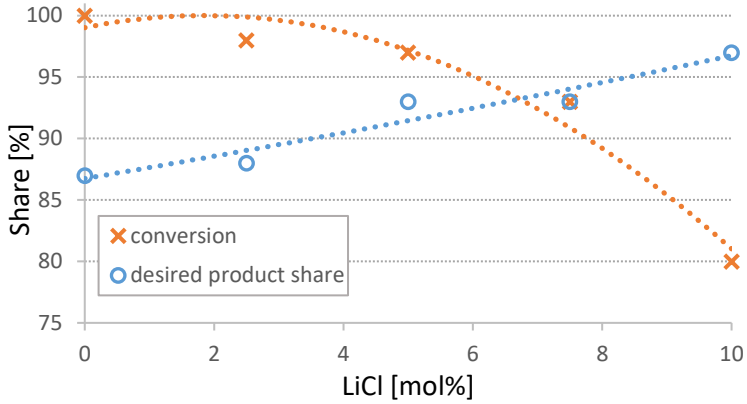

Figure 12: Reaction conversion and share of the desired product alcohol in relation to the added amount of LiCl to the reaction with 50 mol% of KBH_4.

The question remains as to the origin of the unexpected opposite trends in Figure 12 along with the amount of LiCl added to KBH_4. The LiCl additive is expected to increase the amount of $LiBH_4$ by *in situ* formation via metathesis with LiCl, which would lead to a higher reactivity and conversion, but also to more formation of the allylic alcohol due to more active Cp_2TiCl in the solution. However, the experimental results suggest that the additive LiCl has another effect on the concentration of $Cp_2Ti^{III}Cl$. Previous studies by the *Gansäuer* group of reactions using Coll·HCl have shown an effect of this reagent on the catalyst activity beyond its role as a *Brønsted* acid. In solution, $Cp_2Ti^{III}Cl$ is in equilibrium with its chlorine-bridged dimer species (Scheme 56).[83,197] The addition of Coll·HCl shifts this equilibrium by formation of a new hydrogen-bound $[Cp_2Ti^{III}Cl_2]^-$ collidinium adduct. The formation of this *resting state* lowers the concentration of titanocene(III) radicals in solution, preventing catalyst decomposition but also unwanted organic radical trapping and therefore side product formation.

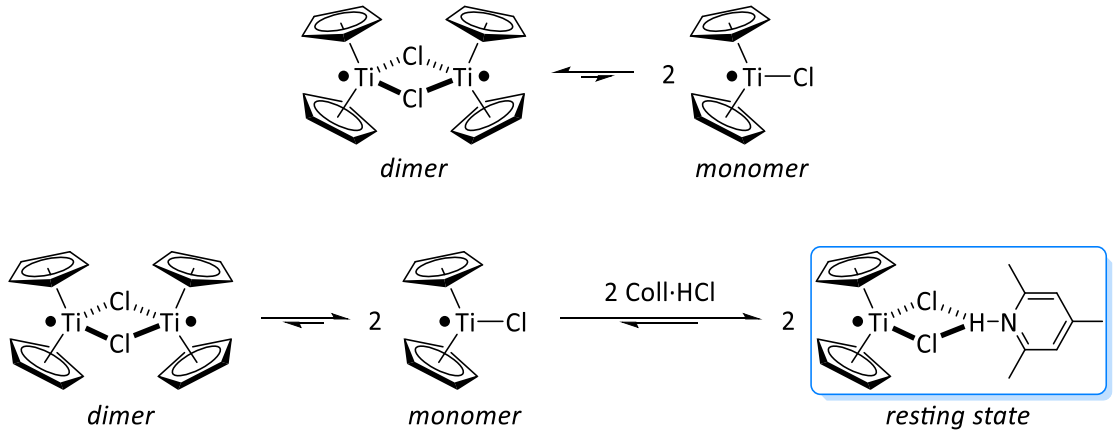

Scheme 56: Equilibria of titanocene(III) species in solution. In presences of Coll·HCl formation of a *resting state* occurs.

Formation of a similar *resting state* can be assumed when LiCl is added to the reaction (Scheme 57). This *resting state* and the resulting lowered concentration of active titanocene radicals in solution explains the prevention of radical trapping and side product formation and is in good agreement with

the observed trend. In addition, it can be assumed that the equilibrium in the presence of LiCl is shifted more towards the *resting state* compared to the equilibrium with Coll·HCl, a trend generally observed with chloride salts.[83] The resulting lowered concentration of active $Cp_2Ti^{III}Cl$ in solution also provides an explanation for the observed decreasing conversions.

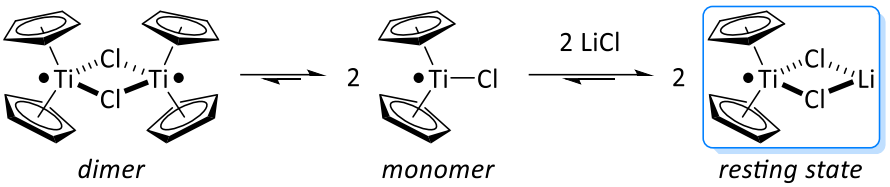

Scheme 57: Proposed *resting state* of active $Cp_2Ti^{III}Cl$ with LiCl.

The identified interim optimal conditions using KBH_4 together with 5 mol% LiCl (Table 12, entry 3), which combine a good conversion with an acceptable product ratio and, importantly, proceed at room temperature, were tested on a scope of epoxides (Table 13).

Table 13: Substrate scope of the cooperative catalytic epoxide opening with KBH_4 and LiCl.[194]

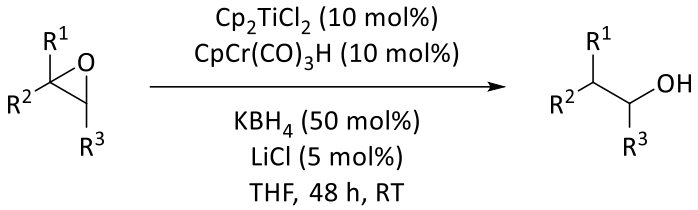

entry	substrate	product	conversion[a] [%]	ratio[a] product/allylic alcohol [%]	yield[c] [%]
1	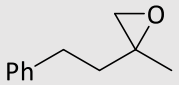 **2**	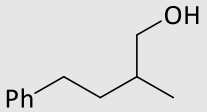 **2a**	92	94/6	57
2	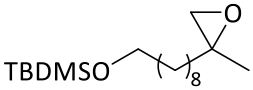 **3**	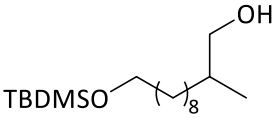 **3a**	89[b]	93/7	68 (96:4)
3	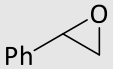 **4**	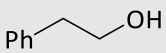 **4a**	100	–	56
4	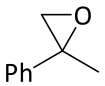 **5**	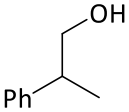 **5a**	100	85/15	83 (86:14)
5	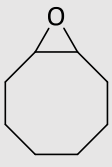 **6**	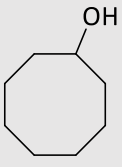 **6a**	85	98/2	43

[a] determined by ^{1}H-NMR of crude reaction mixture. [b] 72 h reaction time. [c] ratio of *anti-Markovnikov* and allylic alcohol in the isolated yield shown in parentheses.

All examined substrates could be converted sufficiently using the described catalytic system, with conversions ranging from 85% to 100%. The formation of the allylic alcohol side products is generally observed. The amount formed varies depending on the substrate structure and is, with exception of substrate **5**, in the expected range of about 95/5. The presence of the side product results in complications of the purification and either lower yields or product and side product mixtures are obtained. Although improvement of the cooperative system at room temperature was achieved, further optimization of the reaction conditions in respect to the product ratio was necessary.

The reaction conditions were further improved in collaboration with *Shizgal* and *Heinz*. One way to control the *Lewis* acidity and the reducing power of the borohydride is by slow and controlled release of the reagent. Besides technical solutions, such as a dosing feeder or a syringe pump, a more elegant and chemical option is to take advantage of the solvent and solubilities. The stronger reducing ability of $LiBH_4$ is caused by Li^+ being a stronger *Lewis* acid than Na^+, but is also related to the much higher solubility of $LiBH_4$ in THF (11.43 mol·L^{-1}, 25°C) compared to $NaBH_4$ (0.02 mol·L^{-1}, 25°C).[198] Therefore, a solvent had to be found that exhibits a reduced solubility for $LiBH_4$. A suitable polar solvent seems to be found in 1,4-dioxane. The solubility of $LiBH_4$ in 1,4-dioxane (0.12 mol·L^{-1}, 18°C)[198] is significantly lower than in THF. At the same time, the coordination properties of 1,4-dioxane are similar to those of THF,[199] which is important for the coordination of the active $Cp_2Ti^{III}Cl$ to form the *Lewis* acidic complex responsible for efficient epoxide coordination and the oxidative addition.

From another perspective, the choice of 1,4-dioxane to adjust the reductive environment is supported by DFT calculated data. As a measure of the reducing ability of metal borohydrides their hydride donating ability (HDA), determined as *Gibbs* free energy ($\Delta G°_{H-}$), can be considered. A lower $\Delta G°_{H-}$ corresponds to a better HDA and a greater ability to transfer a hydride to an organic substrate. The DFT analysis shows a clear dependence of the HDA on the polarity of the media. While the $\Delta G°_{H-}$ of alkali metal and ammonium tetrahydroborates in THF is in the range of 70 to 85 kcal·mol^{-1}, the values in 1,4-dioxane are in the range of 110 to 130 kcal·mol^{-1}.[200] Thus, borohydrides can generally be considered weaker hydridic reductants in 1,4-dioxane than in THF. Based on these findings the combination of $LiBH_4$ and 1,4-dioxane was investigated. The initial results of this catalytic system are presented in Table 14.

Table 14: Application of $LiBH_4$ in 1,4-dioxane.

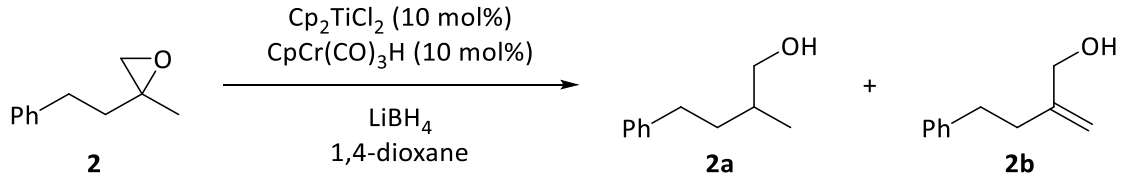

2 **2a** **2b**

entry	$LiBH_4$ [mol%]	T [°C]	t [h]	conversion[a] [%]	ratio[a]	
					2a [%]	2b [%]
1[b]	50	25	24	87	>99	<1
2[b]	50	25	48	92	97	3
3[b]	50	45	24	69	75	25
4[c]	25	25	24	52	96	4
5[b]	100	25	24	55	>99	<1

[a] determined by ^{1}H-NMR of crude reaction mixture. [b] performed by *Shizgal*. [c] performed by *Heinz*.

Fortunately, the desired effect was achieved and the use of 1,4-dioxane led to a significant reduction of side product formation. Looking at entry 1, already after 24 h at room temperature, 87% conversion to **2a** is obtained with no detectable side product. In contrast to KBH_4 in THF, no additive is required to suppress side product formation. A longer reaction time of 48 h (entry 2) increases the conversion, but also 3% of **2b** is observed. The beginning side product formation in the later stage of the reaction can be attributed to the shrinking concentration of the starting material in relation to an approximately equal metal radical concentration. A higher reaction temperature (entry 3) resulted in both, a lower conversion and a poor product ratio, suggesting an over-activation of the titanocene at elevated temperatures also in 1,4-dioxane. For choice of the reaction time, the absence of the side product formation after 24 h is preferable here over a slightly increased conversion after 48 h.

Modifying the borohydride loading from 50 mol% $LiBH_4$ to 25 mol% and 100 mol % (entries 4 and 5) both resulted in a clear reduction of the conversion. This confirms that the previously determined optimal loading of 50 mol% borohydride is also optimal for $LiBH_4$ in 1,4-dioxane. The fact that neither one equivalent borohydride or more, nor the theoretical minimum stoichiometric amount of 0.25 equivalents are advantageous for all investigated systems, seems surprising at first glance. One potential influence is the increased formation of the inactive $Cp_2Ti(BH_4)$ at high concentration of the reductant. Alternatively, the hydride donating ability (HDA) of the borate can be considered here as well. The exchange of a hydride ligand for an alkoxy ligand during the course of the reaction lowers the $\Delta G°_{H^-}$ value, which means the HDA of the borate is increased.[200] A higher ratio of already alkoxy-substituted borate therefore facilitates further relay hydride transfer and catalyst activation. This higher ratio is enforced by a lower loading of the borohydride. However, this is counteracted by the increasing steric demand of the borate with increasing degree of alkoxy substitution, which ultimately

slows down the hydride transfer. This agrees well with the observation that the best reaction results are obtained with 50 mol% of borohydrides, balancing both effects.

Subsequently, the influence of the catalyst loading was investigated (Table 15). However, no improvement of the reaction outcome was achieved by varying one or both catalyst loadings (entries 1–5). Generally, only a higher loading of titanocene (entry 4) or higher than the chromium hydride (entry 3) facilitate formation of **2b**. An increased loading of the chromium hydride (entry 2) does not have this effect. This indicates that the formation of **2b** as shown in Scheme 52 occurs predominantly through β-hydride abstraction by Cp_2TiCl and less by $CpCr(CO)_3$•. Overall, the initial experimental determined optimal loading of 10 mol% for both the titanocene and the chromium hydride catalyst are ideal already.

Table 15: Catalyst loading influence and control experiments.

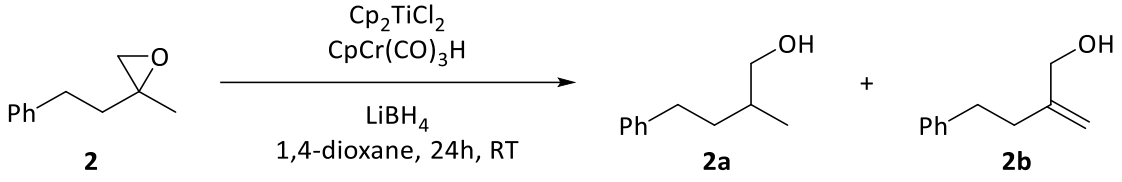

2 **2a** **2b**

entry	Cp_2TiCl_2 [mol%]	$CpCr(CO)_3H$ [mol%]	$LiBH_4$ [mol%]	conversion[a] [%]	ratio[a]	
					2a [%]	**2b [%]**
1[b]	10	10	50	87	>99	<1
2[b]	10	15	50	80	>99	<1
3[b]	10	5	50	71	97	3
4[b]	15	15	50	35	95	5
5[b]	5	5	50	23	>99	<1
6	–	10	50	3	>99	<1
7	10	10	–	10	53	47
8	10	–	50	36	89	11
9	–	–	50	0	–	–

[a] determined by ^{1}H-NMR of crude reaction mixture. [b] performed by *Shizgal*.

To confirm the necessity of all catalysts and reagents in the proposed cooperative mechanism, a series of control experiments were conducted (Table 15, entries 6–9). As anticipated, omitting any of the reagents, led to a failure of the reaction. Surprisingly, when only the Cp_2TiCl_2 catalyst was used without $CpCr(CO)_3H$ (entry 8), a conversion of 36% with a product ratio of 89:11 is observed. This finding suggests that while all reagents are essential for optimal catalysis, Cp_2TiCl_2 and $LiBH_4$ together can partially reduce the epoxide to **2a** in quantities exceeding the stoichiometric amount relative to

titanocene. This indicates a possible direct hydrogen atom transfer mechanism involving a titanocene hydride species, a phenomenon further explored by the Norton group.[201]

Summarizing the condition optimization progress, a combination has been found in $LiBH_4$ and 1,4-dioxane that achieves the desired unprecedented applicability of the borohydride reducing agent as hydrogen atom source within cooperative radical catalysis. The reactivity of the borohydride is tuned by carefully adjusting the cation and solvent effects and by choice of the reaction conditions in such a way that the typical S_N2 reactivity is completely outcompeted. Thus, the same reagent is reprogrammed through activation by cooperative catalysis in a way suppressing its well-known reactivity and resulting in an entirely reversed regioselectivity (Scheme 58).

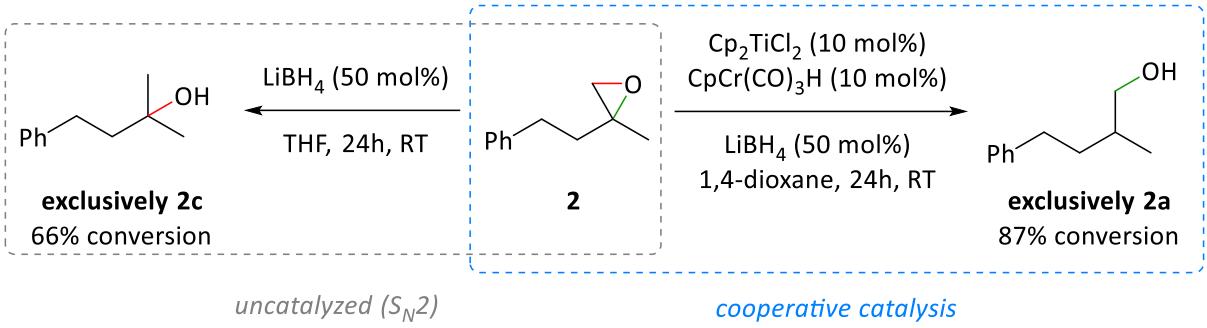

Scheme 58: Reprogramming of the typical borohydride reactivity by cooperative catalysis.

Furthermore, conditions have been identified that avoid the formation of the allylic alcohol and tertiary alcohol side products and require no elevated temperatures. For comparison, some of the borohydride systems tested during the optimization process using **2** are visualized in Figure 13.

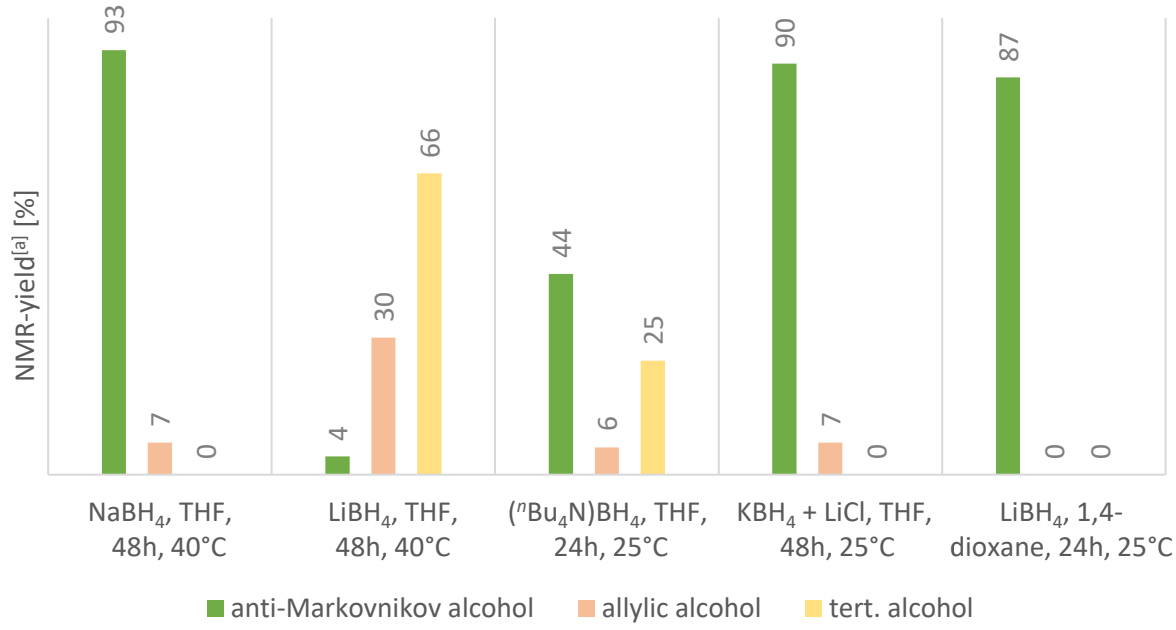

Figure 13: Comparison of different borohydride and solvent combinations in the reaction with **2**. [a] calculated by multiplication of respective conversion rates and product ratios.

The cooperative system using 10 mol% each of Cp_2TiCl_2 and $CpCr(CO)_3H$ alongside with 50 mol% of $LiBH_4$ in 1,4-dioxane (Table 14, entry 1) has been identified as the optimal reaction conditions. It proceeds at room temperature and combines high reactivity with excellent selectivity and has been selected as the starting point for the upcoming applications.

2.5 Application in Reductive Epoxide Openings

With the optimized conditions established, the next step involved testing the applicability of the reaction conditions. The cooperative system utilizing Cp_2TiCl_2 and $CpCr(CO)_3H$, along with $LiBH_4$ in 1,4-dioxane, was applied to different epoxide substrates to evaluate its versatility and efficiency across a broader scope, that is shown in Table 16.

Table 16: Substrate scope of the cooperative catalytic epoxide opening with $LiBH_4$ in 1,4-dioxane.

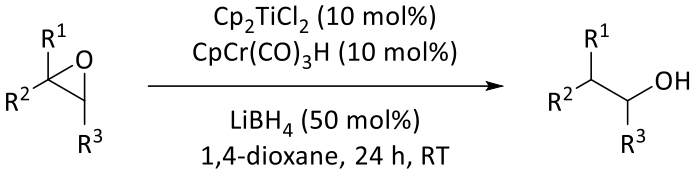

entry	substrate	product	conversion[a] [%]	ratio[a] (product/allylic alcohol) [%]	yield[c] [%]
1[b]	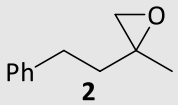 **2**	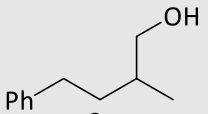 **2a**	87	>99:<1	83
2	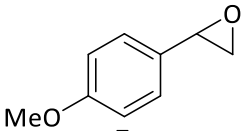 **7**	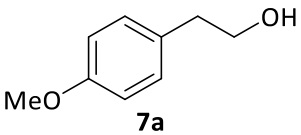 **7a**	100	–	92
3[b]	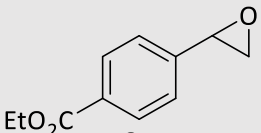 **8**	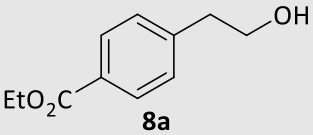 **8a**	100	–	87
4	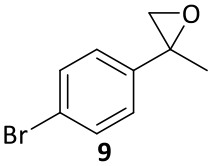 **9**	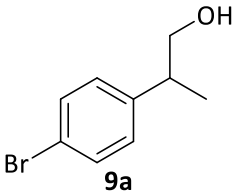 **9a**	100	97:3	76 (98:2)
5[c]	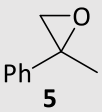 **5**	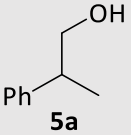 **5a**	100	95:5	80

entry	substrate	product	conversion[a] [%]	ratio[a] product/allylic alcohol [%]	yield[c] [%]
6[c]	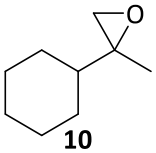 **10**	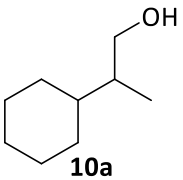 **10a**	100	>99:<1	87
7[b]	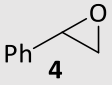 **4**	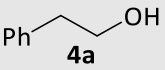 **4a**	100	–	76
8[c]	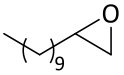 **11**	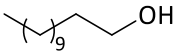 **11a**	100	–	83[e]
9[b]	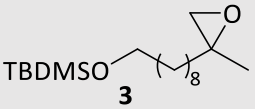 **3**	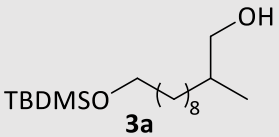 **3a**	100	>99:<1	68
10[c]	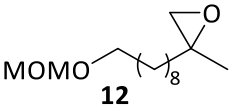 **12**	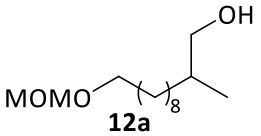 **12a**	80	98:2	68
11	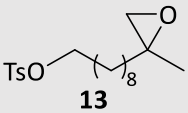 **13**	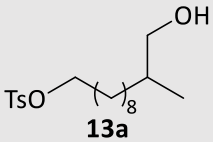 **13a**	66	94:6	64 (94:6)
12	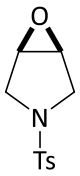 **14**	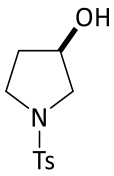 **14a**	88	>99:<1	74
13	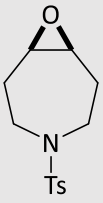 **15**	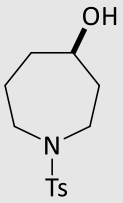 **15a**	75	>99:<1	68
14	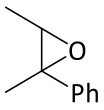 **16**	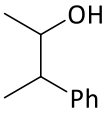 **16a**	78	80:20	54[f] (80:20)
15	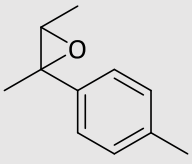 **17**	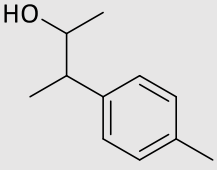 **17a**	74	81:19	56[g] (81:19)

[a] determined by ^{1}H-NMR of crude reaction mixture. [b] performed by *Shizgal*. [c] performed by *Heinz*. [d] ratio of *anti-Markovnikov* alcohol and allylic alcohol in the isolated yield shown in parentheses. [e] obtained as 93:7 mixture of 1- and 2-dodecanol. [f] *syn*:*anti* = 64:36. [g] *syn*:*anti* = 45:55.

The epoxide opening reactions with $LiBH_4$ in 1,4-dioxane gave good to excellent results for almost all epoxide substrates tested, with many reactions proceeding to complete conversion. In general, analysis of the crude products showed excellent product ratios with only trace amounts of by-products observed with only few exceptions. A broad range of mono-, 1,1- and 1,2-substituted epoxides are converted to the corresponding *anti-Markovnikov* alcohols in good to high yields. The mild reaction conditions are tolerant of many functional groups, such as ethers and esters (entries 2–3). The toleration of the halide in **9a** is valuable for further transformations through cross-coupling reactions. Protecting groups such as TBDMS, MOM, and tosyl (entries 9–11) were compatible with the reaction conditions. The acid labile MOM protecting group emphasizes the mild and neutral reaction conditions. The successful reaction of tosylate **13,** under preservation of the good leaving group OTs, ruled out a nucleophilic reaction mechanism, and profs the suppression of the nucleophilic character of the borohydride. Reduction of **4** and **11** to **4a** and **11a**, respectively, indicates the suitability of the method for the reduction of monosubstituted epoxides. Compared to other titanocene-based systems,[202,203] this method exhibits improved regioselectivity in the ring-opening of **11** (93:7).

The lowest yields are obtained for 1,1,2-trisubstituted epoxides **16** and **17**. The steric congestion in these substrates likely slows down the epoxide opening, which explains the relatively low conversions. More importantly, the subsequent HAT by $CpCr(CO)_3H$ to the β-titanoxy radical also seems to be slow in the case of the sterically demanding trisubstituted substrates, resulting in a significant amount of the allylic alcohol. The *d.r.* of the products **16a** and **17a** are close to 50:50, indicating no diastereoselective HAT occurs and, moreover, no intramolecular HAT to the β-titanoxy radical is involved, which would result in stereoconvergence and the formation of only one diastereomer.[204] While trisubstituted substrates can in principle be converted using the presented cooperative system, further optimization work is necessary for this type of substrate.

Significant improvements were achieved in the catalytic reactions using $LiBH_4$ in 1,4-dioxane compared to previous systems that employed $NaBH_4$ or KBH_4 with LiCl in THF. These reactions yielded *anti-Markovnikov* alcohols in high yields in just 24 hours at room temperature, while producing significantly fewer by-products. This reduction in by-product formation simplifies the purification process and enables more efficient synthesis of the target *anti-Markovnikov* alcohols. The combination of $LiBH_4$ and 1,4-dioxane has proven to be well-suited to fit into the gears of cooperative catalysis by adjusting the reducing power and *Lewis* acidity, thereby paving the way for further expansion of this methodology.

2.6 Carbon-Carbon Bond Forming Cyclization Reactions

The next goal was to transfer the cooperative system to 5-*exo* cyclizations and thus to test whether the method is also compatible with the synthesis of more complex molecular structures. Titanocene-catalyzed epoxide openings involving C–C bond forming 5-*exo* cyclizations have been investigated by the *Gansäuer* group.[74,205] Also, the application of the hydrogenation catalyst $CpCr(CO)_3H$ under H_2 pressure in the radical cyclization of olefins has been successfully applied by the *Norton* group as described in chapter 1.6.[136,137] Thus, the cooperative catalysis using titanocenes and $CpCr(CO)_3H$ with $LiBH_4$ to achieve the buildup of cyclic molecular structures appears feasible. Several concurrent reaction steps have to be considered.

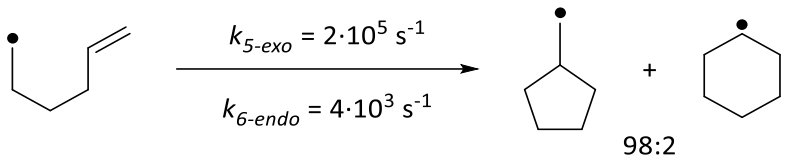

Scheme 59: 5-*exo* vs. 6-*endo* cyclization of the 5-hexenyl radical.

In principle, the addition of an aliphatic radical to a multiple bond allows the formation of 5- and 6-membered rings. In the radical cyclizations of the parent 5-hexenyl radical, the 5-*exo* is strongly favored and proceeds 50 times faster than the 6-*endo* pathway (Scheme 59),[206] which is in accordance with the *Beckwith* rules.[138,207] This preference accounts for the high selectivity observed in the formation of 5-membered rings.

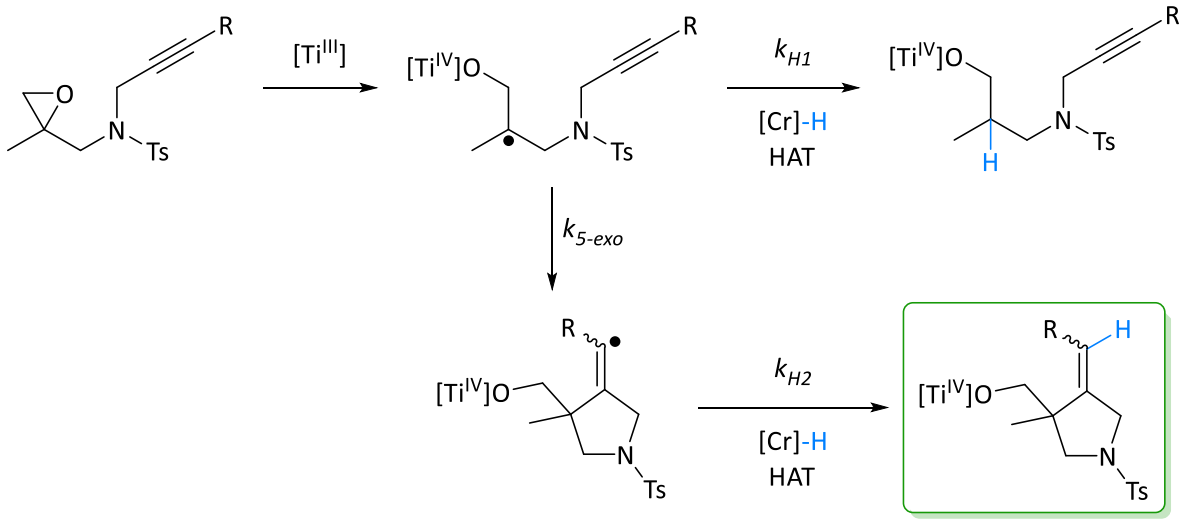

Scheme 60: Kinetic competition in radical cyclization reactions. [Cr]-H = $CpCr(CO)_3H$, [Ti] = Cp_2TiCl.

Premature reduction of the tertiary β-titanoxy radical formed after epoxide opening via HAT by $CpCr(CO)_3H$ may occur as a side reaction. Therefore, $k_{5\text{-}exo}$ for the cyclization must be sufficiently larger than k_{H1} for an efficient reaction (Scheme 60). Direct reduction has not been observed in any of the titanocene-catalyzed cyclizations performed to date and, therefore, seems unlikely. Nevertheless,

after the 5-*exo* ring closure, k_{H2} must still be large enough for efficient HAT to the vinyl radical by $CpCr(CO)_3H$ to yield the cyclic and reduced product.

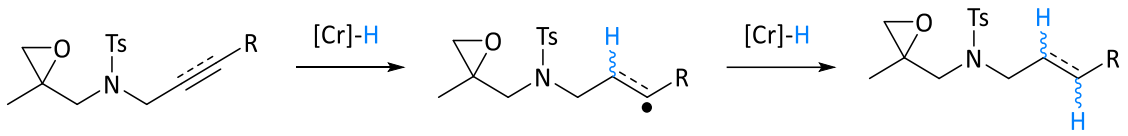

Scheme 61: Undesired hydrogenation of multiple bonds by $CpCr(CO)_3H$ leading to catalyst consumption. Double bonds generally react faster in this reaction than triple bonds. [Cr]-H = $CpCr(CO)_3H$.

In addition, the presence of transition metal hydrides involves the risk for unwanted hydrometallation or HAT to multiple bonds.[208] As shown in Scheme 61, the hydrogenation of the multiple bonds consumes two equivalents of the chromium catalyst, which cannot be regenerated under the reaction conditions with $LiBH_4$. Starting from the alkyne, the hydrogenation can be repeated until the alkane is obtained. This hydrogenation is generally faster for double bonds than for triple bonds and can compete with the rate of cyclization reactions as reported by the *Norton* group.[133,208] This explains the failure of the cyclization reactions of substrates with olefins as radical acceptor in the cooperative catalysis, studied by *Shizgal*.[185] Finally, isomerizations of the double bonds of the products catalyzed by the chromium hydride are possible as side reactions.[137] Taking all these findings into account, the cooperative catalysis system was tested on cyclization reactions using substrates with triple bonds as radical acceptors. Table 17 shows the initial results.

Table 17: Adjustments of the reaction conditions for cyclization reactions.

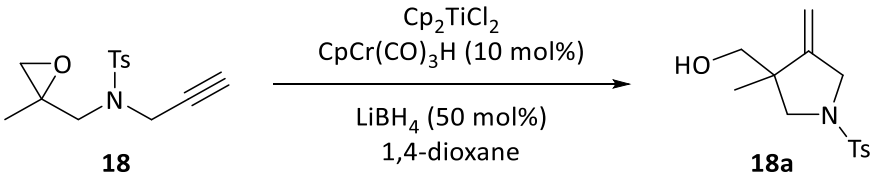

18 **18a**

entry	Cp_2TiCl_2 [mol%]	T [°C]	t [h]	conversion[a] [%]
1[b]	10	25	24	12
2	10	25	72	17
3[c]	15	25	72	19
4	15	45	72	100
5[b]	15	45	48	87

[a] determined by ^{1}H-NMR of crude reaction mixture. [b] performed by *Heinz*. [c] performed by *Schmickler*.

The conditions that were identified and used in the synthesis of the *anti-Markovnikov* alcohols in the previous chapter were chosen as a starting point. However, only 12% conversion to the desired product was detected under these conditions (entry 1). Since the reaction was expected to be slower than the previous reduction of the less complex epoxides, it was necessary to adjust the conditions to

account for the lower reactivity. Extending the reaction time alone (entry 2) or an extended reaction time in combination with an increased titanocene catalyst loading of 15 mol% (entry 3), did not improve the conversion significantly. Eventually, an additional increase of the reaction temperature to 45°C (entry 4), resulted in complete conversion and a clean reaction without any detectable product of the interception of the initially formed β-titanoxy radical or from the hydrometallation or HAT to the alkyne. Finally, a subsequent reduction of the reaction time indicated that 72 h are required, for a complete reaction (entry 5). No additives are necessary for the reaction to proceed efficiently. These adjusted conditions were then applied to a range of substrates to synthesize pyrrolidine derivatives.

Table 18: Scope of cyclization reactions by cooperative catalysis yielding *N*-tosylated pyrrolidine derivatives.

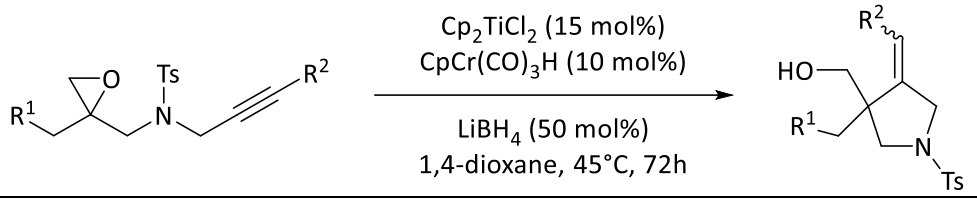

entry	substrate	product	conversion[a] [%]	yield [%]
1	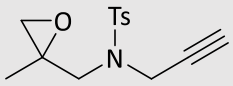 **18**	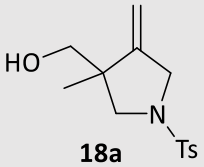 **18a**	100	75[b]
2	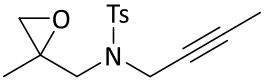 **19**	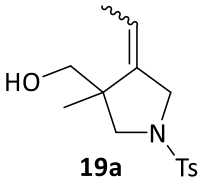 **19a**	100	65[b,c]
3	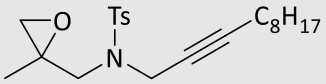 **20**	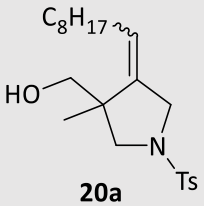 **20a**	100	19[d]
4	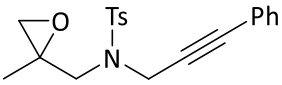 **21**	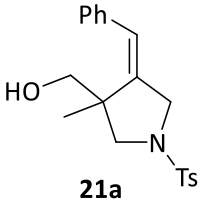 **21a**	100	78[b]
5	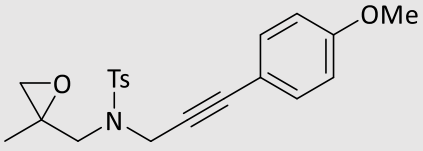 **22**	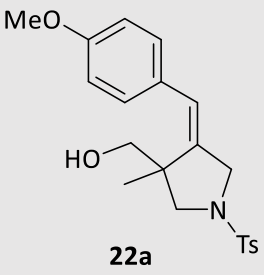 **22a**	100	81[b]

entry	substrate	product	conversion[a] [%]	yield [%]
6	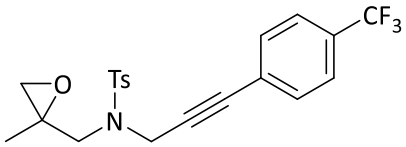 **23**	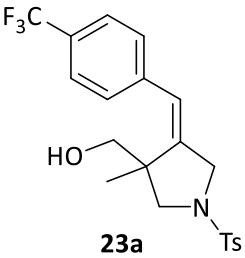 **23a**	100	66[b]
7	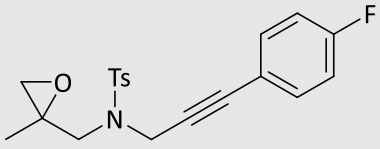 **24**	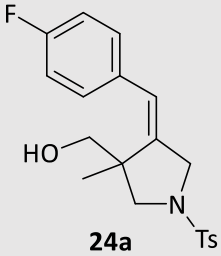 **24a**	100	25
8	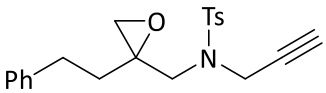 **25**	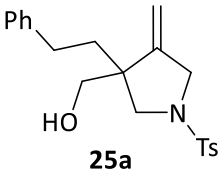 **25a**	100	22
9	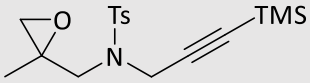 **26**	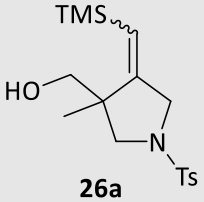 **26a**	25	not isolated
10	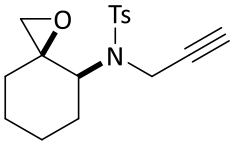 **27**	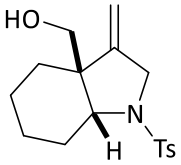 **27a**	50	not isolated

[a] determined by ^{1}H-NMR of crude reaction mixture. [b] performed by *Heinz*. [c] obtained as (*E*):(*Z*) = 70:30. [d] obtained as (*E*):(*Z*) = 50:50.

For this type of starting material, full conversion was achieved for almost all substrates investigated, typically with rather clean reaction mixtures obtained after the work-up. From these, the pyrrolidine derivatives were isolated in good yields, confirming the applicability of the cooperative catalysis for preparing complex structures. Alkyl substituted alkynes led to mixtures of (*E*)- and (*Z*)-olefins. However, in the case of aryl-substituted alkynes, HAT to the vinyl radical resulting from the 5-*exo* cyclization proceeds with full diastereoselectivity, yielding only the (*E*)-olefins (entries 4–7). A NOESY-NMR of **21a** confirming the exclusive formation of the (*E*)-olefin was performed by *Heinz.*

Unfortunately, low yields are obtained for **20a**, **24a** and **25a** after purification, although full conversion of the starting materials is detected. ^{1}H-NMR analysis of the crude reaction mixtures indicated complete consumption of the epoxide and formation of the desired alcohols as main products, but accompanied by complex mixtures of unidentified side products, leading to problems in the

purification. In particular, 4-fluorophenyl substituted **24a** appears to be additionally prone to decomposition during column chromatographic purification with both silica gel and aluminum oxide. TMS-substituted **26a** also turned out to be challenging, with no clean product being isolated. TMS-substituted alkynes are activated towards radical cyclization.[206] However, the accompanying activation for a premature hydrogenation by the chromium catalyst, as shown in Scheme 61, seems to counteract the positive effect. Similarly, a low conversion is observed for bicyclic **27a**, and again a complex mixture of side products prevents isolation of the product. A possible substrate bias in the poorly performing reactions will be investigated later in this chapter (Table 20).

The reaction conditions were then tested with other substrate structures. The synthesis of tetrahydrofuran derivatives and malonate-substituted cyclopentanes was investigated. The results are shown in Table 19.

Table 19: Cyclization reactions by cooperative catalysis of other substrates.

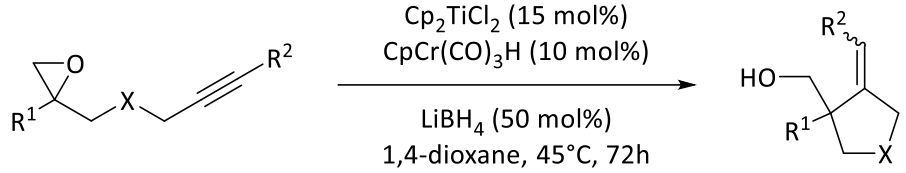

entry	substrate	product	conversion[a] [%]
1	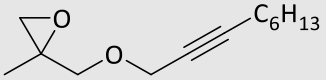 **28**	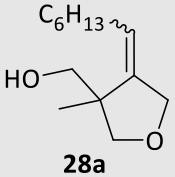 **28a**	decomposition
2	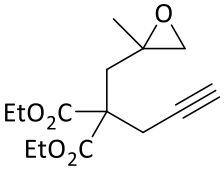 **29**	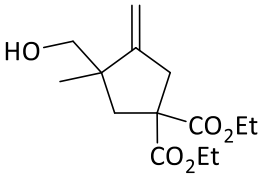 **29a**	22[b]
3	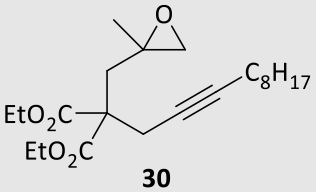 **30**	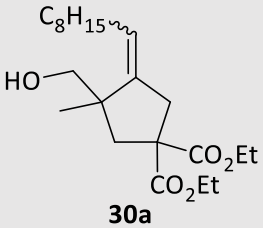 **30a**	30 (*d.r.* = 76:24)
4	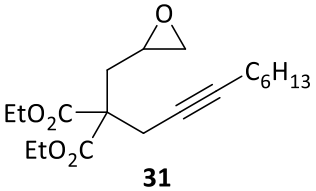 **31**	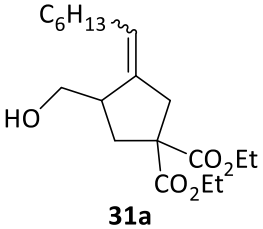 **31a**	0[c]

[a] determined by ^{1}H-NMR of crude reaction mixture. [b] performed by *Shizgal,* T = 25°C. [c] T = 25°C, 5 mol% $CpCr(CO)_3H$.

These reactions proceeded less successfully than the pyrrolidine syntheses shown above. Even under the reaction conditions suitable for the synthesis of pyrrolidines, significantly lower conversions are observed for all substrates. Substrate **28** shows high reactivity with heat development upon addition, and neither the substrate nor the product was found in the crude reaction mixtures after 72 h. Substrates **29** and **30** were converted to the desired products, but only with low conversions. Even the alkyl substitution on the alkyne of **30** seems insufficiently activating. Moreover, substrate **31,** which forms a less stabilized secondary β-titanoxy radical, is not converted at all. The overall low conversions indicate that the found reaction conditions are not yet suitable for these types of substrates, although activated by the *Thorpe-Ingold* effect of the ester substituents (entries 2–4) and require further optimization.

To gain a deeper understanding of the functional group tolerance of the cooperative system and identify or rule out the possibility of a substrate bias, several substrates that yielded unsatisfactory results were cyclized under established conditions.[74,205] Therefore, these were reacted with catalytic amounts of titanocene and stoichiometric amounts of Coll·HCl and manganese (Table 20).

Table 20: Cyclizations of previously uncharacterized products using classic conditions of titanocene catalysis.

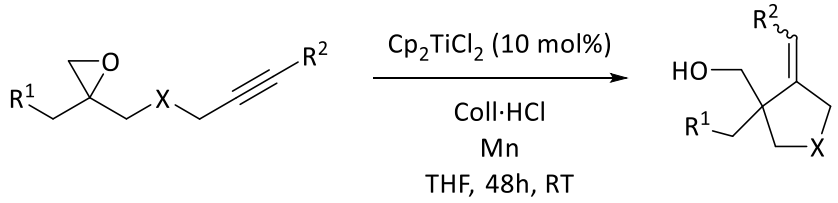

entry	substrate	product	Coll·HCl, Mn [mol%]	conversion[a] [%]	yield [%]
1	**20**	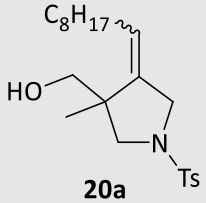 **20a**	300 300	100	86 (*d.r.* = 57:43)
2	**25**	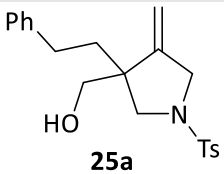 **25a**	250 200	100	46
3	**27**	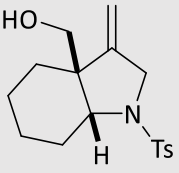 **27a**	250 200	100	94

entry	substrate	product	Coll·HCl, Mn [mol%]	conversion[a] [%]	yield [%]
4	**26**	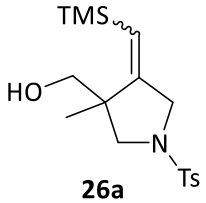 **26a**	250 150	50[b]	not isolated
5	**30**	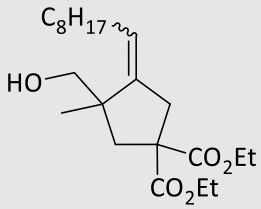 **30a**	300 300	100	26 (*d.r.* = 62:38)

[a] determined by ^{1}H-NMR of crude reaction mixture. [b] performed by *Schmickler,* 5 mol% Cp_2TiCl_2, 72h.

The test reactions of the challenging substrates under established conditions exhibited better results than those with the cooperative catalytic system. With exception of TMS-substituted **26**, for all reactions yielded clean products, mostly in acceptable to good yields. Isolation of **20** and **27** in excellent yields indicates that these are challenging substrates only for the cooperative catalytic system. Although full conversion is achieved for **25** and **30**, the presence of complex mixtures of impurities still hinders their purification and indicates a general bias in radical cyclization reactions of these substrates. The lower conversion observed for **26** and the formation of side products that prevent purification indicate that TMS-protected alkynes are not only unsuitable for the cooperative catalysis but also improper for classic titanocene-catalyzed cyclizations.

Cooperative catalysis has been demonstrated to be an efficient method for synthesizing substituted pyrrolidines, which are common motifs in natural products and drugs.[209] The double bond in the pyrrolidine-derived products enables further synthetic modifications. To showcase the attractiveness of alkynes as radical acceptors in cyclization reactions and the versatility of the resulting olefins, *Heinz* performed hydrogenations of the cyclization products using Crabtree's catalyst (Table 21). These reductions afforded the hydrogenated products in high yields and as single diastereomers.

Table 21: Diastereoselective Ir-catalyzed hydrogenations of cyclization products.

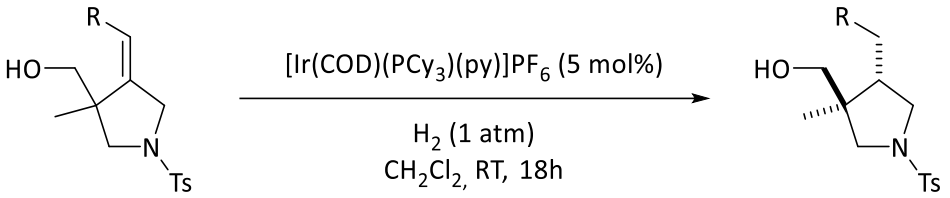

entry	R	yield [%]
1	H	97
2	Me	94
3	*p*-methoxyphenyl	87
4	*p*-(trifluoromethyl)phenyl	98

Reaction conditions: 1.00 eq. olefin, 0.05 eq. $[Ir(COD)(PCy_3)(py)]PF_6$, deoxygenated DCM (15 mL/mmol olefin), H_2 (1 atm), 18 h, 25°C. All reactions performed by *Heinz*.

As pointed out by experimental results,[185] and supported by kinetic data from the literature,[133,208] double bonds as radical acceptors are not tolerated by the cooperative system due to a fast reaction with the chromium hydride catalyst. In contrast, triple bonds have been shown to be tolerated, and cyclization reactions were demonstrated. Therefore, intermolecular additions of the β-titanoxy radical formed after the epoxide opening to triple bonds may also be feasible. Intermolecular additions to double bond containing acrylates have been investigated by *Shizgal* (Scheme 62, top),[185] but with unsatisfactory results due to the aforementioned difficulties with olefin radical acceptor substrates.

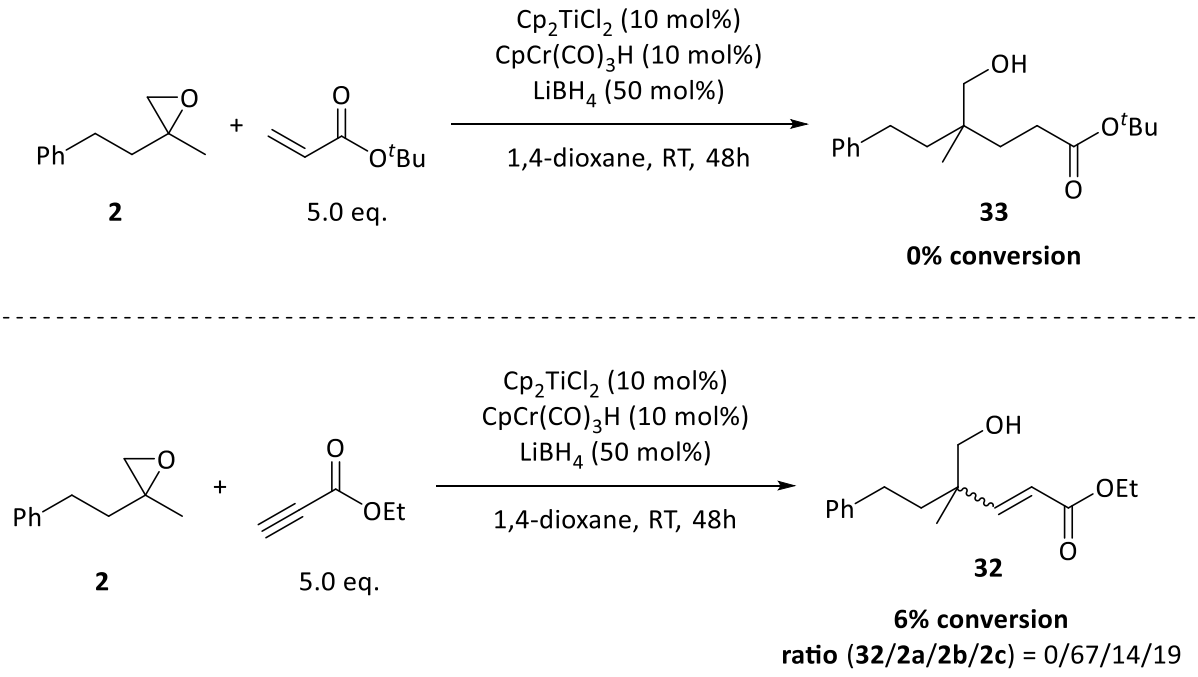

Scheme 62: Intermolecular radical addition to *tert*-butyl acrylate (top) in comparison to intermolecular radical addition to ethyl propiolate (bottom).

Unfortunately, the intermolecular addition to triple bond containing ethyl propiolate was not observed as well (Scheme 62, bottom). One aspect might be that intermolecular addition is too slow to be

efficient, or the back reaction is faster than the subsequent HAT by $CpCr(CO)_3H$. More importantly, the addition of $CpCr(CO)_3H$ or $Cp_2Ti(H)Cl$ to the electron-poor triple bond and thus consumption seems to be favored.[208] Although the addition to alkynes is slower than the addition to olefins, due to the high concentration of the reagent, this possibility cannot be neglected. Besides the absence of the addition product, only a very small conversion of the starting material, mainly to the *anti-Markovnikov* alcohol, is observed. This indicates that not only the radical addition is inhibited, but also the reduction of the epoxide is prohibited. This can be explained by the absence of both catalysts due to the proposed consumption in a side reaction.

In conclusion, the results demonstrated that the developed cooperative catalytic system is, in principle, suitable for the synthesis of cyclic molecular structures, providing potential building blocks for pharmaceutical and natural product syntheses. While several functionalized pyrrolidines were synthesized, further research is required to extend the structural variations. The following chapter will investigate the potential of cooperative catalysis for the targeted synthesis of 1,3- and 1,4-diol units.

2.7 Regiodivergent Epoxide Opening by Cooperative Catalysis

As discussed in chapter 1.4, enantiopure titanocenes can be employed for the desymmetrization of *meso*-epoxides or regiodivergent epoxide openings (REO).[67,90] When *meso*-epoxides are opened using an enantiopure *Kagan* complex, one enantiomer of the alcohol can be synthesized with high enantioselectivity. In the REO of unbiased enantiopure 1,2-disubstituted epoxides using the L- or D-*Kagan* complex (Figure 14), the 1,3- or 1,4-regioisomer is obtained while the configuration of the epoxide's stereocenter is retained. This is because the catalyst is capable of discriminating between the two C–O bonds of the epoxide, despite being electronically similar. This enables the selective cleavage of one of the C–O bonds through the steric interactions of one of the menthyl substituents. Therefore, the REO allows the synthesis of two regioisomers of difunctionalized molecules in enantiopure form at will from a common starting material. Investigations by *Funken* with various hydrogen atom donors have revealed that only the potent $^nBu_3SnH$ led to satisfactory results in the REO under established conditions using chemical reduction.[210] This highlights the necessity for further improvement regarding the hydrogen atom donor system.

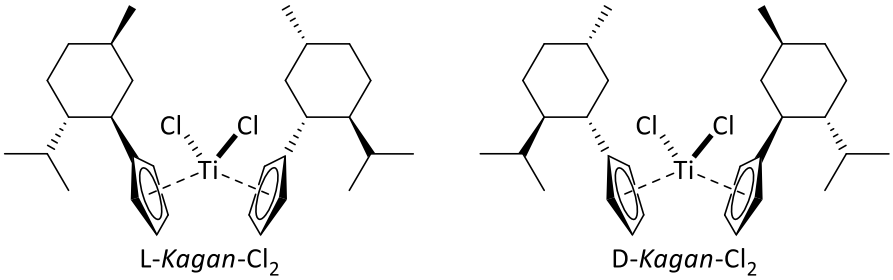

L-*Kagan*-Cl_2 D-*Kagan*-Cl_2

Figure 14: Both enantiomers of the *Kagan* complex.

The borohydride systems for reductive epoxide openings identified in this work were initially tested by replacing the achiral Cp_2TiCl_2 with D-*Kagan*-Cl_2 (Table 22). To take a potentially slower reaction into account, a reaction time of 72 h was selected for all reactions. Epoxide **34** was selected as benchmark substrate for the optimizations as it is readily accessible from ricinoleic acid, which is commercially available as enantiomerically pure natural product.

Table 22: Regiodivergent epoxide opening with previously identified conditions of the reductive epoxide opening.

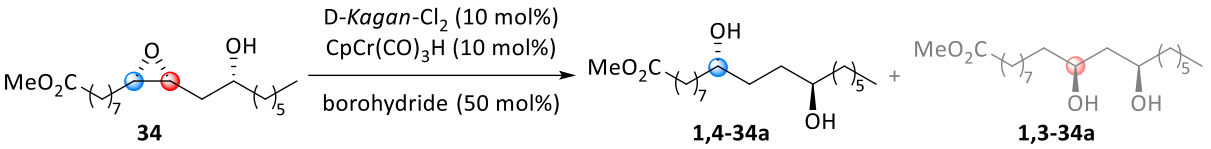

34 **1,4-34a** **1,3-34a**

entry	borohydride	solvent	T [°C], t [h]	conversion[a] [%]	*r.r.*[a] (1,4:1,3)
1	$NaBH_4$	THF	45, 72	38	>99:<1
2[b]	KBH_4	THF	25, 72	25	>99:<1
3[c]	$LiBH_4$	1,4-dioxane	25, 72	36	>99:<1
4[c]	$LiBH_4$	THF	25, 72	6	>99:<1

[a] determined by ^{13}C-NMR of crude reaction mixture. [b] additive: 5 mol% LiCl. [c] performed by *Shizgal*.

The previously identified conditions of the reductive epoxide openings did not yield the desired results from the outset. The conversions for the initial three established systems tested are in the range of 30% (entries 1–3). As expected, $LiBH_4$ in THF exhibited a remarkably low conversion (entry 4). This is presumably due to the deactivation of the catalyst as titanocene borohydride species, as previously described in chapter 2.3. However, in all cases only conversion to the 1,4-diol was observed, which aligns with the expected selectivity of the D-*Kagan* complex and indicates the viability of REO reactions under cooperative conditions. Given the notable disparity in reactivity between the *Kagans* complex and titanocene dichloride, a new screening process for this specific type of reaction was deemed necessary.

The substantial impact of the anionic ligands present in the *Kagan* titanocene on the reactivity observed in the REO has been investigated by *Funken*.[210] Consequently, in addition to the *Kagan* chloride (*Kagan*-Cl_2), the *Kagan* bromide (*Kagan*-Br_2) and *Kagan* tosylate (*Kagan*-$(OTs)_2$) complexes were subjected to test reactions. To account for the potential reduced reactivity of the *Kagan* complexes, reactions with strong reducing $LiBH_4$ in THF were conducted (Table 23), although these conditions were found not optimal for the previous reductive epoxide openings (Table 11).

Table 23: Influence of the *Kagan* complex's anionic ligands in the reaction with $LiBH_4$ in THF.

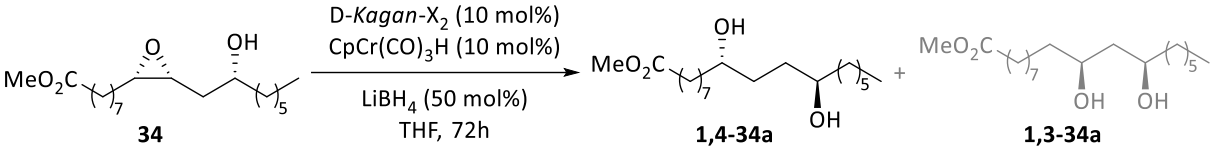

entry	X	T [°C]	conversion[a] [%]	*r.r.*[a] (1,4-*anti*:1,3-*syn*)
1[b]	Cl	25	6	>99:<1
2[b]	Br	25	10	>99:<1
3[b]	OTs	25	5	>99:<1
4[b]	Cl	45	21	>99:<1
5[b]	Br	45	19	>99:<1
6[b]	OTs	45	8	>99:<1

[a] determined by ^{13}C-NMR of crude reaction mixture. [b] performed by *Shizgal*.

The observed conversions are consistently at the lower end, irrespective of the titanocene complex employed. The tosylate complex exhibited the lowest overall reactivity, particularly at elevated temperatures. The bromide and chloride complexes exhibited comparable performance and demonstrated enhanced conversion at elevated temperatures, underscoring the pivotal role of temperature in the reaction. The expected increased reactivity of the bromide in comparison to the chloride complex was not observed in this system. However, both appear to be promising candidates for further screening.

To gain insight into the reactivity of the *Kagan* complex in the presence of borohydrides with varying reactivities, a range of these were investigated. Initially, the less reducing tetrabutylammonium borohydride (^{n}Bu$_4$N)BH$_4$ and sodium cyanoborohydride $NaBH_3CN$ in THF were tested (Table 24).

Table 24: REO reactions using (^{n}Bu$_4$N)BH$_4$ in THF.

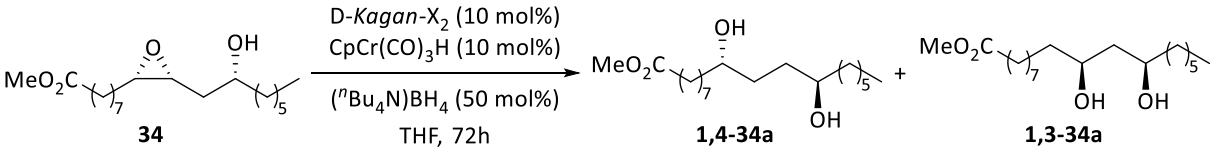

entry	X	T [°C]	conversion[a] [%]	*r.r.*[a] (1,4-*anti*:1,3-*syn*)	*d.r.*[a] (1,4-*anti*:1,4-*syn*)
1[b]	Cl	25	21	>99:<1	>99:<1
2[c]	Cl	25	24	90:10	93:7
3	Br	25	20	85:15	89:11
4[b]	Br	45	55	>99:<1	93:7
5	Br	60	50	>99:<1	>99:<1

[a] determined by ^{13}C-NMR of crude reaction mixture. [b] performed by *Shizgal*. [c] additive: 10 mol% LiCl.

The obtained conversions are overall slightly higher in comparison to the reactions with the more reactive $LiBH_4$ in THF. The addition of 10 mol% of LiCl (entry 2) or the use of *Kagan*-Br_2 instead of *Kagan*-Cl_2 (entry 3) did not result in a notable impact on the conversion. However, it did lead to a decline in regioselectivity. An increase in temperature to 45°C (entry 4) resulted in an elevated conversion rate of 55%, while a further rise to 60°C (entry 5) led to a decrease in conversion. It is noteworthy that the formation of the 1,4-*syn*-diol was observed in some cases. Following the general selectivity scheme of the REO (Scheme 24), the 1,4-*syn*-diol represents the opening product of the *anti*-substrate in reaction with the D-*Kagan* complex. However, as the substrate was employed as *syn* with a *d.r.* of 96:4 and enantiomerically pure D-*Kagan* was used, the theoretically possible amount of 1,4-*syn*-diol is exceeded, and the amount formed requires inversion or reintroduction of a stereocenter. This high ratio of the 1,4-*syn*-diol, the general scrambling of selectivities across the experiments without consistent tendencies, and the complexity of the crude NMR spectra suggest that the reaction proceeds in a partially uncontrolled manner.

A control experiment in the absence of both catalysts (Scheme 63) revealed the conversion of the starting material into a mixture of unidentified side products, accompanied by the complete disappearance of the characteristic epoxide signals in the crude NMR spectra and the complete absence of the diol products. This reactivity of $(^nBu_4N)BH_4$ suggests the potential occurrence of undesired S_N2 reactions and other side reactions in the catalytic process. Accordingly, $(^nBu_4N)BH_4$ was regarded as unsuitable for use in REO reactions under cooperative conditions.

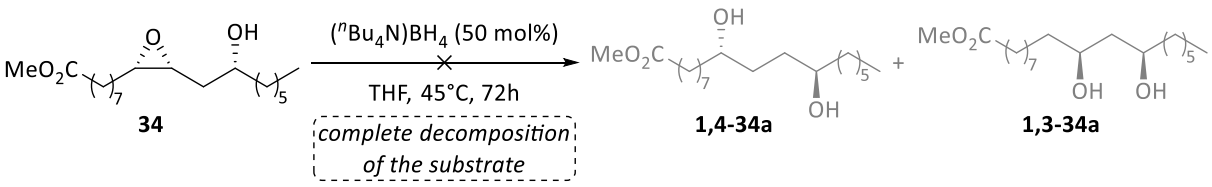

Scheme 63: Control experiment with $(^nBu_4N)BH_4$ without catalysts.

The question remains, what potential side reactions are and how they can be circumvented. Besides the already discussed nucleophilic epoxide openings, an alternative pathway towards alcohols starting from epoxides is a *Meinwald* rearrangement and subsequent reduction of the carbonyl function (Scheme 64).[211] These reactions typically require *Lewis* or *Brønsted* acidic conditions. The sequence proceeding via an achiral intermediate results in loss of the introduced configuration of the epoxide.[212–216] In the case of unbiased 1,2-disubsitituted epoxides, the regioselectivity of the cationic ring opening cannot be controlled, resulting in mixtures of four possible products.

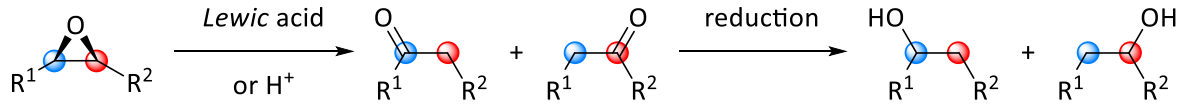

Scheme 64: *Meinwald* rearrangement followed by carbonyl reduction leading to loss of the epoxide configuration and a mixture of regioisomers. R^1 and R^2 are electronically and sterically similar.

The subsequent examination was conducted to determine the potential of the less reducing and milder $NaBH_3CN$ to circumvent possible side reactions (Table 25).

Table 25: REO reactions using $NaBH_3CN$ in THF.

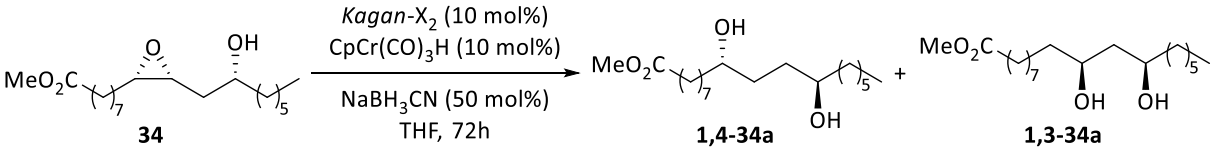

entry	*Kagan*-X_2	T [°C]	conversion[a] [%]	*r.r.*[a] (1,4-*anti*:1,3-*syn*)	*d.r.*[a] (1,4-*anti*:1,4-*syn*)
1	D-*Kagan*-Cl_2	25	22	93:7	>99:<1
2	D-*Kagan*-Br_2	25	30	88:12	>99:<1
3[b]	D-*Kagan*-Cl_2	25	24	89:11	>99:<1
4[c]	D-*Kagan*-Br_2	45	31	>99:<1	>99:<1
5	L-*Kagan*-Br_2	25	20	48:52	>99:<1

[a] determined by ^{13}C-NMR of crude reaction mixture. [b] additive: 10 mol% LiCl. [c] performed by *Shizgal*.

Fortunately, the 1,4-*syn*-diol was no longer detectable in any of the reactions conducted with $NaBH_3CN$. In comparison to the chloride *Kagan* complex, the bromide complex displays enhanced reactivity but diminished regioselectivity at room temperature (entries 1–2). The addition of 10 mol% LiCl (entry 3) did not result in enhanced conversion, but it led to a reduction in regioselectivity. This allows the assumption that the *Lewis* acidic LiCl in THF promotes only an unselective epoxide opening here. Similarly, increasing the reaction temperature to 45°C (entry 4) did not result in an improvement of the system. While the use of the L-enantiomer of the *Kagan* complex should lead to formation of **1,3-34a**, only a ratio of approximately 50:50 was observed (entry 5), which is considerably below the desired selectivity, indicating that the selectivity may be influenced by additional factors. The overall low conversions and only moderate selectivities indicate that $NaBH_3CN$ is not an optimal candidate as well.

Although moderately reducing borohydrides were employed, no conditions were identified that consistently yielded good selectivities. More importantly, sufficient conversions have thus far remained inaccessible. Therefore, reducing the reactivity of the borohydride while continuing to use THF as a solvent proved to be ineffective. Instead, considering again the same manipulation of using a stronger reducing borohydride including a stronger *Lewis* acidic cation, but 'buffered' by the solvent, might prove advantageous. Thus, the combination of $LiBH_4$ and 1,4-dioxane, which was successfully employed in the reductive opening of epoxides beforehand, was examined here (Table 26).

Table 26: REO reactions using $LiBH_4$ in 1,4-dioxane.

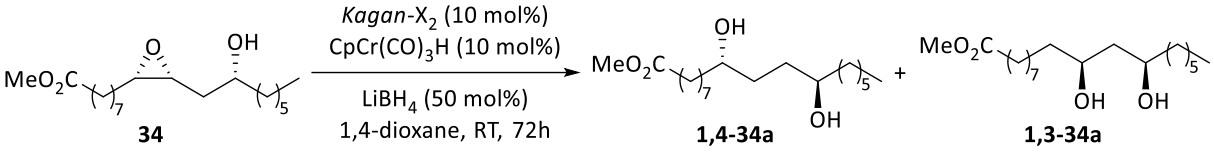

34 **1,4-34a** **1,3-34a**

entry	*Kagan*-X_2	conversion[a] [%]	*r.r.*[a] (1,4-*anti*:1,3-*syn*)
1[b]	D-*Kagan*-Cl_2	36	>99:<1
2[b]	D-*Kagan*-Br_2	25	>99:<1
3[b]	L-*Kagan*-Cl_2	17	5:95

[a] determined by ^{13}C-NMR of crude reaction mixture. [b] performed by *Shizgal*.

The reactions with the D-enantiomers of the chloride and bromide *Kagan* complex (entries 1–2) proceeded with moderate conversions, but exclusive formation of the 1,4-*anti*-diol was detected. Using the L-*Kagan*-Cl_2, resulted mostly in formation of **1,3-34a** with an acceptable *r.r.* of 95:5. However, the lower conversion and worse regioselectivity compared to the reaction with the D-enantiomer indicate a certain substrate bias and an inherent preference of the opening step towards formation of the 1,4-regioisomer, which might be based on steric interactions. The promising results of these test reactions were the foundation for further optimization efforts.

First, the reaction time was again maintained at 72 h to avoid interference with the potentially slow reaction. Furthermore, the reaction temperature was maintained at room temperature initially to prevent any selectivity issues. Instead, the impact of the catalyst loading was examined first to identify the most suitable reaction conditions (Table 27).

Table 27: Influence of the catalyst loadings.

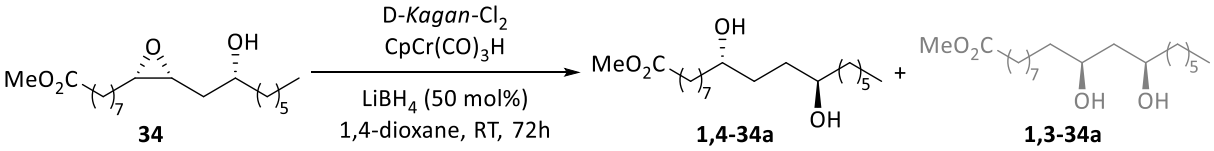

34 **1,4-34a** **1,3-34a**

entry	D-*Kagan*-Cl_2 [mol%]	$CpCr(CO)_3H$ [mol%]	conversion[a] [%]	*r.r.*[a] (1,4-*anti*:1,3-*syn*)
1[b]	10	10	36	>99:<1
2	20	10	55	>99:<1
3	10	20	26	>99:<1
4	20	20	86	>99:<1
5[b,c]	20	20	81	>99:<1

[a] determined by ^{13}C-NMR of crude reaction mixture. [b] performed by *Shizgal*. [c] 100 mol% $LiBH_4$

The reaction conversion was successfully increased to 86% while maintaining the regioselectivity by doubling the loading of the D-*Kagan*-Cl_2 and $CpCr(CO)_3H$ (entry 4). Increasing the concentration of one catalyst individually (entries 2–3) did not achieve the same outcome. Nevertheless, increasing the titanocene loading individually demonstrated a substantial beneficial impact. As already observed in previous screenings, a higher $LiBH_4$ concentration (entry 5) had a slightly detrimental effect, likely due to the deactivation of the titanocene by formation of a titanocene-borohydride species. Although the near-complete conversion was encouraging, the high loadings of titanocene and sensitive $CpCr(CO)_3H$ diminished the efficiency and atom economy of the reaction. Instead, to further optimize the process, additives were employed to accelerate the activation of the less reactive *Kagan* complex and also to stabilize the active titanocene species, as decomposition could occur over the 72-hour reaction time. The selection of the additive was crucial to achieve the optimal balance between stabilization and the avoidance of any inhibitory effects on the reaction.

Sulfonamides are, like squaramides, ureas, or thioureas, examples of so-called anion receptors. These receptors are capable of reversibly abstracting halide ions from $[Cp_2TiX_2]^-$ through hydrogen bonding, forming the catalytically active species Cp_2TiX.[217–219] Their binding abilities are increased by substitution with electron-withdrawing groups, such as trifluoromethyl. Thioureas and squaramides have previously been employed with success in catalytic radical arylation with electrochemical activation of Cp_2TiCl_2.[217,219] Similarly, the sulfonamide anion receptors shift the equilibrium from $[Cp_2TiX_2]^-$ to Cp_2TiX during the formation of the catalytically active species through anion abstraction. The formation of such a supramolecular complex between a sulfonamide and the *Kagan* complex is shown in Figure 15.

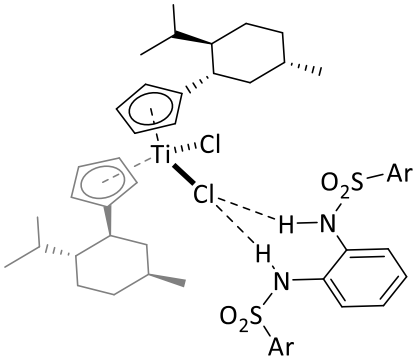

Figure 15: Supramolecular *Kagan*-sulfonamide complex during catalyst activation.[220]

Representatives of sulfonamides, which were also investigated as additives in the cooperative REO systems with the $LiBH_4$ and 1,4-dioxane are shown in Figure 16.

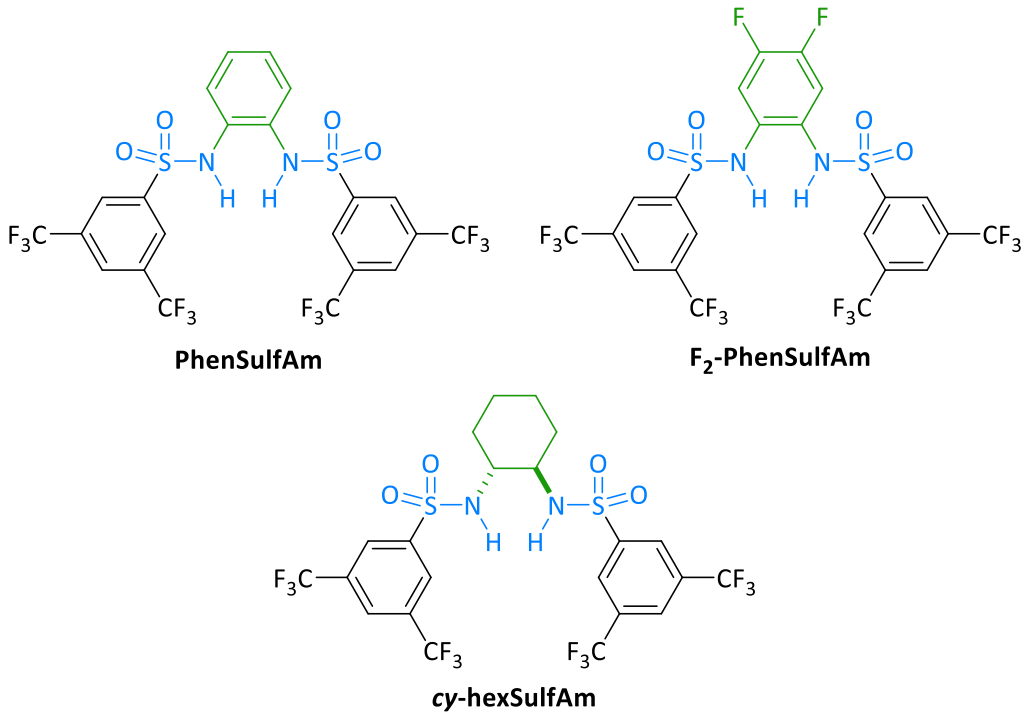

Figure 16: Anion receptors from the class of sulfonamides.

In addition to their role as halide ion acceptors, sulfonamides can form supramolecular complexes with the catalytically active Cp_2TiX, thereby forming stabilizing *resting states*, like Coll·HCl or LiCl introduced in chapter 2.4. Sulfonamides stabilize Ti(III) centers through hydrogen bonding and coordination by an oxygen atom of the sulfonyl group. This increases the electron density at the titanium center and occupies the vacant coordination site. The stabilization calculated through DFT computations is comparable to that of Coll·HCl in the case of sulfonamide **PhenSulfAm**.[218,221] Electrochemical experiments demonstrated that the electron density at the titanium is increased by the coordination, and the redox potential of the titanium complex is advantageously shifted to more negative values.[218] The supramolecular complex formed from sulfonamide **PhenSulfAm** and $Cp_2Ti^{III}Cl$ is illustrated in Figure 17.

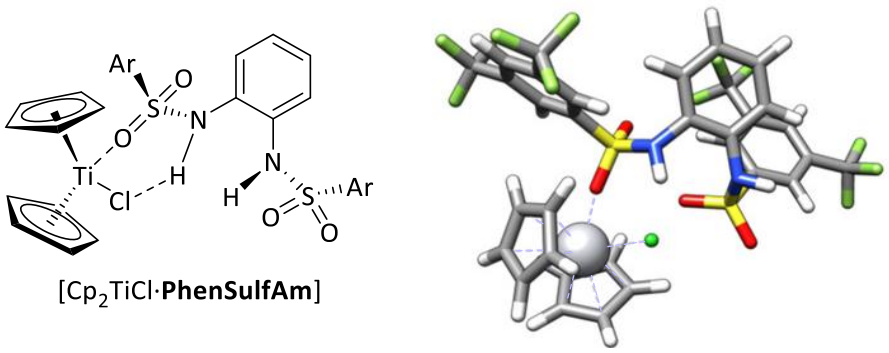

Figure 17: Stabilization of $Cp_2Ti^{III}Cl$ by supramolecular binding of sulfonamide **PhenSulfAm**. Ar = 3,5-$(CF_3)_2C_6H_3$.[218]

The three sulfonamides ***cy*-hexSulfAm**, **F_2-PhenSulfAm**, and **PhenSulfAm** were used in test reactions, and their influence on the conversion and product ratios was investigated. The results of these test reactions are summarized in Table 28.

Table 28: Screening of different sulfonamides as additives for the REO.

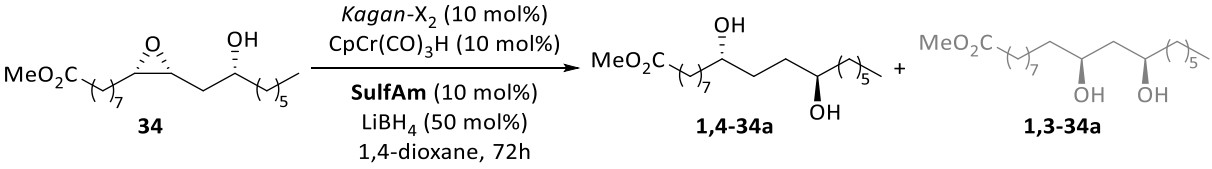

entry	*Kagan*-X_2	SulfAm	T [°C]	conversion[a] [%]	*r.r.*[a] (1,4-*anti*:1,3-*syn*)
1	D-*Kagan*-Cl_2	***cy*-hex-**	25	5	>99:<1
2	D-*Kagan*-Cl_2	**F_2-Phen-**	25	27	>99:<1
3	D-*Kagan*-Cl_2	**Phen-**	25	14	>99:<1
4	D-*Kagan*-Br_2	***cy*-hex-**	25	25	>99:<1
5	D-*Kagan*-Br_2	**F_2-Phen-**	25	32	>99:<1
6	D-*Kagan*-Br_2	**Phen-**	25	50	>99:<1
7	D-*Kagan*-Br_2	**F_2-Phen-**	45	31	>99:<1
8	D-*Kagan*-Br_2	**Phen-**	45	66	>99:<1

[a] determined by ^{13}C-NMR of crude reaction mixture.

The results demonstrate that in the presence of the sulfonamides investigated, the *Kagan*-Cl_2 complex exhibits inferior performance compared to the *Kagan*-Br_2 complex. At room temperature, the reaction proceeds most efficiently with the combination of *Kagan*-Br_2 and sulfonamide **PhenSulfAm** (entry 6), achieving 50% conversion of the starting material and no detectable 1,3-diol (compared to 25% conversion without additive, Table 26, entry 2). These findings suggest that the sulfonamide **PhenSulfAm** may be a promising candidate for facilitating the reaction. Subsequently, the reaction was conducted at a higher temperature. At 45°C, the D-*Kagan*-Br_2 still demonstrated superior performance in combination with **PhenSulfAm** (entry 8), achieving a conversion of already 66%.

In light of the results using the sulfonamide additives and the previously identified beneficial influence of a higher loading of the titanocene catalyst, an examination was conducted on the combination of the additive **PhenSulfAm** and the catalyst loading (Table 29).

Table 29: REO reactions using **PhenSulfAm** in combination with different catalyst loadings and reaction temperatures.

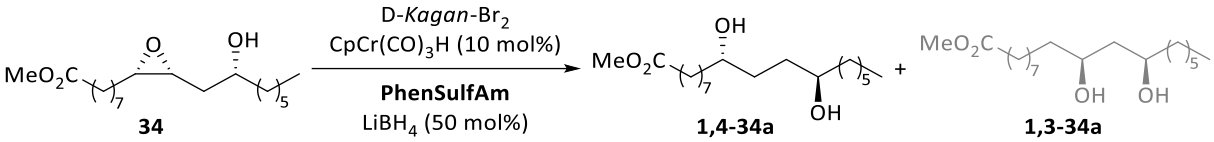

entry	D-*Kagan*-Br_2 [mol%]	PhenSulfAm [mol%]	T [°C]	conversion[a] (isolated yield) [%]	*r.r.*[a] (1,4-*anti*:1,3-*syn*)
1	15	15	25	62	>99:<1
2	10	10	45	66	>99:<1
3	15	15	45	100 (56)[b]	>99:<1
4	20	15	45	100	>99:<1
5[c]	20	15	45	94	>99:<1
6[d]	15	15	45	100	>99:<1

[a] determined by ^{13}C-NMR of crude reaction mixture. [b] isolated in *d.r.* = >99:<1, *r.r.* = >99:<1. [c] 100 mol% $LiBH_4$. [d] reaction time: 48 h.

An increase in both the catalyst and additive loading, while maintaining the temperature at 25°C (entry 1), did not result in satisfactory reaction conversion. However, performing the reaction at 45°C and with a titanocene and additive loading of 15 mol% each finally resulted in complete conversion with only **1,4-34a** being detected (entry 3). The diastereomerically pure compound **1,4-34a** was isolated from this reaction in 56% yield. An additional increase in the titanocene loading to 20 mol% yielded the same reaction conversion. An increase in the loading of $LiBH_4$ 100 mol%, resulted in a slight reduction in conversion, as it has been observed several times during the optimization process. Ultimately, reduction of the reaction time to 48 h (entry 6), resulted in full conversion as well for this substrate.

As sufficient conditions for the REO yielding the 1,4-product were identified, these were subsequently tested for the opening to the 1,3-regioisomer using the L-*Kagan* complex (Table 30).

Table 30: REO reactions under optimized conditions using the L-*Kagan*-Br_2.

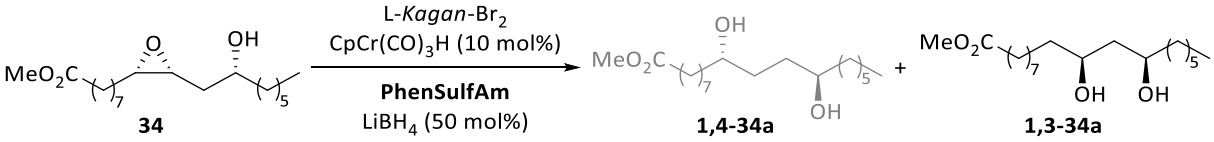

entry	L-*Kagan*-Br_2 [mol%]	PhenSulfAm [mol%]	t [h]	conversion[a] (isolated yield) [%]	*r.r.*[a] (1,4-*anti*:1,3-*syn*)
1	15	15	48	50	1:99
2	15	15	72	63	1:99
3	20	15	72	100 (32)[b]	6:94

[a] determined by ^{13}C-NMR of crude reaction mixture. [b] isolated in *d.r.* = >99:<1, *r.r.* = >99:<1.

The identical conditions that resulted in a complete reaction with the D-*Kagan*-Br_2, did not yield an equivalent outcome with the L-*Kagan*-Br_2. After 48 h only 50% conversion and after 72 h 63% were observed (entries 1–3). Nevertheless, with a titanocene loading of 20 mol%, full conversion to **1,3-34a** was achieved with an *r.r.* of 94:6. These results demonstrate the effectiveness of the cooperative catalytic conditions in achieving the desired regioselectivity of epoxide opening, which is directed by the absolute configuration of the titanocene catalyst. However, it is again evident that the opening to the 1,3-product is more difficult than the opening to the 1,4-product. This suggests a partial substrate control in the otherwise catalyst-controlled reaction. This discrepancy may be due to steric interactions with the bulkier *Kagan* complex or possible formation of 6-membered ring intermediates containing a boron and the two oxygen atoms of the 1,3-diol. These hard to cleave intermediates may result in lowered yield due to loss during the aqueous work-up or the purification. However, these species could not be isolated or detected certainly. Subsequently, the identified reaction conditions were applied to other substrates, starting with substituted ricinolate derivatives (Table 31).

Table 31: REO reactions under cooperative conditions.

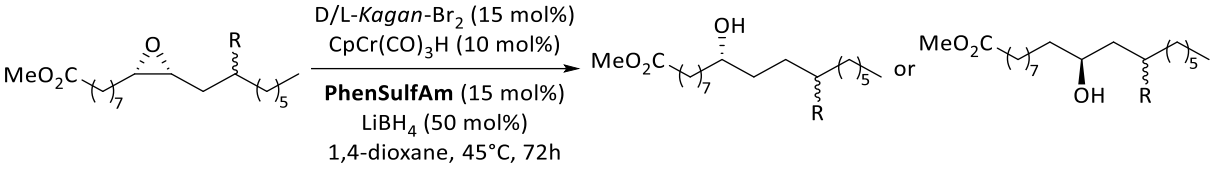

entry	substrate	*Kagan*-Br_2	product	yield [%]
1[a]	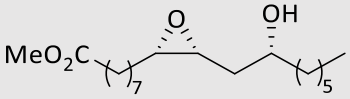 *e.r.* = >99:<1, *d.r.* = 94:6 **34**	D	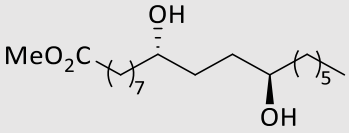 *r.r.* = >99:<1, *d.r.* = >99:<1 **1,4-34a**	78
2[a]	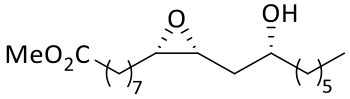 *e.r.* = >99:<1, *d.r.* = 94:6 **34**	L	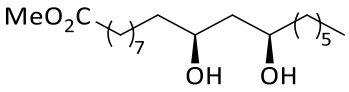 *r.r.* = >99:<1, *d.r.* = >99:<1 **1,3-34a**	57
3[a]	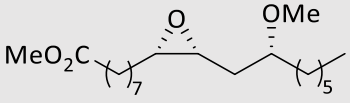 *e.r.* = >99:<1, *d.r.* = 94:6 **35**	D	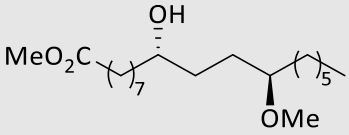 *r.r.* = >99:<1, *d.r.* = >99:<1 **1,4-35a**	78
4[a]	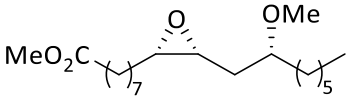 *e.r.* = >99:<1, *d.r.* = 94:6 **35**	L	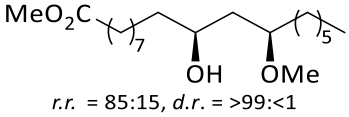 *r.r.* = 85:15, *d.r.* = >99:<1 **1,3-35a**	73

entry	substrate	*Kagan*-Br_2	product	yield [%]
5[a]	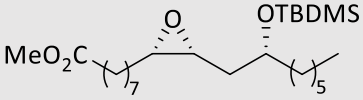 *e.r.* = >99:<1, *d.r.* = 94:6 **36**	D	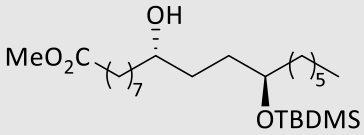 *r.r.* = >99:<1, *d.r.* = >99:<1 **1,4-36a**	81
6[a]	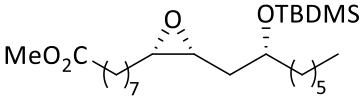 *e.r.* = >99:<1, *d.r.* = 94:6 **36**	L	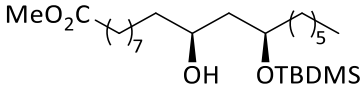 *r.r.* = 80:20, *d.r.* = >99:<1 **1,3-36a**	70
7[a]	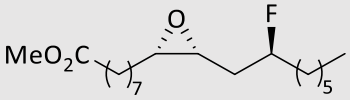 *e.r.* = >99:<1, *d.r.* = >99:<1 **37**	D	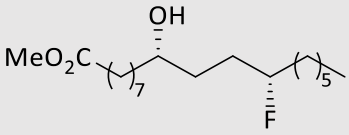 *r.r.* = 96:4, *d.r.* = >99:<1 **1,4-37a**	80
8[a]	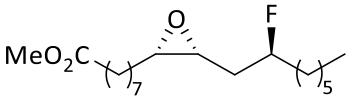 *e.r.* = >99:<1, *d.r.* = >99:<1 **37**	L	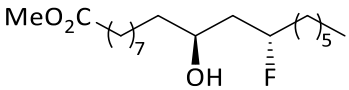 *r.r.* = 95:5, *d.r.* = >99:<1 **1,3-37a**	63

[a] performed by *Heinz*.

The results show that all the employed methyl ricinoleate derivatives could be reacted with full conversion using the optimized conditions both with the L- and the D-*Kagan* complex. The regioselectivities for the reactions to the 1,4-products were excellent in all cases. However, as already observed for **1,3-34a** during the optimization process, 1,3-opening products were obtained in worse regioisomeric ratios in some cases. Particularly the TBDMS-protected **1,3-36a** showed the worst ratio (*r.r.* = 80:20), likely due to increased steric demand in the β-position to the epoxide. While the 1,4-difunctionalized products were generally isolated in good yields, the 1,3-products faced significant challenges in purification. The presence of trace amounts of minor, unidentified by-products hindered purification by column chromatography, resulting in lower yields for 1,3-products. An adjustment of the purification protocol by adding 10% K_2CO_3 to the SiO_2 stationary phase resulted in increased isolated yields, although there is still room for further improvement.

Subsequently, the unprotected β-hydroxy epoxide **38** was reacted using the REO conditions (Table 32), producing **1,4-38a** and **1,3-38a** as single regioisomer and diastereomer. The non-reacting stereocenter in the β-position has been set with excellent stereoselectivity during the substrate synthesis via a HKR reaction. The REO itself features a double asymmetric process (see chapter 1.4 and Scheme 23), leading to the excellent diastereomeric ratio. Thus, as the products are diastereomerically pure and the non-reacting stereocenter has been set before, the obtained products are also enantiomerically pure. Nevertheless, the obtained yields are to be improved further as well.

Table 32: REO reactions under cooperative conditions.

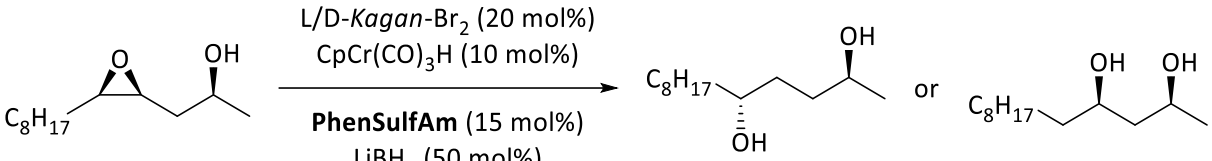

38 **1,4-38a** **1,3-38a**

entry	substrate	*Kagan*-Br_2	product	conversion (yield) [%]
1	 *d.r.* = 94:6 **38**	L	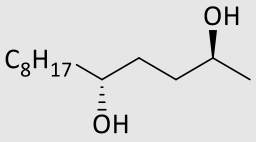 *r.r.* = >99:<1, *d.r.* = >99:<1 **1,4-38a**	100 (24)
2	 *d.r.* = 94:6 **38**	D	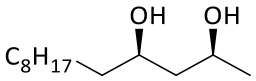 *r.r.* = >99:<1, *d.r.* = >99:<1 **1,3-38a**	100 (18)

[a] determined by ^{13}C-NMR of crude reaction mixture.

Overall, the developed method was shown to be generally applicable for the preparation of diastereomerically and enantiomerically pure 1,3- and 1,4-functionalized molecules from unprotected, fluorinated or silyl-protected enantiomerically pure substrates. Remarkably is the tolerance towards unprotected diols, which is typically not given compared to other methods like photochemical titanocene-catalyzed REO reactions.[220] While the experimental results demonstrate the possible selective synthesis of complex molecular structures by REO in cooperative catalysis, it also indicates the need for improvements in suppressing by-product formation, and purification processes. Further understanding of the mechanism and thus managing the interactions in the formation of the 1,3-products are key challenges for the future.

To broaden the scope of application in the synthesis of enantiopure compounds, the cooperative catalytic method was applied to the desymmetrization of *meso*-epoxides, which are similar to the REO from a conceptional point of view. These were tested first by using the conditions of the reductive epoxide opening, with the *Kagan*-Cl_2 complex at room temperature, and without the halide-binding additive (Table 33).

Table 33: Desymmetrization of *meso*-epoxides under cooperative conditions at room temperature.

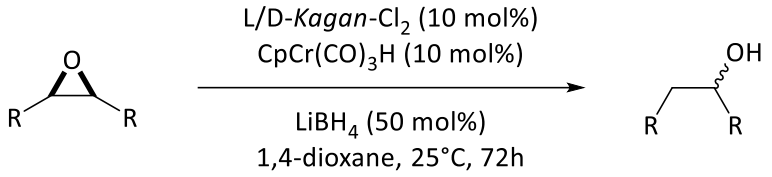

entry	substrate	*Kagan*-Cl₂	product	conversion[a] [%]	yield [%]	*e.r.*
1	 **39**	D	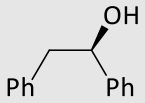 **(*R*)-39a**	50	35	73:27
2	 **39**	L	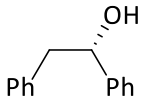 **(*S*)-39a**	64	35	75:25
3	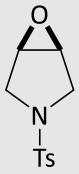 **14**	D	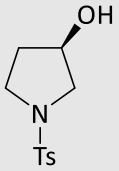 **(*R*)-14a**	43	not isolated	–
4	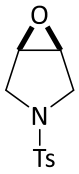 **14**	L	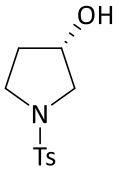 **(*S*)-14a**	38	23	70:30

[a] determined by ^{1}H-NMR of crude reaction mixture.

The obtained enantiomeric ratios of the product alcohols were in the range of about 70:30 for both the (*R*)- and the (*S*)-products, using the corresponding catalyst enantiomer. This generally confirms a catalyst-controlled desymmetrization. However, the selectivity remains suboptimal and does not reach the level of regioselectivity observed in REO reactions. Additionally, the conversions are relatively low, which can be attributed to the diminished reactivity of the *Kagan* complex. The anticipated enhancement in enantioselectivity in the reaction at room temperature was not realized. Subsequently, the desymmetrization was conducted at an elevated temperature, employing the identified conditions from REO reactions (Scheme 65).

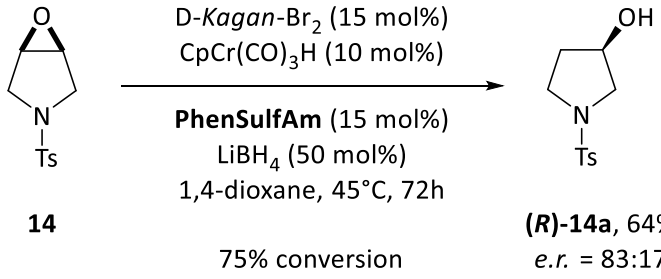

14

75% conversion

(*R*)-14a, 64%
e.r. = 83:17

Scheme 65: Desymmetrization of *meso*-**14** under the cooperative conditions of the REO.

The use of the *Kagan* bromide, addition of the halide binder, and an elevated temperature had a beneficial effect on the desymmetrization as well. Although still no complete conversion was observed, the yield was increased to 64% with an *e.r.* of 83:17. The result has to be compared to the previous analogue experiment performed by *Panfilova* using the $NaBH_4$ and THF system with the D-*Kagan*-Cl_2 at 40°C, which delivered (*R*)-**14a** in 72% yield and *e.r.* = 69:31.[160] It becomes evident that although the enantiomeric ratio was improved in the recent experiment, the difference is not highly. The question remains if the *meso*-epoxides are not well suited for the cooperative catalytic conditions, as the REO reactions shown above proceeded generally with high regioselectivities of the epoxide ring-opening. Also, typically better enantiomeric ratios were obtained in the desymmetrization of *meso*-epoxides with established chemical reduction (Zn, Coll·HCl, 1,4-CHD).[87]

In the investigated conceptual combination of REO and cooperative catalyst, a versatile new tool was developed for the construction of diastereomerically and enantiomerically pure 1,3- and 1,4-units. This approach also provided valuable mechanistic insights. The excellent regioselectivity observed in most epoxide openings, with retention of the epoxide's stereocenter configuration, clearly contradicts a mechanism involving a sequence of *Meinwald* rearrangement and subsequent reduction of the carbonyl group. As outlined in Scheme 64, such a mechanism would lead to a mixture of regioisomers in the opening of unbiased 1,2-disubsitutued epoxides and would not preserve the configuration of the epoxide. Isolation of the REO products as single diastereomers in the optimized system supports the proposed cooperative mechanism and disproves the alternative pathway. The sulfonamide **PhenSulfAm** was found to play an essential role by contributing to catalyst stabilization and activation, particularly by accelerating chloride abstraction. The advantages of the REO under cooperative catalytic conditions are evident compared to the old system. Both monosilyl-protected and unprotected diols can be synthesized with high selectivities. However, purification of the products remained challenging in some cases and needs to be improved to enhance the reliability. Additionally, this method shows significant improvements in sustainability, as it requires only stoichiometric quantities of $LiBH_4$, eliminating the need for (over)stoichiometric amounts of manganese, Lut·HCl, and the toxic $^{n}Bu_3SnH$.

2.8 Alternative Hydrogen Atom Transfer Catalysts

A principal drawback of the presented system remains the handling of the sensitive HAT catalyst $CpCr(CO)_3H$. The complex is highly sensitivity towards oxygen and tends to lose hydrogen even at room temperature. Therefore, the synthesis and all reactions need to be carried out in an inert atmosphere and in deoxygenated solvents, and storage at low temperatures is required. To improve the practicability but also to gain deeper understanding of the nature of the cooperative process and the interplay of transition metal catalysts, the need for improved or alternative HAT catalyst is obvious.

A first approach was to modify a ligand of $CpCr(CO)_3H$. A straightforward modification is exchanging the cyclopentadienyl ligand and use the bulkier and more electron-rich pentamethylcyclopentadienyl ligand (Cp* = C_5Me_5) instead. As discussed in detail in 1.6, the $Cp^*Cr(CO)_3H$ exhibits different properties that the $CpCr(CO)_3H$ analogue. To mention here is the rate of dimerization in solution of the corresponding metal-centered radicals. While the $CpCr(CO)_3\bullet$ dimerizes to a largen extend, $Cp^*Cr(CO)_3\bullet$ is almost completely present as monomer in solution.[153,154]

Although the Cr–H BDE of both complexes is almost identical (61.5 and 62.3 kcal·mol^{-1}), their ability to transfer a hydrogen atom differs (Table 34).[136] The rate constant k_H for the HAT to methyl methacrylate decreases with increasing steric bulk. Similar trends are observed for other metal hydride pairs like $Cp^*Mo(CO)_3H$ and $CpMo(CO)_3H$.[155]

Table 34: BDE values of $(C_5R_5)Cr(CO)_3H$ complexes and their rate constants k_H of the HAT to methyl methacrylate at 35°C.[136]

Metal hydride	BDE (M–H) [kcal·mol^{-1}]	k_H [10^{-3} $M^{-1}\cdot s^{-1}$]
$CpCr(CO)_3H$	61.5	4.0
$Cp^*Cr(CO)_3H$	62.3	0.62
$(C_5Ph_5)Cr(CO)_3H$	64.0	0.51

Although $Cp^*Cr(CO)_3H$ is a less potent HAT reagent value-wise, its investigation was of interest as it is not clear if the HAT from the chromium to the carbon-centered radical is the limiting step of the reaction. In contrast to the $CpCr(CO)_3H$ used before, the $Cp^*Cr(CO)_3H$ does not exhibit the same sensitivity towards temperature and was found to be stable at room temperature. Nevertheless, the compound is still highly sensitive to oxygen, and thus must be handled exclusively under inert atmosphere. The results of the initial test reactions using $Cp^*Cr(CO)_3H$ **53** instead of $CpCr(CO)_3H$ are shown in Table 35.

Table 35: Test reaction of the cooperative system with $Cp^*Cr(CO)_3H$ and Cp_2TiCl_2.

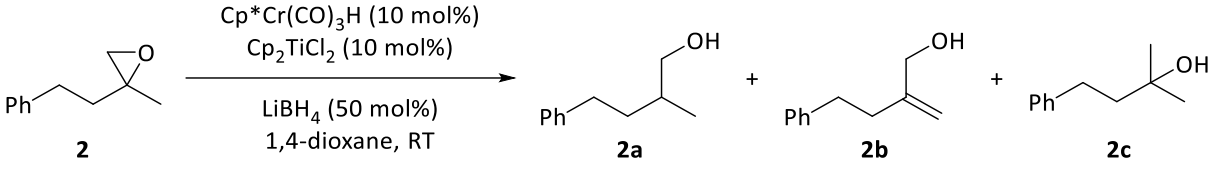

entry	t [h]	conversion[a] [%]	ratio[a] 2a [%]	2b [%]	2c [%]
1	3	47	84	9	7
2	24	79	57	7	36

[a] determined by ^{1}H-NMR of crude reaction mixture.

After a short reaction time of 3 h, a conversion rate of only 47% was observed, accompanied by the formation of small quantities of **2b** and **2c**. Also, after 24 hours, complete conversion is not achieved, and a considerable quantity of the tertiary alcohol **2c** is formed. Therefore, this catalyst system is deficient in reactivity and selectivity and unable to compete with the reaction conditions identified using $CpCr(CO)_3H$ (see Table 15). This indicates that the desired mechanism of epoxide reduction is indeed slower with the bulkier $Cp^*Cr(CO)_3H$, and that over the course of the reaction, the nucleophilic epoxide opening by $LiBH_4$ in 1,4-dioxane, which leads to **2c**, becomes predominant. Thus, the envisioned faster or at least equally selective reaction with the modified chromium HAT catalyst was not achieved.

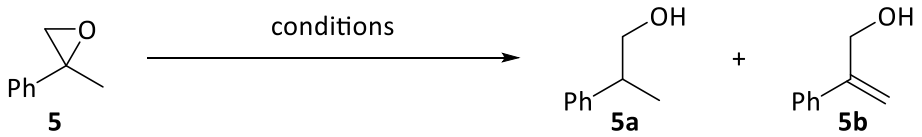

$Cp^*Cr(CO)_3H$ (10 mol%)
Cp_2TiCl_2 (10 mol%)
$LiBH_4$ (50 mol%)
1,4-dioxane, 24h, RT
conversion: 100%
78 : 22
(60% yield[a])

Cp_2TiCl_2 (10 mol%)
$NaBH_4$ (50 mol%)
THF, 48h, 40°C
conversion: 74%
97 : 3

Scheme 66: Epoxide opening of **5** using $Cp^*Cr(CO)_3H$ and Cp_2TiCl_2 vs. Cp_2TiCl_2 alone. [a] isolated as mixture of 78:22 **5a** and allylic alcohol **5b**.

Nevertheless, the reaction conditions were tested in the reaction with substrate **5** (Scheme 66). Although full conversion was achieved for this substrate, **5a** could only be isolated in a moderate yield and as an inseparable 78:22 mixture of **5a** and the allylic alcohol **5b**. The low rate of dimerization of $Cp^*Cr(CO)_3\bullet$ in solution, which results in a higher concentration of free metal-centered radicals, may be a potential explanation for the increased formation of the allylic alcohol side product. A higher concentration of free metal radicals facilitates β-hydrogen abstraction from the β-titanoxy radical, which ultimately leads to formation of the allylic alcohol, as shown earlier in Scheme 52. Although full

conversion of **5** using Cp*Cr(CO)$_3$H seems promising, the high reactivity of this substrate has to be taken into account. In a previous reaction of **5** with Cp_2TiCl_2 and $NaBH_4$ at 40°C without a second catalyst, 74% conversion, with a product ratio **5a**:**5b** = 97:3, was observed.[191]

Subsequently, the Cp*Cr(CO)$_3$H catalyst was evaluated in a cyclization reaction (Scheme 67). Again, the observed conversion rate of 71% is slightly inferior to the reaction conditions that were previously identified (see Table 17).

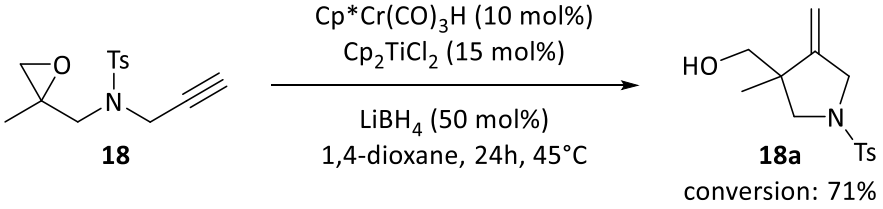

18 **18a** conversion: 71%

Scheme 67: Radical cyclization of **18** using Cp*Cr(CO)$_3$H.

While using Cp*Cr(CO)$_3$H did not lead to enhanced reactivity or results comparable to those of the previously presented systems, a working system has been achieved with the modified HAT catalyst. Despite its reduced reactivity, the catalyst offers better thermal stability, which is a step towards better handling of this reaction. However, this improvement in catalyst stability comes at the expense of reactivity, indicating that the search for a catalyst that is both easier to handle and highly reactive remains a challenge for further research.

Instead of modifying the given chromium complex, another possibility is to change the transition metal instead. However, due to the large number of transition metal hydrides and the different steric, thermodynamic and electrochemical properties, the search is not trivial. In a first study, hydride complexes of tungsten bearing *scorpionate* ligands were investigated by *Shizgal*.[185] With these functional replacements were found, although not yet satisfactory. Considering BDE values, another alternative are hydride complexes of cobalt, which often feature BDE values comparable to CpCr(CO)$_3$H (Table 36). [149,136,222]

Table 36: Bond dissociation energies of cobalt hydrides in comparison to chromium hydrides.

Metal hydride	**BDE (M–H) [kcal·mol^{-1}]**
Co(dmgBF$_2$)$_2$(H$_2$O)H	55
CpCr(CO)$_3$H	62
Cp*Cr(CO)$_3$H	62
Co(CO)$_3$PPh$_3$H	65
Co(CO)$_3$P(OPh)$_3$H	66
Co(CO)$_4$H	67

As previously discussed in chapter 2.3, and illustrated in Scheme 48 and Scheme 49, the mechanism as proposed, in principle does not require the metal hydride species of the HAT catalyst for the initial catalytic turnover. Rather, the metal hydride is formed through HAT from $Cp_2Ti(H)Cl$, giving both the metal hydride and $Cp_2Ti^{III}Cl$. Therefore, it should be possible to not add the metal hydride at onset but generate it *in situ* from a precatalyst. If a cooperative system can be found that does not require a hydride complex at onset, this would not only be advantageous from a practical point of view, but rather be another mechanistical evidence. Based on bimetallic systems that combine titanocenes with cobalt salen complexes, forming cobalt hydrides,[223] and on hydrogenations involving cobalt-based catalysts,[144] a cooperative system was envisioned where cobalt salens and similar complexes would serve as hydrogen atom transfer catalysts.

A screening of potential cobalt complexes as HAT precatalyst was conducted as part of a research exchange within the group of *de Bruin*. Amongst the investigated complexes are cobalt porphyrin, salen and salophen complexes. Salen and salophen ligands, which are formed by condensation of amines and aldehydes, belong to the class of *Shiff*-bases. As early as 1864, *Schiff* published his research on condensation reactions between aniline and aldehydes.[224] The resulting organic compounds, that were later identified to contain imines (–C=N– double bonds), marked the first synthetic description of what would become known as *Schiff*-bases. Although some complexes of *Schiff*-bases and metals have been known since the 19th century,[225,226] they were not investigated systematically from the beginning. The systematic studies on the synthesis of *Schiff*-base metal complexes were conducted by *Pfeiffer* in Bonn starting in 1931,[227,228] thereby laying the foundation for the subsequent developments in salen metal complex chemistry. Both salens and salophens (salens with phenylene backbone) form complexes with transition metals due to their tetradentate coordination site. The cobalt complexes, which were investigated here in the catalyst screening are shown in Figure 18. It must be emphasized that all cobalt complexes shown are insensitive to air and mostly bench-stable. Therefore, they bear the potential for a significant improvement in terms of handling in comparison to the air- and temperature-sensitive $CpCr(CO)_3H$.

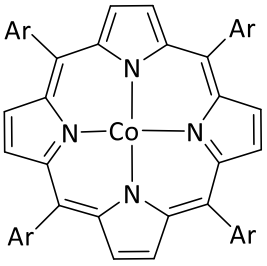

40: Ar = Ph

41: Ar = *p*-CN-C_6H_4

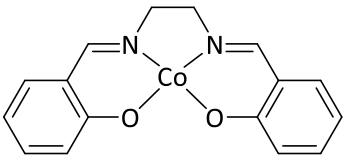

42

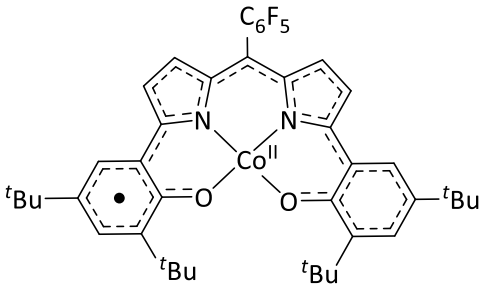

43

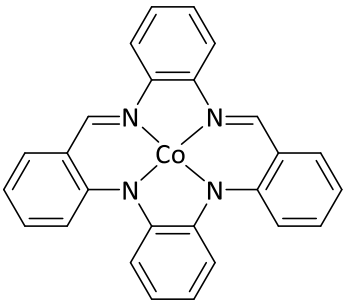

44

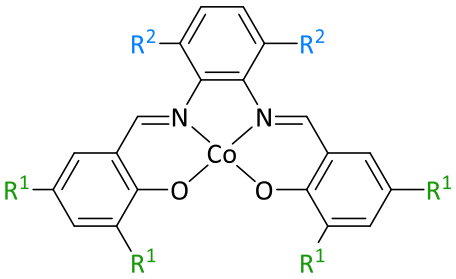

45: $R^1 = R^2 = H$

46: R^1 = Br, R^2 = H

47: R^1 = Br, R^2 = OMe

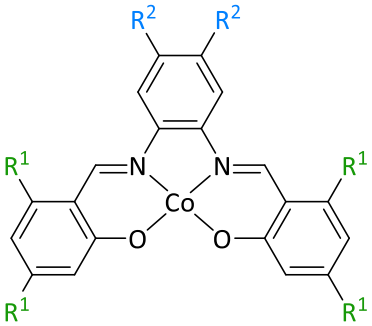

48: R^1 = OMe, R^2 = H

49: R^1 = OMe, R^2 = Cl

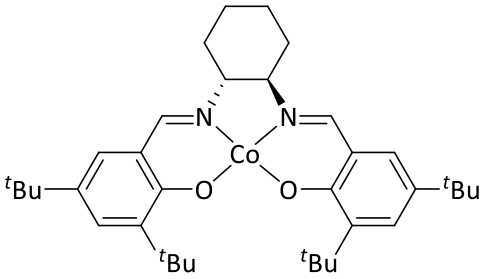

(*R*)-50

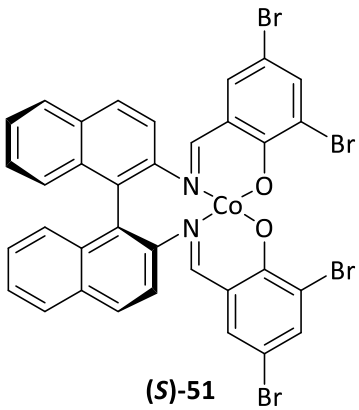

(*S*)-51

Figure 18: Cobalt complexes used in HAT catalyst screening.

The results of the screening reactions with the potential cobalt HAT catalysts are shown in Table 37. Due to the limited amounts of the catalysts, the reactions were caried out on a scale of 0.1 mmol of epoxide. The small amounts of reagents and solvents required adjusted practical execution and might

lead to results that are not fully comparable to the remaining optimization reactions in this work, that were performed on larger scales (usually 1.0 or 0.5 mmol of epoxide, see chapter 2.4). However, these results are comparable between each other and give indications about the reactivity of the cobalt catalysts.

Table 37: Screening reaction of cooperative systems with several cobalt complexes.

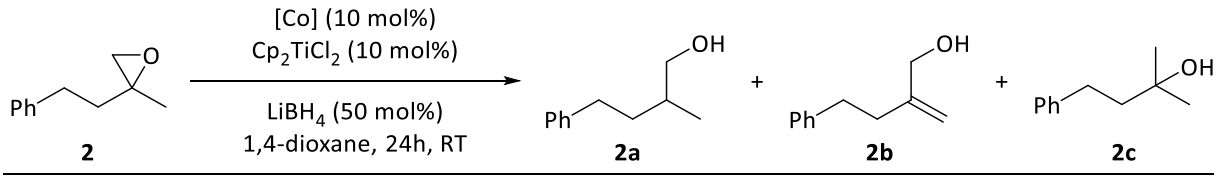

2 **2a** **2b** **2c**

entry	[Co]	conversion[a] [%]	ratio[a] 2a [%]	2b [%]	2c [%]
1	–	19	69	9	22
2	**40**	19	39	51	10
3	**41**	20	69	6	25
4	**42**	36	52	47	1
5	**43**	38	61	26	13
6	**44**	28	74	0	26
7	**45**	42	80	11	9
8	**46**	54	74	10	16
9	**47**	24	93	1	6
10	**48**	49	80	5	15
11	**49**	45	75	22	3
12	**(*R*)-50**	16	61	19	20
13	**(*S*)-51**	5	93	5	3

[a] determined by ^{1}H-NMR of crude reaction mixture. [b] reaction time: 72 h.

To enable a clearer comparison of catalyst performance, a control reaction was conducted without any cobalt catalyst. As previously noted, the titanocene alone catalyzes the epoxide opening, yielding a 19% conversion but also generating substantial amounts of byproducts **2b** and **2c** (entry 1). Attempts to enhance the reaction outcome through cooperative catalysis with porphyrin complexes **40** and **41** (entries 2–3) were unsuccessful. While **41** had no noticeable impact, **40** only significantly increased the formation of the **2b** side product.

The simplest cobalt salen, salcomine **42**, improved the conversion rate but resulted in almost equal amounts of **2a** and the inseparable **2b**. This suggests that β-hydrogen abstraction is strongly promoted by the salen complex.

Subsequent tests involved two complexes containing redox-active ligands, $Co^{II}(DPP^{\bullet 2-})$ **43** (DPP = dipyrrin-bis(*o,p*-di-*tert*-butylphenolato) and $Co(H_2Phen_2TAA)$ **44** (TAA = tetraaza[14]annulene).[229–231] The use of complex **43** led to a 20% increase in conversion compared to the control reaction, but also resulted in significant amounts of **2c** and **2b**. Complex **44**, on the other hand, showed only a 10% increase in conversion. However, interestingly, it completely suppressed the formation of **2b**, despite **2c** remaining at high levels. While these complexes displayed some catalytic activity, neither appeared to be a promising candidate.

More encouraging results were obtained with cobalt salophen complexes (entries 7–11), which feature a more rigid, planar, and aromatic backbone compared to salens. Conversion rates for these cobalt salophens ranged between 42% and 54%, with the exception of **47**. Additionally, the ratio of the desired *anti-Markovnikov* alcohol **2a** was generally above 75%. Among the salophen complexes, unsubstituted salophen **45** and those substituted with bromo or methoxy groups on the phenol ring (**46**, **48**) delivered comparable results, with moderate variations in conversion and selectivity. However, chloro- or methoxy-substitution on the aromatic backbone (**47**, **49**) seemed to have a detrimental effect on the reaction outcome. Although the additionally methoxy substituted **47** (compared to **46**) achieved a high ratio of **2a** of 93%, it suffered from low conversion. Furthermore, the additional chloro-substitution on **49** (compared to **48**) increased the formation of **2b**. Despite these observations, a clear correlation between salophen ligand substitution patterns and reaction outcomes remains elusive.

Lastly, to assess the potential for future applications in enantioselective reactions, asymmetric complexes **(*R*)-50** and **(*S*)-51** were tested. Both complexes exhibit helical chirality. The cobalt salen **(*R*)-50** is known for its use in the hydrolytic kinetic resolution (HKR) of epoxides developed by *Jacobsen*.[63,64] However, as a HAT catalyst in the cooperative catalytic system, this complex showed no significant activity compared to the titanocene alone. Complex **(*S*)-51**, anticipated to mimic the characteristics of salophen **46** while being asymmetric, appeared promising. Unfortunately, the reaction with this complex resulted in only 5% conversion, even lower than that achieved with the titanocene alone, indicating not only a lack of catalytic activity but also inhibition of the titanocene by the second complex. Based on these results, further investigations were limited to achiral complexes at this stage of the research. For a better comparison, the calculated NMR-yields for some of the investigated complexes are shown in Figure 19.

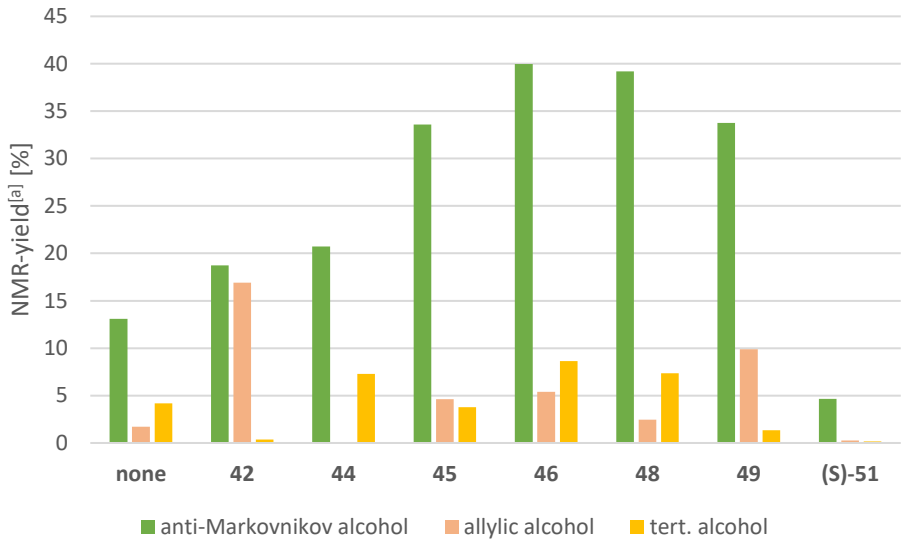

Figure 19: Comparison between some cobalt complexes in the cooperative catalysis with Cp_2TiCl_2 in reaction with **2**. [a] calculated by multiplication of respective conversion rates and product ratios.

In summary, the comparison of reactions catalyzed by salens and salophens reveals that salophens generally produced better results. This suggests that the coordination geometry around the cobalt central atom significantly influences the HAT catalyst's activity. However, the substitution pattern on the salophens had a minor impact on reaction conversions, and no clear correlation to the selectivity was observed. Among the tested cobalt complexes, particularly among the salophens, **45**, **46**, and **48** showed the best combination in terms of conversion and selectivity so far. Subsequent investigations were therefore focused on **45** and **46**.

Table 38: Screening reaction using cobalt salophen **46** in combination with different borohydrides and solvents.

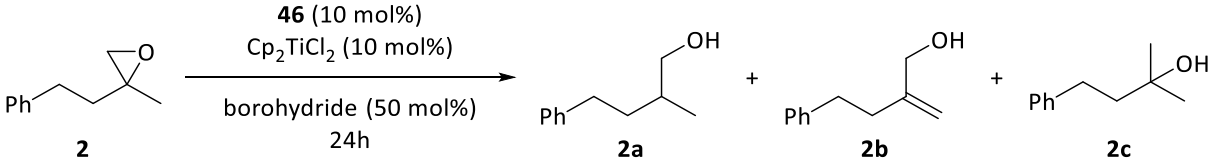

2 **2a** **2b** **2c**

entry	borohydride	solvent	T [°C]	conversion[a] [%]	ratio[a] 2a [%]	2b [%]	2c [%]
1	$LiBH_4$	1,4-dioxane	25	54	74	10	16
2	$NaBH_4$	1,4-dioxane	40	60	61	38	1
3	$NaBH_4$	THF	40	51	72	26	2

[a] determined by ^{1}H-NMR of crude reaction mixture.

To account for the presumably slower reaction with the cobalt HAT catalyst, experiments were conducted using the less reducing and less *Lewis* acidic $NaBH_4$ as the reducing agent in both 1,4-dioxane and THF (Table 38). In both solvents, 1,4-dioxane and THF, the formation of the inseparable byproduct **2b** increased significantly, therefore, no improvement was achieved under

these conditions. However, the observed absence of nucleophilic epoxide opening to **2c** when using $NaBH_4$ supports the hypothesis that the cooperative mechanism involving cobalt is rather slow and prone to being outcompeted by the nucleophilic side reaction, particularly when the stronger reductant $LiBH_4$ is used.

Table 39: Influence of the cobalt catalyst loading.

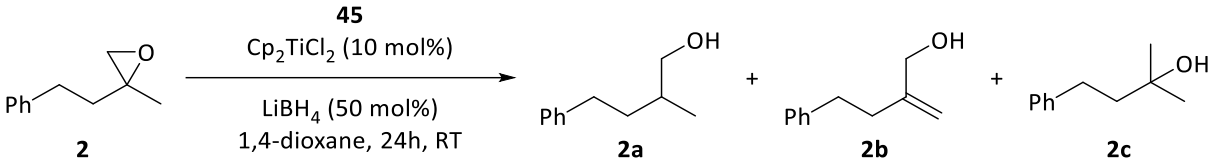

2 **2a** **2b** **2c**

entry	45 [mol%]	conversion[a] [%]	ratio[a] 2a [%]	2b [%]	2c [%]
1	5	30	83	10	7
2	10	42	80	11	9
3	20	34	72	14	14
4[b]	10	39	80	15	5

[a] determined by ^{1}H-NMR of crude reaction mixture. [b] substrate added after 30 min.

The effect of cobalt catalyst loading was subsequently examined using catalyst **45** (Table 39). Varying the catalyst loading from 5 mol% to 20 mol% resulted in only minor deviations in conversion, around 10%. The product ratio also remained consistent across different catalyst loadings. However, the best overall outcome in terms of both conversion and product ratio was observed with 10 mol% of **45**. This suggests that a 1:1 ratio of both catalysts may be optimal, similar to the cooperative system involving chromium and titanium. Also, addition of the substrate after a 30-minute activation period (entry 4) did not significantly change the reaction outcome. This activation period was intended to allow for the potential slow buildup of the cobalt hydride concentration, but the results indicate that the formation of the cobalt hydride alone is not the rate-limiting factor in this system.

A side note should be made regarding the formation of allylic alcohol, which was observed in nearly all reactions. *Lin* previously reported the isomerization of epoxides to allylic alcohols through cooperative catalysis using $Cp_2Ti^{III}Cl$ and cobalt salens.[223] Thus, the occurrence of this isomerization at least as a side reaction in the current study is not surprising. However, it is necessary to identify catalysts and conditions that can suppress this side reaction, as it has been successfully done for the chromium and titanium systems.

The catalytic conditions identified as most effective so far, using the cobalt catalyst **46**, were applied to substrate **5** (Scheme 68).

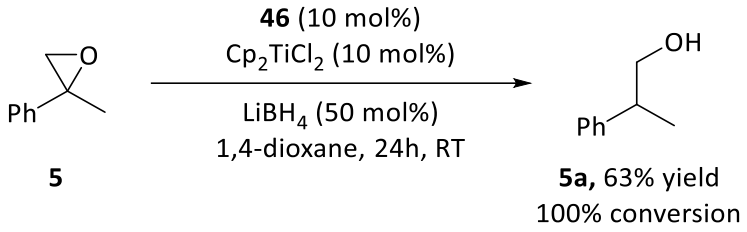

5 **5a,** 63% yield
100% conversion

Scheme 68: Opening of **5** by cooperative cobalt and titanium catalysis.

Under these conditions, full conversion of the epoxide was achieved without the formation of any allylic alcohol **5b** being detected. The desired product **5a**, was isolated in 63% yield. While this result is promising, it is important to note the high reactivity of the substrate **5** (Scheme 66). Nevertheless, the successful isolation of **5a** from the cooperative reaction involving Cp_2TiCl_2 and **46** underscores the overall effectiveness of the cooperative catalysis approach and supports the proposed mechanism, including the *in situ* formation of the cobalt hydride HAT catalyst. Although in general the reaction catalyzed by cobalt instead of chromium appears to proceed as proposed without the direct addition of the HAT catalyst as hydride, the collective data indicate a slower reaction under these conditions, suggesting that further optimization is necessary.

As another part of the research exchange, electron paramagnetic resonance (EPR) experiments were conducted to gain deeper insights into the reaction mechanism. In these experiments, spin traps PBN and DMPO were used to stabilize reactive radical intermediates by converting them into stable spin trap adducts, which can then be detected. EPR samples were collected directly from the reaction mixture under an inert atmosphere after 3 hours and 22 hours, respectively, from reactions catalyzed by **45** and Cp_2TiCl_2. Both spin traps produced similar characteristic spectra, and with the only difference between the spectra obtained after 3 hours and 22 hours being the intensity of the signals. The spectrum obtained using the PBN spin trap and sample extraction after 22 hours is shown in Figure 20.

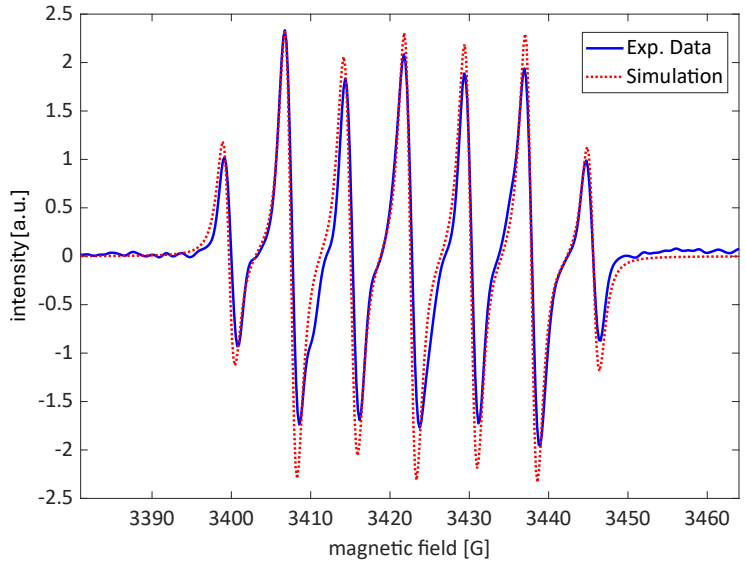

Figure 20: EPR spectrum of a sample taken directly from the reaction mixture after 22 h. Reaction conditions: 1.0 eq. **2**, 0.1 eq. **45**, 0.1 eq. Cp_2TiCl_2, 0.5 eq. $LiBH_4$, 4.0 eq. PBN, 1,4-dioxane, RT.

A comparison of the simulation parameters (*g* value = 2.0067, hyperfine coupling constants = 15.10 G, 7.86 G, line width = 1.027 G) with the *NIEHS* Spin Trap Database,[232,233] enabled identification of the spin adduct shown in Scheme 69.

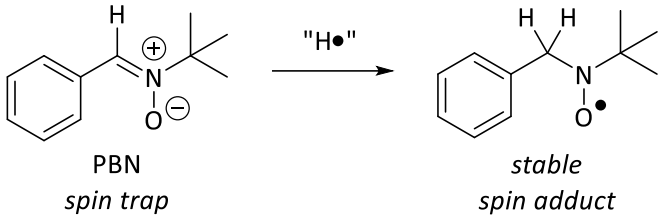

Scheme 69: Persistent radical species formed by HAT to PBN, that was identified from the characteristic EPR spectrum shown in Figure 20.

The identified spin adduct is the result of the trapping of a hydrogen atom.[233] The observed septet arises due to the hyperfine interaction between the unpaired electron and two neighboring hydrogen atoms, as well as the nitrogen atom. Unfortunately, this finding indicates that no other radical intermediates, such as the β-titanoxy radical or a metal-centered radical, could be detected in the reaction mixture. Thus, the experiment only confirms the general presence of any hydrogen atom donor. The exact source of this hydrogen atom remains elusive. It could be the cobalt hydride, the titanocene hydride, or potentially even $LiBH_4$. However, the data suggest that a purely ionic mechanism is unlikely. Further research is needed to fully elucidate the mechanistic details.

Table 40: Cooperative cobalt and titanium catalysis for H_2 activation.

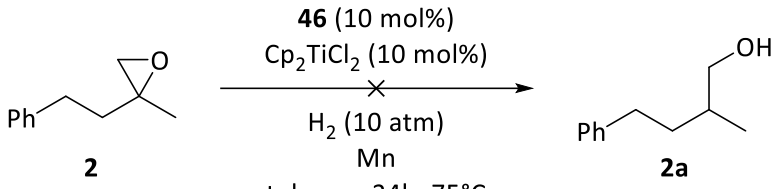

entry	Mn [mol%]	conversion[a] [%]
1	–	0
2	10	0
3	150	0

[a] determined by ^{1}H-NMR of crude reaction mixture.

Furthermore, the potential activation of H_2 by cobalt and titanium cooperative catalysis was investigated (Table 40). In analogy to the activation of H_2 catalyzed by chromium and titanium (see chapter 1.7 and Scheme 42), this catalytic system would require the cobalt complex to function not only as a HAT reagent but also as a *Brønsted* acid and a reducing agent for the titanocene catalyst.[161] Unfortunately, no reaction conversion was observed in the reactions under a 10 atm hydrogen atmosphere. Also, addition of 10 mol% or 150 mol% manganese to the reaction mixture, to facilitate

the initial or continuous reduction of Cp_2TiCl_2 did not lead to any reaction. These results suggest that, under the given conditions, the activation of H_2 by the cobalt salophen and the formation of a cobalt hydride are not feasible. Due to time constraints, no further investigations were conducted in this area.

In summary, it was demonstrated that it is mechanistically feasible to replace the sensitive $CpCr(CO)_3H$ HAT catalyst with more stable cobalt complexes. Among these, cobalt salophens showed promising results, though further research is needed to fully elucidate the underlying mechanisms and optimize the reaction conditions. In addition to their stability, cobalt salophen complexes offer the advantage of straightforward and modular synthesis (see chapter 2.9). However, a key challenge remains in balancing (pre)catalyst stability and catalytic activity. The reaction conversions and product ratios achieved with the cobalt and titanium cooperative system still fall short of those obtained with the chromium and titanium system. Therefore, the identified catalytic systems serve as a 'proof of concept' and provide a foundation for future research aimed at enhancing the practicality and accessibility of cooperative catalytic reactions.

2.9 Synthesis of Catalysts

The following chapter addresses the synthesis of the catalysts, which were an essential part of the conducted investigations. First, the challenging preparation of the chromium hydride complexes will be discussed, followed by the syntheses of the cobalt complexes and enantiomerically pure titanocenes.

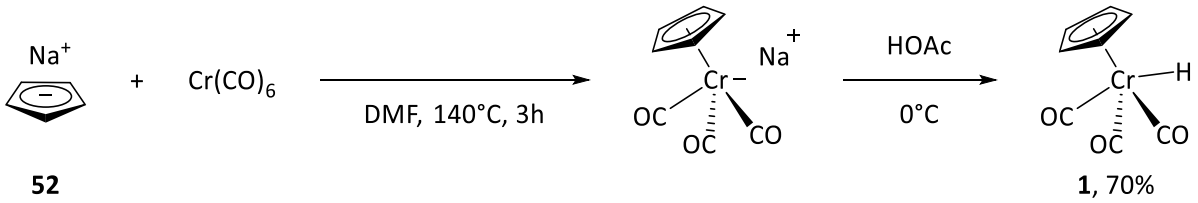

52 **1**, 70%

Scheme 70: Synthesis of $CpCr(CO)_3H$ **1**.

The synthesis of $CpCr(CO)_3H$ starts from commercially available $Cr(CO)_6$. In a one-pot synthesis, $Cr(CO)_6$ is first reacted with NaCp **52**, forming the sodium salt of $CpCr(CO)_3^-$, which is subsequently acidified using a aqueous solution of acetic acid to give the metal hydride (Scheme 70). After purification, **1** is obtained as crystalline, greenish-yellow solid (Figure 21), which is stored in a *glovebox* and at -18°C. Due to its high air- and temperature sensitivity, all synthesis and purification steps were performed using advanced *Schlenk* technique, thoroughly prepared and purified reagents, and degassed solvents, and must be performed consecutively without delays.

Figure 21: $CpCr(CO)_3H$ **1.**

Cyclopentadienyl sodium **52** was prepared by reacting freshly cracked dicyclopentadiene with sodium as shown in Scheme 71. Using this method, **52** is obtained as a white solid, indicating a higher purity compared to other protocols using NaH,[234] which is crucial for the synthesis of **1**.

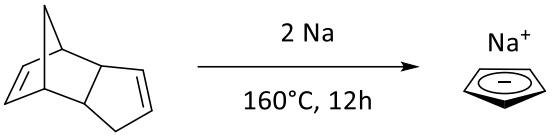

52, 89%

Scheme 71: Synthesis of NaCp **52**.

For the one-pot synthesis of $Cp^*Cr(CO)_3H$ **53** (Scheme 72), first $Cr(CO)_6$ is refluxed in MeCN to give $Cr(CO)_3(MeCN)_3$. The highly reactive nitrile complex is reacted directly with commercially available pentamethylcyclopentadiene (Cp*H) to give **53**. After purification **53** is obtained as a brownish-yellow, highly air sensitive solid and is stored in a *glovebox*. In contrast to $CpCr(CO)_3H$, $Cp^*Cr(CO)_3H$ exhibits significantly reduced sensitivity towards temperature, allowing it to be stored at RT.

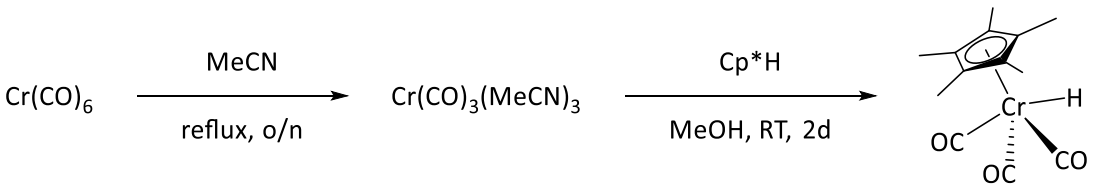

53, 30%

Scheme 72: Synthesis of $Cp^*Cr(CO)_3H$ **53**.

Salen and salophen ligands can be easily and modularly synthesized in high yields by condensation of diamines and aldehydes (Table 41), which are both commercially available in a wide variety of substitution patterns.

Table 41: Synthesis of ligands **54** and **(*S*)-55**.

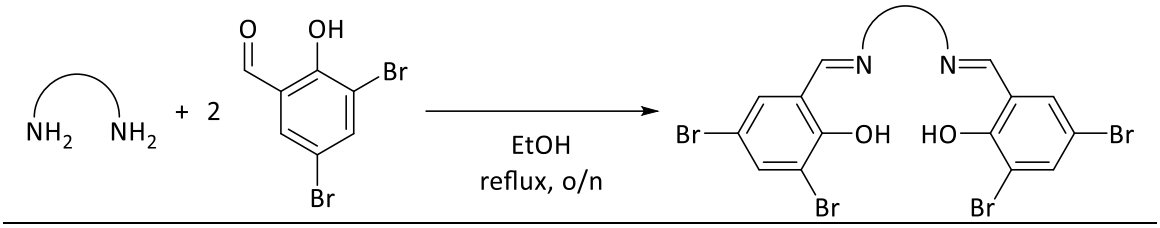

diamine	**ligand**
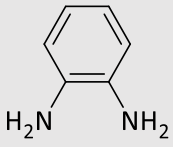	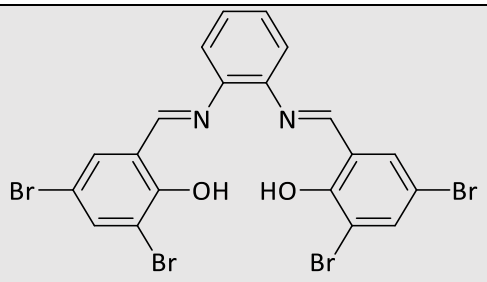 **54**, 94%
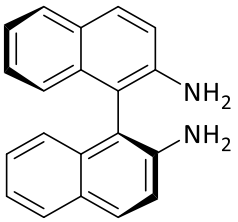	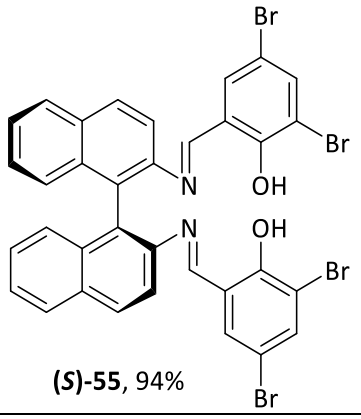 **(*S*)-55**, 94%

Ligands **56**, **57** and **58** were synthesized and provided by *InCatT B.V.*, Amsterdam. Ligand **59** was synthesized and provided by the group of *de Bruin*.

Metalation of the tetradentate ligands was carried out using $Co(OAc)_2 \cdot 4H_2O$, giving the cobalt complexes generally in high yields (Table 42). Lower yields (**44** and **48**) were the result of the high solubility in MeOH and thus partial loss during the purification.

Table 42: Synthesis of cobalt complexes by metalation with $Co(OAc)_2 \cdot 4H_2O$.

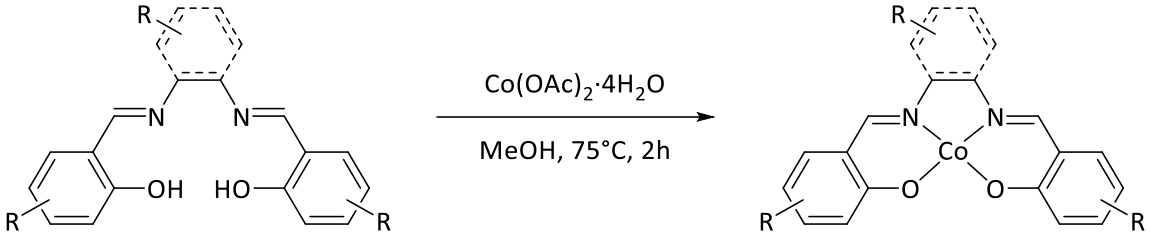

ligand	cobalt complex
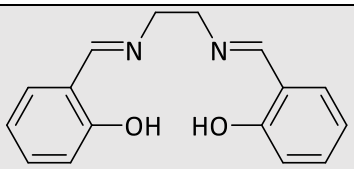 **56**	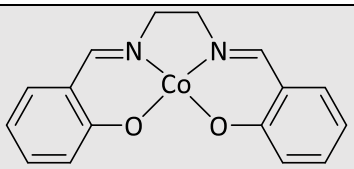 **42,** 71%
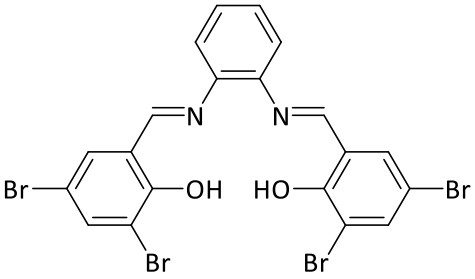 **54**	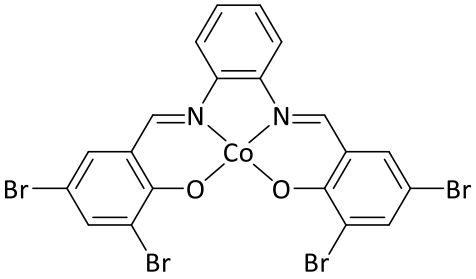 **46**, 97%
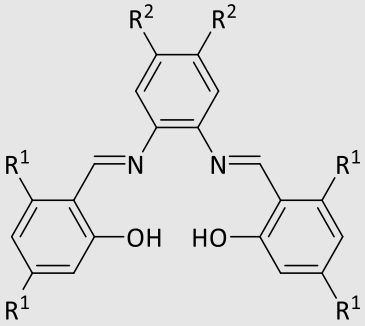 **57**: R^1 = OMe, R^2 = H **58**: R^1 = OMe, R^2 = Cl	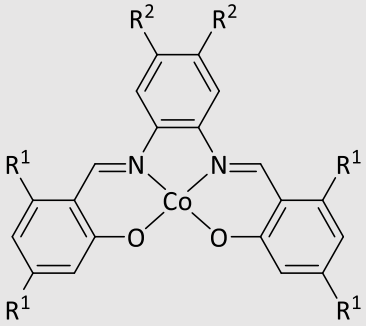 **48**: R^1 = OMe, R^2 = H, 10% **49**: R^1 = OMe, R^2 = Cl, 65%

ligand	cobalt complex
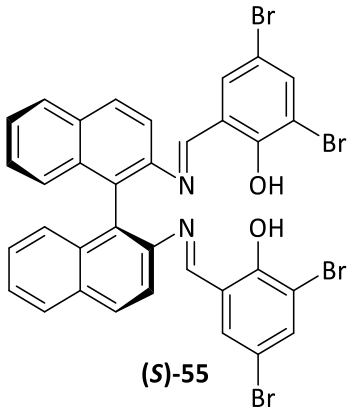 **(*S*)-55**	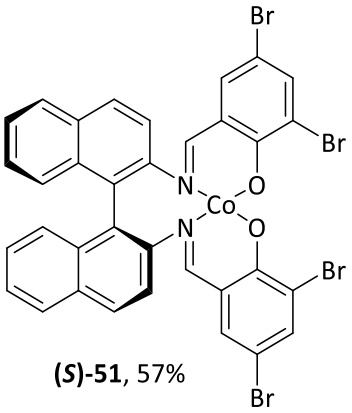 **(*S*)-51**, 57%
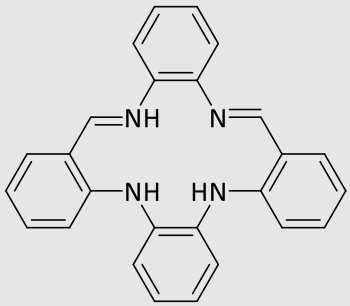 **59**	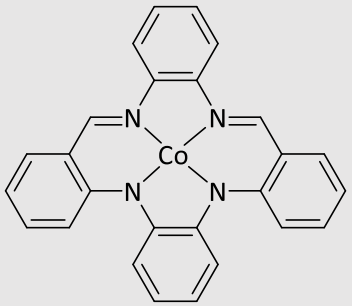 **44**, 18%

Alternatively, cobalt salophens can be obtained in a one-pot synthesis, starting from the diamine, the aldehyde, and cobalt acetate, as shown for **47** (Scheme 73).

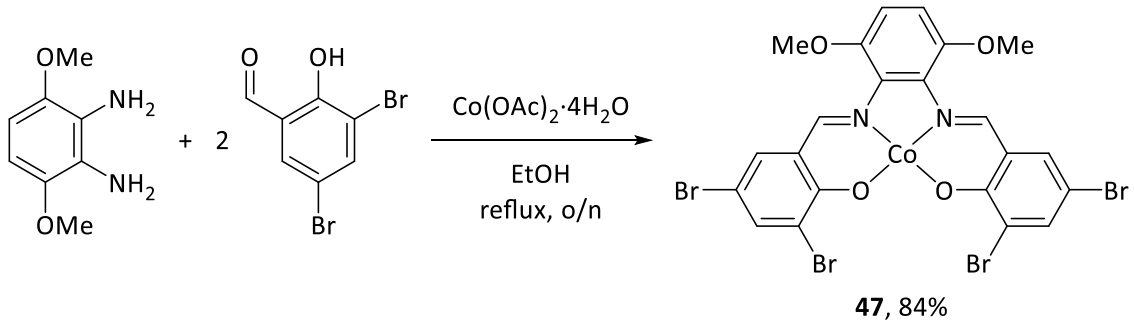

47, 84%

Scheme 73: One-step synthesis of **47**.

Complexes **40**, **41**, **43**, and **45** were synthesized and provided by the group of *de Bruin*. The *Jacobsen* catalyst **(*R*)-50** is commercially available.

The enantiopure *Kagan* complex was synthesized according to an established protocol. The Sequence starts with a *Mitsunobu* inversion of D-menthol to give L-neomenthol **60** (Scheme 74).

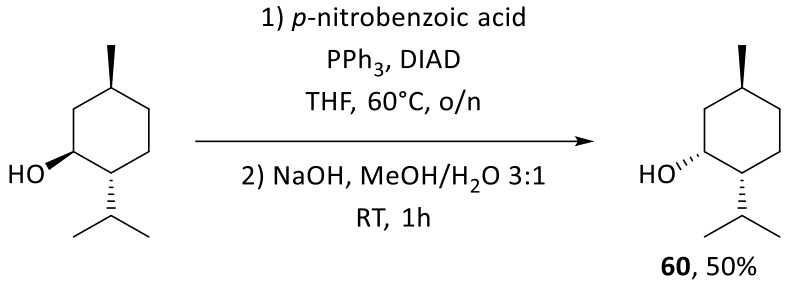

60, 50%

Scheme 74: Synthesis of L-neomenthol **60**.

The L-neomenthol is converted to the mesylate **61**, which is then reacted in a S_N2 reaction with *in situ* generated cyclopentadienyl sodium to give the D-menthol-substituted cyclopentadienyl ligand **62** (Scheme 75). These two steps were performed without purification and **62** was used immediately for the subsequent metalation.

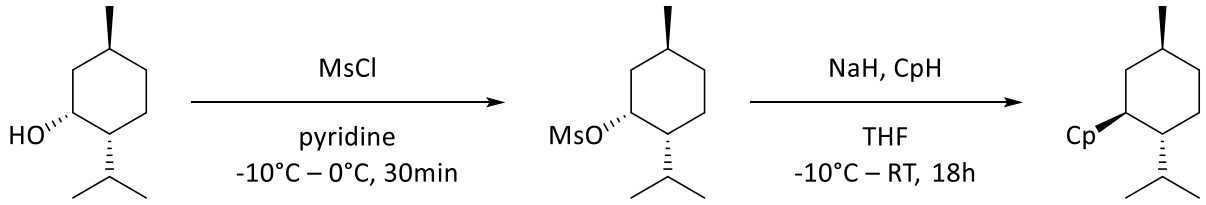

60 **61** **62**

Scheme 75: Synthesis of D-menthylcyclopentadiene **62**.

The metalation is carried out by deprotonation of **62** with ^{n}BuLi and reaction with $TiCl_4$ (Scheme 76). After recrystallization, D-*Kagan*-Cl_2 **63** was obtained as a fluffy orange solid. L-*Kagan*-Cl_2 was synthesized by *Slak* analogously to the synthesis of **63**.

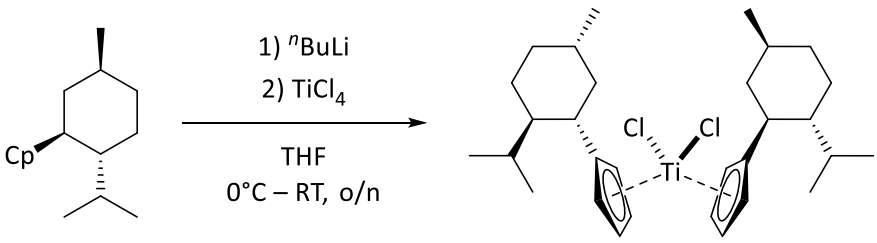

62 **63**, 31%

Scheme 76: Metalation of D-*Kagan*-Cl_2 **63**.

The D-*Kagan*-Br_2 **64** was synthesized starting from **63** (Scheme 77). First, the D-*Kagan*-Cl_2 is converted to the semi-stable dimethyl titanocene using methyl lithium, which is then reacted with HBr to give D-*Kagan*-Br_2 **64**. L-*Kagan*-Br_2 **65** was synthesized following the same procedure shown in Scheme 77, starting with L-*Kagan*-Cl_2.

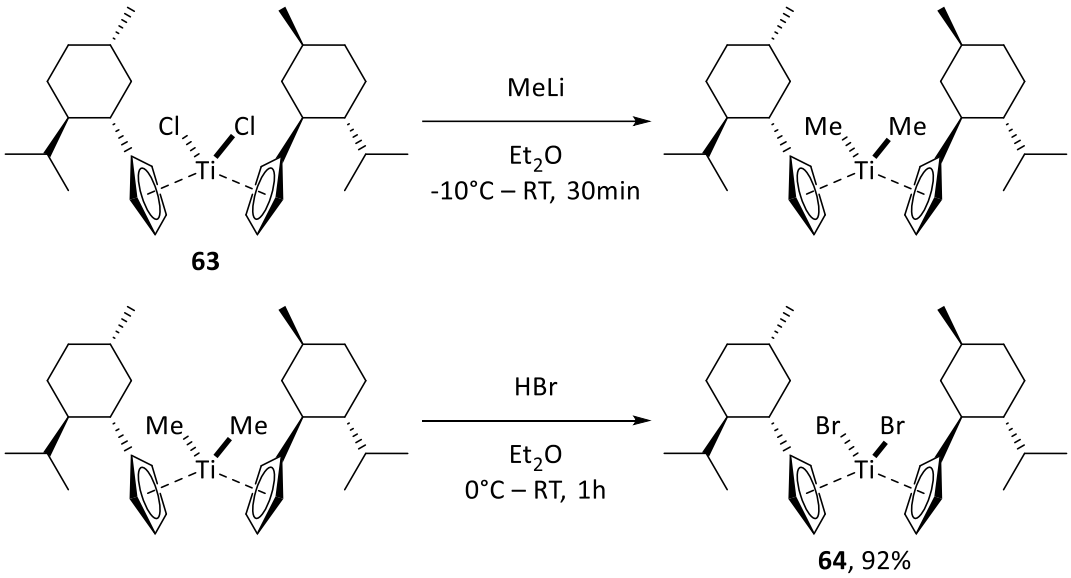

Scheme 77: Synthesis of D-*Kagan*-Br_2 **64.**

The sulfonamides **F_2-PhenSulfAm**, and **PhenSulfAm** were synthesized by *Zhang* and ***cy*-hexSulfAm** by *Schäfer* according to reported procedures.[218]

2.10 Synthesis of Substrates

Following the synthesis of the catalysts, this chapter covers the synthesis of the employed substrate epoxides. Many of the epoxides could be synthesized directly from commercially available precursors or required only few synthetic steps.

1,1-Disubsituted epoxides were obtained from the corresponding ketones using the *Corey-Chaykovsky* reaction with sulfur ylides (Table 43).

Table 43: *Corey-Chaykovsky* epoxidation of ketones.

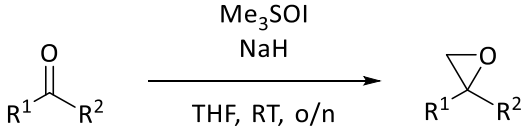

substrate	product	yield [%]	substrate	product	yield [%]
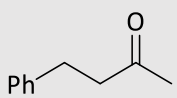	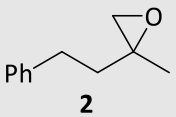 **2**	85	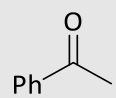	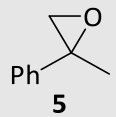 **5**	65
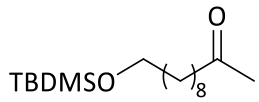 **67**	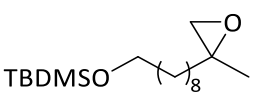 **3**	68[a]	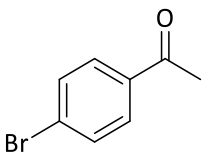	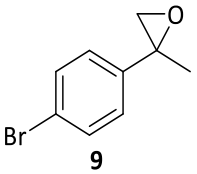 **9**	67

[a] performed by *Plato*.

The synthesis of **7** from the aldehyde required using Me_3SI instead of Me_3SOI (Scheme 78). Moreover, the unstable and temperature sensitive **7** does not tolerate temperatures above 25°C during work-up or purification and could only be purified by column chromatography using Al_2O_3 instead of SiO_2.

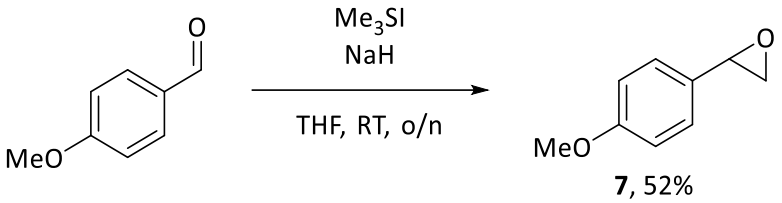

Scheme 78: Synthesis of **7** by modified *Corey-Chaykovsky* epoxidation.

The ketone **67** was synthesized starting with a *Wacker* oxidation of 10-undecen-1-ol, giving ketone **66** (Scheme 79). The free alcohol required protection with TBDMSCl, resulting in **67**, to tolerate the subsequent *Corey-Chaykovsky* epoxidation.

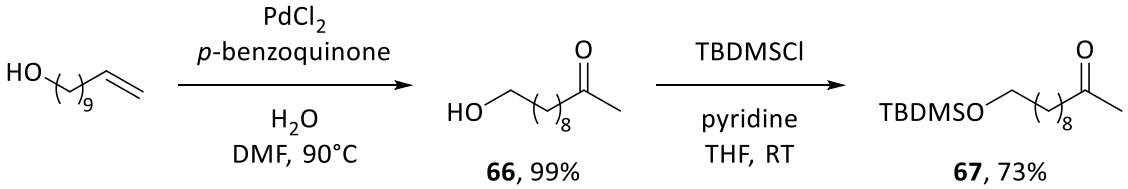

Scheme 79: Synthesis of ketone **67** (performed by *Plato*).

The synthesis of epoxide **13** in Scheme 80 was performed by deprotection of the silyl group with TBAF and protection of the hydroxy group with tosyl chloride.

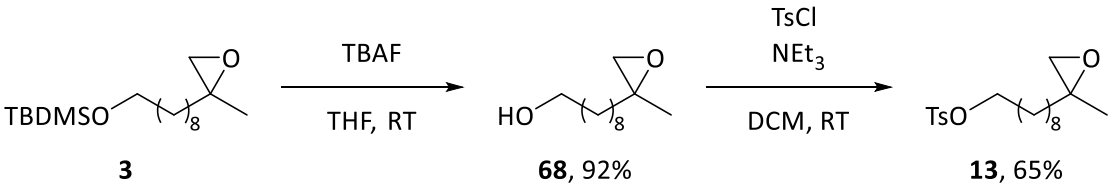

Scheme 80: Synthesis of epoxide **13**.

Olefins were converted to the corresponding epoxides in the *Prilezhaev* reaction by using *meta*-chloroperoxybenzoic acid (Table 44).

Table 44: *Prilezhaev* epoxidation of olefins.

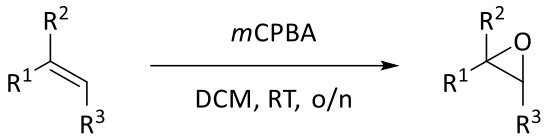

substrate	product	yield [%]	substrate	product	yield [%]
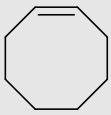	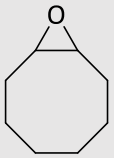 **6**	80	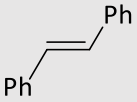	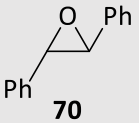 **70**	91
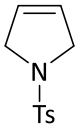 **69**	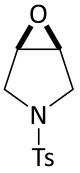 **14**	53	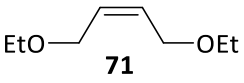 **71**	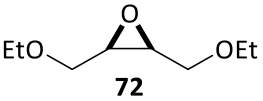 **72**	78
	 **39**	89	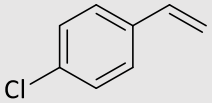	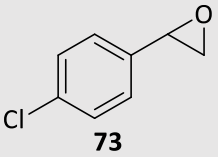 **73**	68

The olefin precursors **69** and **71** were synthesized by the S_N2 reactions shown in Scheme 81.

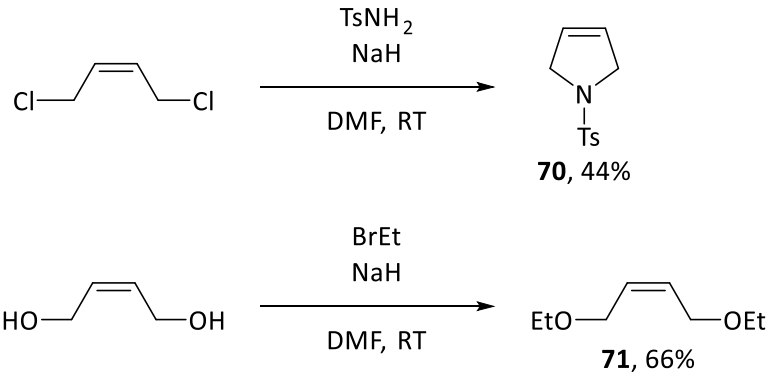

Scheme 81: Synthesis of olefins **69** and **71**.

Epoxides **4**, **8**, and **15** were synthesized by *Shizgal* and epoxides **10**, **11**, and **12** by *Heinz*, according to reported procedures.

Trisubstituted epoxide **16** was prepared via *Matteson* epoxidation of acetophenone with 1,1-dibromoethane (Scheme 81). Epoxide **17** was prepared accordingly by *Höthker*.

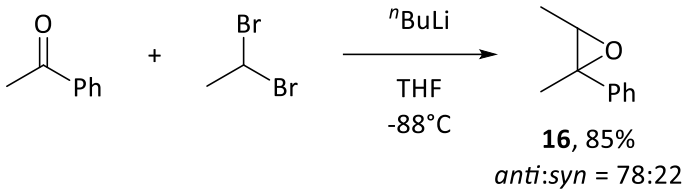

Scheme 82: *Matteson* epoxidation of acetophenone.

Substrates for the radical cyclization reactions were synthesized in a modular way in few synthetical steps. The common precursor olefin **75** was synthesized, starting from propargyl amine, which is tosyl protected first to give **74**. The secondary amine is reacted with 3-chlor-2-methylpropen in a S_N2 reaction using potassium carbonate, and potassium iodide, giving **75** in high yield.

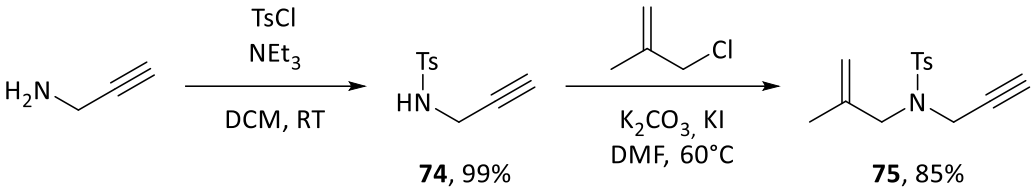

Scheme 83: Synthesis of precursor olefin **75**.

The olefin precursor **75** can either be epoxidized directly or the alkyne group can be further functionalized before. As shown in Scheme 84, the derivatization of **75** was performed either by deprotonation of the alkyne with ^{n}BuLi and subsequent reaction with TMSCl or 1-iodoctane (**76** and **77**), or by a *Sonogashira* cross-coupling, introducing an aromatic substituent (**78**).

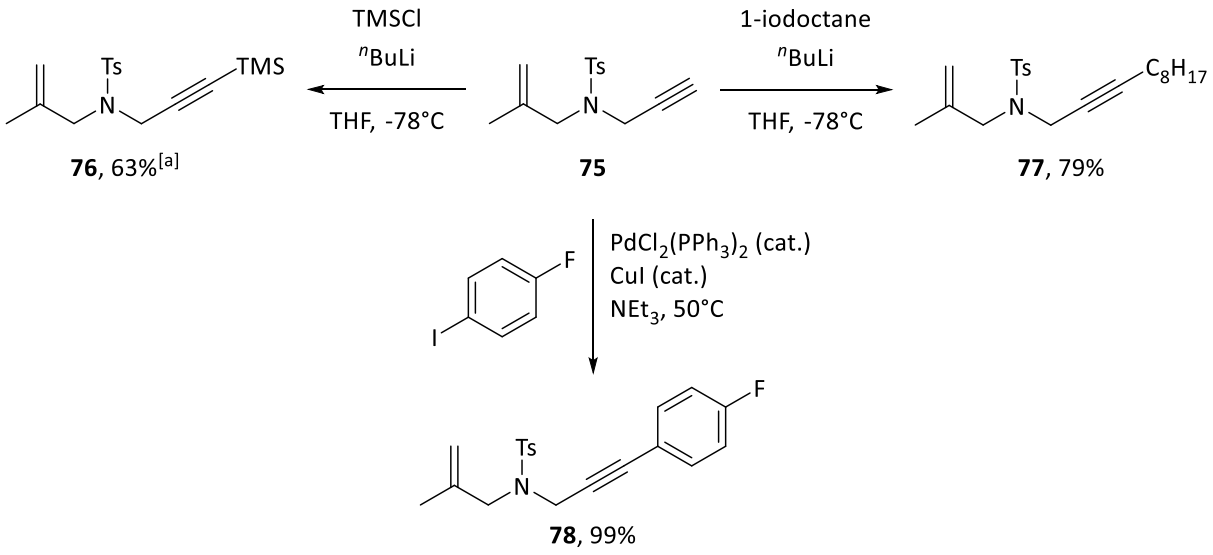

Scheme 84: Derivatizations of **75**. [a] performed by *Schmickler*.

Subsequently, the olefins were converted to the corresponding epoxides with the *Prilezhaev* reaction (Scheme 85).

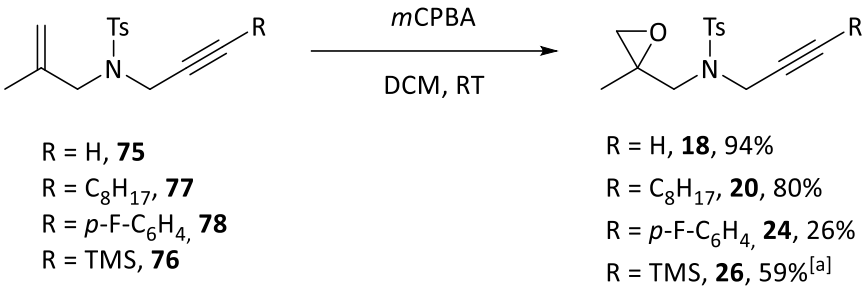

Scheme 85: *Prilezhaev* epoxidation of the olefin precursors. [a] performed by *Schmickler*.

Only for **24** a low yield was obtained in the epoxidation step. However, **24** could be synthesized in high yield by *Sonogashira* reaction directly from **18** (Scheme 86).

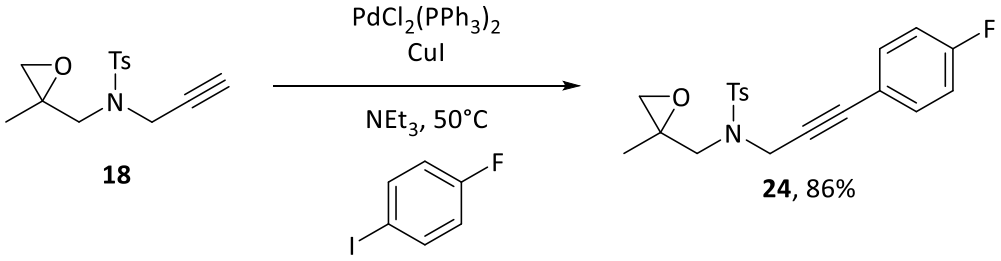

Scheme 86: Alternative synthetic route to **24** from **18**.

Substrates **19**, **21**, **22**, and **23** were synthesized by *Heinz* according to reported procedures.

For the synthesis of **25** (Scheme 87), the *Grignard* reagent generated *in suit* from (2-bromoethyl) benzene was reacted with propargyl alcohol catalyzed by CuI to give **2b**. **2b** was then reacted with sulfonamide **74** in a *Mitsunobu*-like reaction to obtain **79**. The subsequent *Prilezhaev* epoxidation led to **25**.

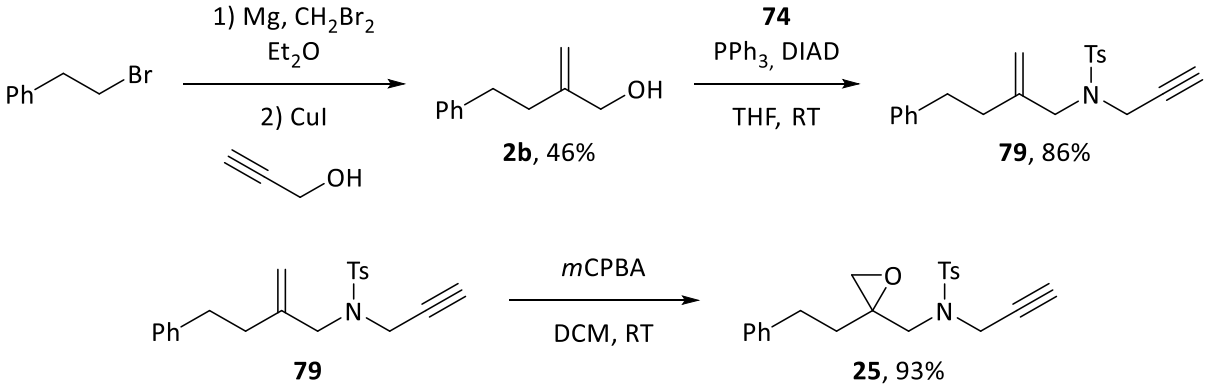

Scheme 87: Synthesis of **25**.

The synthesis of **27** proceeds over four consecutive steps (Scheme 88). Cyclohexene oxide is reacted in a nucleophilic epoxide opening with propargyl amine assisted by *Lewis* acidic $AlEt_3$. After tosyl-

protection of the secondary amine, the hydroxy group in **80** is oxidized to ketone **82**, using the *Swern* oxidation. *Corey-Chaykovsky* epoxidation of **82** was unsuccessful, due to the C–H acidity of the alkyne. However, by applying the *Matteson* epoxidation, **27** was obtained in good yield and with excellent diastereoselectivity.

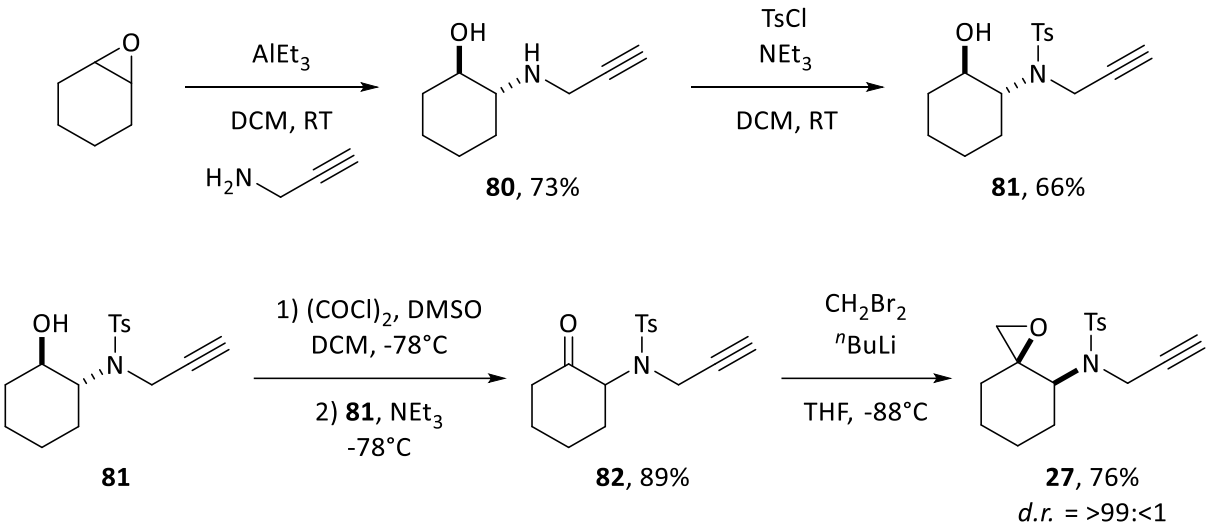

Scheme 88: Synthesis of **27**.

Terminal alkene substrate **85** was synthesized in a S_N2 reaction of tosyl-protected allylamine **83** and epoxide **84** (Scheme 89). Despite bromide being a good leaving group and the prolonged reaction time, **85** could only be obtained in 10% yield.

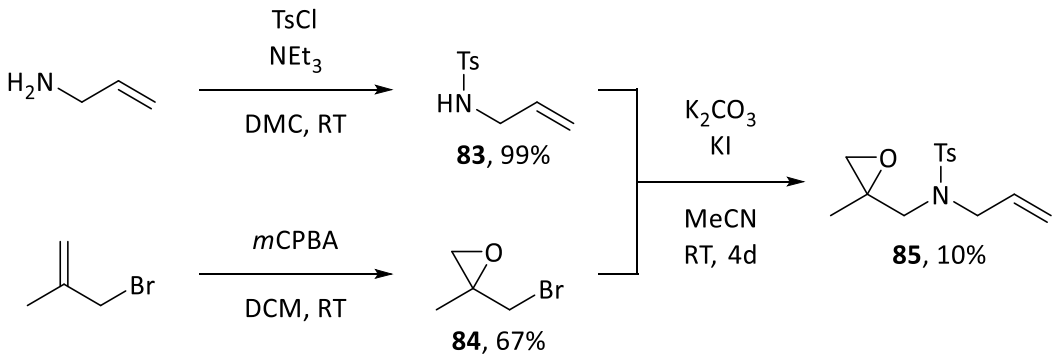

Scheme 89: Synthesis of **85**.

The synthesis of TMS-alkene substrate **88** required the synthesis of TMS-akene **87** first. For this purpose, the alkyne of tosyl protected propargyl amine **74** was TMS protected. The following (*Z*)-selective reduction with colloidal P-2 nickel and hydrogen gas resulted in TMS-alkene **87** and the S_N2 reaction with epoxide **84** gave **88**.

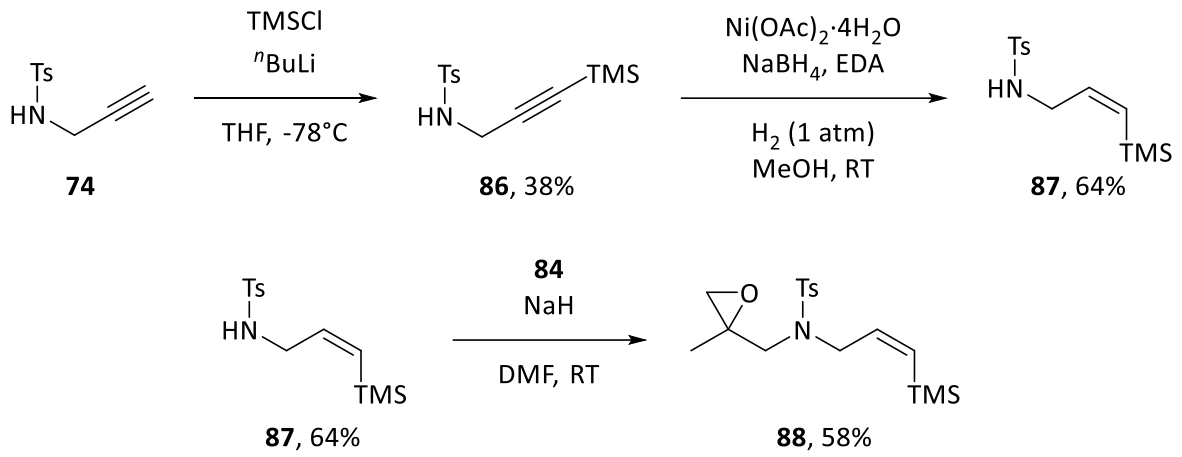

74 **86**, 38% **87**, 64% **87**, 64% **88**, 58%

Scheme 90: Synthesis of **88**.

For the synthesis of malonate-derived cyclization substrates, synthesis of propargyl bromides **91** and **92** was necessary (Scheme 91). These were synthesized by addition of deprotonated alkynes to paraformaldehyde, giving propargylic alcohols **89** and **90**, which were then converted in an *Appel*-like reaction to the propargyl bromides.

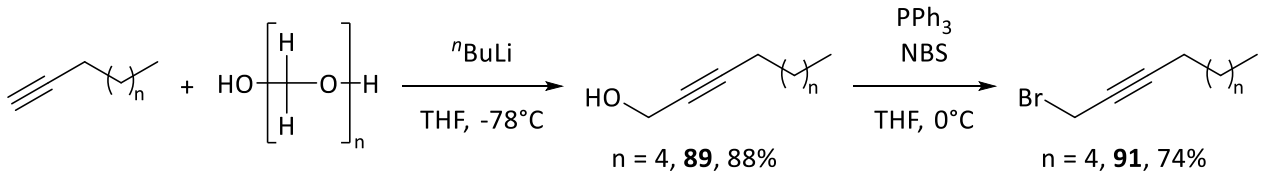

n = 4, **89**, 88%
n = 6, **90**, 80%[a]
n = 4, **91**, 74%
n = 6, **92**, 87%[a]

Scheme 91: Synthesis of substituted propargyl alcohols and propargyl bromides. [a] performed by *Heinrichs*.

The second building block of the malonate-derived cyclization substrates is epoxide **94**, which was synthesized by an S_N2 reaction of commercially available diethylmalonate and 3-chlor-2-methylpropen to give **93**, followed by *Prilezhaev* epoxidation (Scheme 92). Epoxide **95** was synthesized accordingly by *Shizgal*.

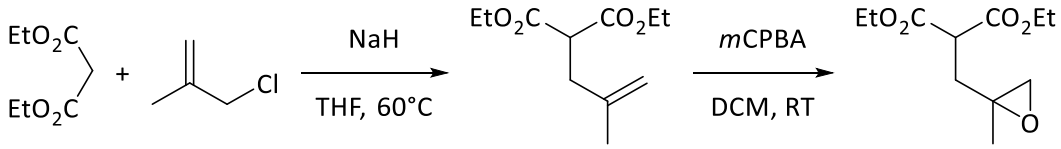

93, 46% **94**, 85%

Scheme 92: Synthesis of epoxide **94** (performed by *Heinrichs*).

Epoxides **94** and **95** were subsequently reacted with the propargyl bromides to give the malonate-derived cyclization substrates (Scheme 93).

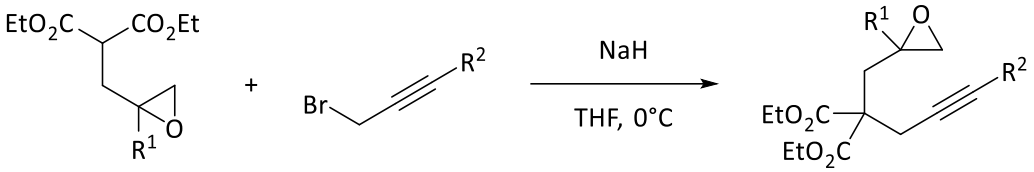

R^1 = H, **95** | R^2 = H, propargyl bromide | R^1 = H, R^2 = C_6H_{13}, **31**, 70%

R^1 = Me, **94** | R^2 = C_6H_{13}, **91** | R^1 = Me, R^2 = H, **29**, 82%[a]

R^2 = C_8H_{17}, **92** | R^1 = Me, R^2 = C_8H_{17}, **30**, 91%[a]

Scheme 93: Synthesis of **29**, **30**, and **31**.

The alcohol intermediate **89** was also used for the synthesis of **28** by S_N2 reaction with 3-brom-2-methylpropen and subsequent *Prilezhaev* epoxidation (Scheme 94).

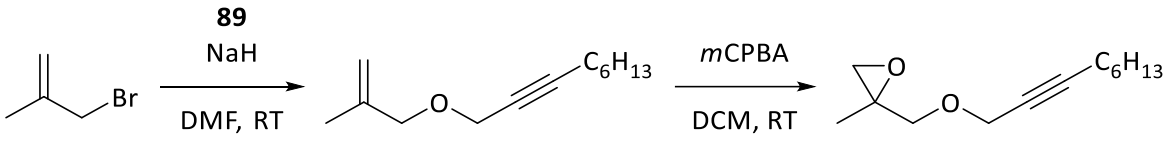

Scheme 94: Synthesis of **28**.

The first synthetic step towards the β-epoxy alcohol REO substrate is a hydrolytic kinetic resolution (HKR). This reaction is well-suited for chiral resolution of the terminal propene oxide (Scheme 95). By using the oligomeric *Jacobsen*-(*S,S*)-salen-cobalt(III) catalyst, the undesired epoxide enantiomer is efficiently converted to the diol and the desired epoxide enantiomer **(*S*)-97** is obtained after distillation in excellent enantiomeric excess. The reduced yield is explained by the maximum yield of 45% in this kinetic resolution (0.55 eq. of H_2O), and additionally by the high volatility of propene oxide. In the next step, the alkyne addition of the deprotonated alkyne to **(*S*)-97** takes place. The epoxide is activated by the *Lewis* acid BF_3·THF towards the nucleophilic attacked. Maintaining the low reaction temperature is essential here for a clean reaction. Subsequently, the alkyne **98** is reduced in a (*Z*)-selective hydrogenation with colloidal P-2 nickel and hydrogen gas to (*Z*)-β-hydroxy alkene **99**.

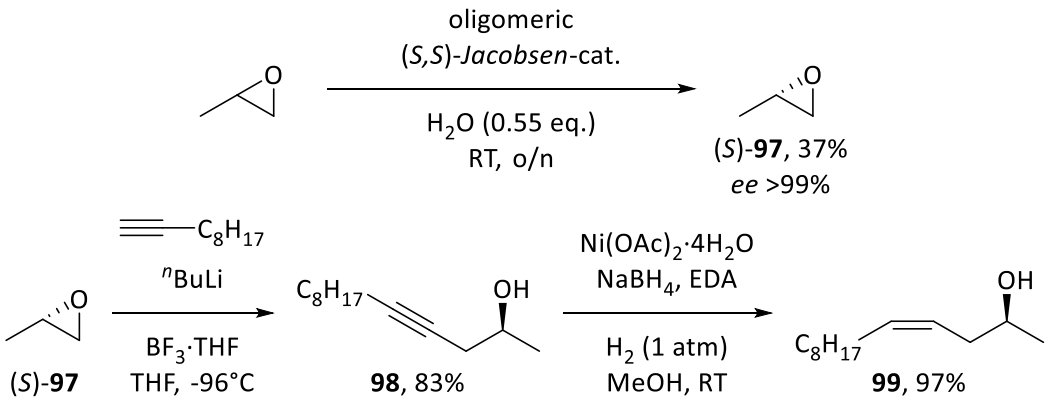

Scheme 95: Synthesis of (*Z*)-β-hydroxy alkene **99**.

In a *syn*-selective epoxidation using the $VO(acac)_2$ catalyst and TBHP (Table 45), **99** is converted to the REO substrate **38**. Analogously, REO substrate **34** was accessible from commercially available and enantiomerically pure (*R*)-methyl ricinoleate. Both substrates were obtained in very good diastereomeric ratios. Substituted REO substrates **35**, **36** and **37** were synthesized by *Heinz* according to reported procedures.

Table 45: Synthesis of **38** and **34** by *syn*-selective epoxidation of β-hydroxy alkenes catalyzed by $VO(acac)_2$.

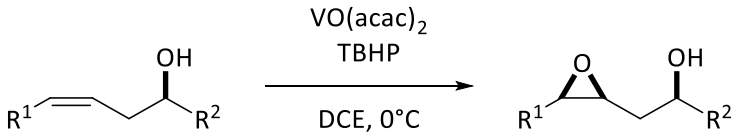

substrate	product
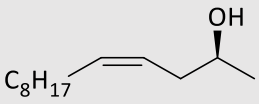 **99**	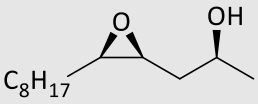 **38**, 80% *d.r.* = 94:6
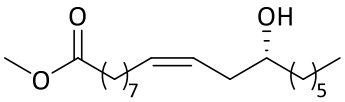	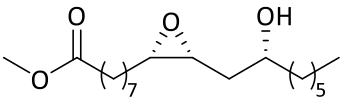 **34**, 68% *d.r.* = 96:4

2.11 Conclusion

A new synthetic method was developed, demonstrating an innovative application of readily available, affordable, and reasonably safe borohydrides as hydrogen atom and electron donors in cooperative catalysis of radical reactions. This was achieved by coupling the unique reactivities of the earth abundant metals titanium and chromium in a reactive network. The catalytic system is based on the synergistic combination of titanocenes, especially Cp_2TiCl_2, known for their efficiency in radical epoxide opening reactions, and $CpCr(CO)_3H$, which is a well-established catalyst in radical hydrogenations of olefins.

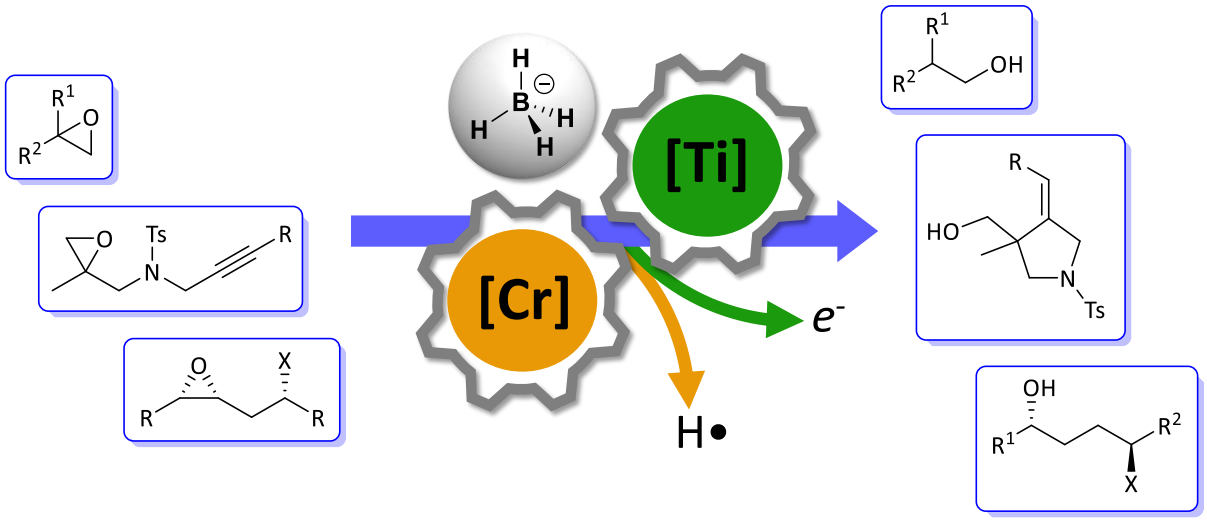

The key step to achieve the envisioned reprogrammed reactivity of borohydride in the cooperative mechanism is an unprecedented relay hydrogen atom transfer process. Initially, a hydride is transferred from the borohydride to the Cp_2TiCl_2 precatalyst. Subsequently, a hydrogen atom is transferred from the $Cp_2Ti(H)Cl$ intermediate to the $CpCr(CO)_3$• species, simultaneously generating both the electron transfer catalyst Cp_2TiCl and the hydrogen atom transfer catalyst $CpCr(CO)_3H$ in equimolar amounts. In this way, the hydride is transferred by the two transition-metal catalysts as electron and hydrogen atom, allowing the use of borohydrides as hydrogen atom and electron donors. In this way, the typical nucleophilic hydric reduction character of the BH_4^- anion is completely outcompeted, and its reactivity is successfully reprogrammed. The mechanistic details have been elucidated through both computational and experimental studies, which allowed the experimental realization of our proposed catalytic 'globe'. The truly interconnected cycles of the chromium-catalyzed hydrogen atom transfer with the titanium-catalyzed epoxide opening makes this reaction a strong example of cooperative catalysis, achieving a reactivity which was not possible before.

Optimal performance of this reaction has been achieved by identifying the combination of strongly reducing and *Lewis* acidic $LiBH_4$ with the solvent 1,4-dioxane, which controls the reactivity of the

borohydride through solubility, ensuring a controlled and precise delivery of the reagent via a 'chemical syringe pump'. This orchestral combination of titanium and chromium catalysts with lithium borohydride in 1,4-dioxane enables high reactivity paired with minimal formation of side products. The mildness and functional group tolerance of the reaction conditions were demonstrated in the synthesis of a broad range of *anti-Markovnikov* alcohols.

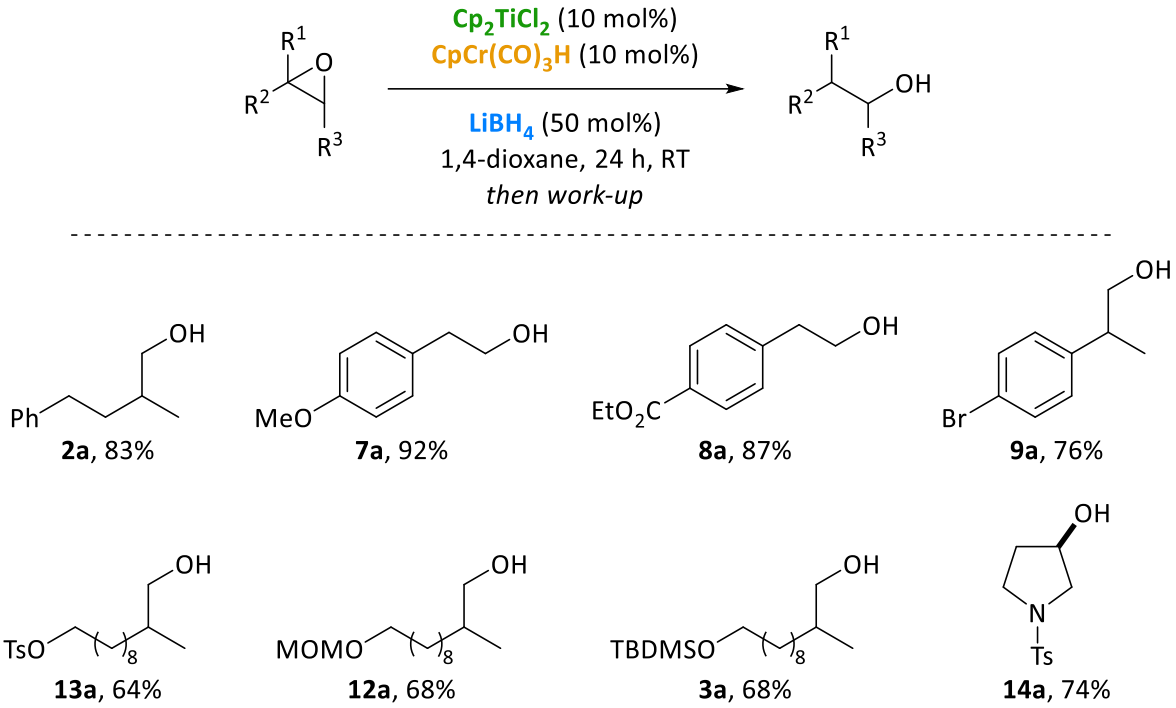

Moreover, our method has been extended to realize C–C bond-forming cyclization reactions and regiodivergent epoxide openings. These transformations address previous limitations in the applicability of cooperative catalysis. However, to achieve these synthetically extensions, careful adjustments of reaction conditions were again necessary. The synthesis of pyrrolidine derivatives by radical cyclization was achieved by adjusting catalyst loading, temperature, and reaction time.

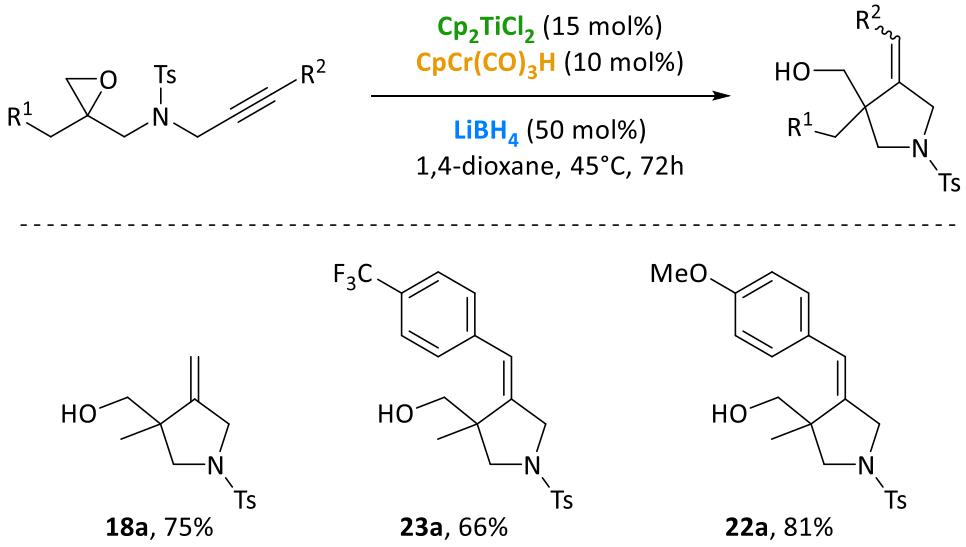

Furthermore, the successful combination of regiodivergent epoxide openings with cooperative catalysis, was achieved through two additional major modifications. First, the *Kagan*-Br_2 titanocene was chosen as regiodivergent catalyst. Second, sulfonamide additives had to be introduced to ensure proper reactivity. These sulfonamides play a dual role: they facilitate the activation of the titanocene by halide abstraction and stabilize the active titanocene catalyst by forming a *resting state*. This approach enables the synthesis of enantiopure 1,3- and 1,4-difunctionalized units from common starting materials. This is realized by first introducing the epoxide and the neighboring stereocenter stereoselectively into the substrate using well-established methods (HKR, $VO(acac)_2$-catalyzed epoxidation, etc.), followed by regiodivergent epoxide opening, which retains the configuration of the epoxide. Particularly attractive is the possibility to directly obtain unprotected 1,3- and 1,4-diols, circumventing the need for additional introduction and removal of protection group. Achieving REO reactions has previously been unattainable through radical cooperative catalysis or epoxide reductions involving a *Meinwald* rearrangement followed by carbonyl reduction.

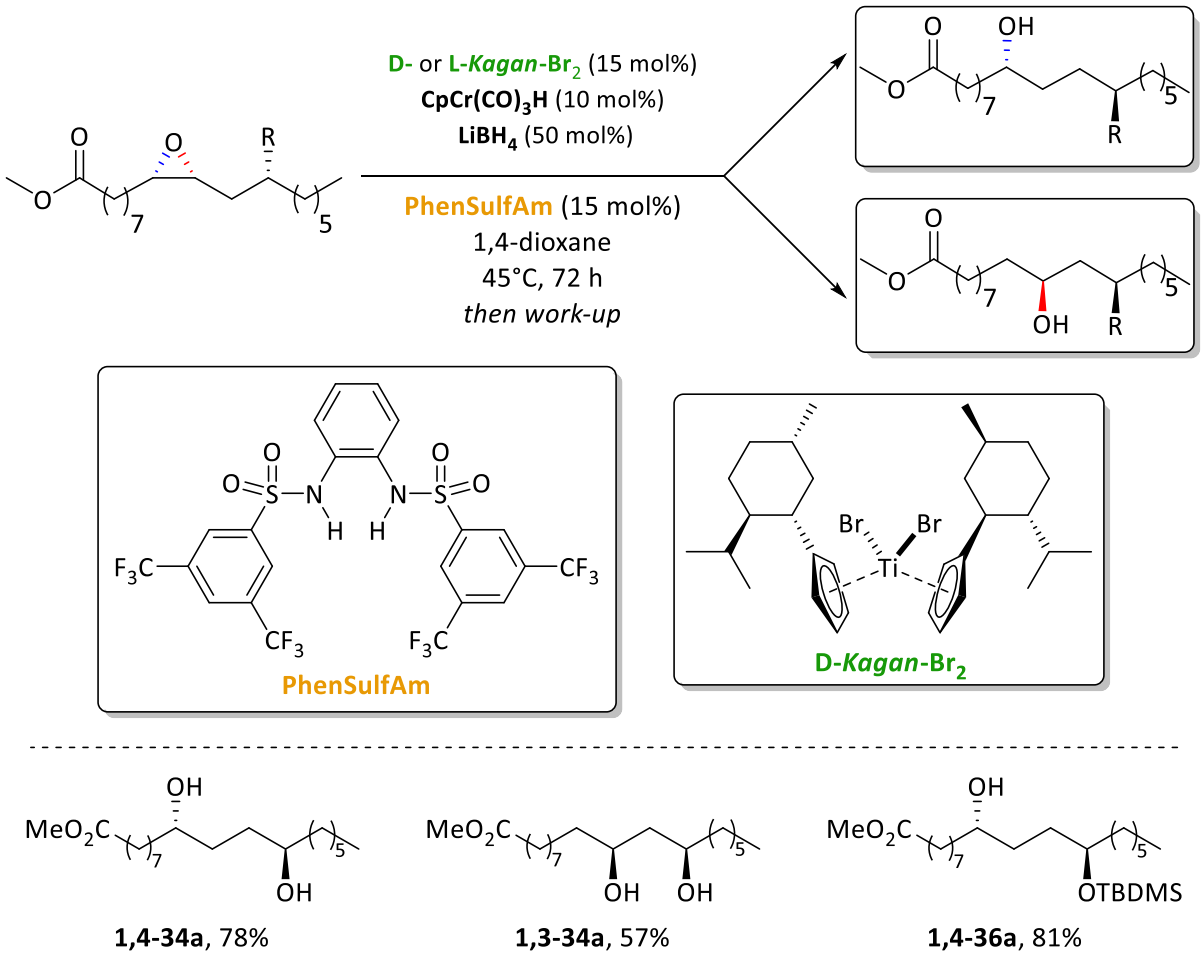

These improved regiodivergent epoxide opening and C–C bond-forming cyclization reactions provide a more sustainable access to molecular structures that may serve as key intermediates in the synthesis of complex natural products and drugs. A key advantage across all the above-mentioned systems over

earlier developed titanocene-catalyzed epoxide openings is the elimination of the need for both stoichiometric *Brønsted* acids and toxic hydrogen atom donors like 1,4-cyclohexadiene or $^{n}Bu_3SnH$. Instead, the only stoichiometric reagent required is the borohydride. This improvement enhances atom economy and thus sustainability, and environmental compatibility, bringing the process more closely to the principles of green chemistry. At the same time, the use of pressurized and highly flammable hydrogen gas, as previously used in chromium and titanium cooperative catalysis, is circumvented by employing easily handled borohydrides, facilitating safer and better manageable experimental procedures in research laboratories.

3 Experimental Part

3.1 General Information

All air- or moisture-sensitive reagents, products, and reactions were handled in glassware previously oven-dried or flame-dried under vacuum and under argon atmosphere using standard *Schlenk* technique. Liquid reagents and dry solvents were transferred into the reaction flasks via argon flushed plastic syringes or transfer cannulas through septa. Small volumes were measured using glass syringes by *Hamilton* of type *Gastight 1700 Series.* Solid reagents were added to the reaction flask using a *glovebox* or under argon counterflow. Filtrations of air- or moisture-sensitive mixtures were performed using sintered glass filter sticks or filter cannulas with glass microfiber filters.

Commercially available chemicals were purchased from *Sigma Aldrich, Merck, abcr, TCI Chemicals, Alfa Aesar, Carl Roth, BLDpharm* or *Fischer Scientific* and used without further purification, unless otherwise noted.

All reactions were monitored by thin layer chromatography (TLC) on *Merck* silica gel 60 F_{254} plates using UV light as visualizing agent (if applicable) or a solution of vanillin (43 g/l) and concentrated H_2SO_4 (12.5 mL/L) in ethanol or a solution of $(NH_4)_6Mo_7O_{24}{\cdot}4\ H_2O$ (25 g/L) and $Ce(SO_4)_2{\cdot}4\ H_2O$ (10 g/L) in 10% aq. solution of H_2SO_4 as developing agent. Reaction products were purified via flash column chromatography on *Merck* silica gel 60 or *Merck* aluminum oxide neutral. The solvent mixtures used as eluent are denoted in the respective reaction procedures.

3.1.1 Analytics

^{1}H-, ^{13}C-, and ^{19}F-NMR spectra were recorded on a *Bruker Avance I 300 MHz, Bruker Avance I 400 MHz, Bruker Avance I 500 MHz* or *Bruker Avance III HD 500 MHz* instrument at room temperature. Chemical shifts (δ) are denoted in ppm and were calibrated by using the residual undeuterated solvent signals as internal reference for ^{1}H-NMR ($CDCl_3$: 7.26 ppm, C_6D_6: 7.16 ppm and THF-d_8: 3.58 ppm) and ^{13}C-NMR ($CDCl_3$: 77.16 ppm, C_6D_6: 128.06 ppm and THF-d_8: 67.57 ppm). H,H-coupling constants (J) are reported in Hz.

IR spectra were measured using a *Thermo Nicolet 380 FT-IR-ATR* or *Shimadzu IRSpirit-T FT-IR-ATR* Spectrometer as neat film. Wavenumbers (ν) were denoted in cm^{-1}.

High resolution mass spectra were measured using electron spray ionization (ESI) on a time-of-flight spectrometer *microTOF-Q* by *Bruker Daltonic*, atmospheric-pressure chemical ionization (APCI) on an

Orbitrap XL spectrometer and electron ionization (EI) a on sector field mass analyzers *MAT 90* and *MAT 95 XL* by *Thermo Finnigan*.

Analytical high performance liquid chromatography (HPLC) for the determination of enantiomeric excesses (*ee*) was performed by *A. Schneider* on a *Knauer Azura HPG* device using *Chiralpak* IH-U 1.6 µm columns with a flow rate of 0.85 mL/min and ^{n}hexane/ethanol or ^{n}heptane/isopropanol mixtures as eluent.

Optical rotations ($[\alpha]_D^{20}$) were measured on the *Anton Paar MCP 150* polarimeter with a concentration of 10 g/L.

Melting points (M_p) were measured on a *DigiMelt MPA 161* by *SRS*.

3.1.2 Solvent Purification

Acetonitrile (MeCN)	Obtained from *M. Braun MB SPS 800* solvent drying system under an argon stream.
Dichloromethane (DCM)	Obtained from *M. Braun MB SPS 800* solvent drying system under an argon stream or purchased as a p.a. solvent and used without further purification.
Dichloroethane (DCE)	Purchased as a p.a. solvent and used without further purification.
Diethyl ether (Et_2O)	Obtained from *M. Braun MB SPS 800* solvent drying system under an argon stream or pre-dried over CaH_2 and distilled under an argon atmosphere and stored over molecular sieves.
Dimethylformamide (DMF)	Obtained from *M. Braun MB SPS 800* solvent drying system under an argon stream.
1,4-Dioxane	Refluxed over sodium/benzophenone and distilled under argon before use.
Methanol (MeOH)	Obtained from *M. Braun MB SPS 800* solvent drying system under an argon stream or purchased in *AcroSeal* bottles under inert atmosphere over molecular sieves.

^{n}Pentane	Pre-dried over CaH_2 and distilled under an argon atmosphere and stored over molecular sieves or purchased in *AcroSeal* bottles under inert atmosphere over molecular sieves.
Pyridine	Obtained from *M. Braun MB SPS 800* solvent drying system under an argon stream.
Tetrahydrofuran (THF)	Obtained from *M. Braun MB SPS 800* solvent drying system under an argon stream or refluxed over sodium/benzophenone and distilled under argon before use.

Solvents for highly air-sensitive reactions are additionally degassed by using the freeze-pump-thaw process. The dry solvent is placed in a *Schlenk* tube under static argon and cooled with liquid N_2. When the solvent is frozen, the flask is evacuated for 5 min, closed, and the solvent is allowed to thaw under static vacuum. The process is repeated two more times. After the final thawing, the flask is backfilled with argon when at room temperature.

Degassed water is prepared by refluxing deionized water for 30 min while purging argon through it. The water is cooled down to room temperature while continuing the purging with argon.

3.1.3 Chromatography Solvents

Cyclohexane (CH)	Separation of high boiling impurities by distillation at normal pressure.
Dichloromethane (DCM)	Purchased as a p.a. solvent and used without further purification.
Diethyl ether (Et_2O)	Purchased as a p.a. solvent and used without further purification.
Ethyl acetate (EA)	Separation of high boiling impurities by distillation at normal pressure.
Methanol (MeOH)	Purchased as a p.a. solvent and used without further purification.
^{n}Pentane	Purchased as a p.a. solvent and used without further purification.

3.2 General Procedures

General procedure **GP-1**: Epoxidation of ketones (*Corey-Chaykovsky* reaction)

In a flame-dried *Schlenk* flask, to a suspension of trimethylsulfoxonium iodide (1.40 eq.) in dry THF (1 mL/mmol ketone) is added sodium hydride (60% in mineral oil, 1.20 eq.), and the mixture is stirred for 1 h at RT. The ketone (1.00 eq.) is added slowly, and the reaction mixture is stirred overnight at RT. Water is added and the layers are separated. The aqueous layer is extracted with EA (3x), the combined organic layers are washed with water and brine, dried over $MgSO_4$ and the solvent is removed *in vacuo*. The crude product is purified via flash column chromatography or distillation.

General procedure **GP-2**: Epoxidation of olefins (*Prilezhaev* reaction)

In a round-bottom flask, to a solution of the olefin (1.00 eq.) in DCM (3 mL/mmol olefin) is added *m*CPBA (70%, 1.20 eq.) at 0°C. The reaction mixture is stirred overnight at RT. Sat. aq. Na_2CO_3 solution is added, and the layers are separated. The aqueous layer is extracted with DCM (4x), the combined organic layers are washed with sat. aq. Na_2CO_3 solution (2x) and brine, dried over $MgSO_4$ and the solvent is removed *in vacuo*. The crude product is purified via flash column chromatography or distillation.

General procedure **GP-3**: Ligand metalation with cobalt(II) acetate tetrahydrate

In a flame-dried *Schlenk* tube, the ligand (1.00 eq.) and cobalt acetate tetrahydrate (1.00 eq.) are suspended in dry MeOH (1 mL/mmol ligand) and refluxed for 2 h. The mixture is cooled to 0°C and the resulting dark precipitate is filtered off. The crude product is washed with as little as possible cold MeOH (cooled on dry ice) and ^{n}pentane and is dried *in vacuo* to obtain the cobalt complex.

General procedure **GP-4**: Titanocene- and chromium-catalyzed epoxide opening with $LiBH_4$

In a flame-dried *Schlenk* flask, Cp_2TiCl_2 (0.10 eq.) is added and the flask is transferred into a *glovebox* where $CpCr(CO)_3H$ (0.10 eq.) and $LiBH_4$ (0.50 eq.) are added. Freshly distilled 1,4-dioxane (2 mL/mmol of epoxide) and epoxide (1.00 eq.) are added in argon counterflow, and the reaction is stirred for 24 h at RT. NaOH solution (2 M, 2 mL/mmol of epoxide) is added and the mixture is stirred for 30 min at RT. The layers are separated, the aqueous layer is extracted with Et_2O, the combined organic layers are filtered through a silica plug and the solvent is removed *in vacuo.* The product is purified via flash column chromatography.

General procedure **GP-5**: Titanocene-catalyzed cyclization using Coll·HCl and manganese

In a flame-dried *Schlenk* flask, freshly resublimed 2,4,6-collidine hydrochloride (2.50 eq.), Mn (2.00 eq.) and Cp_2TiCl_2 (0.10 eq.) are suspended in freshly distilled THF (10 mL/mmol of epoxide) and stirred for

30 min until a color change to green is observed. The epoxide (1.00 eq.) is added, and the reaction mixture is stirred for 48 h at RT. The mixture is diluted with Et_2O, the organic layer is washed with aq. HCl (1 M), water, sat. aq. $NaHCO_3$ solution, water, dried over $MgSO_4$ and the solvent is removed in vacuo. The product is purified via flash column chromatography.

General Procedure **GP-6**: Titanocene- and chromium-catalyzed cyclization

In a flame-dried *Schlenk* flask, Cp_2TiCl_2 (0.15 eq.) is added and the flask is transferred into a *glovebox* where $CpCr(CO)_3H$ (0.10 eq.) and $LiBH_4$ (0.50 eq.) are added. Freshly distilled 1,4-dioxane (2 mL/mmol of epoxide) and the epoxide (1.00 eq.) are added in argon counterflow, and the reaction is stirred for 72 h at 45°C. NaOH solution (2 M, 2 mL) is added, and the mixture is stirred for 30 min at RT. The layers are separated, the aqueous layer is extracted with Et_2O, the combined organic layers are filtered through a silica plug and the solvent is removed *in vacuo.* The product is purified via flash column chromatography.

General procedure **GP-7**: Desymmetrization of *meso*-epoxides

In a flame-dried *Schlenk* flask, L-*Kagan*-Cl_2 or D-*Kagan*-Cl_2 (0.10 eq.) is added and the flask is transferred into a *glovebox* where $CpCr(CO)_3H$ (0.10 eq.) and $LiBH_4$ (0.50 eq.) are added. Freshly distilled 1,4-dioxane (2 mL/mmol of epoxide) and the *meso*-epoxide (1.00 eq.) are added in argon counterflow, and the reaction is stirred for 72 h at RT. Pyridine-*N*-oxide (2.00 eq.) is added and the mixture is stirred for 30 min at RT. The layers are separated, the aqueous layer is extracted with Et_2O, the combined organic layers are washed with water, dried over $MgSO_4$ and the solvent is removed *in vacuo.* The product is purified via flash column chromatography.

General procedure **GP-8:** Titanocene- and chromium-catalyzed regiodivergent epoxide opening

In a flame-dried *Schlenk* flask, L-Kagan-Br_2 **65** or D-Kagan-Br_2 **64** (0.15 eq.) is added and the flask is transferred into a *glovebox* where $CpCr(CO)_3H$ (0.10 eq.), sulfonamide **PhenSulfAm** (0.15 eq.) and $LiBH_4$ (0.50 eq.) are added. Freshly distilled 1,4-dioxane (2 mL/mmol of epoxide) and the epoxide (1.00 eq.) are added in argon counterflow, and the reaction is stirred for 72 h at 45°C. Pyridine-*N*-oxide (2.00 eq.) is added and the mixture is stirred for 30 min at RT. The layers are separated, the aqueous layer is extracted with Et_2O, the combined organic layers are washed with water, dried over $MgSO_4$ and the solvent is removed *in vacuo.* The product is purified via flash column chromatography.

General procedure **GP-9**: Titanocene- and chromium-catalyzed epoxide opening with KBH_4 and LiCl

In a flame-dried *Schlenk* flask, Cp_2TiCl_2 (0.10 eq.) is added and the flask is transferred into a *glovebox* where $CpCr(CO)_3H$ (0.10 eq.), KBH_4 (0.50 eq.) and LiCl (0.05 eq.) are added. Freshly distilled THF (2 mL/mmol of epoxide) and epoxide (1.00 eq.) are added in argon counterflow, and the reaction is

stirred for 48 h at RT. NaOH solution (2 M, 2 mL/mmol of epoxide) is added and the mixture is stirred for 30 min at RT. The layers are separated, the aqueous layer is extracted with EA, the combined organic layers are washed with water, brine, dried over $MgSO_4$ and the solvent was removed *in vacuo*. The product is purified via flash column chromatography.

General procedure **GP-10:** Optimization of cyclization reactions

In a flame-dried *Schlenk* flask, Cp_2TiCl_2 is added and the flask is transferred into a *glovebox* where $CpCr(CO)_3H$ and $LiBH_4$ are added. Freshly distilled 1,4-dioxane (2 mL/mmol of epoxide) and the epoxide (1.00 eq.) are added in argon counterflow, and the reaction is stirred for the specified time at the specified temperature. NaOH solution (2 M, 2 mL/mmol of epoxide) is added, and the mixture is stirred for 30 min at RT. The layers are separated, the aqueous layer is extracted with Et_2O, the combined organic layers are filtered through a silica plug and the solvent is removed *in vacuo.*

General procedure **GP-11:** Optimization of regiodivergent epoxide opening

In a flame-dried *Schlenk* flask, L-Kagan or D-Kagan is added and the flask is transferred into a *glovebox* where $CpCr(CO)_3H$, the sulfonamide, and the borohydride are added. Freshly distilled 1,4-dioxane or THF (2 mL/mmol of epoxide) and the epoxide (1.00 eq.) are added in argon counterflow, and the reaction is stirred for the specified time at the specified temperature. Pyridine-*N*-oxide (2.00 eq.) is added, and the mixture is stirred for 30 min at RT. The layers are separated, the aqueous layer is extracted with Et_2O, the combined organic layers are washed with water, dried over $MgSO_4$ and the solvent is removed *in vacuo.*

General procedure **GP-12:** Titanocene- and cobalt-catalyzed epoxide opening

In a flame-dried *Schlenk* flask, Cp_2TiCl_2 (0.10 eq.) and the cobalt complex (0.10 eq.) are added, and the flask is transferred into a *glovebox* where $LiBH_4$ (0.50 eq.) is added. 2-Methyl-2-(2-phenylethyl)-oxirane **2** (1.0 eq) is added via micropipette and 1,4-dioxane, previously dried over MS and degassed (2 mL/mmol of epoxide), is added via syringe in argon counterflow. The reaction is stirred for 24 h at RT. NaOH solution (2 M, 2 mL/mmol of epoxide) is added and the mixture is stirred for 30 min at RT. The layers are separated, the aqueous layer is extracted with Et_2O, the organic layers are filtered through a short silica plug and the solvent is removed *in vacuo.*

3.3 Substrate Synthesis

2-Methyl-2-(2-phenylethyl)-oxirane **2**

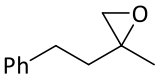

According to **GP-1**, 4-Phenylbutan-2-one (14.82 g, 0.10 mol, 1.00 eq.), trimethylsulfoxonium iodide (30.81 g, 0.14 mol, 1.40 eq.) and sodium hydride (60% in mineral oil, 4.80 g, 0.12 mol, 1.20 eq.) are reacted in THF (100 mL) overnight. After purification via distillation (4 mbar, 84°C) 2-Methyl-2-(2-phenylethyl)-oxirane **2** (13.75 g, 84.76 mmol, 85%) is obtained as a colorless oil.

^{1}H-NMR (500 MHz, $CDCl_3$, 298 K) δ [ppm] = 7.31 – 7.26 (m, 2H), 7.22 – 7.17 (m, 3H), 2.75 – 2.70 (m, 2H), 2.61 (d, *J* = 4.8 Hz, 1H), 2.58 (d, *J* = 4.9 Hz, 1H), 1.97 – 1.90 (m, 1H), 1.88 – 1.81 (m, 1H), 1.38 (s, 3H).

^{13}C-NMR (125 MHz, $CDCl_3$, 298 K) δ [ppm] = 141.7, 128.6, 128.4, 126.1, 56.8, 54.1, 38.7, 31.6, 21.2.

The analytical data is in agreement with the literature.[212]

11-Hydroxyundecan-2-one **66**

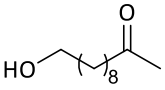

A round-bottom flask is charged with palladium(II) chloride (0.089 g, 0.05 mmol, 0.01 eq.) and *p*-benzoquinone (5.40 g, 50.0 mmol, 1.00 eq.) in DMF (150). 10-Undecanol (10.3 mL, 8.51 g, 50.0 mmol, 1.00 eq.) and water (10.0 mL) are added dropwise at 0°C. The mixture is stirred for 4 h at 90°C under air and is then poured into water (150 mL). The layers are separated, the aqueous layer is extracted with EA (4x), the combined organic layers are washed with water (2x) and sat. aq. NH_4Cl solution (2x), dried over $MgSO_4$ and the solvent is removed *in vacuo*. After purification via flash column chromatography (SiO_2, CH:EA = 70:30) 11-hydroxyundecan-2-one **66** (9.314 g, 50.0 mmol, >99%) is obtained as a pale yellow oil.

R_f (CH:EA = 70:30) = 0.15

^{1}H-NMR (500 MHz, $CDCl_3$, 298 K) δ [ppm] = 3.63 (t, *J* = 6.6 Hz, 2H), 2.41 (t, *J* = 7.5 Hz, 2H), 2.13 (s, 3H), 1.60-1.51 (m, 4H), 1.39 – 1.22 (m, 10H).

^{13}C-NMR (125 MHz, $CDCl_3$, 298 K) δ [ppm] = 209.7, 63.2, 43.9, 32.9, 30.0, 29.5, 29.46, 29.43, 29.3, 25.8, 24.0.

The analytical data is in agreement with the literature.[235]

11-((*tert*-Butyldimethylsilyl)oxy)undecan-2-one **67**

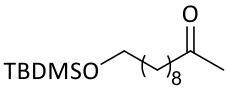

In a flame-dried *Schlenk* flask, to a solution of *tert*-butyldimethylsilyl chloride (8.14 g, 54.2 mmol, 1.20 eq.) and dry pyridine (10 mL) in dry THF (100 mL) is

added 11-hydroxyundecan-2-one **66** (8.42 g, 45.2 mmol, 1.00 eq.) dropwise at 0°C. The mixture is stirred overnight while it is allowed to warm up to RT. The white precipitate is filtered off and washed with Et_2O. The filtrate is washed with water (3x) and brine, dried over $MgSO_4$ and the solvent is removed *in vacuo*. The crude product is filtered through celite using Et_2O to obtain 11-((*tert*-butyldimethylsilyl)oxy)undecan-2-one **67** (9.90 g, 32.9 mmol, 73%) as a pale yellow oil without further purification.

^{1}H-NMR (500 MHz, $CDCl_3$, 298 K) δ [ppm] = 3.59 (t, J = 6.6 Hz, 2H), 2.41 (t, J = 7.5 Hz, 2H), 2.13 (s, 3H), 1.60 – 1.45 (m, 4H), 1.33 – 1.25 (m, 10H), 0.89 (s, 9H), 0.04 (s, 6H).

^{13}C-NMR (125 MHz, $CDCl_3$, 298 K) δ [ppm] = 209.7, 63.5, 44.0, 33.0, 29.6, 29.51, 29.47, 29.3, 26.1, 25.9, 25.8, 24.0, 18.5, -5.1.

The analytical data is in agreement with the literature.[113]

tert-Butyldimethyl((9-(2-methyloxiran-2-yl)nonyl)oxy)silane **3**

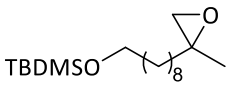

According to **GP-1**, 11-((*tert*-butyldimethylsilyl)oxy)undecan-2-one **67** (84%, 8.96 g, 25.00 mmol, 1.00 eq.), trimethylsulfoxonium iodide (7.70 g, 35.00 mmol, 1.40 eq.) and sodium hydride (60% in mineral oil, 1.20 g, 30.00 mmol, 1.20 eq.) are reacted in THF (35 mL) for 24 h. After purification via flash column chromatography (SiO_2, CH:EA = 90:10) *tert*-butyldimethyl((9-(2-methyloxiran-2-yl)nonyl)oxy)silane **3** (5.38 g, 17.1 mmol, 68%) is obtained as a pale yellow oil.

R_f (CH:EA = 90:10) = 0.48

^{1}H-NMR (500 MHz, $CDCl_3$, 298 K) δ [ppm] = 3.59 (t, J = 6.6 Hz, 2H), 2.60 (d, J = 5.0 Hz, 1H), 2.56 (d, J = 5.0 Hz, 1H), 1.61 – 1.53 (m, 2H), 1.53 – 1.24 (m, 14H), 1.30 (s, 3H), 0.89 (s, 9H), 0.04 (s, 6H).

^{13}C-NMR (125 MHz, $CDCl_3$, 298 K) δ [ppm] = 63.5, 57.2, 54.1, 36.9, 33.0, 29.8, 29.67, 29.66, 29.6, 26.1, 25.9, 25.4, 21.1, 18.5, -5.1.

The analytical data is in agreement with the literature.[113]

9-(2-Methyloxiran-2-yl)nonan-1-ol **68**

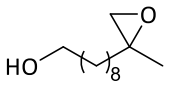

In a flame-dried *Schlenk* flask, to a solution of *tert*-butyldimethyl((9-(2-methyloxiran-2-yl)nonyl)oxy)silane **3** (3.595 g, 11.4 mol, 1.0 eq.) in dry THF (20 mL) TBAF solution (1.0 M in THF, 17.1 mL, 17.1 mmol, 1.5 eq.) is added dropwise. The mixture is stirred for 5 h at RT and the solvent is removed *in vacuo.* After purification via flash column chromatography (SiO_2, CH:EA = 80:20 to 70:30) 9-(2-methyloxiran-2-yl)nonan-1-ol **68** (2.100 g, 10.48 mmol, 92%) is obtained as a colorless oil.

R_f (CH:EA = 70:30) = 0.25

^{1}H-NMR (400 MHz, $CDCl_3$, 298 K) δ [ppm] = 3.63 (t, *J* = 6.7 Hz, 2H), 2.61 – 2.55 (m, 2H), 1.68 – 1.24 (m, 18H), 1.29 (s, 3H).

^{13}C-NMR (100 MHz, $CDCl_3$, 298 K) δ [ppm] = 63.2, 57.2, 54.1, 36.9, 32.9, 29.8, 29.6, 29.6, 29.5, 25.8, 25.4, 21.0.

The analytical data is in agreement with the literature.[203]

9-(2-Methyloxiran-2-yl)nonyl 4-methylbenzenesulfonate **13**

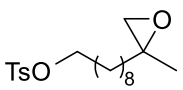

In a flame-dried *Schlenk* flask, 9-(2-methyloxiran-2-yl)nonan-1-ol **68** (2.003 g, 10.00 mmol, 1.00 eq.)) and *p*-toluenesulfonyl chloride (2.097 g, 11.0 g, 1.10 eq.) are dissolved in dry DCM (30). NEt_3 (3.47 mL, 2.530 g, 25.00 mmol, 2.50 eq.) is added dropwise and the mixture is stirred for 4 h at RT. and sat. aq. NH_4Cl solution and water are added. The layers are separated, the aqueous layer is extracted with Et_2O (3x), the combined organic layers are washed with water and brine, dried over $MgSO_4$ and the solvent is removed *in vacuo*. After purification via flash column chromatography (SiO_2, CH:EA:NEt_3 = 80:19:1) 9-(2-methyloxiran-2-yl)nonyl 4-methylbenzenesulfonate **13** (2.320 g, 6.54 mmol, 65%) is obtained as a colorless oil.

^{1}H-NMR (500 MHz, $CDCl_3$, 298 K) δ [ppm] = 7.82 – 7.76 (m, 2H), 7.37 – 7.32 (m, 2H), 4.01 (t, *J* = 6.5 Hz, 2H), 2.59 (d, *J* = 4.9 Hz, 1H), 2.56 (d, *J* = 4.9 Hz, 1H), 2.45 (s, 3H), 1.67 – 1.18 (m, 19H).

^{13}C-NMR (125 MHz, $CDCl_3$, 298 K) δ [ppm] = 144.6, 133.3, 129.8, 127.9, 70.7, 57.1, 54.0, 36.7, 29.6, 29.4, 29.3, 28.91, 28.8, 25.3, 25.2, 21.6, 20.9.

The analytical data is in agreement with the literature.[74]

2-Methyl-2-phenyloxirane **5**

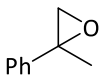

According to **GP-1**, acetophenone (5.95 mL, 6.003 g, 50.00 mmol, 1.00 eq.), trimethylsulfoxonium iodide (15.405 g, 70.00 mmol, 1.40 eq.) and sodium hydride (60% in mineral oil, 2.400 g, 60.00 mmol, 1.20 eq.) are reacted in THF (50 mL) overnight. After purification via flash column chromatography (SiO_2, CH:EA:NEt_3 = 95:4:1) 2-methyl-2-phenyloxirane **5** (4.373 g, 32.59 mmol, 65%) is obtained as a colorless oil.

R_f (CH:EA:NEt_3 = 95:4:1) = 0.2

^{1}H-NMR (500 MHz, $CDCl_3$, 298 K) δ [ppm] = 7.41 – 7.24 (m, 5H), 2.98 (d, *J* = 5.4 Hz, 1H), 2.81 (d, *J* = 5.4 Hz, 1H), 1.73 (s, 3H).

^{13}C-NMR (125 MHz, $CDCl_3$, 298 K) δ [ppm] = 141.32, 128.46, 127.59, 125.44, 57.16, 56.89, 21.95.

The analytical data is in agreement with the literature.[236]

Cycloocten oxide **6**

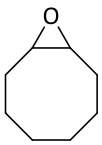

According to **GP-2,** cyclooctene (95%, 12.72 g, 110.0 mmol, 1.00 eq.) and *m*CPBA (75%, 38.0 g, 165.0 mmol, 1.50 eq.) are reacted in DCM (320 mL) overnight. After purification via flash column chromatography (SiO_2, CH:EA = 95:5) and distillation (75°C, 12 mbar) cyclooctene oxide **6** (11.05 g, 87.6 mmol, 80%) is obtained as colorless crystals.

R_f (CH:EA = 95:5) = 0.3

^{1}H-NMR (400 MHz, $CDCl_3$, 298 K) δ [ppm] = 2.93 – 2.87 (m, 2H), 2.18 – 2.11 (m, 2H), 1.67 – 1.39 (m, 8H), 1.33 – 1.22 (m, 2H).

^{13}C-NMR (100 MHz, $CDCl_3$, 298 K) δ [ppm] = 55.8, 26.7, 26.4, 25.7.

The analytical data is in agreement with the literature.[237]

2-(4-Methoxyphenyl)oxirane **7**

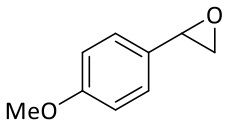

In a flame-dried *Schlenk* flask, trimethylsulfonium iodide (98%, 5.99 g, 28.75 mmol, 1.15 eq.) is dissolved in dry THF (50 mL). Sodium hydride (60% in mineral oil, 1.20 g, 30.00 mmol, 1.20 eq.) is added and the reaction is stirred at RT for 1 h. 2-(4-Methoxyphenyl)acetaldehyde (98%, 3.47 g, 25.00 mmol, 1.00 eq.) is added dropwise at 0°C and the reaction is stirred overnight while it is allowed to warm up to RT. The reaction mixture is poured on ice. The layers are separated, the aqueous layer is extracted with Et_2O, the combined organic layers are washed with water and brine, dried over $MgSO_4$ and the solvent is removed *in vacuo*. After purification via flash column chromatography (Al_2O_3, CH:EA = 70:30) 2-(4-methoxyphenyl)oxirane **7** (1.96 g, 13.10 mmol, 52%) is obtained as a temperature sensitive yellow oil.

^{1}H-NMR (500 MHz, $CDCl_3$, 298 K) δ [ppm] = 7.22 – 7.18 (m, 2H), 6.90 – 6.87 (m, 2H), 3.82 (dd, *J* = 4.0, 2.6 Hz, 1H), 3.81 (s, 3H), 3.12 (dd, *J* = 5.3, 4.0 Hz, 1H), 2.81 (dd, *J* = 5.3, 2.6 Hz, 1H).

^{13}C-NMR (125 MHz, $CDCl_3$, 298 K) δ [ppm] = 159.8, 129.6, 127.0, 114.1, 55.4, 52.4, 51.1.

The analytical data is in agreement with the literature.[238]

2-(4-Bromophenyl)-2-methyloxirane **9**

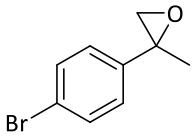

According to **GP-1**, 4-bromoacetophenone (5.00 g, 24.62 mmol, 1.00 eq.), trimethylsulfoxonium iodide (7.74 g, 34.47 mmol, 1.40 eq.) and sodium hydride (60% in mineral oil, 1.18 g, 29.54 mmol, 1.20 eq.) are reacted in THF (25 mL) overnight. After purification via flash column chromatography (SiO_2, CH:EA = 90:10) and distillation

(4 mbar, 91°C) 2-(4-bromophenyl)-2-methyloxirane **9** (3.60 g, 16.90 mmol, 67%) is obtained as a colorless oil.

R_f (CH:EA = 90:10) = 0.34

^{1}H-NMR (500 MHz, $CDCl_3$, 298 K) δ [ppm] = 7.47 – 7.44 (m, 2H), 7.25 – 7.22 (m, 2H), 2.97 (d, *J* = 5.4 Hz, 1H), 2.75 (dd, *J* = 5.4, 0.7 Hz, 1H), 1.69 (d, *J* = 0.7 Hz, 3H).

^{13}C-NMR (125 MHz, $CDCl_3$, 298 K) δ [ppm] = 140.5, 131.6, 127.3, 121.6, 57.1, 56.5, 21.7.

The analytical data is in agreement with the literature.[239]

1-Tosyl-2,5-dihydro-1*H*-pyrrole **69**

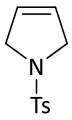

In a flame-dried *Schlenk* flask, (*Z*)-1,4-dichlorobut-2-ene (95%, 6.57 g, 50.00 mmol, 1.00 eq.) and *p*-toluenesulfonamide (10.27 g, 60.00 mmol, 1.10 eq.) are added into dry DMF (60 mL). Sodium hydride (60% in mineral oil, 2.00 g, 50.00 mmol, 1.00 eq.) is added portion wise and the reaction mixture is stirred at RT for 2 h. After addition of water (200 mL) the mixture is stirred for 30 min. The precipitate is filtered off, washed with water, ^{n}pentane and dried *in vacuo* to obtain 1-tosyl-2,5-dihydro-1*H*-pyrrole **69** (4.84 g, 21.90 mmol, 44%) as pale yellow solid.

^{1}H-NMR (500 MHz, $CDCl_3$, 298 K) δ [ppm] = 7.73 – 7.70 (m, 2H), 7.34 – 7.29 (m, 2H), 5.65 (s, 2H), 4.12 (s, 4H), 2.42 (s, 3H).

^{13}C-NMR (125 MHz, $CDCl_3$, 298 K) δ [ppm] = 143.6, 134.5, 129.9, 127.6, 125.6, 55.0, 21.7.

The analytical data is in agreement with the literature.[240]

3-Tosyl-6-oxa-3-azabicyclo[3.1.0]hexane **14**

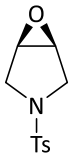

According to **GP-2**, 1-tosyl-2,5-dihydro-1*H*-pyrrole **69** (4.88 g, 21.90 mmol, 1.00 eq.) and *m*CPBA (70%, 6.48 g, 26.30 mmol, 1.20 eq.) are reacted in DCM (45 mL) overnight. After purification via recrystallization from EA and flash column chromatography (SiO_2, CH:EA = 60:40) 3-tosyl-6-oxa-3-azabicyclo[3.1.0]hexane **14** (2.79 g, 11.66 mmol, 53%) is obtained as a white crystalline solid.

R_f (CH:EA = 60:40) = 0.2

^{1}H-NMR (400 MHz, $CDCl_3$, 298 K) δ [ppm] = 7.70 – 7.62 (m, 2H), 7.34 – 7.27 (m, 2H), 3.69 (d, *J* = 12.3 Hz, 2H), 3.58 (s, 2H), 3.36 (d, *J* = 12.2 Hz, 2H), 2.42 (s, 3H).

^{13}C-NMR (100 MHz, $CDCl_3$, 298 K) δ [ppm] = 143.7, 134.8, 129.8, 127.6, 55.2, 48.9, 21.7.

The analytical data is in agreement with the literature.[241]

2,3-Dimethyl-2-phenyloxirane **16**

In a flame-dried *Schlenk* flask, acetophenone (1.75 mL, 1.802 g, 15.00 mmol, 1.00 eq.) and 1,1-dibromoethane (1.50 mL, 3.100 g, 16.50 mmol, 1.10 eq.) are dissolved in dry THF (60 mL). ^{n}BuLi (2.5 M in hexane, 6.6 mL, 16.5 mmol, 1.10 eq.) is added over 30 min at -88°C (^{i}PrOH/N_2) and the mixture is stirred overnight while it is allowed to warm up to RT. Sat. aq. NH_4Cl solution (30 mL) and water (30 mL) are added, and the layers are separated. The aqueous layer is extracted with Et_2O (2x), the combined organic layers are washed with water and brine, dried over $MgSO_4$ and the solvent is removed *in vacuo*. After purification via flash column chromatography (SiO_2, CH:EA:NEt_3 = 95:4:1) 2,3-dimethyl-2-phenyloxirane **16** (1.890 g, 12.75 mmol, 85%, *anti*:*syn* = 78:22) is obtained as a colorless oil.

R_f (CH:EA = 95:4:1) = 0.38

^{1}H-NMR (500 MHz, $CDCl_3$, 298 K) δ [ppm] = major (*anti*): 7.37 – 7.31 (m, 5H), 2.95 (q, *J* = 5.5 Hz, 1H), 1.66 (s, 3H), 1.43 (d, *J* = 5.5 Hz, 3H), minor (*syn*): 7.29 – 7.24 (m, 5H), 3.18 (q, *J* = 5.4 Hz, 1H), 1.65 (s, 3H), 0.99 (d, *J* = 5.3 Hz, 3H).

^{13}C-NMR (125 MHz, $CDCl_3$, 298 K) δ [ppm] = major (*anti*): 143.2, 128.4, 127.3, 125.2, 62.7, 60.5, 17.5, 14.6, minor (*syn*): 139.8, 128.2, 127.3, 126.7, 62.8, 61.4, 24.7, 14.6.

The analytical data is in agreement with the literature.[242]

cis-Stilbene oxide **39**

According to **GP-2,** *cis*-stilbene (97%, 1.86 g, 10.0 mmol, 1.00 eq.) and *m*CPBA (70%, 2.96 g, 12.0 mmol, 1.20 eq.) are reacted in DCM (30 mL) overnight. After purification via flash column chromatography (SiO_2, CH:EA = 90:10) *cis*-stilbene oxide **39** (1.737 g, 8.86 mmol, 89%) is obtained as white waxy solid.

^{1}H-NMR (400 MHz, $CDCl_3$, 298 K) δ [ppm] = 7.20 – 7.13 (m, 10H), 4.37 (s, 2H).

^{13}C-NMR (100 MHz, $CDCl_3$, 298 K) δ [ppm] = 134.5, 127.9, 127.6, 127.0, 59.9.

The analytical data is in agreement with the literature.[243]

trans-Stilbene oxide **70**

According to **GP-2,** *trans*-stilbene (98%, 3.68 g, 20.0 mmol, 1.00 eq.) and *m*CPBA (70%, 5.42 g, 22.0 mmol, 1.10 eq.) are reacted in DCM (80 mL) overnight. After purification via flash column chromatography (SiO_2, CH:EA = 90:10) *trans*-stilbene oxide **70** (3.588 g, 18.3 mmol, 91%) is obtained as white solid.

^{1}H-NMR (400 MHz, $CDCl_3$, 298 K) δ [ppm] = 7.43 – 7.33 (m, 10H), 3.89 (s, 2H).

^{13}C-NMR (100 MHz, $CDCl_3$, 298 K) δ [ppm] = 137.3, 128.7, 128.5, 125.6, 63.0.

The analytical data is in agreement with the literature.[244]

(*Z*)-1,4-diethoxybut-2-ene **71**

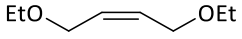

In a flame-dried *Schlenk* flask, to a suspension of sodium hydride (60% in mineral oil, 4.20 g, 105.0 mmol, 2.10 eq.) in dry DMF (50 mL) was added (*Z*)-2-butene-1,4-diol dropwise at -15°C. After 15 min a solution of 1-bromo ethane in dry DMF (50 mL) is added over 30 min. The mixture is stirred for 30 min at -15°C and overnight at RT. The mixture is purred on water (200 mL). The layers are separated, the aqueous layer is extracted with EA (3x), the combined organic layers are washed with water (2x) and brine (1x), dried over $MgSO_4$ and the solvent is removed *in vacuo*. After purification via distillation (50 mbar, 76 – 86°C) (*Z*)-1,4-diethoxybut-2-ene **71** (4.777 g, 33.13 mmol, 66%) is obtained as a colorless oil.

^{1}H-NMR (400 MHz, $CDCl_3$, 298 K) δ [ppm] = 5.73 – 5.70 (m, 2H), 4.08 – 4.01 (m, 4H), 3.48 (q, *J* = 7.0 Hz, 4H), 1.21 (t, *J* = 7.0 Hz, 6H).

^{13}C-NMR (100 MHz, $CDCl_3$, 298 K) δ [ppm] = 129.5, 66.4, 65.9, 15.4.

The analytical data is in agreement with the literature.[245]

cis-2,3-Bis(ethoxymethyl)oxirane **72**

According to **GP-2**, (*Z*)-1,4-diethoxybut-2-ene **71** (3.00 g, 20.80 mmol, 1.00 eq.) and *m*CPBA (70%, 6.15 g, 24.96 mmol, 1.20 eq.) are reacted in DCM (60 mL) overnight. After purification via flash column chromatography (SiO_2, CH:EA = 80:20) *cis*-2,3-bis(ethoxymethyl)oxirane **72** (2.60 g, 16.24 mmol, 78%) is obtained as a white crystalline solid.

^{1}H-NMR (500 MHz, $CDCl_3$, 298 K) δ [ppm] = 3.70 – 3.47 (m, 8H), 3.23 – 3.19 (m, 2H), 1.22 (t, *J* = 7.0 Hz, 6H).

^{13}C-NMR (125 MHz, $CDCl_3$, 298 K) δ [ppm] = 68.6, 66.9, 54.7, 15.3.

The analytical data is in agreement with the literature.[246]

2-(4-Chlorophenyl)oxirane **73**

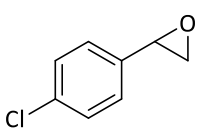

According to **GP-2,** 1-chloro-4-vinylbenzene (97%, 4.33 mL, 5.00 g, 35.0 mmol, 1.00 eq.) and *m*CPBA (70%, 7.25 g, 42.0 mmol, 1.20 eq.) are reacted in DCM (100 mL) overnight. After purification via flash column chromatography (SiO_2,

CH:EA:NEt_3 = 80:19:1) 2-(4-chlorophenyl)oxirane **73** (3.695 g, 23.9 mmol, 68%) is obtained as a colorless oil.

R_f (CH:EA = 80:20) = 0.41

^{1}H-NMR (400 MHz, $CDCl_3$, 298 K) δ [ppm] = 7.34 – 7.29 (m, 2H), 7.23 – 7.18 (m, 2H), 3.84 (dd, *J* = 4.1, 2.5 Hz, 1H), 3.14 (dd, *J* = 5.5, 4.1 Hz, 1H), 2.75 (dd, *J* = 5.5, 2.5 Hz, 1H).

^{13}C-NMR (100 MHz, $CDCl_3$, 298 K) δ [ppm] = 136.3, 134.1, 128.9, 127.0, 51.9, 51.4.

The analytical data is in agreement with the literature.[247]

N-propargyl-*p*-toluenesulfonamide **74**

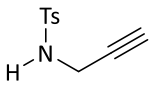

In a flame-dried *Schlenk* flask, propargylamine (97%, 5.28 mL, 4.54 g, 80.00 mmol, 1.00 eq.) is dissolved in DCM (250 mL). Tosyl chloride (97% 16.78 g, 88.00 mmol, 1.10 eq.) and NEt_3 (27.72 mL, 20.24 g, 200.0 mmol, 2.50 eq.) are added and the mixture is stirred for 1 h at RT. The mixture is diluted with 2 M HCl (200 mL). The layers are separated, the aqueous layer is extracted with DCM (3x) and Et_2O (1x), the combined organic layers are washed with brine and then dried over $MgSO_4$, and the solvent is removed *in vacuo*. After purification via flash column chromatography (SiO_2, CH:EA = 1:1) *N*-propargyl-*p*-toluenesulfonamide **74** (16.640 g, 79.52 mmol, 99%) is obtained as a light yellow solid.

R_f (CH:EA = 1:1) = 0.5

^{1}H-NMR (500 MHz, $CDCl_3$, 298 K) δ [ppm] = 7.79 – 7.76 (m, 2H), 7.34 – 7.30 (m, 2H), 4.66 (s, 1H), 3.83 (dd, *J* = 6.1, 2.5 Hz, 2H), 2.43 (s, 3H), 2.10 (t, *J* = 2.5 Hz, 1H).

^{13}C-NMR (125 MHz, $CDCl_3$, 298 K) δ [ppm] = 144.0, 136.7, 129.9, 127.5, 78.1, 73.1, 33.0, 21.7.

The analytical data is in agreement with the literature.[248]

4-Methyl-*N*-(2-methyl-2-propen-1-yl)-*N*-2-propyn-1-ylbenzenesulfonamide **75**

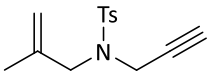

In a flame-dried *Schlenk* flask, *N*-propargyl-*p*-toluenesulfonamide **74** (3.650 g, 17.44 mmol, 1.00 eq.), potassium carbonate (4.820 g, 34.88 mmol, 2.00 eq.) and potassium iodide (5.790 g, 34.88 mmol, 2.0 eq.) are mixed in dry DMF (50 mL). 3-Chloro-2-methylpropene (5.13 mL, 4.738 g, 52.32 mmol, 3.00 eq.) is added dropwise at 0°C and the mixture is stirred overnight at 60°C. Sat. aq. NH_4Cl solution is added, and the layers are separated. The aqueous layer is extracted with EA (3x), the combined organic layers are washed with water and brine, dried over $MgSO_4$, and the solvent is removed *in vacuo*. After purification via flash column chromatography (SiO_2, CH:EA = 80:20) 4-methyl-*N*-(2-methyl-2-propen-1-yl)-*N*-2-propyn-1-ylbenzenesulfonamide **75** (3.884 g, 14.76 mmol, 85%) is obtained as a colorless solid.

^{1}H-NMR (500 MHz, $CDCl_3$, 298 K) δ [ppm] = 7.76 – 7.73 (m, 2H), 7.31 – 7.27 (m, 2H), 5.00 – 4.94 (m, 2H), 4.05 (d, *J* = 2.4 Hz, 2H), 3.73 (s, 2H), 2.42 (s, 3H), 1.96 (t, *J* = 2.5 Hz, 1H), 1.76 (s, 3H).

^{13}C-NMR (125 MHz, $CDCl_3$, 298 K) δ [ppm] = 143.6, 139.3, 136.2, 129.6, 128.0, 115.7, 76.5, 73.8, 52.5, 35.6, 21.7, 19.8.

The analytical data is in agreement with the literature.[205]

4-Methyl-*N*-(2-methylallyl)-*N*-(3-(trimethylsilyl)prop-2-yn-1-yl)benzenesulfonamide **76**

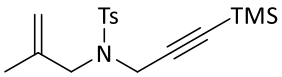

In a flame-dried *Schlenk* flask, to a solution of 4-methyl-*N*-(2-methyl-2-propen-1-yl)-*N*-2-propyn-1-ylbenzenesulfonamide **75** (7.36 g, 28.1 mmol, 1.00 eq.) in dry THF (60 mL) ^{n}BuLi (2.5 M in hexane, 15.0 mL, 36.5 mmol, 1.30 eq.) is added dropwise at -78°C and stirred for 30 min. TMSCl (7.2 mL, 56.2 mmol, 2.05 eq.) is added dropwise at -78 °C and the reaction mixture is stirred at RT for 4 h. After addition of water (50 mL) the layers are separated, and the aqueous layer is extracted with EA (3x). The combined organic layers are washed with water and brine, dried over $MgSO_4$ and the solvent is removed *in vacuo*. After purification via flash column chromatography (SiO_2, CH:EA = 94:6) 4-methyl-*N*-(2-methylallyl)-*N*-(3-(trimethylsilyl)prop-2-yn-1-yl)benzenesulfonamide **76** (5.93 g, 17.7 mmol, 63%) is obtained as a white solid.

R_f (CH:EA = 94:6) = 0.27

^{1}H-NMR (400 MHz, $CDCl_3$, 298 K) δ [ppm] = 7.76 – 7.71 (m, 2H), 7.31 – 7.27 (m, 2H), 4.96 (d, *J* = 6.69 Hz, 2H), 4.05 (s, 2H), 3.73 (s, 2H), 2.42 (s, 3H), 1.77 (t, *J* = 1.1 Hz, 3H), -0.02 (s, 9H).

^{13}C-NMR (100 MHz, $CDCl_3$, 298 K) δ [ppm] = 143.4, 139.3, 136.2, 129.6, 127.9, 115.7, 97.8, 91.1, 52.5, 36.6, 21.7, 19.8, -0.3.

The analytical data is in agreement with the literature.[249]

4-Methyl-*N*-(2-methylallyl)-*N*-(undec-2-yn-1-yl)benzenesulfonamide **77**

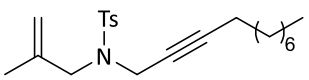

In a flame-dried *Schlenk* flask, to a solution of 4-methyl-*N*-(2-methyl-2-propen-1-yl)-*N*-2-propyn-1-ylbenzenesulfonamide **75** (2.634 g, 10.0 mmol, 1.00 eq.) in dry THF (100 mL) ^{n}BuLi (2.5 M in hexane, 4.48 mL, 11.2 mmol, 1.12 eq.) is added dropwise at -78°C and stirred for 10 min at RT. 1-Iodoctane (9.10 mL, 12.007 g, 50.0 mmol, 5.0 eq.) is added dropwise at -78 °C and the reaction mixture is stirred at RT for 18 h. The mixture is diluted with Et_2O (100 mL) and sat. aq. $NaHCO_3$ solution (100 mL). The layers are separated, and the aqueous layer is extracted with Et_2O (2x). The combined organic layers are washed with water and brine, dried over $MgSO_4$ and the solvent is removed *in vacuo*. The crude product is purified by filtration with a silica plug (SiO_2, CH:EA = 100:0 to 90:10) and flash column chromatography (SiO_2, CH:EA = 95:5) to obtain 4-

methyl-*N*-(2-methylallyl)-*N*-(undec-2-yn-1-yl)benzenesulfonamide **77** (3.104 g, 7.9 mmol, 79%) is obtained as a yellowish oil.

R_f (CH:EA = 95:5) = 0.19

^{1}H-NMR (400 MHz, $CDCl_3$, 298 K) δ [ppm] = 7.76 – 7.72 (m, 2H), 7.30 – 7.26 (m, 2H), 4.97 – 4.94 (m, 2H), 4.01 (t, *J* = 2.2 Hz, 2H), 3.71 (s, 2H), 2.42 (s, 3H), 1.86 (ddt, *J* = 6.8, 4.4, 2.4 Hz, 2H), 1.77 (s, 3H), 1.35 – 1.14 (m, 12H), 0.89 (t, *J* = 7.0 Hz, 3H).

^{13}C-NMR (100 MHz, $CDCl_3$, 298 K) δ [ppm] = 143.2, 139.6, 136.5, 129.4, 128.0, 115.3, 86.4, 72.3, 52.4, 36.2, 32.0, 29.3, 29.2, 29.0, 28.5, 22.8, 21.7, 19.9, 18.6, 14.2.

HRMS (ESI+): m/z calculated for $[M+H]^+$ = 376.2305, found = 376.2312.

IR ν_{max} [cm^{-1}] = 2926, 2856, 1349, 1170, 1096, 1015, 904, 813, 764, 708, 694, 656, 571, 554.

N-(3-(4-fluorophenyl)prop-2-yn-1-yl)-4-methyl-*N*-(2-methylallyl)benzenesulfonamide **78**

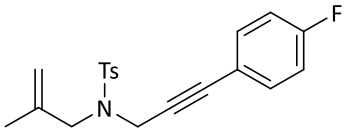

In a flame-dried *Schlenk* flask, bis(triphenylphosphin)palladium(II) dichloride (0.121 g, 0.17 mmol, 0.20 eq.), copper(I) iodide (0.033 g, 0.17 mmol, 0.20 eq.), 1-fluoro-4-iodobenzene (2.107 g, 9.49 mmol, 1.10 eq.) and 4-methyl-*N*-(2-methyl-2-propen-1-yl)-*N*-2-propyn-1-ylbenzenesulfonamide **75** (2.274 g, 8.63 mmol, 1.00 eq.) are dissolved in freshly distilled NEt_3 (100 mL). The mixture is stirred overnight at 50°C. The reaction mixture is diluted with Et_2O and purred on water. The aqueous layer is extracted with Et_2O (3x), the combined organic layers are washed with water (3x), dried over $MgSO_4$ and the solvent is removed *in vacuo*. After purification via flash column chromatography (SiO_2, CH:EA = 90:10) *N*-(3-(4-fluorophenyl)prop-2-yn-1-yl)-4-methyl-*N*-(2-methylallyl)benzenesulfonamide **78** (3.083 g, 8.63 mmol, >99%) is obtained as a brownish oil.

R_f (CH:EA = 90:10) = 0.3

^{1}H-NMR (500 MHz, $CDCl_3$, 298 K) δ [ppm] = 7.79 – 7.76 (m, 2H), 7.26 – 7.23 (m, 2H), 7.04 – 7.00 (m, 2H), 6.95 – 6.90 (m, 2H), 5.00 (d, *J* = 1.0 Hz, 2H), 4.23 (s, 2H), 3.79 (s, 2H), 2.34 (s, 3H), 1.81 (s, 3H).

^{13}C-NMR (125 MHz, $CDCl_3$, 298 K) δ [ppm] = 162.59 (d, *J* = 249.9 Hz), 143.51, 139.46, 136.29, 133.50 (d, *J* = 8.4 Hz), 129.60, 127.99, 118.47 (d, *J* = 3.5 Hz), 115.69, 115.53 (d, *J* = 22.1 Hz), 84.70, 81.55 (d, *J* = 1.5 Hz), 52.91, 36.47, 21.56, 19.89.

The analytical data is in agreement with the literature.[250]

4-Methyl-N-((2-methyloxiran-2-yl)methyl)-N-(prop-2-yn-1-yl)benzenesulfonamide **18**

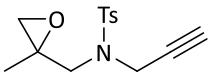

According to **GP-2**, 4-methyl-*N*-(2-methyl-2-propen-1-yl)-*N*-2-propyn-1-ylbenzenesulfonamide **75** (3.800 g, 14.40 mmol, 1.00 eq.) and *m*CPBA (70%, 2.981 g, 17.28 mmol, 1.20 eq.) are reacted in DCM (30 mL) overnight. After purification via flash column chromatography (SiO_2, CH:EA = 80:20) 4-methyl-N-((2-methyloxiran-2-yl)methyl)-N-(prop-2-yn-1-yl)benzenesulfonamide **18** (3.787 g, 13.56 mmol, 94%) is obtained as a white crystalline solid.

^{1}H-NMR (500 MHz, $CDCl_3$, 298 K) δ [ppm] = 7.74 – 7.69 (m, 2H), 7.31 – 7.26 (m, 2H), 4.30 – 4.17 (m, 2H), 3.40 (d, *J* = 14.7 Hz, 1H), 3.27 (d, *J* = 14.4 Hz, 1H), 2.77 (d, *J* = 4.6 Hz, 1H), 2.64 (d, *J* = 4.7 Hz, 1H), 2.42 (s, 3H), 1.97 (t, *J* = 2.5 Hz, 1H), 1.40 (s, 3H).

^{13}C-NMR (125 MHz, $CDCl_3$, 298 K) δ [ppm] = 143.9, 136.0, 129.6, 127.9, 76.6, 74.1, 55.7, 51.7, 51.0, 37.8, 21.7, 19.0.

The analytical data is in agreement with the literature.[205]

4-Methyl-*N*-((2-methyloxiran-2-yl)methyl)-*N*-(undec-2-yn-1-yl)benzenesulfonamide **20**

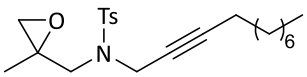

According to **GP-2**, 4-methyl-*N*-(2-methylallyl)-*N*-(undec-2-yn-1-yl)benzenesulfonamide **77** (2.629 g, 7.0 mmol, 1.00 eq.) and *m*CPBA (70%, 2.070 g, 8.40 mmol, 1.20 eq.) are reacted in DCM (15 mL) overnight. After purification via flash column chromatography (SiO_2, CH:EA = 80:20) 4-Methyl-*N*-((2-methyloxiran-2-yl)methyl)-*N*-(undec-2-yn-1-yl)benzenesulfonamide **20** (2.197 g, 5.61 mmol, 80%) is obtained as a white crystalline solid.

R_f (CH:EA = 80:20) = 0.4

^{1}H-NMR (500 MHz, $CDCl_3$, 298 K) δ [ppm] = 7.75 – 7.69 (m, 2H), 7.30 – 7.24 (m, 2H), 4.28 – 4.20 (m, 1H), 4.18 – 4.09 (m, 1H), 3.32 (d, *J* = 14.2 Hz, 1H), 3.27 (d, *J* = 14.2 Hz, 1H), 2.77 (dd, *J* = 4.7, 0.8 Hz, 1H), 2.63 (d, *J* = 4.7 Hz, 1H), 2.41 (s, 3H), 1.87 – 1.82 (m, 2H), 1.40 (d, *J* = 0.6 Hz, 3H), 1.33 – 1.13 (m, 12H), 0.89 (t, *J* = 7.1 Hz, 3H).

^{13}C-NMR (125 MHz, $CDCl_3$, 298 K) δ [ppm] = 143.5, 136.3, 129.5, 128.0, 86.7, 72.3, 55.7, 51.9, 50.9, 38.4, 32.0, 29.3, 29.2, 29.0, 28.5, 22.6, 21.7, 19.1, 18.6, 14.2.

The analytical data is in agreement with the literature.[251]

N-(3-(4-fluorophenyl)prop-2-yn-1-yl)-4-methyl-*N*-((2-methyloxiran-2-yl)methyl)benzene sulfonamide **24**

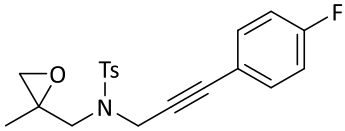

Route A: In a flame-dried *Schlenk* flask, bis(triphenylphosphin)palladium(II) dichloride (0.140 g, 0.20 mmol, 0.21 eq.), copper(I) iodide (0.038 g, 0.20 mmol, 0.21 eq.), 1-fluoro-4-

iodobenzene (2.137 g, 9.7 mmol, 1.00 eq.) and 4-methyl-N-((2-methyloxiran-2-yl)methyl)-N-(prop-2-yn-1-yl)benzenesulfonamide **18** (2.794 g, 10.0 mmol, 1.03 eq.) are dissolved in freshly distilled NEt_3 (100 mL). The mixture is stirred overnight at 50°C. The reaction mixture is diluted with Et_2O and purred on water. The aqueous layer is extracted with Et_2O (3x), the combined organic layers are washed with water (3x), dried over $MgSO_4$ and the solvent is removed *in vacuo*. After purification via flash column chromatography (SiO_2, CH:EA:NEt_3 = 80:19:1) *N*-(3-(4-fluorophenyl)prop-2-yn-1-yl)-4-methyl-*N*-((2-methyloxiran-2-yl)methyl)benzenesulfonamide **24** (3.104 g, 8.3 mmol, 86%) is obtained as a yellow oil.

Route B: According to **GP-2**, *N*-(3-(4-fluorophenyl)prop-2-yn-1-yl)-4-methyl-*N*-(2-methylallyl) benzenesulfonamide **78** (3.085 g, 8.63 mmol, 1.00 eq.) and *m*CPBA (70%, 2.553 g, 10.36 mmol, 1.20 eq.) are reacted in DCM (20 mL) for 24 h. After purification via flash column chromatography (SiO_2, CH:EA:NEt_3 = 80:19:1) *N*-(3-(4-fluorophenyl)prop-2-yn-1-yl)-4-methyl-*N*-((2-methyloxiran-2-yl)methyl)benzenesulfonamide **24** (0.874 g, 2.26 mmol, 26%) is obtained as a yellow oil.

R_f (CH:EA = 80:20) = 0.2

^{1}H-NMR (500 MHz, $CDCl_3$, 298 K) δ [ppm] = 7.78 – 7.72 (m, 2H), 7.24 (d, *J* = 8.0 Hz, 2H), 7.04 – 6.97 (m, 2H), 6.96 – 6.87 (m, 2H), 4.49 – 4.35 (m, 2H), 3.43 (d, *J* = 14.3 Hz, 1H), 3.34 (d, *J* = 14.3 Hz, 1H), 2.81 (d, *J* = 4.6 Hz, 1H), 2.66 (d, *J* = 4.6 Hz, 1H), 2.33 (s, 3H), 1.44 (s, 3H).

^{13}C-NMR (125 MHz, $CDCl_3$, 298 K) δ [ppm] = 162.6 (d, *J* = 250.0 Hz), 143.7, 136.2, 133.5 (d, *J* = 8.3 Hz), 129.7, 127.9, 118.4 (d, *J* = 3.5 Hz), 115.5 (d, *J* = 22.0 Hz), 84.8, 81.6 (d, *J* = 1.6 Hz), 55.9, 51.7, 51.2, 38.7, 21.6, 19.1.

^{19}F-NMR (470 MHz $CDCl_3$, 298 K) δ [ppm] = -110.48.

IR ν_{max} [cm^{-1}] = 2990, 2925, 1600, 1505, 1347, 1220, 1160, 1089, 1045, 1020, 925, 902, 837, 813, 748, 673, 652, 565, 542, 530.

HRMS (ESI+): m/z calculated for $[M+Na]^+$ = 396.1040, found = 396.1039.

4-Methyl-*N*-((2-methyloxiran-2-yl)methyl)-*N*-(3-(trimethylsilyl)prop-2-yn-1-yl)benzenesulfonamide **26**

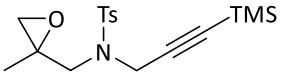

According to **GP-2**, 4-methyl-*N*-(2-methylallyl)-*N*-(3-(trimethylsilyl)prop-2-yn-1-yl)benzenesulfonamide **76** (5.93 g, 17.7 mmol, 1.00 eq.) and *m*CPBA (70%, 4.53 g, 23.0 mmol, 1.30 eq.) are reacted in DCM (300 mL) overnight. After purification via flash column chromatography (SiO_2, CH:EA:NEt_3 = 85:14:1) 4-methyl-*N*-((2-methyloxiran-2-yl)methyl)-*N*-(3-(trimethylsilyl)prop-2-yn-1-yl)benzenesulfonamide **26** (3.65 g, 10.4 mmol, 59%) is obtained as a white crystalline solid.

R_f (CH:EA = 85:15) = 0.24

^{1}H-NMR (500 MHz, $CDCl_3$, 298 K) δ [ppm] = 7.74 – 7.68 (m, 2H), 7.30 – 7.26 (m, 2H), 4.32 – 4.13 (m, 2H), 3.42 – 3.21 (m, 2H), 2.78 (d, *J* = 4.7 Hz, 1H), 2.63 (d, *J* = 4.7 Hz, 1H), 2.41 (s, 3H), 1.41 (s, 3H), -0.04 (s, 9H).

^{13}C-NMR (125 MHz, $CDCl_3$, 298 K) δ [ppm] = 143.6, 136.1, 129.7, 127.9, 97.9, 91.3, 55.6, 52.0, 50.9, 38.8, 21.7, 19.1, -0.3.

IR ν_{max} [cm^{-1}] = 1337, 1247, 1161, 997, 808, 752, 667, 647, 569, 544.

2-Methylene-4-phenylbutan-1-ol **2b**

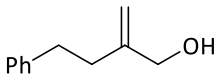

A flame-dried three-necked flask is equipped with reflux condenser and dropping funnel. Magnesium turnings (4.011 g, 165.0 mmol, 3.30 eq.) are added and stirred under vacuum overnight. Dibromo methane (0.05 mL) and dry Et_2O (9 mL) are added and stirred for 15 min. A solution of (2-bromoethyl)benzene in dry Et_2O (54 mL) is slowly added over 30 min via dropping funnel (maintaining gentle refluxing) and further stirred for 1 h. The mixture is cooled to 0°C, transferred into a freshly prepared suspension of copper(I) iodide (1.619 g, 8.5 mmol, 0.17 eq.) in dry Et_2O via transfer canula at 0°C and stirred for 15 min. Propargylic alcohol (2.803 g, 50 mmol, 1.0 eq.) is added over 30 min at 0°C and the mixture is stirred overnight at RT. Aq. sat. NH_4Cl solution is added at 0°C and the layers are separated. The organic layer is extracted with Et_2O (3x), the combined organic layers are washed with brine dried over $MgSO_4$ and the solvent is removed *in vacuo*. After purification via flash column chromatography (SiO_2, CH:EA = 80:20) 2-methylene-4-phenylbutan-1-ol **2b** (3.720 g, 22.9 mmol, 46%) is obtained as yellow oil.

^{1}H-NMR (500 MHz, $CDCl_3$, 298 K) δ [ppm] = 7.32 – 7.25 (m, 2H), 7.23 – 7.16 (m, 3H), 5.08 – 5.06 (m, 1H), 4.93 (d, *J* = 1.3 Hz, 1H), 4.10 (d, *J* = 6.1 Hz, 2H), 2.82 – 2.77 (m, 2H), 2.42 – 2.37 (m, 2H), 1.45 – 1.41 (m, 1H).

^{13}C-NMR (125 MHz, $CDCl_3$, 298 K) δ [ppm] = 148.6, 142.0, 128.50, 128.46, 126.1, 110.0, 66.2, 34.8, 34.4.

The analytical data is in agreement with the literature.[252]

4-Methyl-*N*-(2-methylene-4-phenylbutyl)-*N*-(prop-2-yn-1-yl)benzenesulfonamide **79**

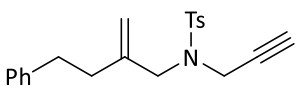

In a flame-dried *Schlenk* flask, 2-methylene-4-phenylbutan-1-ol **2b** (2.596 g, 16.0 mmol, 1.00 eq.), *N*-propargyl-p-toluenesulfonamide **74** (3.348 g, 16.0 mmol, 1.00 eq.), and PPh_3 (4.196 g, 16.0 mmol, 1.00 eq.) are dissolved in dry THF (160 mL). Diisopropyl azodicarboxylate (3.15 mL, 3.235 g, 16.0 mmol, 1.00 eq.) is added and the mixture is stirred overnight at RT. The solvent is removed *in vacuo* and the crude product is dissolved

in CH. The white precipitate is filtered off and the solvent is removed *in vacuo*. After purification via flash column chromatography (SiO_2, CH:EA 80:20) 4-methyl-*N*-(2-methylene-4-phenylbutyl)-*N*-(prop-2-yn-1-yl)benzenesulfonamide **79** (4.845 g, 13.7 mmol, 86%) is obtained as white solid.

R_f (CH:EA = 80:20) = 0.4

^{1}H-NMR (400 MHz, $CDCl_3$, 298 K) δ [ppm] = 7.78 – 7.71 (m, 2H), 7.32 – 7.24 (m, 4H), 7.24 – 7.14 (m, 3H), 5.03 (d, *J* = 10.0 Hz, 2H), 4.02 (d, *J* = 2.4 Hz, 2H), 3.78 (s, 2H), 2.85 – 2.76 (m, 2H), 2.42 (s, 3H), 2.42 – 2.36 (m, 2H), 1.95 (t, *J* = 2.4 Hz, 1H).

^{13}C-NMR (125 MHz, $CDCl_3$, 298 K) δ [ppm] = 143.7, 142.5, 141.7, 136.1, 129.6, 128.6, 128.5, 128.0, 126.0, 115.6, 76.5, 74.0, 51.3, 35.6, 34.8, 34.0, 21.7.

IR ν_{max} [cm^{-1}] = 3290, 3030, 2920, 1650, 1600, 1460, 1347, 1170, 1093, 898, 814, 762, 698, 657, 570, 542.

HRMS (ESI+): m/z calculated for $[M+H]^+$ = 354.1522, found = 354.1520.

M_p = 58°C

4-Methyl-*N*-((2-phenethyloxiran-2-yl)methyl)-*N*-(prop-2-yn-1-yl)benzenesulfonamide **25**

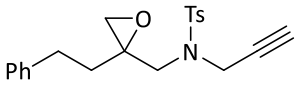

According to **GP-2**, 4-methyl-*N*-(2-methylene-4-phenylbutyl)-*N*-(prop-2-yn-1-yl)benzenesulfonamide **79** (1.767 g, 5.00 mmol, 1.00 eq.) and *m*CPBA (70%, 1.601 g, 6.50 mmol, 1.30 eq.) are reacted in DCM (10 mL) overnight. After purification via flash column chromatography (SiO_2, CH:EA = 90:10) 4-methyl-*N*-((2-phenethyloxiran-2-yl)methyl)-*N*-(prop-2-yn-1-yl)benzenesulfonamide **25** (1.711 g, 4.63 mmol, 93%) is obtained as a white crystalline solid.

R_f (CH:EA = 80:20) = 0.35

^{1}H-NMR (400 MHz, $CDCl_3$, 298 K) *δ* [ppm] = 7.77 – 7.69 (m, 2H), 7.33 – 7.24 (m, 4H), 7.25 – 7.15 (m, 3H), 4.32 – 4.16 (m, 2H), 3.48 (d, *J* = 14.4 Hz, 1H), 3.32 (d, *J* = 14.4 Hz, 1H), 2.81 – 2.72 (m, 2H), 2.72 (dd, *J* = 4.5, 0.8 Hz, 1H), 2.63 (d, *J* = 4.5 Hz, 1H), 2.42 (s, 3H), 2.21 – 2.08 (m, 1H), 1.96 (t, *J* = 2.4 Hz, 1H), 1.93 – 1.80 (m, 1H).

^{13}C-NMR (100 MHz, $CDCl_3$, 298 K) *δ* [ppm] = 143.9, 141.3, 135.8, 129.7, 128.6, 128.5, 128.0, 126.2, 76.5, 74.3, 57.9, 50.4, 49.4, 37.9, 33.9, 30.8, 21.7.

IR ν_{max} [cm^{-1}] = 3265, 2930, 1600, 1432, 1330, 1290, 1162, 1094, 962, 932, 911, 886, 816, 794, 702, 660, 565, 541, 515, 489.

HRMS (ESI+): m/z calculated for $[M+H]^+$ = 392.1291, found = 392.1290.

M_p = 106°C

trans-2-(Prop-2-yn-1-ylamino)cyclohexan-1-ol **80**

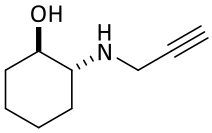

In a flame-dried *Schlenk* flask, to a solution of propargylamine (3.20 mL, 2.754 g, 50.00 mmol, 1.00 eq.) in dry DCM (150 mL) is added triethylaluminium (1.3 M in heptane, 38.5 mL, 50.00 mmol, 1.00 eq.) at 0°C and stirred for 30 min. Cyclohexene oxide (5.06 mL, 4.908 g, 50.00 mmol, 1.00 eq.) is added at 0°C and the mixture is stirred overnight at RT. 2 M NaOH is added carefully (gas evolution) and the layers are separated. The aqueous layer is extracted with DCM (3x), the combined organic layers are dried over $MgSO_4$, and the solvent is removed *in vacuo*. After purification via flash column chromatography (SiO_2, DCM:MeOH = 95:5) *trans*-2-(prop-2-yn-1-ylamino)cyclohexan-1-ol **80** (5.589 g, 36.47 mmol, 73%) is obtained as a yellowish solid.

R_f (DCM:MeOH = 95:5) = 0.16

^{1}H-NMR (400 MHz, $CDCl_3$, 298 K) δ [ppm] = 3.54 (dd, *J* = 16.9, 2.5 Hz, 1H), 3.43 (dd, *J* = 16.9, 2.4 Hz, 1H), 3.27 – 3.20 (m, 1H), 2.41 (ddd, *J* = 11.3, 9.3, 4.0 Hz, 1H), 2.28 (br s, 2H), 2.22 (t, *J* = 2.4 Hz, 1H), 2.13 – 2.06 (m, 1H), 2.05 – 1.96 (m, 1H), 1.78 – 1.66 (m, 2H), 1.35 – 1.17 (m, 3H), 1.05 – 0.93 (m, 1H).

^{13}C-NMR (125 MHz, $CDCl_3$, 298 K) δ [ppm] = 82.6, 74.1, 71.4, 62.7, 35.8, 33.8, 30.4, 25.0, 24.5.

The analytical data is in agreement with the literature.[253]

N-(*trans*-2-hydroxycyclohexyl)-4-methyl-*N*-(prop-2-yn-1-yl)benzenesulfonamide **81**

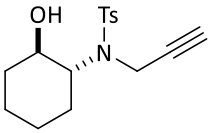

In a flame-dried *Schlenk* flask, *trans*-2-(prop-2-yn-1-ylamino)cyclohexan-1-ol **80** (7.662 g, 50.00 mmol, 1.00 eq.) is dissolved in DCM (150 mL). Tosyl chloride (9.532 g, 50.00 mmol, 1.00 eq.) and NEt_3 (13.94 mL, 10.119 g, 100.0 mmol, 2.00 eq.) are added and the mixture is stirred for 1 h at RT. The mixture is diluted with 2 M HCl (200 mL). The layers are separated, the aqueous layer is extracted with DCM (3x), the combined organic layers are washed with water and brine, dried over $MgSO_4$, and the solvent is removed *in vacuo*. After purification via flash column chromatography (SiO_2, CH:EA = 60:40 to 50:50) *N*-(*trans*-2-hydroxycyclohexyl)-4-methyl-*N*-(prop-2-yn-1-yl)benzenesulfonamide **81** (10.130 g, 32.95 mmol, 66%) is obtained as a light yellow oil.

R_f (CH:EA = 60:40) = 0.3

^{1}H-NMR (500 MHz, $CDCl_3$, 298 K) δ [ppm] = 7.82 – 7.78 (m, 4H), 7.30 – 7.26 (m, 4H), 4.25 (dd, *J* = 18.6, 2.5 Hz, 2H), 4.03 (dd, *J* = 18.6, 2.5 Hz, 2H), 3.64 – 3.50 (m, 2H), 2.41 (s, 3H), 2.34 (d, *J* = 3.2 Hz, 1H), 2.21 (t, *J* = 2.5 Hz, 1H), 2.12 – 2.06 (m, 1H), 1.73 – 1.65 (m, 2H), 1.63 – 1.57 (m, 1H), 1.51 – 1.41 (m, 1H), 1.34 – 1.13 (m, 3H).

^{13}C-NMR (125 MHz, $CDCl_3$, 298 K) δ [ppm] = 143.7, 137.6, 129.6, 127.6, 79.9, 72.9, 69.9, 64.2, 34.0, 32.3, 29.2, 25.3, 24.2, 21.7.

HRMS (ESI+): m/z calculated for $[M+Na]^+$ = 330.1134, found = 330.1139.

IR ν_{max} [cm^{-1}] = 3854, 3845, 3751, 3743, 3736, 3249, 2946, 2859, 1655, 1458, 1441, 1429, 1352, 1328, 1308, 1289, 1161, 1147, 1127, 1089, 1071, 1034, 1017, 969, 883, 858, 820, 802, 786, 769, 726, 691, 662, 615, 576, 543.

4-Methyl-*N*-(2-oxocyclohexyl)-*N*-(prop-2-yn-1-yl)benzenesulfonamide **82**

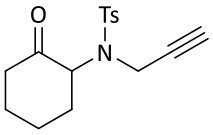

In a flame-dried *Schlenk* flask, to a solution of oxalyl chloride (2.62 mL, 3.808 g, 30.0 mmol, 1.50 eq.) in dry DCM (90 mL) is added DMSO (4.26 mL, 4.688 g, 60.0 mmol, 3.00 eq.) dropwise at -78°C (gas evolution) and stirred for 10 min. A solution of *N*-(*trans*-2-hydroxycyclohexyl)-4-methyl-*N*-(prop-2-yn-1-yl)benzenesulfonamide **81** (6.148 g, 20.0 mmol, 1.00 eq.) in dry DCM (20 mL) is added into the reaction mixture and is stirred for 30 min. NEt_3 (16.73 mL, 12.143 g, 120.0 mmol, 6.00 eq.) is added at -78°C and the mixture is stirred overnight at RT. The mixture is purred on water and the layers are separated. The aqueous layer is extracted with DCM (3x), the combined organic layers are washed with water and brine, dried over $MgSO_4$ and the solvent is removed *in vacuo*. After purification via flash column chromatography (SiO_2, CH:EA = 80:20) 4-methyl-*N*-(2-oxocyclohexyl)-*N*-(prop-2-yn-1-yl)benzenesulfonamide **82** (5.208 g, 17.1 mmol, 89%) is obtained as crystalline white solid.

^{1}H-NMR (500 MHz, $CDCl_3$, 298 K) δ [ppm] = 7.75 – 7.70 (m, 2H), 7.29 – 7.24 (m, 2H), 4.54 (dd, *J* = 12.9, 5.8 Hz, 1H), 4.38 (dd, *J* = 18.9, 2.5 Hz, 1H), 3.81 (dd, *J* = 18.9, 2.5 Hz, 1H), 2.50 – 2.44 (m, 1H), 2.40 (s, 3H), 2.34 – 2.25 (m, 2H), 2.17 (t, *J* = 2.5 Hz, 1H), 2.12 – 1.94 (m, 3H), 1.77 – 1.55 (m, 2H).

^{13}C-NMR (125 MHz, $CDCl_3$, 298 K) δ [ppm] = 205.8, 143.6, 137.2, 129.6, 127.5, 80.4, 72.5, 65.4, 41.8, 34.8, 33.7, 26.8, 25.1, 21.7.

HRMS (ESI+): m/z calculated for $[M+H]^+$ = 306.1158, found = 306.1155.

IR ν_{max} [cm^{-1}] = 3264, 2945, 2858, 1721, 1596, 1449, 1434, 1332, 1309, 1298, 1298, 1286, 1154, 1114, 1089, 1045, 1016, 998, 897, 883, 823, 803, 778, 738, 688, 662, 620, 581, 554, 525, 501, 473, 452.

4-Methyl-*N*-(prop-2-yn-1-yl)-*N*-(*cis*-1-oxaspiro[2.5]octan-4-yl)benzenesulfonamide **27**

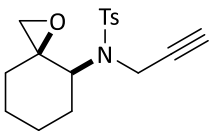

In a flame-dried *Schlenk* flask, to a solution of 4-methyl-*N*-(2-oxocyclohexyl)-*N*-(prop-2-yn-1-yl)benzenesulfonamide **82** (1.527 g, 5.00mmol, 1.00 eq.) and dibromomethane (0.38 mL, 0.956 g, 5.50 mmol, 1.10 eq.) in dry THF (20 mL) is added ^{n}BuLi (2.5 M in hexane, 2.20 mL, 5.50 mmol, 1.10 eq.) over 30 min at -88°C. The mixture is

stirred overnight while it is allowed to warm up to RT. Sat. aq. NH_4Cl solution (10 mL) and water (10 mL) are added. The layers are separated, the aqueous layer is extracted with Et_2O (3x), the combined organic layers are washed with water and brine, dried over $MgSO_4$ and the solvent is removed *in vacuo*. After purification via flash column chromatography (SiO_2, CH:EA:NEt_3 = 80:19:1) 4-methyl-*N*-(prop-2-yn-1-yl)-*N*-(*cis*-1-oxaspiro[2.5]octan-4-yl)benzenesulfonamide **27** (1.211 g, 3.79 mmol, 76%, *d.r.* = >99:<1) is obtained as a crystalline white solid.

R_f (CH:EA = 80:20) = 0.33

^{1}H-NMR (500 MHz, $CDCl_3$, 298 K) δ [ppm] = 7.83 – 7.78 (m, 2H), 7.29 – 7.26 (m, 2H), 4.30 (dd, *J* = 18.9, 2.5 Hz, 1H), 4.20 (dd, *J* = 18.9, 2.5 Hz, 1H), 4.03 (dd, *J* = 12.8, 4.1 Hz, 1H), 3.07 (d, *J* = 4.3 Hz, 1H), 2.52 (d, *J* = 4.4 Hz, 1H), 2.42 (s, 3H), 2.01 (t, *J* = 2.5 Hz, 1H), 1.94 (td, *J* = 13.9, 4.5 Hz, 1H), 1.89 – 1.76 (m, 2H), 1.73 – 1.47 (m, 3H), 1.38 – 1.27 (m, 2H).

^{13}C-NMR (125 MHz, $CDCl_3$, 298 K) δ [ppm] = 143.5, 137.7, 129.5, 127.7, 80.3, 72.5, 61.9, 56.4, 51.8, 34.1, 33.9, 29.2, 26.0, 23.2, 21.7.

HRMS (ESI+): m/z calculated for $[M+H]^+$ = 320.1315, found = 320.1298.

IR ν_{max} [cm^{-1}] = 3264, 2936, 2864, 1443, 1333, 1164, 1154, 1090, 1039, 923, 902, 803, 189, 679, 661, 578, 512.

N-Allyl-*p*-toluenesulfonamide **83**

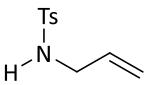

In a flame-dried *Schlenk* flask, allylamine (98%, 3.83 mL, 2.911 g, 50.00 mmol, 1.00 eq.) is dissolved in DCM (150 mL). Tosyl chloride (97% 10.809 g, 55.00 mmol, 1.10 eq.) and NEt_3 (17.33 mL, 12.649 g, 125.0 mmol, 2.50 eq.) are added and the mixture is stirred for 1 h at RT. The mixture is diluted with 2 M HCl (200 mL). The layers are separated, the aqueous layer is extracted with DCM (3x) and Et_2O (1x), the combined organic layers are washed with brine and then dried over $MgSO_4$, and the solvent is removed *in vacuo*. After purification via flash column chromatography (SiO_2, CH:EA = 1:1) *N*-allyl-*p*-toluenesulfonamide **83** (10.518 g, 49.78 mmol, >99%) is obtained as a light yellow solid.

R_f (CH:EA = 1:1) = 0.57

^{1}H-NMR (500 MHz, $CDCl_3$, 298 K) δ [ppm] = 7.78 – 7.74 (m, 2H), 7.33 – 7.29 (m, 2H), 5.72 (ddt, *J* = 17.1, 10.2, 5.8 Hz, 1H), 5.16 (dq, *J* = 17.1, 1.5 Hz, 1H), 5.09 (dq, *J* = 10.2, 1.3 Hz, 1H), 4.59 – 4.52 (m, 1H), 3.58 (tt, *J* = 6.1, 1.5 Hz, 2H), 2.43 (s, 3H).

^{13}C-NMR (125 MHz, $CDCl_3$, 298 K) δ [ppm] = 143.7, 137.1, 133.1, 129.9, 127.3, 117.9, 45.9, 21.7.

The analytical data is in agreement with the literature.[254]

2-(Bromomethyl)-2-methyloxirane **84**

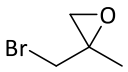

According to **GP-2**, 3-bromo-2-methylpropene (95%, 5.00 g, 35.19 mmol, 1.00 eq.) and *m*CPBA (70%, 10.41 g, 42.23 mmol, 1.20 eq.) are reacted in DCM (150 mL) overnight. After purification via distillation (30 mbar, 50°C) 2-(bromomethyl)-2-methyloxirane **84** (3.541 g, 23.45mmol, 67%) is obtained as a colorless liquid.

^{1}H-NMR (500 MHz, $CDCl_3$, 298 K) δ [ppm] = 3.40 (d, J = 10.4 Hz, 1H), 3.33 (d, J = 10.5 Hz, 1H), 2.84 – 2.78 (m, 3H), 1.50 (s, 4H).

^{13}C-NMR (125 MHz, $CDCl_3$, 298 K) δ [ppm] = 56.1, 55.3, 38.1, 19.3.

The analytical data is in agreement with the literature.[255]

N-allyl-4-methyl-N-((2-methyloxiran-2-yl)methyl)benzenesulfonamide **85**

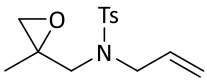

In a flame-dried *Schlenk* flask, *N*-allyl-*p*-toluenesulfonamide **83** (0.277 g, 2.00 mmol, 1.00 eq.), potassium carbonate (0.263 g, 1.90 mmol, 1.52 eq.) and potassium iodide (0.208 g, 1.25 mmol, 1.0 eq.) are mixed in dry acetonitrile (10 mL). 2-(bromomethyl)-2-methyloxirane **84** (0.302 g, 2.0 mmol, 1.60 eq.) is added dropwise at 0°C and the mixture is stirred overnight at RT. The solvent is removed *in vacuo* and the residue is dissolved in EA, washed with water and brine, dried over $MgSO_4$, and the solvent is removed *in vacuo*. After purification via flash column chromatography (SiO_2, CH:EA:NEt_3 = 80:19:1) *N*-allyl-4-methyl-N-((2-methyloxiran-2-yl)methyl) benzenesulfonamide **85** (0.054 g, 0.19 mmol, 10%) is obtained as a colorless solid.

R_f (CH:EA = 80:20) = 0.23

^{1}H-NMR (400 MHz, $CDCl_3$, 298 K) δ [ppm] = 7.71 – 7.67 (m, 2H), 7.32 – 7.27 (m, 2H), 5.58 – 5.47 (m, 1H), 5.18 – 5.09 (m, 2H), 3.96 – 3.82 (m, 2H), 3.37 (d, J = 14.6 Hz, 1H), 3.16 (d, J = 14.7 Hz, 1H), 2.66 (d, J = 4.6 Hz, 1H), 2.61 (d, J = 4.6 Hz, 1H), 2.42 (s, 3H), 1.36 (s, 3H).

^{13}C-NMR (100 MHz, $CDCl_3$, 298 K) δ [ppm] = 143.6, 137.3, 132.4, 129.9, 127.3, 119.7, 56.1, 52.1, 52.0, 51.4, 21.7, 19.1.

4-Methyl-*N*-(3-(trimethylsilyl)prop-2-yn-1-yl)benzenesulfonamide **86**

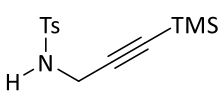

In a flame-dried *Schlenk* flask, to a solution of *N*-propargyl-*p*-toluenesulfonamide **74** (2.091 g, 10.00 mmol, 1.00 eq.) in dry THF (20 mL) is added ^{n}BuLi (2.5 M in hexane, 4.8 mL, 12.00 mmol, 1.20 eq.) dropwise at -78°C The mixture is stirred for 45 min at RT, cooled again to 0°C and TMSCl (2.45 mL, 20.00 mmol, 2.00 eq.) is added dropwise. The mixture is stirred overnight while it is allowed to warm up to RT. The mixture is purred on water and the layers are separated. The aqueous layer is extracted with Et_2O (3x) and EA (1x), the combined organic layers are

washed with water and brine, dried over $MgSO_4$ and the solvent is removed *in vacuo*. After purification via flash column chromatography (SiO_2, ^{n}pentane:Et_2O = 60:40) 4-methyl-*N*-(3-(trimethylsilyl)prop-2-yn-1-yl)benzenesulfonamide **86** (1.059 g, 3.76 mmol, 38%) is obtained as an off-white solid.

R_f (^{n}pentane:Et_2O = 60:40) = 0.31

^{1}H-NMR (500 MHz, $CDCl_3$, 298 K) δ [ppm] = 7.79 – 7.76 (m, 2H), 7.33 – 7.29 (m, 2H), 4.60 – 4.55 (m, 1H), 3.86 (d, *J* = 6.0 Hz, 2H), 2.43 (s, 3H), 0.02 (s, 9H).

^{13}C-NMR (125 MHz, $CDCl_3$, 298 K) δ [ppm] = 143.8, 136.9, 129.8, 127.2, 99.5, 90.0, 34.0, 21.7, -0.3.

The analytical data is in agreement with the literature.[256]

(*Z*)-4-methyl-*N*-(3-(trimethylsilyl)allyl)benzenesulfonamide **87**

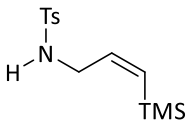

In a flame-dried *Schlenk* flask, to a solution of $Ni(OAc)_2{\cdot}4H_2O$ (0.234 g, 0.94 mmol, 0.25 eq.) in dry MeOH (23 mL) is added $NaBH_4$ (0.036 g, 0.94 mmol, 0.25 eq.) at 0°C. An immediate color change to black is observed. The solution is warmed to RT and 1,2-diaminoethane (0.13 mL, 0.114 g, 1.89 mmol, 0.50 eq.) and 4-methyl-*N*-(3-(trimethylsilyl)prop-2-yn-1-yl)benzenesulfonamide **86** (1.059 g, 3.77 mmol, 1.00 eq.) are added. A hydrogen-filled ballon with attached valve is connected to the flask. The flask is evacuated till boiling of the solvent is observed and refilled with hydrogen. The purging process is repeated five times. The mixture is vigorously stirred for 48 h under hydrogen atmosphere. The mixture is filtered through a silica plug using Et_2O and the solvent is removed *in vacuo*. To avoid spontaneous ignition, the black residue in the filter plug is immediately reacted with 6 M HCl until the color changes completely to green. After purification via flash column chromatography (SiO_2, EH:EA = 90:10) (*Z*)-4-methyl-*N*-(3-(trimethylsilyl)allyl)benzenesulfonamide **87** (0.686 g, 2.42 mmol, 64%) is obtained as a white solid.

R_f (CH:EA = 90:10) = 0.19

^{1}H-NMR (500 MHz, $CDCl_3$, 298 K) δ [ppm] = 7.78 – 7.73 (m, 2H), 7.34 – 7.29 (m, 2H), 6.11 (dt, *J* = 13.9, 6.9 Hz, 1H), 5.67 (dd, *J* = 14.1, 1.4 Hz, 1H), 4.40 (br s, 1H), 3.61 (ddd, *J* = 7.1, 6.0, 1.3 Hz, 2H), 2.43 (s, 3H), 0.02 (s, 9H).

^{13}C-NMR (125 MHz, $CDCl_3$, 298 K) δ [ppm] = 143.7, 141.6, 137.0, 134.8, 129.9, 127.3, 45.2, 21.7, 0.0.

(*Z*)-4-methyl-*N*-((2-methyloxiran-2-yl)methyl)-*N*-(3-(trimethylsilyl)allyl)benzenesulfonamide **88**

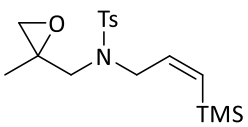

In a flame-dried *Schlenk* flask, to a suspension of sodium hydride (60% in mineral oil, 0.080 g, 2.00 mmol, 1.02 eq) in dry DMF (25) is added (*Z*)-4-methyl-*N*-(3-(trimethylsilyl)allyl)benzenesulfonamide **87** (0.680 g, 2.40 mmol, 1.21 eq.) at 0°C and stirred for 30 min. 2-(Bromomethyl)-2-methyloxirane **84** (0.299 g, 1.98 mmol, 1.00 eq.) is

added dropwise at 0°C and the mixture is stirred for 4 d at RT. The mixture is purred on water and the layers are separated. The aqueous layer is extracted with Et_2O, the combined organic layers are washed with water, dried over $MgSO_4$ and the solvent is removed *in vacuo*. After purification via flash column chromatography (Al_2O_3, CH:EA = 90:10) (*Z*)-4-methyl-*N*-((2-methyloxiran-2-yl)methyl)-*N*-(3-(trimethylsilyl)allyl)benzene sulfonamide **88** (0.405 g, 1.15 mmol, 58% in 93% purity) is obtained as an off-white solid.

R_f (Al_2O_3, CH:EA = 90:10) = 0.24

^{1}H-NMR (500 MHz, $CDCl_3$, 298 K) δ [ppm] = 7.70 – 7.66 (m, 2H), 7.31 – 7.27 (m, 2H), 5.91 (dt, *J* = 14.4, 6.3 Hz, 1H), 5.60 (dt, *J* = 14.5, 1.8 Hz, 1H), 4.00 (d, *J* = 6.2 Hz, 2H), 3.31 (d, *J* = 14.9 Hz, 1H), 3.23 (d, *J* = 14.7 Hz, 1H), 2.72 (d, *J* = 4.6 Hz, 1H), 2.61 (d, *J* = 4.6 Hz, 1H), 2.42 (s, 3H), 1.38 (s, 3H), 0.11 (s, 9H).

^{13}C-NMR (125 MHz, $CDCl_3$, 298 K) δ [ppm] = 143.6, 142.2, 137.2, 133.6, 129.9, 127.4, 56.1, 52.2, 52.0, 50.7, 21.7, 19.3, 0.0.

Non-2-yn-1-ol **89**

In a flame-dried *Schlenk* flask, to a solution of 1-octyne (6.65 mL, 4.959 g, 45.00 mmol, 1.00 eq.) in THF (70 mL) is added ^{n}BuLi (2.5 M in hexane, 22.00 mL, 54.90 mmol, 1.22 eq.) at -78°C and is stirred for 40 min. Paraformaldehyde (1.622 g, 54.00 mmol, 1.20 eq.) is added and the mixture is stirred overnight while it is allowed to warm up to RT. Sat. aq. NH_4Cl solution (70 mL) is added and the layers are separated. The aqueous layer is extracted with Et_2O (4x), the combined organic layers are washed with brine, dried over $MgSO_4$ and the solvent is removed *in vacuo*. After purification via flash column chromatography (SiO_2, CH:EA = 80:20) non-2-yn-1-ol **89** (5.563 g, 39.67 mmol, 88%) is obtained as a colorless oil.

R_f (CH:EA = 80:20) = 0.3

^{1}H-NMR (500 MHz, $CDCl_3$, 298 K) δ [ppm] = 4.25 (t, *J* = 2.2 Hz, 2H), 2.21 (tt, *J* = 7.2, 2.2 Hz, 2H), 1.55 – 1.47 (m, 2H), 1.41 – 1.23 (m, 6H), 0.89 (t, *J* = 7.0 Hz, 3H).

^{13}C-NMR (125 MHz, $CDCl_3$, 298 K) δ [ppm] = 86.8, 78.4, 51.6, 31.5, 28.7, 28.7, 22.7, 18.9, 14.2.

The analytical data is in agreement with the literature.[257]

Undec-2-yn-1-ol **90**

In a flame-dried *Schlenk* flask, to a solution of 1-dectyne (8.56 mL, 6.22 g, 45.0 mmol, 1.00 eq.) in THF (70 mL) is added ^{n}BuLi (2.5 M in hexane, 22.0 mL, 54.9 mmol, 1.22 eq.) at -78°C and is stirred for 40 min. Paraformaldehyde (1.62 g, 54.0 mmol, 1.20 eq.) is added and the mixture is stirred overnight while it is allowed to warm up to RT. Sat. aq. NH_4Cl

solution (70 mL) is added and the layers are separated. The aqueous layer is extracted with Et_2O (4x), the combined organic layers are washed with brine, dried over $MgSO_4$ and the solvent is removed *in vacuo*. After purification via flash column chromatography (SiO_2, CH:EA = 80:20) undec-2-yn-1-ol **90** (6.08 g, 36.2 mmol, 80%) is obtained as a colorless oil.

R_f (CH:EA = 80:20) = 0.3

^{1}H-NMR (500 MHz, $CDCl_3$, 298 K) δ [ppm] = 4.25 (t, *J* = 2.5 Hz, 2H), 2.20 (tt, *J* = 7.0, 2.5 Hz, 2H), 1.58 (br s, 1H), 1.53 – 1.47 (m, 2H), 1.38 – 1.33 (m, 2H), 1.22 – 1.31 (m, 8H), 0.88 (t, *J* = 7.0 Hz, 3H).

^{13}C-NMR (125 MHz, $CDCl_3$, 298 K) δ [ppm] = 86.8, 78.4, 51.6, 32.0, 29.3, 29.2, 29.0, 28.8, 22.8, 18.9, 14.2.

The analytical data is in agreement with the literature.[258]

1-Bromonon-2-yne **91**

In a flame-dried *Schlenk* flask, to a solution of non-2-yn-1-ol **89** (1.402 g, 10.00 mmol, 1.00 eq.) and triphenylphosphane (3.410 g, 13.00 mmol, 1.30 eq.) in dry THF (25 mL) is added *N*-bromosuccinimide (2.136 g, 12.00 mmol, 1.20 eq.) portion wise at 0°C. The mixture is stirred for 2 h at 0°C and diluted with ^{n}hexane (25 mL). The white precipitate is filtered off and the solvent is removed *in vacuo*. After purification via flash column chromatography (SiO_2, CH) 1-bromonon-2-yne **91** (1.493 g, 7.35 mmol, 74%) is obtained as a colorless oil.

R_f (CH) = 0.5

^{1}H-NMR (500 MHz, $CDCl_3$, 298 K) δ [ppm] = 3.93 (t, *J* = 2.4 Hz, 2H), 2.23 (tt, *J* = 7.1, 2.4 Hz, 2H), 1.55 – 1.47 (m, 2H), 1.41 – 1.23 (m, 6H), 0.89 (t, *J* = 7.0 Hz, 3H).

^{13}C-NMR (125 MHz, $CDCl_3$, 298 K) δ [ppm] = 88.5, 75.4, 31.4, 28.7, 28.5, 22.7, 19.1, 16.0, 14.2.

The analytical data is in agreement with the literature.[257]

1-Bromoundec-2-yne **92**

In a flame-dried *Schlenk* flask, to a solution of undec-2-yn-1-ol **90** (3.36 g, 20.00 mmol, 1.00 eq.) and triphenylphosphane (6.82 g, 26.00 mmol, 1.30 eq.) in dry THF (50 mL) is added *N*-bromosuccinimide (4.27 g, 24.00 mmol, 1.20 eq.) portion wise at 0°C. The mixture is stirred for 2 h at 0°C and diluted with ^{n}hexane (50 mL). The white precipitate is filtered off and the solvent is removed *in vacuo*. After purification via flash column chromatography (SiO_2, CH) 1-bromoundec-2-yne **92** (4.00 g, 17.3 mmol, 87%) is obtained as a colorless oil.

R_f (CH) = 0.4

^{1}H-NMR (400 MHz, $CDCl_3$, 298 K) δ [ppm] = 3.93 (t, *J* = 2.4 Hz, 2H), 2.23 (tt, *J* = 7.2, 2.4 Hz, 2H), 1.57 – 1.46 (m, 2H), 1.41 – 1.22 (m, 10H), 0.92 – 0.85 (m, 3H).

^{13}C-NMR (100 MHz, $CDCl_3$, 298 K) δ [ppm] = 88.5, 75.4, 31.9, 29.3, 29.2, 29.0, 28.5, 22.8, 19.1, 16.0, 14.3.

The analytical data is in agreement with the literature.[259]

Diethyl 2-(2-methylallyl)malonate **93**

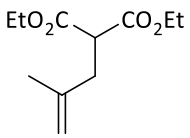

In a flame-dried *Schlenk* flask, to a suspension of sodium hydride (60% in mineral oil, 3.690 g, 99.0 mmol, 1.00 eq.) in dry THF (100 mL) is added diethylmalonate (15.0 mL, 99.0 mmol, 1.00 eq.) dropwise. 3-Chloro-2-methylpropene (9.64 mL, 99.0 mmol, 1.00 eq.) is added dropwise and the reaction mixture is stirred for 24 h at 60°C. The mixture is purred on water and the layers are separated. The aqueous layer is extracted with Et_2O, die combined organic layers are dried over $MgSO_4$ and the solvent is removed *in vacuo*. After purification via flash column chromatography (SiO_2, CH:EA = 90:10) diethyl 2-(2-methylallyl)malonate **93** (9.800 g, 45.7 mmol, 46%) is obtained as a colorless oil.

R_f (CH:EA = 90:10) = 0.2

^{1}H-NMR (500 MHz, $CDCl_3$, 298 K) δ [ppm] = 4.78 (m, 1H), 4.72 (m, 1H), 4.19 (qd, *J* = 7.1, 0.8 Hz, 4H), 3.57 (t, *J* = 7.8 Hz, 1H), 2.61 (d, *J* = 7.5 Hz, 2H), 1.74 (t, *J* = 1.2 Hz, 3H), 1.26 (t, *J* = 7.1 Hz, 6H).

^{13}C-NMR (125 MHz, $CDCl_3$, 298 K) δ [ppm] = 169.3, 141.9, 112.4, 61.5, 50.7, 36.6, 22.4, 14.2.

The analytical data is in agreement with the literature.[260]

Diethyl 2-((2-methyloxiran-2-yl)methyl)malonate **94**

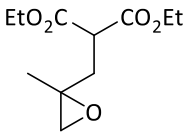

According to **GP-2**, diethyl 2-(2-methylallyl)malonate **93** (5.360 g, 25.0 mmol, 1.00 eq.) and *m*CPBA (70%, 7.394 g, 30.0 mmol, 1.20 eq.) are reacted in DCM (50 mL) overnight. After purification via flash column chromatography (SiO_2, CH:EA = 80:20) diethyl 2-((2-methyloxiran-2-yl)methyl)malonate **94** (4.870 g, 21.2 mmol, 85%) is obtained as a colorless oil.

R_f (CH:EA = 80:20) = 0.2

^{1}H-NMR (500 MHz, C_6D_6, 298 K) δ [ppm] = 4.00 – 3.92 (m, 4H), 3.45 (dd, *J* = 8.0, 6.8 Hz, 1H), 2.39 – 2.30 (m, 2H), 2.26 (dd, *J* = 14.5, 6.7, 1H), 2.11 (d, *J* = 4.7 Hz, 1H), 1.05 (s, 3H), 0.94 – 0.90 (m, 6H).

^{13}C-NMR (125 MHz, C_6D_6, 298 K) δ [ppm] = 169.1, 169.0, 61.4, 61.3, 54.7, 52.7, 48.7, 35.3, 21.3, 14.0.

The analytical data is in agreement with the literature.[261]

Diethyl 2-((2-methyloxiran-2-yl)methyl)-2-(prop-2-yn-1-yl)malonate **29**

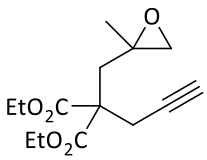

In a flame-dried *Schlenk* flask, to a solution of diethyl 2-((2-methyloxiran-2-yl)methyl)malonate **94** (1.150 g, 5.00 mmol, 1.00 eq.) and propargyl bromide (1.670 g, 14.00 mmol 2.80 eq.) in dry THF (30 mL) is added sodium hydride (60% in mineral oil, 0.220 g, 5.50 mmol, 1.10 eq.) portion wise at 0°C and the mixture is stirred for 96 h while it is allowed to warm up to RT. The mixture is diluted with Et_2O (50 mL), washed with water (3x), dried over $MgSO_4$ and the solvent is removed *in vacuo*. After purification via flash column chromatography (SiO_2, CH:EA = 90:10) diethyl 2-((2-methyloxiran-2-yl)methyl)-2-(prop-2-yn-1-yl)malonate **29** (1.100 g, 4.10 mmol, 82%) is obtained as a colorless oil.

R_f (CH:EA = 90:10) = 0.13

^{1}H-NMR (500 MHz, C_6D_6, 298 K) δ [ppm] = 3.95 (m, 4H), 3.30 – 3.05 (m, 2H), 2.77 – 2.51 (m, 3H), 2.13 (dd, *J* = 5.2, 1.0 Hz, 1H), 1.73 – 1.70 (m, 1H), 1.20 – 1.16 (m, 3H), 0.90 (t, *J* = 7.1 Hz, 6H).

^{13}C-NMR (125 MHz, C_6D_6, 298 K) δ [ppm] = 169.9, 169.7, 79.6, 72.3, 61.7, 56.2, 54.2, 53.9, 38.7, 24.1, 22.3, 13.9, 13.9.

The analytical data is in agreement with the literature.[74]

Diethyl 2-((2-methyloxiran-2-yl)methyl)-2-(undec-2-yn-1-yl)malonate **30**

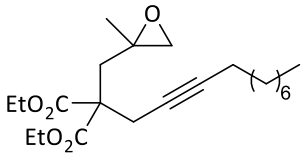

In a flame-dried *Schlenk* flask, to a solution of diethyl 2-((2-methyloxiran-2-yl)methyl)malonate **94** (1.150 g, 5.00 mmol, 1.00 eq.) and 1-bromoundec-2-yne **92** (1.495 g, 6.50 mmol 1.30 eq.) in dry THF (30 mL) is added sodium hydride (60% in mineral oil, 0.220 g, 5.50 mmol, 1.10 eq.) portion wise at 0°C and the mixture is stirred for 72 h at RT. The mixture is diluted with Et_2O (50 mL), washed with water (3x), dried over $MgSO_4$ and the solvent is removed *in vacuo*. After purification via flash column chromatography (SiO_2, CH:EA = 90:10) diethyl 2-((2-methyloxiran-2-yl)methyl)-2-(undec-2-yn-1-yl)malonate **30** (1.740 g, 4.57 mmol, 91%) is obtained as a colorless oil.

R_f (CH:EA = 90:10) = 0.25

^{1}H-NMR (500 MHz, C_6D_6, 298 K) δ [ppm] = 4.06 – 3.93 (m, 4H), 3.37 (dt, *J* = 17.0, 2.4 Hz, 1H), 3.18 (dt, *J* = 17.0, 2.4 Hz, 1H), 2.85 (d, *J* = 14.7 Hz, 1H), 2.68 (d, *J* = 14.9 Hz, 1H), 2.66 – 2.64 (m, 1H), 2.21 (dd, *J* = 5.3, 1.1 Hz, 1H), 2.00 (tt, *J* = 7.0, 2.4 Hz, 2H), 1.42 – 1.34 (m, 2H), 1.34 – 1.16 (m, 13H), 0.96 – 0.88 (m, 9H).

^{13}C-NMR (125 MHz, C_6D_6, 298 K) δ [ppm] = 170.3, 170.0, 84.4, 75.5, 61.6, 61.5, 56.64, 54.1, 54.0, 39.0, 32.2, 29.7, 29.5, 29.3, 29.1, 24.6, 23.1, 22.4, 19.0, 14.4, 14.0, 13.9.

HRMS (ESI+): m/z calculated for $[M+H]^+$ = 381.2636, found = 381.2631.

IR ν_{max} [cm^{-1}] = 2928, 2857, 2359, 1741, 1447, 1390, 1369, 1288, 1273, 1241, 1200, 1095, 1048, 1014, 975, 904, 859, 788, 723, 668, 613, 530, 459.

Diethyl 2-(non-2-yn-1-yl)-2-(oxiran-2-ylmethyl)malonate **31**

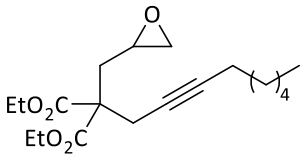

In a flame-dried *Schlenk* flask, to a solution of diethyl 2-(oxiran-2-ylmethyl)malonate **95** (1.011 g, 5.00 mmol, 1.00 eq.) and 1-bromonon-2-yne **91** (1.320 g, 6.50 mmol 1.30 eq.) in dry THF (30 mL) is added sodium hydride (60% in mineral oil, 0.220 g, 5.50 mmol, 1.10 eq.) portion wise at 0°C and the mixture is stirred for 96 h while it is allowed to warm up to RT. The mixture is diluted with Et_2O (50 mL), washed with water (3x), dried over $MgSO_4$ and the solvent is removed *in vacuo*. After purification via flash column chromatography (SiO_2, ^{n}pentane:Et_2O = 80:20) diethyl 2-(non-2-yn-1-yl)-2-(oxiran-2-ylmethyl)malonate **31** (1.183 g, 3.50 mmol, 70%) is obtained as a colorless oil.

R_f (^{n}pentane:Et_2O = 80:20) = 0.2

^{1}H-NMR (400 MHz, C_6D_6, 298 K) δ [ppm] = 4.08 – 3.98 (m, 4H), 3.30 – 3.18 (m, 2H), 2.99 (dtd, *J* = 7.0, 4.2, 2.5 Hz, 1H), 2.69 (dd, *J* = 14.5, 4.5 Hz, 1H), 2.39 – 2.29 (m, 2H), 2.16 (dd, *J* = 5.3, 2.5 Hz, 1H), 1.99 (tt, *J* = 7.0, 2.4 Hz, 2H), 1.40 – 1.09 (m, 8H), 0.95 (td, *J* = 7.1, 6.3 Hz, 6H), 0.87 (t, *J* = 7.2 Hz, 3H).

^{13}C-NMR (100 MHz, C_6D_6, 298 K) δ [ppm] = 170.12, 170.11, 84.2, 75.1, 61.62, 61.59, 56.6, 48.3, 46.2, 36.6, 31.7, 29.2, 28.8, 24.7, 23.0, 19.0, 14.3, 14.0.

HRMS (EI): m/z calculated for [M] = 338.2093, found = 338.2092.

IR ν_{max} [cm^{-1}] = 2932, 2859, 1726, 1466, 1445, 1368, 1321, 1288, 1261, 1189, 1097, 1032, 8567, 445, 436.

1-((2-Methylallyl)oxy)non-2-yne **96**

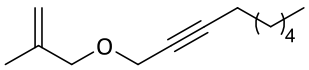

In a flame-dried *Schlenk* flask, to a solution of non-2-yn-1-ol **89** (1.402 g, 10.00 mmol, 1.00 eq.) in dry DMF (13 mL) is added sodium hydride ((60% in mineral oil, 0.400 g, 10.00 mmol, 1.00 eq.) at 0°C and stirred for 2 h. 3-Bromo-2-methylpropene (1.17 mL, 1.485 g, 11.00 mmol, 1.10 eq.) is added at 0°C and the reaction mixture is stirred for 68 h at RT. The mixture is diluted with CH (100 mL), washed with water (3x) and brine, dried over $MgSO_4$ and the solvent is removed *in vacuo.* 1-((2-Methylallyl)oxy)non-2-yne **96** (1.942 g, 10.0 mmol, >99%) is obtained as a colorless oil.

^{1}H-NMR (500 MHz, $CDCl_3$, 298 K) δ [ppm] = 4.99 – 4.97 (m, 1H), 4.92 – 4.90 (m, 1H), 4.11 (t, *J* = 2.2 Hz, 2H), 3.95 (s, 2H), 2.22 (tt, *J* = 7.2, 2.2 Hz, 2H), 1.75 (s, 3H), 1.56 – 1.48 (m, 2H), 1.42 – 1.24 (m, 6H), 0.89 (t, *J* = 7.0 Hz, 3H).

^{13}C-NMR (125 MHz, $CDCl_3$, 298 K) δ [ppm] = 141.9, 112.9, 87.2, 76.1, 73.5, 57.7, 31.5, 28.8, 28.7, 22.70, 19.7, 18.9, 14.2.

The analytical data is in agreement with the literature.[262]

2-methyl-2-((non-2-yn-1-yloxy)methyl)oxirane **28**

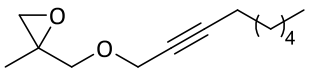

According to **GP-2**, 1-((2-methylallyl)oxy)non-2-yne **96** (1.943 g, 10.00 mmol, 1.00 eq.) and *m*CPBA (70%, 2.957 g, 12.00 mmol, 1.20 eq.) are reacted in DCM (20 mL) overnight. After purification via flash column chromatography (SiO_2, CH:EA:NEt_3 = 90:9:1) 2-methyl-2-((non-2-yn-1-yloxy)methyl)oxirane **28** (1.085 g, 5.16 mmol, 52%) is obtained as a colorless oil.

R_f (CH:EA = 90:10) = 0.2

^{1}H-NMR (400 MHz, $CDCl_3$, 298 K) δ [ppm] = 4.17 (q, *J* = 2.2 Hz, 2H), 3.57 (d, *J* = 10.9 Hz, 1H), 3.50 (d, *J* = 10.8 Hz, 1H), 2.77 (d, *J* = 4.9 Hz, 1H), 2.63 (d, *J* = 4.9 Hz, 1H), 2.21 (tt, *J* = 7.2, 2.2 Hz, 2H), 1.55 – 1.46 (m, 2H), 1.42 – 1.22 (m, 9H), 0.89 (t, *J* = 6.9 Hz, 3H).

^{13}C-NMR (125 MHz, $CDCl_3$, 298 K) δ [ppm] = 87.6, 75.7, 72.9, 59.2, 56.0, 51.9, 31.7, 28.7, 28.7, 22.7, 18.9, 18.7, 14.2.

The analytical data is in agreement with the literature.[262]

(*S*)-propene oxide **(*S*)-97**

In a round-bottom flask, oligomeric (*S,S*)-*Jacobsen*-catalyst (0.005 g) is added to *rac*-propene oxide (70.0 mL, 58.08 g, 1.00 mol, 1.00 eq.) and cooled to 0°C. Water (9.911 g, 0.55 mol, 0.55 eq.) is added dropwise and the mixture is vigorously stirred overnight while it is allowed to warm up to RT. After purification via distillation (1 atm, 34°C) (*S*)-propene oxide **(*S*)-97** (21.370 g, 0.37 mol, 37%, *ee* >99%) is obtained as a volatile colorless liquid.

^{1}H-NMR (500 MHz, $CDCl_3$, 298 K) δ [ppm] = 3.02 – 2.94 (m, 1H), 2.77 – 2.72 (m, 1H), 2.45 – 2.40 (m, 1H), 1.31 (d, *J* = 4.7 Hz, 3H).

^{13}C-NMR (125 MHz, $CDCl_3$, 298 K) δ [ppm] = 48.4, 48.2, 18.2.

The analytical data is in agreement with the literature.[263]

(*S*)-tridec-4-yn-2-ol **98**

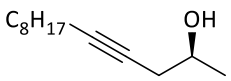

In a flame-dried *Schlenk* flask, to a solution of 1-decyne (98%, 9.20 mL 7.054 g, 50.00 mmol, 1.20 eq.) in dry THF (80 mL) is added ^{n}BuLi (2.5 M in hexane, 20.00 mL, 50.00 mmol, 1.20 eq.) dropwise at -96°C and stirred for 1 h. BF_3·THF (4.60 mL, 5.834 g, 41.70 mmol, 1.00 eq.) and (*S*)-propene oxide **(*S*)-97** (2.92 mL, 2.422 g, 41.70 mmol, 1.00 eq.) are added simultaneously dropwise and the mixture is stirred for 2 h at -96°C. The reaction mixture is treated with sat. aq. $NaHCO_3$ solution and the layers are separated. The aqueous layer is extracted with Et_2O, the combined organic layers are dried over $MgSO_4$ and the solvent is removed *in vacuo*. After purification via flash column chromatography (SiO_2, CH:EA = 80:20) (*S*)-tridec-4-yn-2-ol **98** (6.762 g, 34.44 mmol, 83%) is obtained as a colorless oil.

R_f (CH:EA = 80:20) = 0.3

^{1}H-NMR (500 MHz, $CDCl_3$, 298 K) δ [ppm] = 3.93 – 3.86 (m, 1H), 2.40 – 2.34 (m, 1H), 2.30 – 2.24 (m, 1H), 2.16 (tt, *J* = 7.1, 2.4 Hz, 2H), 1.97 (br s, 1H), 1.53 – 1.45 (m, 2H), 1.40 – 1.21 (m, 10H), 0.88 (t, *J* = 6.9 Hz, 3H).

^{13}C-NMR (125 MHz, $CDCl_3$, 298 K) δ [ppm] = 83.5, 76.2, 66.7, 32.0, 29.6, 29.3, 29.2, 29.2, 29.1, 22.8, 22.3, 18.9, 14.2.

The analytical data is in agreement with the literature.[91]

(*S,Z*)-tridec-4-en-2-ol **99**

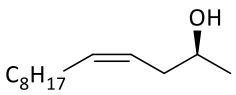

In a flame-dried *Schlenk* flask, to a solution of $Ni(OAc)_2$·$4H_2O$ (2.140 g, 8.60 mmol, 0.25 eq.) in dry MeOH (80 mL) is added $NaBH_4$ (0.325 g, 8.60 mmol, 0.25 eq.) at 0°C. An immediate color change to black is observed. The solution is warmed to RT and 1,2-diaminoethane (1.15 mL, 1.034 g, 17.20 mmol, 0.50 eq.) and (*S*)-tridec-4-yn-2-ol **98** (6.762 g, 34.40 mmol, 1.00 eq.) are added. A hydrogen-filled ballon with attached valve is connected to the flask. The flask is evacuated till boiling of the solvent is observed and refilled with hydrogen. The purging process is repeated five times. The mixture is vigorously stirred overnight under hydrogen atmosphere. The solution is concentrated *in vacuo*, the residue is suspended in Et_2O, filtered through a silica plug and the solvent is removed *in vacuo.* (*S,Z*)-tridec-4-en-2-ol **99** (6.648 g,33.52 mmol, 97%) is obtained as a colorless oil without further purification. To avoid spontaneous ignition, the black residue in the filter plug is immediately reacted with 6 M HCl until the color changes completely to green.

^{1}H-NMR (500 MHz, $CDCl_3$, 298 K) δ [ppm] = 5.61 – 5.52 (m, 1H), 5.44 – 5.34 (m, 1H), 3.87 – 3.77 (m, 1H), 2.30 – 2.13 (m, 2H), 2.05 (q, *J* = 7.2 Hz, 2H), 1.39 – 1.17 (m, 15H), 0.88 (t, *J* = 6.9 Hz, 3H).

^{13}C-NMR (125 MHz, $CDCl_3$, 298 K) δ [ppm] = 133.7, 125.1, 67.9, 37.3, 32.03, 29.8, 29.6, 29.5, 29.4, 27.6, 22.9, 22.8, 14.2.

The analytical data is in agreement with the literature.[91]

(2*S*,4*S*,5*R*)-4,5-epoxy-tridecane-2-ol **38**

In a flame-dried *Schlenk* flask, to a solution of (*S,Z*)-tridec-4-en-2-ol **99** (6.648 g, 33.50 mmol, 1.00 eq.) and $VO(acac)_2$ (0.435 g, 1.70 mmol, 0.05 eq.) in DCE (70 mL) is added TBHP (5.5 M in decane, 9.15 mL, 50.30 mmol, 1.50 eq.) dropwise at 0°C. The reaction mixture is stirred overnight while it is allowed to warm up to RT. The mixture is treated with sat. aq. $Na_2S_2O_3$ solution. The layers are separated, the aqueous layer is extracted with EA (3x), the combined organic layers are washed with water and brine, dried over $MgSO_4$ and the solvent is removed *in vacuo*. After purification via flash column chromatography (SiO_2, CH:EA = 80:20) (2*S*,4*S*,5*R*)-4,5-epoxy-tridecane-2-ol **38** (5.716 g, 26.67 mmol, 80%, *d.r.* = 94:6) is obtained as a yellowish oil.

R_f (CH:EA = 80:20) = 0.1

^{1}H-NMR (500 MHz, $CDCl_3$, 298 K) δ [ppm] = 4.17 – 4.08 (m, 1H), 3.10 (dt, *J* = 8.6, 4.2 Hz, 1H), 2.96 – 2.88 (m, 1H), 2.29 (br s, 1H), 1.78 (dt, *J* = 14.3, 4.0 Hz, 1H), 1.58 – 1.21 (m, 18H), 0.88 (t, *J* = 6.7 Hz, 3H).

^{13}C-NMR (125 MHz, $CDCl_3$, 298 K) δ [ppm] = 67.2, 56.5, 55.5, 36.5, 32.0, 29.6, 29.6, 29.3, 28.1, 26.6, 23.6, 22.8, 14.2.

The analytical data is in agreement with the literature.[91]

Methyl 8-((2*S*,3*R*)-3-((*R*)-2-hydroxyoctyl)oxiran-2-yl)octanoate **34**

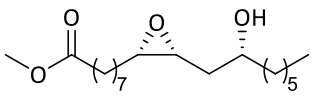

In a flame-dried *Schlenk* flask, to a solution of methyl ricinoleate (75%, 45.29 mL, 41.665 g, 100.0 mmol, 1.00 eq.) and $VO(acac)_2$ (1.326 g, 5.0 mmol, 0.05 eq.) in DCE (200 mL) is added TBHP (5.5 M in decane, 27.0 mL, 150.0 mmol, 1.50 eq.) dropwise at -10°C. The reaction mixture is stirred overnight while it is allowed to warm up to RT. The mixture is treated with sat. aq. $Na_2S_2O_3$ solution. The layers are separated, the aqueous layer is extracted with EA, the combined organic layers are washed with water and brine, dried over $MgSO_4$ and the solvent is removed *in vacuo*. After purification via flash column chromatography (SiO_2, CH:EA = 80:20) methyl 8-((2*S*,3*R*)-3-((*R*)-2-hydroxyoctyl)oxiran-2-yl)octanoate **34** (22.346 g, 68.0 mmol, 68%, *d.r.* = 96:4) is obtained as a colorless oil.

R_f (CH:EA = 80:20) = 0.1

^{1}H-NMR (500 MHz, $CDCl_3$, 298 K) δ [ppm] = 3.95 – 3.86 (m, 1H), 3.66 (s, 3H), 3.12 (dt, *J* = 8.5, 4.3 Hz, 1H), 2.94 – 2.88 (m, 1H), 2.30 (t, *J* = 7.5 Hz, 2H), 2.24 (s, 1H), 1.80 (dt, *J* = 14.2, 3.8 Hz, 1H), 1.66 – 1.57 (m, 2H), 1.56 – 1.24 (m, 20H), 0.91 – 0.85 (m, 3H).

^{13}C-NMR (125 MHz, $CDCl_3$, 298 K) δ [ppm] = 174.4, 71.1, 56.4, 55.6, 51.6, 37.6, 34.9, 34.2, 32.0, 29.43, 29.39, 29.3, 29.1, 28.0, 26.5, 25.6, 25.0, 22.8, 14.2.

The analytical data is in agreement with the literature.[91]

3.4 Synthesis of Catalysts

Sodium cyclopentadienyl **52**

A flame-dried three-necked flask equipped with reflux condenser and argon inlet is charged with sodium (3.750 g, 163.8 mmol, 1.00 eq.) and dicyclopentadiene (300.0 g). The mixture is slowly heated up and refluxed at 160°C for 12 h (during heat-up, the mixture turns blue initially then discolors as the sodium melts and white precipitate is forming). After the sodium is fully reacted and the hydrogen gas evolution stops, the mixture is cooled to RT. The precipitate is filtered off using a sintered glass filter stick, washed with freshly dried and deoxygenized ^{n}pentane (5x 50 mL) and dried *in vacuo* for 2 h. Sodium cyclopentadienyl **52** (12.928 g, 146.5 mmol, 89%) is obtained as off-white solid, which is stored in the *glovebox*.

^{1}H-NMR (500 MHz, THF-d_8, 298 K) δ [ppm] = 5.67 (s, 5H).

^{13}C-NMR (125 MHz, THF-d_8, 298 K) δ [ppm] = 103.5.

The analytical data is in agreement with the literature.[264]

Cyclopentadienylchromium tricarbonyl hydride **1**

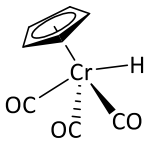

A flame-dried three-necked flask is charged with sodium cyclopentadienyl **52** (2.246 g, 25.5 mmol, 1,02 eq) inside the glovebox. A flame-dried reflux condenser is attached and chromium hexacarbonyl (5.502 g, 25.0 mmol, 1.0 eq) and dry DMF (85 mL) are added. The mixture is slowly heated up to 140°C and stirred for 3 h until no further CO evolution is observed. The mixture is cooled to RT and the solvent is removed *in vacuo* using a cooling trap. The brown residue is dissolved in deoxygenated aq. NaOH (0.5 M, 25 mL). The solution is washed with deoxygenated Et_2O (5x 20 mL) and remaining Et_2O is removed *in vacuo* into a cooling trap. The solution is filtered using a sintered glass filter stick. The clear solution is cooled to 0°C and deoxygenated aq. HOAc (2 M, 25 mL) is added dropwise. The yellow precipitate is filtered off using a sintered glass filter stick, washed with deoxygenated H_2O (3x 20 mL) and dried over P_2O_5. The residue is dissolved in deoxygenated Et_2O (30 mL), filtrated through a sintered glass filter stick and the solvent is removed *in vacuo* to obtain cyclopentadienylchromium tricarbonyl hydride **1** (3.563 g, 17.6 mmol, 70%) as an olive-green air sensitive solid which is stored in the *glovebox* at -18°C.

^{1}H-NMR (500 MHz, C_6D_6, 298 K) δ [ppm] = 4.07 (s, 5H), -5.62 (s, 1H).

^{13}C-NMR (125 MHz, C_6D_6, 298 K) δ [ppm] = 86.1.

The analytical data is in agreement with the literature.[265]

Pentamethylcyclopentadienylchromium tricarbonyl hydride **53**

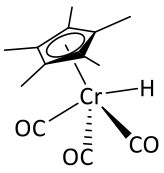

A flame-dried three-necked flask equipped with reflux condenser and argon inlet is charged with chromium hexacarbonyl (4.401 g, 20.0 mmol, 1.00 eq.) in deoxygenated MeCN (120 mL). The mixture is refluxed for 5 h, stirred overnight at 65°C and refluxed for another 3 h to ensure a quantitative conversion. The mixture is cooled to RT and the solvent is removed *in vacuo* into a cooling trap. The yellow precipitate is dissolved in deoxygenated MeOH (60 mL) and deoxygenated sodium pentamethylcyclopentadienyl (3.24 mL, 2.725 g, 20.0 mmol, 1.00 eq.) is added. The reaction mixture is stirred for 2 d at RT and the solvent is removed *in vacuo* into a cooling trap. The brown residue is extracted with deoxygenated ^{n}hexane (100 mL) and the remaining residue is filtered off using a sintered glass filter stick. The brown clear filtrate is concentrated *in vacuo* (approx. 15 mL) and cooled to -78°C to precipitate a yellow solid. The remaining liquid is filtered off using a filter cannula. Another portion of ^{n}hexane (10 mL) is added and filtered off after washing. The residue is dried *in vacuo* to obtain pentamethylcyclopentadienylchromium tricarbonyl hydride **53** (1.639 g, 6.0 mmol, 30%) as yellow to brownish solid.

^{1}H-NMR (400 MHz, C_6D_6, 298 K) δ [ppm] = 1.54 (s, 15H), -5.52 (s, 1H).

^{13}C-NMR (100 MHz, C_6D_6, 298 K) δ [ppm] = 99.9, 10.5.

The analytical data is in agreement with the literature.[266]

L-Neomenthol **60**

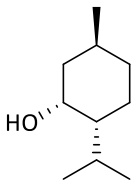

A round-bottom flask is charged with D-menthol (46.88 g, 300.0 mmol, 1.00 eq.), *p*-nitrobenzoic acid (70.19 g, 420.0 mmol, 1.40 eq.) and triphenylphosphine (106.23 g, 405.0 mmol, 1.35 eq.) in THF (600 mL) and cooled to 0°C. Diisopropyl azodicarboxylate (82.45 mL, 84.92 g, 420.0 mmol, 1.40 eq.) is added over 2 h and the mixture is stirred overnight at 60°C. Sat. aq. $NaHCO_3$ solution is added and the layers are separated. The aqueous layer is extracted with Et_2O, the combined organic layers are washed with water and brine, dried over $MgSO_4$ and the solvent is removed *in vacuo*. The residue is diluted with Et_2O and an excess CH. Et_2O is removed at 300 mbar and maximum speed on the rotary evaporator, the white precipitate is filtered off with a silica plug using CH and the solvent is removed *in vacuo*. The crude product is dissolved in THF (120 mL). MeOH (230 mL), water (70 mL) and NaOH (60.00 g, 1.50 mol, 5.00 eq.) are added and the mixture is stirred for 1 h at RT. The layers are separated, and the aqueous layer is extracted with Et_2O (3x), washed

with water and brine, dried over $MgSO_4$ and the solvent is removed *in vacuo*. After purification via distillation (3 mbar, 71°C) L-neomenthol **60** (23.659 g, 151.40 mmol, 50%) is obtained as a colorless oil.

^{1}H-NMR (500 MHz, $CDCl_3$, 298 K) δ [ppm] = 4.12 – 4.09 (m, 1H), 1.83 (dtd, *J* = 13.7, 3.5, 2.4 Hz, 1H), 1.77 – 1.63 (m, 4H), 1.52 (dsept, *J* = 9.3, 6.7 Hz, 1H), 1.32 – 1.23 (m, 2H), 1.08 (ddd, *J* = 13.9, 12.2, 2.6 Hz, 1H), 0.96 (d, *J* = 6.6 Hz, 3H), 0.92 (d, *J* = 6.7 Hz, 3H), 0.87 (d, *J* = 6.3 Hz, 3H).

^{13}C-NMR (125 MHz, $CDCl_3$, 298 K) δ [ppm] = 67.9, 48.1, 42.7, 35.2, 29.4, 26.0, 24.3, 22.45, 21.3, 20.9.

The analytical data is in agreement with the literature.[267]

L-Mesylneomenthol **61**

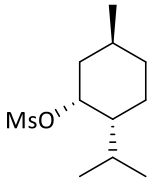

In a flame-dried *Schlenk* flask, to a solution of mesyl chloride (8.13 mL, 12.03 g, 105.0 mmol, 1.40 eq.) in dry pyridine (45 mL) is added a solution of L-neomenthol **60** (11.72 g, 75.0 mmol, 1.00 eq.) in dry pyridine (10 mL) dropwise at -10°C. The mixture is stirred for 30 min at -10°C and 5 h at 0°C. The reaction mixture is purred on a mixture of HCl (50 mL, 37%) and ice (150 g). The layers are separated, the aqueous layer is extracted with Et_2O, the combined organic layers are dried over $MgSO_4$ and the solvent is removed *in vacuo*. L-Mesylneomenthol **61** is obtained as a yellow oil and used without further purification.

D-Menthylcyclopentadiene **62**

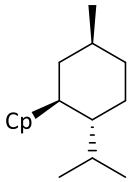

In a flame-dried *Schlenk* flask, to a suspension of sodium hydride (60% in mineral oil, 6.90 g, 172.5 mmol, 2.30 eq.) in dry THF (150 mL) is added freshly cracked cyclopentadiene (15.14 mL, 11.90 g, 180.0 mmol, 2.40 eq.) over 15 min at -10°C and stirred for 1 h. Into the pink solution is added a solution of L-mesylneomenthol **61** (17.58 g, 75.0 mmol, 1.00 eq.) in dry THF (50 mL) slowly via transfer cannula at -10°C and the reaction mixture is stirred for 18 h at RT. Water (200 mL) is added and the layers are separate. The aqueous layer is extracted with ^{n}pentane (3x), the combined organic layers are washed with water (2x) and brine, dried over $MgSO_4$ and the solvent is removed *in vacuo*. The crude product is filtered through a silica plug using petrol ether and the solvent is removed *in vacuo* to obtain D-menthylcyclopentadiene **62** as a dark yellow oil which is used without further purification.

D-*Kagan*-Cl_2 **63**

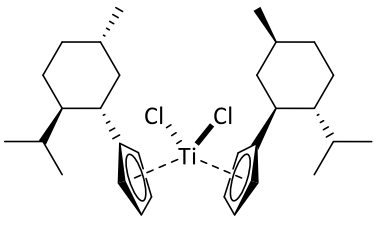

In a flame-dried *Schlenk* flask, to a solution of D-menthylcyclopentadiene **62** (13.28 g, 65.0 mmol, 1.00 eq.) in dry THF (130 mL) is added ^{n}BuLi (2.5 M in hexane, 27.3 mL, 68.3 mmol, 1.05 eq.) at 0°C. In a second flame-dried *Schlenk* flask, titanium tetrachloride (3.42 mL, 5.920 g, 31.2 mmol, 0.48 eq.) is

dissolved in Et_2O and cooled to 0°C. The second solution is transferred slowly into the first solution via transfer cannula. The reaction mixture is stirred overnight while it is allowed to warm up to RT. The solvent is removed *in vacuo*, the residue is dissolved in DCM and washed with a HCl/NaCl solution (1 M HCl, 10% NaCl). The organic layer is dried over $MgSO_4$, and ^{n}heptane (150 mL) is added. DCM is removed under reduced pressure and the suspension is filtered over a plug of Celite and washed with CH until the filtrate becomes colorless. The filter residue is dissolved in DCM and the solvent is removed *in vacuo*. After purification via recrystallization (DCM:Et_2O = 2:1) D-*Kagan*-Cl_2 **63** (5.088 g, 9.7 mmol, 31%) is obtained as an orange fluffy solid.

^{1}H-NMR (500 MHz, $CDCl_3$, 298 K) δ [ppm] = 6.74 (td, *J* = 3.2, 2.0 Hz, 2H), 6.40 (q, *J* = 2.3 Hz, 2H), 6.28 (dt, *J* = 3.3, 2.2 Hz, 2H), 6.19 (q, *J* = 2.8 Hz, 2H), 2.74 (td, *J* = 11.3, 3.0 Hz, 2H), 1.81 – 1.73 (m, 2H), 1.69 (dq, *J* = 13.0, 3.3 Hz, 2H), 1.64 – 1.56 (m, 2H), 1.44 (dddd, *J* = 32.4, 14.8, 8.2, 2.9 Hz, 4H), 1.18 – 0.91 (m, 8H), 0.89 (d, *J* = 6.5 Hz, 6H), 0.85 (d, *J* = 6.8 Hz, 6H), 0.79 (d, *J* = 6.9 Hz, 6H).

^{13}C-NMR (125 MHz, $CDCl_3$, 298 K) δ [ppm] = 145.6, 126.9, 121.2, 115.1, 109.6, 51.0, 42.2, 40.9, 35.3, 32.5, 27.5, 24.8, 22.9, 21.8, 15.7.

The analytical data is in agreement with the literature.[268]

D-*Kagan*-Br_2 **64**

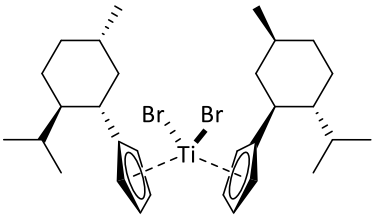

In a flame-dried *Schlenk* flask, to a solution of D-Kagan-Cl_2 **63** (2.000 g, 3.81 mmol, 1.00 eq.) in dry Et_2O (20 mL) is added methyl lithium (1.6 M in Et_2O, 5.2 mL, 8.38 mmol, 2.20 eq.) dropwise at -10°C. The mixture is stirred for 10 min at -10°C and for 30 min at RT. NH_4Cl solution (6%, 20 mL) is added at 0°C and the layers are separated. The organic layer is washed with water and brine, dried over $MgSO_4$ and the solvent is removed *in vacuo*. The light-orange solid is dissolved in dry Et_2O (180 mL) and HBr (48%, 1.9 mL, 11.43 mmol, 3.00 eq) is added dropwise at 0°C. The mixture is stirred for 1 h at RT and sat. aq. $NaHCO_3$ solution (80 mL) is added. The layers are separated, the organic layer is washed with water and brine, dried over $MgSO_4$ and the solvent is removed *in vacuo*. D-Kagan-Br_2 **64** (2.146 g, 3.50 mmol, 92%) is obtained as a red-brown solid.

^{1}H-NMR (500 MHz, $CDCl_3$, 298 K) δ [ppm] = 7.04 – 7.01 (m, 2H), 6.64 – 6.61 (m, 2H), 6.41 (q, *J* = 2.3 Hz, 2H), 6.17 – 6.13 (m, 2H), 2.87 (td, *J* = 11.3, 3.0 Hz, 2H), 1.80 – 1.74 (m, 2H), 1.73 – 1.67 (m, 2H), 1.62 – 1.31 (m, 6H), 1.17 – 0.91 (m, 8H), 0.89 (d, *J* = 6.9 Hz, 6H), 0.87 (d, *J* = 6.5 Hz, 6H), 0.81 (d, *J* = 6.9 Hz, 6H).

^{13}C-NMR (125 MHz, $CDCl_3$, 298 K) δ [ppm] = 145.1, 127.3, 122.3, 114.4, 110.2, 51.3, 43.05, 41.1, 35.2, 32.4, 27.6, 24.7, 22.8, 21.8, 15.7.

The analytical data is in agreement with the literature.[91]

L-*Kagan*-Br_2 **65**

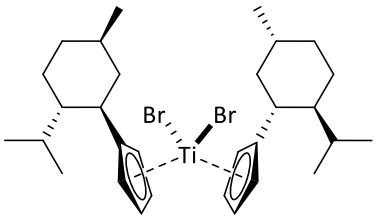

L-*Kagan*-Br_2 **65** is synthesized according to the procedure described for D-*Kagan*-Br_2 **64** using L-Kagan-Cl_2 (0.890 g, 1.69 mmol, 1.00 eq.) as starting material and methyl lithium (1.6 M in Et_2O, 2.3 mL, 3.73 mmol, 2.20 eq.) and HBr (48%, 0.85 mL, 5.07 mmol, 3.00 eq). L-Kagan-Br_2 **65** (2.146 g, 3.50 mmol, 92%) is obtained as a red-brown solid.

^{1}H-NMR (500 MHz, $CDCl_3$, 298 K) δ [ppm] = 7.03 – 7.01 (m, 2H), 6.63 – 6.61 (m, 2H), 6.41 (q, *J* = 2.3 Hz, 2H), 6.15 (q, *J* = 2.8 Hz, 2H), 2.87 (td, *J* = 11.3, 3.0 Hz, 2H), 1.80 – 1.74 (m, 2H), 1.73 – 1.67 (m, 2H), 1.62 – 1.31 (m, 6H), 1.17 – 0.91 (m, 8H), 0.89 (d, *J* = 6.9 Hz, 6H), 0.87 (d, *J* = 6.5 Hz, 6H), 0.81 (d, *J* = 6.9 Hz, 6H).

^{13}C-NMR (125 MHz, $CDCl_3$, 298 K) δ [ppm] = 145.0, 127.3, 122.3, 114.4, 110.2, 51.3, 43.0, 41.1, 35.2, 32.4, 27.6, 24.7, 22.8, 21.8, 15.7.

HRMS (EI): m/z calculated for [M] = 612.1446, found = 612.1448.

The analytical data is in agreement with the literature.[91]

N,N'-Bis(salicylidene)ethylenediaminocobalt(II) **42**

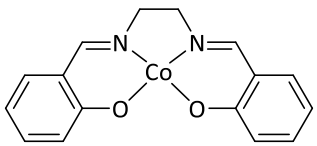

According to **GP-3,** *N,N*'-bis(salicyliden)ethylendiamin **56** (0.537 g, 2.00 mmol, 1.00 eq.) and cobalt(II) acetate tetrahydrate (0.498 g, 2.00 mmol, 1.00 eq.) are reacted in dry MeOH (20 mL) for 1 h at 75°C. *N,N*'-Bis(salicylidene)ethylenediaminocobalt(II) **42** (0.460 g, 1.41 mmol, 71%) is obtained as dark red solid.

HRMS (ESI+): m/z calculated for $[M]^+$ = 325.0382, found = 325.0376.

IR ν_{max} [cm^{-1}] = 3053, 3019, 2960, 2931, 2567, 1528, 1448, 1429, 1195, 1125, 1053, 749, 730, 620, 588, 463.

The analytical data is in agreement with the literature.[269]

N,N'-o-phenylenebis(3,5-dibromosalicylideneimine) **54**

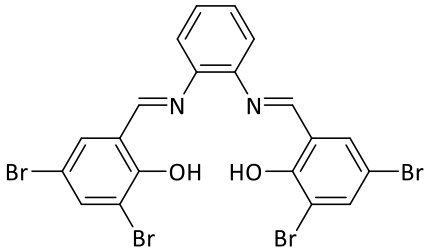

In a flame-dried *Schlenk* flask with attached reflux condenser, 1,2-phenylenediamine (0.541 g, 5.00 mmol, 1.00 eq.) and 3,5-dibromosalicylaldehyde (2.799 g, 10.00 mmol, 2.00 eq.) are refluxed in dry EtOH (50 mL) overnight. The precipitate is filtered off, washed with hot EtOH, and dried in vacuo to obtain *N,N*'-o-phenylenebis(3,5-dibromosalicylideneimine) **54** (2.985 g, 4.72 mmol, 94%) as an orange solid.

^{1}H-NMR (500 MHz, $CDCl_3$, 298 K) δ [ppm] = 8.52 (s, 2H), 7.76 (d, J = 2.3 Hz, 2H), 7.48 (d, J = 2.3 Hz, 2H), 7.40 (dd, J = 5.9, 3.4 Hz, 2H), 7.23 (dd, J = 5.9, 3.4 Hz, 2H).

^{13}C-NMR (125 MHz, $CDCl_3$, 298 K) δ [ppm] = 162.35, 142.14, 141.5, 138.82, 135.07, 133.78, 128.78, 120.83, 120.43, 110.54.

HRMS (APCI): m/z calculated for $[M+H]^+$ = 632.7666, found = 632.7665.

IR ν_{max} [cm^{-1}] = 1610, 1436, 1357, 1270, 1156, 1105, 859, 841, 822, 809, 759, 750, 736, 685, 663.

The analytical data is in agreement with the literature.[270]

6,6'-((1E,1'E)-(1,2-phenylenebis (azanylylidene)) bis(methanylylidene)) bis(2,4-dibromophenol) cobalt(II) **46**

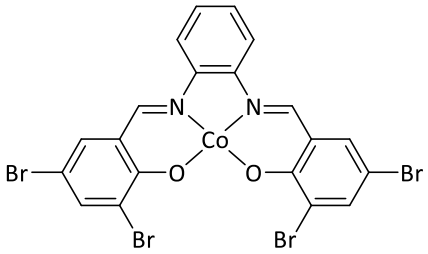

According to **GP-3,** *N,N'*-o-phenylenebis(3,5-dibromosalicylideneimine) **54** (0.631 g, 1.00 mmol, 1.00 eq.) and cobalt(II) acetate tetrahydrate (0.249 g, 1.00 mmol, 1.00 eq.) are reacted in dry MeOH (3.0 mL) for 3 h at 75°C. 6,6'-((1E,1'E)-(1,2-phenylenebis (azanylylidene)) bis(methanylylidene)) bis(2,4-dibromophenol) cobalt(II) **46** (0.652 g, 0.97 mmol, 97%) is obtained as black solid.

HRMS (ESI+): m/z calculated for $[M+H]^+$ = 689.6840, found = 689.6836.

IR ν_{max} [cm^{-1}] = 3055, 3024, 1571, 1489, 1422, 1366, 1334, 1198, 1169, 1158, 858, 740, 716, 702, 571, 542.

The analytical data is in agreement with the literature.[270]

6,6'-((1E,1'E)-(1,2-phenylenebis (azanylylidene)) bis(methanylylidene)) bis(3,5-dimethoxyphenol) cobalt(II) **48**

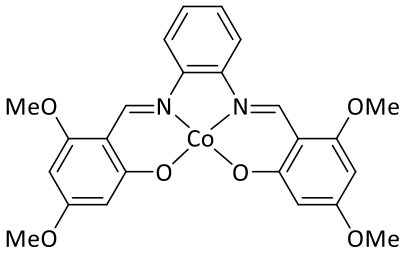

According to **GP-3,** 2,2'-[1,2-phenylenebis(nitrilomethylidyne)] bis[3,5-dimethoxyphenol] **57** (0.043 g, 0.10 mmol, 1.00 eq.) and cobalt(II) acetate tetrahydrate (0.025 g, 0.010 mmol, 1.00 eq.) are reacted in dry MeOH (1.0 mL) for 3 h at 75°C. 6,6'-((1E,1'E)-(1,2-phenylenebis (azanylylidene)) bis(methanylylidene)) bis(3,5-dimethoxyphenol) cobalt(II) **48** (0.007 g, 0.01 mmol, 10%) is obtained as dark brown solid.

HRMS (ESI+): m/z calculated for $[M]^+$ = 493.0810, found = 493.0801.

6,6'-((1E,1'E)-(4,5-dichloro-1,2-phenylene (azanylylidene)) bis(methanylylidene)) bis(3,5-dimethoxyphenol) cobalt(II) **49**

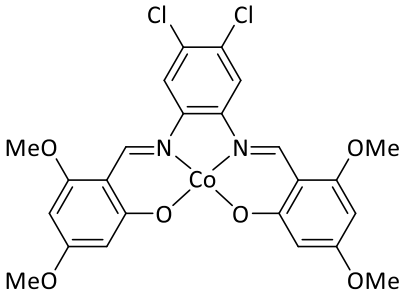

According to **GP-3,** 2,2'-[(4,5-dichloro-1,2-phenylene)bis(nitrilomethylidyne)] bis[3,5-methoxyphenol] **58** (0.086 g, 0.17 mmol, 1.00 eq.) and cobalt(II) acetate tetrahydrate (0.042 g, 0.017 mmol, 1.00 eq.) are reacted in dry MeOH (1.0 mL) for 3 h at 75°C. 6,6'-((1E,1'E)-(4,5-dichloro-1,2-phenylene (azanylylidene)) bis(methanylylidene)) bis(3,5-dimethoxyphenol) cobalt(II) **49** (0.062 g, 0.11 mmol, 65%) is obtained as dark brown solid.

HRMS (ESI+): m/z calculated for $[M]^+$ = 561.0030, found = 561.0027.

IR ν_{max} [cm^{-1}] = 2938, 2838, 1610, 1567, 1531, 1430, 1416, 1376, 1357, 1324, 1258, 1235, 1215, 1155, 1121, 1112, 811, 554, 429.

6,6'-((1E,1'E)-(3,6-dimethoxy-1,2-phenylene (azanylylidene)) bis(methanylylidene)) bis(2,4-dibromophenol) cobalt(II) **47**

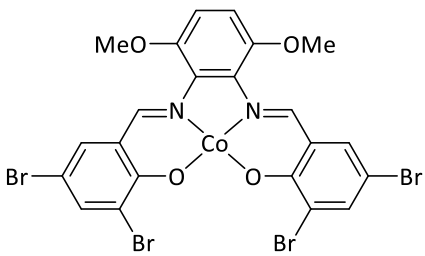

In a flame-dried *Schlenk* flask with attached reflux condenser, 3,5-dibromosalicylaldehyde (0.560 g, 2.00 mmol, 2.00 eq.), 3,6-dimethoxy-1,2-benzenediamine (0.168 g, 1.00 mmol, 1.00 eq.) and cobalt(II) acetate tetrahydrate (0.249 g, 1.00 mmol, 1.00 eq.) are refluxed in dry EtOH (15 mL) overnight. The mixture is concentrated in vacuo and the precipitate is filtered off. The residue is washed with cold MeOH and ^{n}pentane and is died *in vacuo* to obtain 6,6'-((1E,1'E)-(3,6-dimethoxy-1,2-phenylene (azanylylidene)) bis(methanylylidene)) bis(2,4-dibromophenol) cobalt(II) **47** (0.628 g, 0.84 mmol, 84%) as dark brown solid.

HRMS (ESI+): m/z calculated for $[M]^+$ = 748.6971, found = 748.6978.

IR ν_{max} [cm^{-1}] = 2934, 2837, 1581, 1551, 1494, 1435, 1375, 1263, 1217, 1168, 1105, 1063, 983, 946, 862, 786, 752, 712, 611, 547, 537.

cobalt(II) diphenyleneltetraaza[14]annulene [Co(PheTAA)] **44**

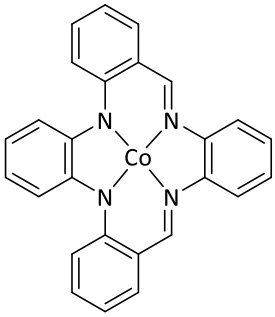

According to **GP-3,** diphenyleneltetraaza[14]annulene **59** (0.194 g, 0.5 mmol, 1.00 eq.) and cobalt(II) acetate tetrahydrate (0.125 g, 0.5 mmol, 1.00 eq.) are reacted in dry MeOH (1.0 mL) for 3 h at 75°C. Cobalt(II) diphenyleneltetraaza[14]annulene **44** (0.041 g, 0.09 mmol, 18%) is obtained as dark brown solid.

HRMS (ESI+): m/z calculated for $[M]^+$ = 445.0863, found = 445.0869.

IR ν_{max} [cm^{-1}] = 3060, 3006, 1605, 1564, 1517, 1455, 1435, 1416, 1366, 1340, 1192, 1165, 735, 720, 511, 469.

N,*N*'-((*S*)-[1,1'-binaphthalene]-2,2'-diyl)bis(3,5-dibromosalicylideneimine) **(*S*)-55**

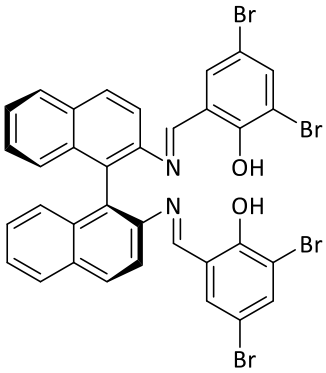

In a flame-dried *Schlenk* flask with attached reflux condenser, (*S*)-1,1'-binaphthyl-2,2'-diamine (0.284 g, 1.00 mmol, 1.00 eq.) and 3,5-dibromosalicylaldehyde (0.560 g, 2.00 mmol, 2.00 eq.) are refluxed in dry EtOH (10 mL) overnight. The precipitate is filtered off, washed with hot EtOH, and dried in vacuo to *N*,*N*'-((*S*)-[1,1'-binaphthalene]-2,2'-diyl)bis(3,5-dibromosalicylideneimine) **(*S*)-55** (0.763 g, 0.944 mmol, 94%) as an orange solid.

^{1}H-NMR (500 MHz, $CDCl_3$, 298 K) δ [ppm] = 12.92 (br s, 2H), 8.50 (s, 2H), 8.10 (d, *J* = 9.3 Hz, 2H), 7.97 (d, *J* = 8.1 Hz, 2H), 7.58 (d, *J* = 8.9 Hz, 2H), 7.56 (d, *J* = 2.4 Hz, 2H), 7.47 (ddd, *J* = 8.1, 6.7, 1.2 Hz, 2H), 7.28 (ddd, *J* = 8.2, 6.8, 1.3 Hz, 2H), 7.25 (d, *J* = 2.4 Hz, 2H), 7.18 (dd, *J* = 8.4, 1.0 Hz, 2H).

^{13}C-NMR (125 MHz, $CDCl_3$, 298 K) δ [ppm] = 160.5, 156.9, 143.0, 138.0, 133.5, 133.3, 133.0, 130.7, 129.4, 128.6, 127.5, 126.6, 126.6, 121.0, 117.1, 111.9, 110.1.

The analytical data is in agreement with the literature.[271]

N,*N*'-((*S*)-[1,1'-binaphthalene]-2,2'-diyl)bis(3,5-dibromosalicylideneimine) cobalt (II) **(*S*)-51**

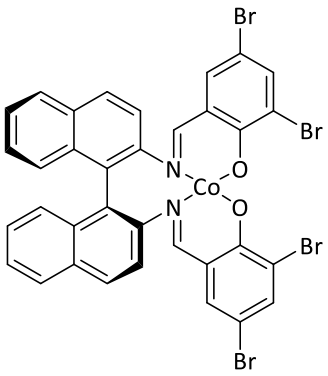

In a flame-dried *Schlenk* flask, *N*,*N*'-((*S*)-[1,1'-binaphthalene]-2,2'-diyl)bis(3,5-dibromosalicylideneimine) **(*S*)-55** (0.762 g, 0.94 mmol, 1.00 eq.) and cobalt(II) acetate tetrahydrate (0.234 g, 0.94 mmol, 1.00 eq.) are suspended in dry MeOH and MeCN (2 mL and 1 mL) and refluxed for 3 d. The mixture is cooled to 0°C and the precipitate is filtered off. The residue is washed with MeOH (cooled on dry ice) and ^{n}pentane. The crude product is dissolved in DCM, remaining unreacted insoluble ligand is filtered off and the solvent is removed *in vacuo*. *N*,*N*'-((*S*)-[1,1'-binaphthalene]-2,2'-diyl)bis(3,5-dibromosalicylideneimine) cobalt (II) **(*S*)-51** (0.466 g, 0.54 mmol, 57%) is obtained as dark brown solid.

HRMS (ESI+): m/z calculated for $[M]^+$ = 864.7395, found = 864.7391.

IR ν_{max} [cm^{-1}] = 3056, 1584, 1499, 1422, 1402, 1306, 1195, 1145, 862, 814, 748, 712, 684, 528.

The analytical data is in agreement with the literature.[272]

3.5 Experimental Details of Optimizations and Screenings

Optimization and screening reactions, as well as reactions that did not result in product isolation were performed using the following experimental details. The conversion rates and product ratios were determined based on the integrals of clearly separated signals observed in the ^{1}H and ^{13}C NMR spectra of the reaction mixtures.

Experimental details for Scheme 54:

$LiBH_4$ (0.011 g, 0.5 mmol, 0.5 eq.) is added to a flame-dried *Schlenk* flask inside a *glovebox*. Freshly distilled THF (2 mL) and 2-methyl-2-(2-phenylethyl)-oxirane **2** (0.162 g, 1.0 mmol, 1.00 eq.) are added in argon counterflow, and the reaction is stirred for 24 h at RT. NaOH solution (2 M, 2 mL) is added and the mixture is stirred for 30 min at RT. The layers are separated, the aqueous layer is extracted with Et_2O, the combined organic layers are filtered through a silica plug and the solvent is removed *in vacuo.*

Experimental details for Table 15:

The general procedure **GP-4** was conducted with 2-methyl-2-(2-phenylethyl)-oxirane **2** (0.162 g, 1.0 mmol, 1.0 eq) and the specified conditions given below.

entry	Cp_2TiCl_2	$CpCr(CO)_3H$	$LiBH_4$
6	–	0.020 g 0.1 mmol 0.1 eq.	0.011 0.5 mmol 0.5 eq.
7	0.025 g 0.1 mmol 0.1 eq.	0.020 g 0.1 mmol 0.1 eq.	–
8	0.025 g 0.1 mmol 0.1 eq.	–	0.011 0.5 mmol 0.5 eq.
9	–	–	0.011 0.5 mmol 0.5 eq.

Experimental details for Table 17:

The general procedure **GP-10** was conducted with 4-methyl-*N*-((2-methyloxiran-2-yl)methyl)-*N*-(prop-2-yn-1-yl)benzenesulfonamide **18** (0.279 g, 1.0 mmol, 1.0 eq) and the specified conditions given below.

entry	Cp_2TiCl_2	$CpCr(CO)_3H$	$LiBH_4$	T [°C], t [h]
2	0.025 g 0.1 mmol 0.1 eq.	0.020 g 0.1 mmol 0.1 eq.	0.011 0.5 mmol 0.5 eq.	25, 24
3	0.037 g 0.15 mmol 0.15 eq.	0.020 g 0.1 mmol 0.1 eq.	0.011 0.5 mmol 0.5 eq.	25, 72
4	0.037 g 0.15 mmol 0.15 eq.	0.020 g 0.1 mmol 0.1 eq.	0.011 0.5 mmol 0.5 eq.	45, 72

Experimental details for Table 18:

The general procedure **GP-6** was conducted with the specified conditions and substrates given below.

entry	substrate	Cp_2TiCl_2	$CpCr(CO)_3H$	$LiBH_4$
9	**26** 0.351 g 1.0 mmol 1.0 eq.	0.037 g 0.15 mmol 0.15 eq.	0.020 g 0.1 mmol 0.1 eq.	0.011 0.5 mmol 0.5 eq.
10	**27** 0.160 g 0.5 mmol 1.0 eq.	0.019 g 0.075 mmol 0.15 eq.	0.010 g 0.05 mmol 0.1 eq.	0.005 0.25 mmol 0.5 eq.

Experimental details for Table 19:

The general procedure **GP-6** was conducted with the specified conditions and substrates given below.

entry	substrate	Cp_2TiCl_2	$CpCr(CO)_3H$	$LiBH_4$	T [°C], t [h]
1	**28** 0.210 g 1.0 mmol 1.0 eq	0.037 g 0.15 mmol 0.15 eq.	0.020 g 0.1 mmol 0.1 eq.	0.011 0.5 mmol 0.5 eq.	45, 72
3	**30** 0.190 g 0.5 mmol 1.0 eq.	0.019 g 0.075 mmol 0.15 eq.	0.010 g 0.05 mmol 0.1 eq.	0.005 0.25 mmol 0.5 eq.	45, 72
4	**31** 0.176 g 0.5 mmol 1.0 eq.	0.019 g 0.075 mmol 0.15 eq.	0.005 g 0.025 mmol 0.05 eq.	0.005 0.25 mmol 0.5 eq.	25, 72

Experimental details for Table 20:

Entry 4: The general procedure **GP-5** was conducted with Cp_2TiCl_2 (0.006 g, 0.03 mmol, 0.05 eq.), Mn powder (0.041 g, 0.75 mmol, 1.50 eq.), Coll·HCl (0.197 g, 1.25 mmol, 2.50 eq.) 4-methyl-*N*-((2-methyloxiran-2-yl)methyl)-*N*-(3-(trimethylsilyl)prop-2-yn-1-yl)benzenesulfonamide **26** (0.176 g, 0.50 mmol, 1.00 eq.) are reacted in THF (5 mL) at RT for 72 h.

Experimental details for Scheme 62:

In a flame-dried *Schlenk* flask, Cp_2TiCl_2 (0.025 g, 0.10 mmol, 0.10 eq.) is added and the flask is transferred into a *glovebox* where $CpCr(CO)_3H$ (0.020 g, 0.10 mmol, 0.10 eq.) and $LiBH_4$ (0.011 g, 0.50 mmol, 0.50 eq.) are added. Freshly distilled 1,4-dioxane (2 mL), 2-methyl-2-(2-phenylethyl)-oxirane **2** (0.162 g, 1.0 mmol, 1.0 eq), and ethyl propiolate (0.491 g, 5.00 mmol, 5.00 eq.) are added in argon counterflow, and the reaction is stirred for 48 h at RT. NaOH solution (2 M, 2 mL) is added and the mixture is stirred for 30 min at RT. The layers are separated, the aqueous layer is extracted with Et_2O, the combined organic layers are filtered through a silica plug and the solvent is removed *in vacuo.*

Experimental details for Table 22:

The general procedure **GP-11** was conducted with methyl 8-((2*S*,3*R*)-3-((*R*)-2-hydroxyoctyl)oxiran-2-yl)octanoate **34** (1.0 eq.) and the specified conditions given below.

entry	34	D-*Kagan*-Cl_2	$CpCr(CO)_3H$	borohydride	LiCl	solvent	T [°C], t [h]
1	0.082 g 0.25 mmol 1.0 eq.	0.013 g 0.025 mmol 0.1 eq.	0.005 g 0.025 mmol 0.1 eq.	$NaBH_4$ 0.005 g 0.125 mmol 0.50 eq.	–	THF	45, 72
2	0.164 g 0.50 mmol 1.0 eq.	0.026 g 0.05 mmol 0.1 eq.	0.010 g 0.05 mmol 0.1 eq.	KBH_4 0.013 g 0.25 mmol 0.50 eq.	0.001 g 0.025 mmol 0.05 eq.	THF	25, 72

Experimental details for Table 24:

The general procedure **GP-11** was conducted with methyl 8-((2*S*,3*R*)-3-((*R*)-2-hydroxyoctyl)oxiran-2-yl)octanoate **34** (0.082 g, 0.25 mmol, 1.0 eq.) and the specified conditions given below.

entry	D-*Kagan*-X_2	$CpCr(CO)_3H$	$(^nBu_4N)BH_4$	LiCl	solvent	T [°C], t [h]
2	D-*Kagan*-Cl_2 0.013 g 0.025 mmol 0.1 eq.	0.005 g 0.025 mmol 0.1 eq.	0.032 g 0.125 mmol 0.50 eq.	0.001 g 0.025 mmol 0.10 eq.	THF	25, 72
3	D-*Kagan*-Br_2 0.015 g 0.025 mmol 0.1 eq.	0.005 g 0.025 mmol 0.1 eq.	0.032 g 0.125 mmol 0.50 eq.	–	THF	25, 72
5	D-*Kagan*-Br_2 0.015 g 0.025 mmol 0.1 eq.	0.005 g 0.025 mmol 0.1 eq.	0.032 g 0.125 mmol 0.50 eq.	–	THF	60, 72

Experimental details for Scheme 63:

$(^nBu_4N)BH_4$ (0.032 g, 0.125 mmol, 0.50 eq.) is added to a flame-dried *Schlenk* flask inside a *glovebox*. Freshly distilled THF (0.5 mL) and methyl 8-((2*S*,3*R*)-3-((*R*)-2-hydroxyoctyl)oxiran-2-yl)octanoate **34** (0.082 g, 0.25 mmol, 1.0 eq.) are added in argon counterflow, and the reaction is stirred for 72 h at 45°C. Pyridine-*N*-oxide (2.00 eq.) is added, and the mixture is stirred for 30 min at RT. The layers are separated, the aqueous layer is extracted with Et_2O, the combined organic layers are washed with water, dried over $MgSO_4$ and the solvent is removed *in vacuo.*

Experimental details for Table 25:

The general procedure **GP-11** was conducted with methyl 8-((2*S*,3*R*)-3-((*R*)-2-hydroxyoctyl)oxiran-2-yl)octanoate **34** (0.082 g, 0.25 mmol, 1.0 eq.) and the specified conditions given below.

entry	*Kagan*-X_2	$CpCr(CO)_3H$	$NaBH_3CN$	LiCl	solvent	T [°C], t [h]
1	D-*Kagan*-Cl_2 0.013 g 0.025 mmol 0.10 eq.	0.005 g 0.025 mmol 0.10 eq.	0.008 g 0.125 mmol 0.50 eq.	–	THF	25, 72
2	D-*Kagan*-Br_2 0.015 g 0.025 mmol 0.10 eq.	0.005 g 0.025 mmol 0.10 eq.	0.008 g 0.125 mmol 0.50 eq.	–	THF	25, 72
3	D-*Kagan*-Cl_2 0.013 g 0.025 mmol 0.10 eq.	0.005 g 0.025 mmol 0.10 eq.	0.008 g 0.125 mmol 0.50 eq.	0.001 g 0.025 mmol 0.10 eq.	THF	25, 72
5	L-*Kagan*-Cl_2 0.013 g 0.025 mmol 0.10 eq.	0.005 g 0.025 mmol 0.10 eq.	0.008 g 0.125 mmol 0.50 eq.	–	THF	25, 72

Experimental details for Table 27:

The general procedure **GP-11** was conducted with methyl 8-((2*S*,3*R*)-3-((*R*)-2-hydroxyoctyl)oxiran-2-yl)octanoate **34** (0.082 g, 0.25 mmol, 1.0 eq.) in 1,4-dioxane for 72 h at RT and the specified conditions given below.

entry	D-*Kagan*-Cl_2	$CpCr(CO)_3H$	$LiBH_4$
2	0.026 g 0.050 mmol 0.20 eq.	0.005 g 0.025 mmol 0.10 eq.	0.003 g 0.125 mmol 0.50 eq.
3	0.013 g 0.025 mmol 0.10 eq.	0.010 g 0.050 mmol 0.20 eq.	0.003 g 0.125 mmol 0.50 eq.
4	0.026 g 0.050 mmol 0.20 eq.	0.010 g 0.050 mmol 0.20 eq.	0.003 g 0.125 mmol 0.50 eq.

Experimental details for Table 28:

The general procedure **GP-11** was conducted with methyl 8-((2*S*,3*R*)-3-((*R*)-2-hydroxyoctyl)oxiran-2-yl)octanoate **34** (0.082 g, 0.25 mmol, 1.0 eq.) in 1,4-dioxane and the specified conditions given below.

entry	D-*Kagan*-X_2	$CpCr(CO)_3H$	$LiBH_4$	SulfAm	T [°C], t [h]
1	D-*Kagan*-Cl_2 0.013 g 0.025 mmol 0.10 eq.	0.005 g 0.025 mmol 0.10 eq.	0.003 g 0.125 mmol 0.50 eq.	***cy*-hexSulfAm** 0.017 g 0.025 mmol 0.10 eq.	25, 72
2	D-*Kagan*-Cl_2 0.013 g 0.025 mmol 0.10 eq.	0.005 g 0.025 mmol 0.10 eq.	0.003 g 0.125 mmol 0.50 eq.	**F_2-PhenSulfAm** 0.017 g 0.025 mmol 0.10 eq.	25, 72
3	D-*Kagan*-Cl_2 0.013 g 0.025 mmol 0.10 eq.	0.005 g 0.025 mmol 0.10 eq.	0.003 g 0.125 mmol 0.50 eq.	**PhenSulfAm** 0.017 g 0.025 mmol 0.10 eq.	25, 72
4	D-*Kagan*-Br_2 0.015 g 0.025 mmol 0.10 eq.	0.005 g 0.025 mmol 0.10 eq.	0.003 g 0.125 mmol 0.50 eq.	***cy*-M SulfAm** 0.017 g 0.025 mmol 0.10 eq.	25, 72
5	D-*Kagan*-Br_2 0.015 g 0.025 mmol 0.10 eq.	0.005 g 0.025 mmol 0.10 eq.	0.003 g 0.125 mmol 0.50 eq.	**F_2-PhenSulfAm** 0.017 g 0.025 mmol 0.10 eq.	25, 72
6	D-*Kagan*-Br_2 0.015 g 0.025 mmol 0.10 eq.	0.005 g 0.025 mmol 0.10 eq.	0.003 g 0.125 mmol 0.50 eq.	**PhenSulfAm** 0.017 g 0.025 mmol 0.10 eq.	25, 72

entry	D-*Kagan*-X_2	$CpCr(CO)_3H$	$LiBH_4$	SulfAm	T [°C], t [h]
7	D-*Kagan*-Br_2 0.015 g 0.025 mmol 0.10 eq.	0.005 g 0.025 mmol 0.10 eq.	0.003 g 0.125 mmol 0.50 eq.	**F_2-PhenSulfAm** 0.017 g 0.025 mmol 0.10 eq.	45, 72
8	D-*Kagan*-Br_2 0.015 g 0.025 mmol 0.10 eq.	0.005 g 0.025 mmol 0.10 eq.	0.003 g 0.125 mmol 0.50 eq.	**PhenSulfAm** 0.017 g 0.025 mmol 0.10 eq.	45, 72

Experimental details for Table 29:

The general procedure **GP-11** was conducted with methyl 8-((2*S*,3*R*)-3-((*R*)-2-hydroxyoctyl)oxiran-2-yl)octanoate **34** (0.082 g, 0.25 mmol, 1.0 eq.) in 1,4-dioxane and the specified conditions given below.

entry	D-*Kagan*-Br_2	$CpCr(CO)_3H$	$LiBH_4$	PhenSulfAm	T [°C], t [h]
1	0.023 g 0.0375 mmol 0.15 eq.	0.005 g 0.025 mmol 0.10 eq.	0.003 g 0.125 mmol 0.50 eq.	0.025 g 0.0375 mmol 0.15 eq.	25, 72
2	0.015 g 0.025 mmol 0.10 eq.	0.005 g 0.025 mmol 0.10 eq.	0.003 g 0.125 mmol 0.50 eq.	0.017 g 0.025 mmol 0.10 eq.	45, 72
3	0.023 g 0.0375 mmol 0.15 eq.	0.005 g 0.025 mmol 0.10 eq.	0.003 g 0.125 mmol 0.50 eq.	0.025 g 0.0375 mmol 0.15 eq.	45, 72
4	0.031 g 0.050 mmol 0.20 eq.	0.005 g 0.025 mmol 0.10 eq.	0.003 g 0.125 mmol 0.50 eq.	0.025 g 0.0375 mmol 0.15 eq.	45, 72
5	0.031 g 0.050 mmol 0.20 eq.	0.005 g 0.025 mmol 0.10 eq.	0.006 g 0.25 mmol 1.0 eq.	0.025 g 0.0375 mmol 0.15 eq.	45, 72
6	0.023 g 0.0375 mmol 0.15 eq.	0.005 g 0.025 mmol 0.10 eq.	0.003 g 0.125 mmol 0.50 eq.	0.025 g 0.0375 mmol 0.15 eq.	45, 48

Experimental details for Table 30:

The general procedure **GP-11** was conducted with methyl 8-((2*S*,3*R*)-3-((*R*)-2-hydroxyoctyl)oxiran-2-yl)octanoate **34** (1.0 eq.) in 1,4-dioxane and the specified conditions given below.

entry	34	L-*Kagan*-Br_2	$CpCr(CO)_3H$	$LiBH_4$	PhenSulfAm	T [°C], t [h]
1	0.328 g 1.00 mmol 1.00 eq.	0.092 g 0.15 mmol 0.15 eq.	0.020 g 0.10 mmol 0.10 eq.	0.011 g 0.50 mmol 0.50 eq.	0.099 g 0.10 mmol 0.15 eq.	45, 48
2	0.164 g 0.50 mmol 1.00 eq.	0.046 g 0.075 mmol 0.15 eq.	0.010 g 0.05 mmol 0.10 eq.	0.005 g 0.25 mmol 0.50 eq.	0.050 g 0.075 mmol 0.15 eq.	45, 72
3	0.082 g 0.25 mmol 1.00 eq.	0.031 g 0.050 mmol 0.20 eq.	0.005 g 0.025 mmol 0.10 eq.	0.003 g 0.125 mmol 0.50 eq.	0.025 g 0.0375 mmol 0.15 eq.	45, 72

Experimental details for Table 33:

Entry 3: The general procedure **GP-7** was conducted, with D-*Kagan*-Cl_2 (0.053 g, 0.1 mmol, 0.1 eq.), $CpCr(CO)_3H$ (0.020 g, 0.10 mmol, 0.10 eq.), $LiBH_4$ (0.011 g, 0.50 mmol, 0.50 eq.), and 3-tosyl-6-oxa-3-azabicyclo[3.1.0]hexane **14** (0.239 g, 0.5 mmol, 1.0 eq.) for 72 h at RT.

Experimental details for Table 35:

The general procedure **GP-4** was conducted with 2-methyl-2-(2-phenylethyl)-oxirane **2** (0.081 g, 0.5 mmol, 1.0 eq), and the specified conditions given below.

entry	Cp_2TiCl_2	$Cp^*Cr(CO)_3H$	$LiBH_4$	T [°C], t [h]
1	0.012 g 0.05 mmol 0.10 eq.	0.014 g 0.05 mmol 0.10 eq.	0.005 g 0.25 mmol 0.50 eq.	25, 3
2	0.012 g 0.05 mmol 0.10 eq.	0.014 g 0.05 mmol 0.10 eq.	0.005 g 0.25 mmol 0.50 eq.	25, 24

Experimental details for Scheme 67:

In a flame-dried *Schlenk* flask, Cp_2TiCl_2 (0.019 g, 0.075 mmol, 0.15 eq.) is added and the flask is transferred into a *glovebox* where $Cp^*Cr(CO)_3H$ (0.014 g, 0.05 mmol, 0.10 eq.) and $LiBH_4$ (0.005 g, 0.25 mmol, 0.50 eq.) are added. Freshly distilled 1,4-dioxane (1 mL) and 4-methyl-*N*-((2-methyloxiran-2-yl)methyl)-*N*-(prop-2-yn-1-yl)benzenesulfonamide **18** (0.140 g, 0.50 mmol, 1.00 eq.) are added in argon counterflow, and the reaction is stirred for 24 h at 45°C. NaOH solution (2 M, 2 mL) is added, and the mixture is stirred for 30 min at RT. The layers are separated, the aqueous layer is extracted with Et_2O, the combined organic layers are filtered through a silica plug and the solvent is removed *in vacuo.*

Experimental details for Table 37:

The general procedure **GP-12** was conducted with the specified conditions given below.

entry	2	[Co]	Cp_2TiCl_2	$LiBH_4$
1	16.8 µL 0.1 mmol 1.0 eq.	–	0.0025 g 0.01 mmol 0.10 eq.	0.0011 g 0.005 mmol 0.50 eq.
2	16.8 µL 0.1 mmol 1.0 eq.	**40** 0.0067 g 0.01 mmol 0.1 eq.	0.0025 g 0.01 mmol 0.10 eq.	0.0011 g 0.005 mmol 0.50 eq.
3	16.8 µL 0.1 mmol 1.0 eq.	**41** 0.0077 g 0.01 mmol 0.1 eq.	0.0025 g 0.01 mmol 0.10 eq.	0.0011 g 0.005 mmol 0.50 eq.

entry	2	[Co]	Cp_2TiCl_2	$LiBH_4$
4	0.081 g 0.5 mmol 1.0 eq.	**42** 0.016 g 0.05 mmol 0.1 eq.	0.012 g 0.05 mmol 0.1 eq.	0.005 g 0.25 mmol 0.5 eq.
5	16.8 µL 0.1 mmol 1.0 eq.	**43** 0.0077 g 0.01 mmol 0.1 eq.	0.0025 g 0.01 mmol 0.10 eq.	0.0011 g 0.005 mmol 0.50 eq.
6	16.8 µL 0.1 mmol 1.0 eq.	**44** 0.0045 g 0.01 mmol 0.1 eq.	0.0025 g 0.01 mmol 0.10 eq.	0.0011 g 0.005 mmol 0.50 eq.
7	16.8 µL 0.1 mmol 1.0 eq.	**45** 0.0037 g 0.01 mmol 0.1 eq.	0.0025 g 0.01 mmol 0.10 eq.	0.0011 g 0.005 mmol 0.50 eq.
8	16.8 µL 0.1 mmol 1.0 eq.	**46** 0.0067 g 0.01 mmol 0.1 eq.	0.0025 g 0.01 mmol 0.10 eq.	0.0011 g 0.005 mmol 0.50 eq.
9	0.081 g 0.5 mmol 1.0 eq.	**47** 0.037 g 0.05 mmol 0.1 eq.	0.012 g 0.05 mmol 0.1 eq.	0.005 g 0.25 mmol 0.5 eq.
10	16.8 µL 0.1 mmol 1.0 eq.	**48** 0.0049 g 0.01 mmol 0.1 eq.	0.0025 g 0.01 mmol 0.10 eq.	0.0011 g 0.005 mmol 0.50 eq.
11	0.081 g 0.5 mmol 1.0 eq.	**49** 0.026 g 0.05 mmol 0.1 eq.	0.012 g 0.05 mmol 0.1 eq.	0.005 g 0.25 mmol 0.5 eq.
12	16.8 µL 0.1 mmol 1.0 eq.	**(*R*)-50** 0.0060 g 0.01 mmol 0.1 eq.	0.0025 g 0.01 mmol 0.10 eq.	0.0011 g 0.005 mmol 0.50 eq.
13	0.081 g 0.5 mmol 1.0 eq.	**(*S*)-51** 0.043 g 0.05 mmol 0.1 eq.	0.012 g 0.05 mmol 0.1 eq.	0.005 g 0.25 mmol 0.5 eq.

Experimental details for Table 38:

The general procedure **GP-12** was conducted with the specified conditions given below.

entry	2	46	Cp_2TiCl_2	borohydride	solvent	T [°C], t [h]
1	16.8 µL 0.1 mmol 1.0 eq.	0.0067 g 0.01 mmol 0.1 eq.	0.0025 g 0.01 mmol 0.10 eq.	$LiBH_4$ 0.0011 g 0.005 mmol 0.50 eq.	1,4-dioxane	25, 24
2	16.8 µL 0.1 mmol 1.0 eq.	0.0067 g 0.01 mmol 0.1 eq.	0.0025 g 0.01 mmol 0.10 eq.	$NaBH_4$ 0.0018 g 0.005 mmol 0.50 eq.	1,4-dioxane	40, 24
3	16.8 µL 0.1 mmol 1.0 eq.	0.0067 g 0.01 mmol 0.1 eq.	0.0025 g 0.01 mmol 0.10 eq.	$NaBH_4$ 0.0018 g 0.005 mmol 0.50 eq.	THF	40, 24

Experimental details for Table 39:

The general procedure **GP-12** was conducted with the specified conditions given below.

entry	2	45	Cp_2TiCl_2	$LiBH_4$
1	16.8 µL 0.1 mmol 1.0 eq.	0.0019 g 0.005 mmol 0.05 eq.	0.0025 g 0.01 mmol 0.10 eq.	0.0011 g 0.005 mmol 0.50 eq.
2	16.8 µL 0.1 mmol 1.0 eq.	0.0037 g 0.01 mmol 0.1 eq.	0.0025 g 0.01 mmol 0.10 eq.	0.0011 g 0.005 mmol 0.50 eq.
3	16.8 µL 0.1 mmol 1.0 eq.	0.0075 g 0.02 mmol 0.2 eq.	0.0025 g 0.01 mmol 0.10 eq.	0.0011 g 0.005 mmol 0.50 eq.

Entry 4: In a flame-dried *Schlenk* flask, Cp_2TiCl_2 (0.0025 g, 0.01 mmol, 0.10 eq.) and the cobalt complex **45** (0.0037 g, 0.01 mmol, 0.1 eq.) are added, and the flask is transferred into a *glovebox* where $LiBH_4$ (0.0011 g, 0.005 mmol, 0.50 eq.) is added. 1,4-dioxane, previously dried over MS and degassed (0.2 mL), is added via syringe in argon counterflow and the mixture is stirred for 30 min. 2-Methyl-2-(2-phenylethyl)-oxirane **2** (16.8 µL, 0.1 mmol, 1.0 eq.) is added via micropipette and the reaction is stirred for 24 h at RT. NaOH solution (2 M, 0.2 mL) is added and the mixture is stirred for 30 min at RT. The layers are separated, the aqueous layer is extracted with Et_2O, the organic layers are filtered through a short silica plug and the solvent is removed *in vacuo.*

Experimental details for Figure 20:

In a flame-dried *Schlenk* flask, Cp_2TiCl_2 (0.0025 g, 0.01 mmol, 0.10 eq.) and the cobalt complex **45** (0.0037 g, 0.01 mmol, 0.1 eq.) are added, and the flask is transferred into a *glovebox* where $LiBH_4$ (0.0011 g, 0.005 mmol, 0.50 eq.), and phenyl-*N*-*tert*-butylnitrone (0.0709 g, 0.4 mmol, 4.0 eq.) or 5,5-dimethyl-1-pyrroline-*N*-oxide (0.0453 g, 0.4 mmol, 4.0 eq.) are added. 2-Methyl-2-(2-phenylethyl)-

oxirane **2** (16.8 µL, 0.1 mmol, 1.0 eq.) is added via micropipette, and 1,4-dioxane, previously dried over MS and degassed (0.2 mL), is added via syringe in argon counterflow. The reaction is stirred at RT and EPR samples are taken from the reaction mixture after 3 h, and after 22 h using a glass cannula, which is immediately transferred into an argon-flushed EPR-tube. EPR spectra were recorded at RT on a standard X-band EPR spectrometer.

Experimental details for Table 40:

The cobalt complex **46**, Cp_2TiCl_2, and Mn powder are placed in an oven-dried glass vial. The vial is placed in a *Schlenk* bottle and flushed with argon several times. 2-Methyl-2-(2-phenylethyl)-oxirane **2** is added via micropipette, and toluene, previously refluxed over sodium and distilled (0.2 mL), is added via syringe in argon counterflow. The vial is transferred into a high-pressure reactor autoclave and flushed with argon several times. The argon atmosphere is exchanged for a 10-bar hydrogen atmosphere, and the mixture is stirred for 24 h at 75°C. After slow venting of the hydrogen pressure, the reaction mixture is diluted with Et_2O, filtered through a short silica plug, and the solvent is removed *in vacuo.*

entry	2	46	Cp_2TiCl_2	Mn
1	16.8 µL 0.1 mmol 1.0 eq.	0.0067 g 0.01 mmol 0.1 eq.	0.0025 g 0.01 mmol 0.10 eq.	–
2	16.8 µL 0.1 mmol 1.0 eq.	0.0067 g 0.01 mmol 0.1 eq.	0.0025 g 0.01 mmol 0.10 eq.	0.0011 g 0.01 mmol 0.1 eq
3	16.8 µL 0.1 mmol 1.0 eq.	0.0067 g 0.01 mmol 0.1 eq.	0.0025 g 0.01 mmol 0.10 eq.	0.0082 g 0.15 mmol 1.5 eq

3.6 Catalysis Products

2-(4-Bromophenyl)propan-1-ol **9a**

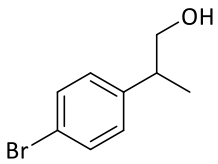

According to **GP-4**, Cp_2TiCl_2 (0.025 g, 0.10 mmol, 0.10 eq.), $CpCr(CO)_3H$ (0.020 g, 0.10 mmol, 0.10 eq.), $LiBH_4$ (0.011 g, 0.50 mmol, 0.50 eq.) and 2-(4-bromophenyl)-2-methyloxirane **9** (0.213 g, 1.00 mmol, 1.00 eq.) are reacted in 1,4-dioxane (2 mL) for 24 h. After purification via flash column chromatography (SiO_2, CH:EA = 60:40) 2-(4-bromophenyl)propan-1-ol **9a** (0.164 g, 0.76 mmol, 76%) is obtained together with 2% of the allylic alcohol by-product as a yellow oil.

R_f (CH:EA = 60:40) = 0.3

^{1}H-NMR (500 MHz, $CDCl_3$, 298 K) δ [ppm] = 7.47 – 7.43 (m, 2H), 7.14 – 7.10 (m, 2H), 3.72 – 3.64 (m, 2H), 2.92 (sext, *J* = 7.0 Hz, 1H), 1.42 (br s, 1H) 1.26 (d, *J* = 7.0 Hz, 3H).

^{13}C-NMR (125 MHz, $CDCl_3$, 298 K) δ [ppm] = 142.9, 131.8, 129.4, 120.5, 68.6, 42.1, 17.6.

The analytical data is in agreement with the literature.[273]

2-(4-Methoxyphenyl)ethan-1-ol **7a**

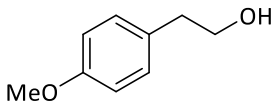

According to **GP-4**, Cp_2TiCl_2 (0.025 g, 0.10 mmol, 0.10 eq.), $CpCr(CO)_3H$ (0.020 g, 0.10 mmol, 0.10 eq.), $LiBH_4$ (0.011 g, 0.50 mmol, 0.50 eq.) and 2-(4-methoxyphenyl)oxirane **7** (0.150 g, 1.00 mmol, 1.00 eq.) are reacted in 1,4-dioxane (2 mL) for 24 h. After purification via flash column chromatography (Al_2O_3, DCM:MeOH = 95:5) 2-(4-methoxyphenyl)ethan-1-ol **7a** (0.140 g, 0.92 mmol, 92%) is obtained as a white solid.

R_f (Al_2O_3, DCM:MeOH = 95:5) = 0.5

^{1}H-NMR (500 MHz, $CDCl_3$, 298 K) δ [ppm] = 7.15 (d, *J* = 8.6 Hz, 2H), 6.86 (d, *J* = 8.6 Hz, 2H), 3.82 (t, *J* = 6.5 Hz, 2H), 3.79 (s, 3H), 2.81 (t, *J* = 6.5 Hz, 2H) 1.48 (br s, 1H).

^{13}C-NMR (125 MHz, $CDCl_3$, 298 K) δ [ppm] = 158.4, 130.5, 130.1, 114.2, 64.0, 55.4, 38.4.

The analytical data is in agreement with the literature.[274]

1-Tosylpyrrolidin-3-ol **14a**

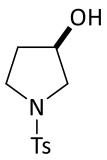

According to **GP-4**, Cp_2TiCl_2 (0.025 g, 0.10 mmol, 0.10 eq.), $CpCr(CO)_3H$ (0.020 g, 0.10 mmol, 0.10 eq.), $LiBH_4$ (0.011 g, 0.50 mmol, 0.50 eq.) and 3-tosyl-6-oxa-3-azabicyclo[3.1.0]hexane **14** (0.239 g, 1.00 mmol, 1.00 eq.) are reacted in 1,4-dioxane (2 mL) for 24 h. After purification via flash column chromatography (SiO_2, DCM:MeOH = 95:5) 1-tosylpyrrolidin-3-ol **14a** (0.178 g, 0.74 mmol, 74%) is obtained as a white solid.

R_f (DCM:MeOH = 95:5) = 0.3

^{1}H-NMR (400 MHz, $CDCl_3$, 298 K) δ [ppm] = 7.71 (d, *J* = 8.2 Hz, 2H), 7.32 (d, *J* = 8.2 Hz, 2H), 4.36 (tt, *J* = 4.7, 2.3 Hz, 1H), 3.41 – 3.32 (m, 3H), 3.23 (ddd, *J* = 11.1, 2.2, 1.4 Hz, 1H), 2.42 (s, 3H), 1.96 – 1.78 (m, 3H).

^{13}C-NMR (100 MHz, $CDCl_3$, 298 K) δ [ppm] = 143.7, 133.8, 129.8, 127.7, 70.9, 56.2, 46.1, 34.4, 21.7.

The analytical data is in agreement with the literature.[203]

1-Tosylazepan-4-ol **15a**

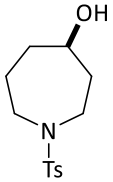

According to **GP-4**, Cp_2TiCl_2 (0.025 g, 0.10 mmol, 0.10 eq.), $CpCr(CO)_3H$ (0.020 g, 0.10 mmol, 0.10 eq.), $LiBH_4$ (0.011 g, 0.50 mmol, 0.50 eq.) and 4-tosyl-8-oxa-4-azabicyclo[5.1.0]octane **15** (0.267 g, 1.00 mmol, 1.00 eq.) are reacted in 1,4-dioxane (2 mL)

for 24 h. After purification via flash column chromatography (SiO_2, DCM:MeOH = 95:5) 1-tosylazepan-4-ol **15a** (0.183 g, 0.68 mmol, 68%) is obtained as a white solid.

R_f (DCM:MeOH = 95:5) = 0.2

^{1}H-NMR (400 MHz, $CDCl_3$, 298 K) δ [ppm] = 7.66 (d, J = 8.2 Hz, 2H), 7.29 (d, J = 8.2 Hz, 2H), 3.93 (m, 1H), 3.40 – 3.29 (m, 2H), 3.27 – 3.13 (m, 2H), 2.41 (s, 2H), 2.05 – 1.54 (m, 7H).

^{13}C-NMR (100 MHz, $CDCl_3$, 298 K) δ [ppm] = 143.3, 136.2, 129.8, 127.1, 70.2, 47.9, 42.7, 37.9, 35.0, 22.6, 21.6.

IR ν_{max} [cm^{-1}] = 3450 (br), 2920, 2850, 1323, 1152, 1090, 1040, 946, 888, 815, 713, 696, 648, 574, 550, 491.

HRMS (APCI): m/z calculated for $[M+H]^+$ = 270.1158, found = 270.1154.

M_p = 65.4 °C

11-Hydroxy-10-methylundecyl 4-methylbenzenesulfonate **13a**

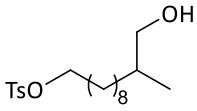

According to **GP-4**, Cp_2TiCl_2 (0.012 g, 0.05 mmol, 0.10 eq.), $CpCr(CO)_3H$ (0.010 g, 0.05 mmol, 0.10 eq.), $LiBH_4$ (0.005 g, 0.25 mmol, 0.50 eq.) and 9-(2-methyloxiran-2-yl)nonyl 4-methylbenzenesulfonate **13** (0.177 g, 0.50 mmol, 1.00 eq.) are reacted in 1,4-dioxane (1 mL) for 24 h. After purification via flash column chromatography (SiO_2, CH:EA = 80:20) 11-hydroxy-10-methylundecyl 4-methyl benzenesulfonate **13a** (0.113 g, 0.32 mmol, 64%) is obtained together with 6% of the allylic alcohol by-product as a colorless oil.

^{1}H-NMR (500 MHz, $CDCl_3$, 298 K) δ [ppm] = 7.78 (d, J = 8.4 Hz, 2H), 7.34 (d, J = 8.0 Hz, 2H), 4.01 (t, J = 6.5 Hz, 2H), 3.50 (dd, J = 10.5, 5.8 Hz, 1H), 3.41 (dd, J = 10.5, 6.5 Hz, 1H), 2.44 (s, 3H), 1.67 – 1.55 (m, 2H), 1.49 – 1.03 (m, 14H), 0.91 (d, J = 6.7 Hz, 3H).

^{13}C-NMR (125 MHz, $CDCl_3$, 298 K) δ [ppm] = 144.7, 133.4, 129.9, 128.0, 70.8, 68.5, 35.9, 33.3, 30.0, 29.6, 29.5, 29.0, 29.0, 27.1, 25.5, 21.8, 16.7.

The analytical data is in agreement with the literature.[74]

11-((*tert*-Butyldimethylsilyl)oxy)-2-methylundecan-1-ol **3a**

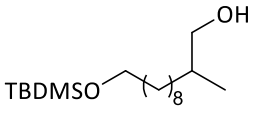

According to **GP-9**, Cp_2TiCl_2 (0.024 g, 0.1 mmol, 0.10 eq.), $CpCr(CO)_3H$ (0.020 g, 0.1 mmol, 0.10 eq.), KBH_4 (0.027 g, 0.50 mmol, 0.50 eq.), LiCl (0.002 g, 0.05 mmol, 0.05 eq.) and *tert*-butyldimethyl((9-(2-methyloxiran-2-yl)nonyl)oxy)silane **3** (0.315 g, 1.00 mmol, 1.00 eq.) are reacted in THF (2 mL) for 72 h. After purification via flash column chromatography (SiO_2, CH:EA:NEt_3 = 80:19:1= 70:30) 11-((*tert*-

butyldimethylsilyl)oxy)-2-methylundecan-1-ol **3a** (0.215 g, 0.68 mmol, 68%) is obtained together with 4% of the allylic alcohol by-product as a colorless oil.

R_f (CH:EE:NEt_3 = 80:19:1) = 0.3

^{1}H-NMR (500 MHz, $CDCl_3$, 298 K) δ [ppm] = 3.59 (t, *J* = 6.6 Hz, 2H), 3.51 (dd, *J* = 10.5 Hz, 5.7 Hz, 1H), 3.41 (dd, *J* = 10.5 Hz, 6.6 Hz, 1H), 1.64–1.23 (m, 16H), 0.91 (d, *J* = 6.7 Hz, 3H), 0.89 (s, 9H), 0.05 (s, 6H).

^{13}C-NMR (125 MHz, $CDCl_3$, 298 K) δ [ppm] = 68.6, 63.5, 35.9, 33.3, 33.0, 30.1, 29.8, 29.7, 29.6, 27.1, 26.1, 25.9, 18.5, 16.7, -5.1.

The analytical data is in agreement with the literature.[113]

3-Phenylbutan-2-ol **16a**

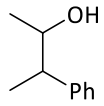

According to **GP-4**, Cp_2TiCl_2 (0.037 g, 0.15 mmol, 0.15 eq.), $CpCr(CO)_3H$ (0.020 g, 0.10 mmol, 0.10 eq.), $LiBH_4$ (0.011 g, 0.50 mmol, 0.50 eq.) and 2,3-dimethyl-2-phenyloxirane **16** (0.177 g, 1.00 mmol, 1.00 eq., *d.r.* = 78:22) are reacted in 1,4-dioxane (2 mL) for 24 h. After purification via flash column chromatography (SiO_2, ^{n}pentane:Et_2O = 95:5) 3-phenylbutan-2-ol **16a** (0.081 g, 0.54 mmol, 54%, *d.r.* = 64:36) is obtained together with 20% of the allylic alcohol by-product as a colorless oil.

^{1}H-NMR (500 MHz, $CDCl_3$, 298 K) δ [ppm] = *major/syn:* 7.42 – 7.28 (m, 3H), 7.28 – 7.18 (m, 2H), 3.92 – 3.84 (m, 1H), 2.78 – 2.71 (m, 1H), 1.33 (d, *J* = 7.1 Hz, 3H), 1.09 (d, *J* = 6.3 Hz, 3H); *minor/anti:* 7.41 – 7.29 (m, 3H), 7.27 – 7.19 (m, 2H), 3.88 – 3.82 (m, 1H), 2.71 – 2.64 (m, 1H), 1.27 (d, *J* = 7.1 Hz, 3H), 1.23 (d, *J* = 6.2 Hz, 3H).

^{13}C-NMR (125 MHz, $CDCl_3$, 298 K) δ [ppm] = *major/syn:* 144.4, 128.6, 128.0, 126.6, 72.5, 47.3, 21.2, 16.1; *minor/anti:* 143.7, 128.8, 128.2, 127.0, 72.5, 48.1, 20.8, 18.0.

The analytical data is in agreement with the literature.[275]

3-(*p*-Tolyl)butan-2-ol **17a**

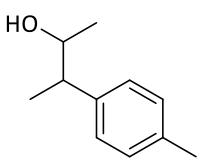

According to **GP-4**, Cp_2TiCl_2 (0.025 g, 0.10 mmol, 0.10 eq.), $CpCr(CO)_3H$ (0.020 g, 0.10 mmol, 0.10 eq.), $LiBH_4$ (0.011 g, 0.50 mmol, 0.50 eq.) and 2,3-dimethyl-2-(*p*-tolyl)oxirane **17** (0.162 g, 1.00 mmol, 1.00 eq.) are reacted in 1,4-dioxane (2 mL) for 48 h. After purification via flash column chromatography (SiO_2, ^{n}pentane:Et_2O = 90:10) 3-(*p*-tolyl)butan-2-ol **17a** (0.092 g, 0.56 mmol, 56%, *d.r.* = 55:45) is obtained together with 19% of the allylic alcohol by-product as a colorless oil.

^{1}H-NMR (500 MHz, $CDCl_3$, 298 K) δ [ppm] = *major/anti:* 7.18 – 7.08 (m, 4H), 3.90 – 3.83 (m, 1H), 2.64 (p, *J* = 7.2 Hz, 1H), 2.33 (s, 3H), 1.25 (d, *J* = 7.1 Hz, 3H), 1.23 (d, *J* = 6.1 Hz, 3H); *minor/syn:* 7.18 – 7.08

(m, 4H), 3.85 – 3.79 (m, 1H), 2.71 (p, *J* = 6.9 Hz, 1H), 2.34 (s, 3H), 1.31 (d, *J* = 7.0 Hz, 3H), 1.09 (d, *J* = 6.3 Hz, 3H).

^{13}C-NMR (125 MHz, $CDCl_3$, 298 K) *δ* [ppm] = *major/anti:* 141.8, 136.4, 129.3, 127.9, 72.5, 46.8, 21.13, 21.11, 16.1; *minor/syn:* 140.6, 136.1, 129.5, 128.0, 72.6, 47.7, 21.2, 20.8, 18.1.

The analytical data is in agreement with the literature.[204]

2-Methyl-4-phenylbutan-1-ol **2a**

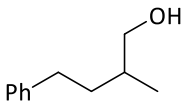

In a flame-dried *Schlenk* flask, Cp_2TiCl_2 (0.025 g, 0.10 mmol, 0.10 eq.) is added and the flask is transferred into a *glovebox* where $CpCr(CO)_3H$ (0.020 g, 0.10 mmol, 0.10 eq.) and $NaBH_4$ (0.019 g, 0.50 mmol, 0.50 eq.) are added. Freshly distilled THF (2 mL) and 2-methyl-2-(2-phenylethyl)-oxirane **2** (0.162 g, 1.00 mmol, 1.00 eq.) are added in argon counterflow, and the reaction is stirred for 48 h at RT. NaOH solution (2 M, 2 mL) is added and the mixture is stirred for 30 min at RT. The layers are separated, the aqueous layer is extracted with Et_2O, the combined organic layers are filtered through a silica plug and the solvent is removed *in vacuo.* After purification via flash column chromatography (SiO_2, ^{n}pentane:Et_2O = 50:50) 2-methyl-4-phenylbutan-1-ol **2a** (0.133 g, 0.81 mmol, 81%) is obtained together with 10% of the allylic alcohol by-product as a colorless oil.

According to **GP-9**, Cp_2TiCl_2 (0.024 g, 0.1 mmol, 0.10 eq.), $CpCr(CO)_3H$ (0.020 g, 0.1 mmol, 0.10 eq.), KBH_4 (0.027 g, 0.50 mmol, 0.50 eq.), LiCl (0.002 g, 0.005 mmol, 0.05 eq.) and 2-methyl-2-(2-phenylethyl) oxirane **2** (0.162 g, 1.00 mmol, 1.00 eq.) are reacted in THF (2 mL) for 48 h. After purification via flash column chromatography (SiO_2, ^{n}pentane:Et_2O = 50:50) 2-methyl-4-phenylbutan-1-ol **2a** (0.094 g, 0.57 mmol, 57%) is obtained as a colorless oil

R_f (^{n}pentane:Et_2O = 50:50) = 0.3

^{1}H-NMR (500 MHz, $CDCl_3$, 298 K) *δ* [ppm] = 7.31 – 7.26 (m, 2H), 7.22 – 7.16 (m, 3H), 3.54 (dd, *J* = 10.5, 5.8 Hz, 1H), 3.48 (dd, *J* = 10.5, 6.4 Hz, 1H), 2.75 – 2.68 (m, 1H), 2.64 – 2.57 (m, 1H), 1.81 – 1.73 (m, 1H), 1.72 – 1.64 (m, 1H), 1.49 – 1.41 (m, 1H), 1.37 (br s, 1H), 0.99 (d, *J* = 6.7 Hz, 3H).

^{13}C-NMR (125 MHz, $CDCl_3$, 298 K) *δ* [ppm] = 142.7, 128.5, 125.9, 110.0, 68.3, 35.5, 35.1, 33.4, 16.6.

The analytical data is in agreement with the literature.[276]

2-Phenylethan-1-ol **4a**

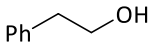

According to **GP-9**, Cp_2TiCl_2 (0.024 g, 0.1 mmol, 0.10 eq.), $CpCr(CO)_3H$ (0.020 g, 0.1 mmol, 0.10 eq.), KBH_4 (0.027 g, 0.50 mmol, 0.50 eq.), LiCl (0.002 g, 0.005 mmol, 0.05 eq.) and 2-phenyloxirane **4** (0.120 g, 1.00 mmol, 1.00 eq.) are reacted in THF (2 mL) for 48 h. After

purification via flash column chromatography (SiO_2, CH:EA = 50:50 and ^{n}pentane:Et_2O = 30:70) 2-phenylethan-1-ol **4a** (0.069 g, 0.56 mmol, 56%) is obtained as a colorless oil.

R_f (CH:EA = 50:50) = 0.4

^{1}H-NMR (500 MHz, $CDCl_3$, 298 K) δ [ppm] = 7.35 – 7.30 (m, 2H), 7.27 – 7.22 (m, 3H), 3.88 (t, J = 6.5 Hz, 2H), 2.88 (t, J = 6.5 Hz, 2H), 1.50 (br s, 1H).

^{13}C-NMR (125 MHz, $CDCl_3$, 298 K) δ [ppm] = 138.6, 129.2, 128.8, 126.6, 63.9, 39.4.

The analytical data is in agreement with the literature.[277]

Cyclooctanol **6a**

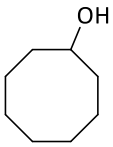

According to **GP-9**, Cp_2TiCl_2 (0.024 g, 0.1 mmol, 0.10 eq.), $CpCr(CO)_3H$ (0.020 g, 0.1 mmol, 0.10 eq.), KBH_4 (0.027 g, 0.50 mmol, 0.50 eq.), LiCl (0.002 g, 0.005 mmol, 0.05 eq.) and cyclooctene oxide **6** (0.126 g, 1.00 mmol, 1.00 eq.) are reacted in THF (2 mL) for 48 h. After purification via flash column chromatography (SiO_2, CH:EA = 80:20) cyclooctanol **6a** (0.055 g, 0.43 mmol, 43%) is obtained as a colorless oil.

R_f (CH:EA = 80:20) = 0.2

^{1}H-NMR (500 MHz, $CDCl_3$, 298 K) δ [ppm] = 3.85 (tt, J = 7.9 Hz, 3.7 Hz, 1H), 1.87 – 1.78 (m, 2H), 1.74 – 1.39 (m, 12H).

^{13}C-NMR (125 MHz, $CDCl_3$, 298 K) δ [ppm] = 72.4, 34.9, 27.6, 25.4, 22.8.

The analytical data is in agreement with the literature.[278]

2-Phenylpropan-1-ol **5a**

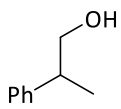

According to **GP-9**, Cp_2TiCl_2 (0.024 g, 0.1 mmol, 0.10 eq.), $CpCr(CO)_3H$ (0.020 g, 0.1 mmol, 0.10 eq.), KBH_4 (0.027 g, 0.50 mmol, 0.50 eq.), LiCl (0.002 g, 0.005 mmol, 0.05 eq.) and 2-methyl-2-phenyloxirane **5** (0.134 g, 1.00 mmol, 1.00 eq.) are reacted in THF (2 mL) for 48 h. After purification via flash column chromatography (SiO_2, CH:EA = 70:30) 2-phenylpropan-1-ol **5a** (0.113 g, 0.83 mmol, 83%) is obtained together with 14% of the allylic alcohol by-product as a colorless oil.

In a flame-dried *Schlenk* flask, Cp_2TiCl_2 (0.025 g, 0.10 mmol, 0.10 eq.) is added and the flask is transferred into a *glovebox* where $Cp^*Cr(CO)_3H$ (0.027 g, 0.10 mmol, 0.10 eq.) and $LiBH_4$ (0.011 g, 0.50 mmol, 0.50 eq.) are added. Freshly distilled 1,4-dioxane (2 mL) and 2-methyl-2-phenyloxirane **5** (0.134 g, 1.00 mmol, 1.00 eq.) are added in argon counterflow and the reaction is stirred for 24 h at RT. NaOH solution (2 M, 2 mL) is added and the mixture is stirred for 30 min at RT. The layers are

separated, the aqueous layer is extracted with Et_2O, the combined organic layers are filtered through a silica plug and the solvent is removed *in vacuo.* After purification via flash column chromatography (SiO_2, ^{n}pentane:Et_2O = 90:10) 2-Phenylpropan-1-ol **5a** (0.082 g, 0.60 mmol, 60%) is obtained together with 22% of the allylic alcohol by-product as a colorless oil.

In a flame-dried *Schlenk* flask, Cp_2TiCl_2 (0.025 g, 0.10 mmol, 0.10 eq.) and 6,6'-((1E,1'E)-(1,2-phenylenebis (azanylylidene)) bis(methanylylidene)) bis(2,4-dibromophenol) cobalt(II) **46** (0.069 g, 0.10 mmol, 0.10 eq.) are added and the flask is transferred into a *glovebox* where $LiBH_4$ (0.011 g, 0.50 mmol, 0.50 eq.) is added. Freshly distilled 1,4-dioxane (2 mL) and 2-methyl-2-phenyloxirane **5** (0.134 g, 1.00 mmol, 1.00 eq.) are added in argon counterflow and the reaction is stirred for 24 h at RT. NaOH solution (2 M, 2 mL) is added and the mixture is stirred for 30 min at RT. The layers are separated, the aqueous layer is extracted with Et_2O, the combined organic layers are filtered through a silica plug and the solvent is removed *in vacuo.* After purification via flash column chromatography (SiO_2, CH:EA = 80:20) 2-Phenylpropan-1-ol **5a** (0.086 g, 0.63 mmol, 63%) is obtained as a colorless oil.

R_f (CH:EA = 80:20) = 0.15

^{1}H-NMR (500 MHz, $CDCl_3$, 298 K) δ [ppm] = 7.36 – 7.32 (m, 2H), 7.27 – 7.22 (m, 3H), 3.71 (d, *J* = 6.8 Hz, 2H), 2.96 (sext, *J* = 7.0 Hz, 1H), 1.53 (br s, 1H), 1.28 (d, *J* = 7.0 Hz, 3H).

^{13}C-NMR (125 MHz, $CDCl_3$, 298 K) δ [ppm] = 143.8, 128.8, 127.6, 126.8, 68.8, 42.6, 17.7.

The analytical data is in agreement with the literature.[279]

3-Methyl-4-methylene-1-[(4-methylphenyl)sulfonyl]-3-pyrrolidinemethanol **18a**

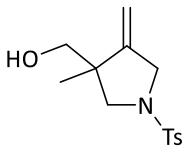

According to **GP-6**, Cp_2TiCl_2 (0.025 g, 0.075 mmol, 0.15 eq.), $CpCr(CO)_3H$ (0.010 g, 0.05 mmol, 0.10 eq.), $LiBH_4$ (0.005 g, 0.25 mmol, 0.50 eq.), and 4-methyl-*N*-((2-methyloxiran-2-yl)methyl)-*N*-(prop-2-yn-1-yl)benzenesulfonamide **18** (0.140 g, 0.50 mmol, 1.00 eq.) are reacted in 1,4-dioxane (1 mL). After purification via flash column chromatography (SiO_2, ^{n}pentane:Et_2O = 50:50) 3-methyl-4-methylene-1-[(4-methylphenyl)sulfonyl]-3-pyrrolidinemethanol **18** (0.035 g, 0.125 mmol, 25%) is obtained as a colorless oil.

R_f (^{n}pentane:Et_2O = 50:50) = 0.1

^{1}H-NMR (400 MHz, $CDCl_3$, 298 K) δ [ppm] = 7.72 – 7.68 (m, 2H), 7.36 – 7.32 (m, 2H), 5.01 (t, *J* = 2.1 Hz, 1H), 4.89 (t, *J* = 2.4 Hz, 1H), 3.93 (dt, *J* = 14.1, 2.3 Hz, 1H), 3.79 (dt, *J* = 14.1, 2.2 Hz, 1H), 3.46 – 3.41 (m, 2H), 3.32 (d, *J* = 11.0 Hz, 1H), 2.86 (d, *J* = 9.5 Hz, 1H), 2.44 (s, 3H), 1.68 (br s, 1H), 1.10 (s, 3H).

^{13}C-NMR (125 MHz, $CDCl_3$, 298 K) δ [ppm] = 149.6, 143.9, 132.6, 129.9, 128.0, 107.4, 67.6, 56.5, 52.5, 47.9, 21.7, 20.9.

The analytical data is in agreement with the literature.[205]

(3-methyl-4-nonylidene-1-tosylpyrrolidin-3-yl)methanol **20a**

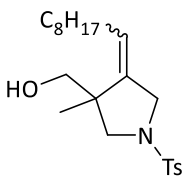

According to **GP-5**, Cp_2TiCl_2 (0.012 g, 0.05 mmol, 0.10 eq.), 2,4,6-collidine hydrochloride (0.236 g, 1.50 mmol, 3.00 eq.), Mn (0.082 g, 1.50 mmol, 3.00 eq.) and 4-Methyl-*N*-((2-methyloxiran-2-yl)methyl)-*N*-(undec-2-yn-1-yl)benzenesulfonamide **20** (0.196 g, 0.50 mmol, 1.00 eq.) are reacted in THF (5 mL) for 48 h. After purification via flash column chromatography (SiO_2, ^{n}pentane:Et_2O = 50:50) (3-methyl-4-nonylidene-1-tosylpyrrolidin-3-yl)methanol **20a** (0.170 g, 0.43 mmol, 86%, *d.r.* = 57:43) is obtained as a colorless oil.

According to **GP-6**, Cp_2TiCl_2 (0.037 g, 0.15 mmol, 0.15 eq.), $CpCr(CO)_3H$ (0.020 g, 0.10 mmol, 0.10 eq.), $LiBH_4$ (0.011 g, 0.50 mmol, 1.00 eq.) and 4-Methyl-*N*-((2-methyloxiran-2-yl)methyl)-*N*-(undec-2-yn-1-yl)benzenesulfonamide **20** (0.392 g, 1.00 mmol, 1.00 eq.) are reacted in 1,4-dioxane (2 mL) for 72 h. After purification via flash column chromatography (SiO_2, ^{n}pentane:Et_2O = 50:50) (3-methyl-4-nonylidene-1-tosylpyrrolidin-3-yl)methanol **20a** (0.076 g, 0.19 mmol, 19%, *d.r.* = 50:50) is obtained as a colorless oil.

R_f (^{n}pentane:Et_2O = 50:50) = 0.2

^{1}H-NMR (500 MHz, $CDCl_3$, 298 K) δ [ppm] = *major diastereomer:* 7.74 – 7.66 (m, 2H), 7.37 – 7.31 (m, 2H), 5.21 – 5.14 (m, 1H), 3.90 – 3.71 (m, 1H), 3.64 – 3.25 (m, 4H), 2.81 (d, J = 9.3 Hz, 1H), 2.44 (s, 3H), 2.13 – 1.85 (m, 2H), 1.34 – 1.19 (m, 12H), 1.07 (s, 3H), 0.90 – 0.85 (m, 3H); *minor diastereomer:* 7.74 – 7.66 (m, 2H), 7.37 – 7.31 (m, 2H), 5.35 – 5.27 (m, 1H), 3.74 – 3.67 (m, 1H), 3.64 – 3.25 (m, 4H), 2.82 (d, *J* = 9.3 Hz, 1H), 2.44 (s, 3H), 2.13 – 1.85 (m, 2H), 1.34 – 1.19 (m, 12H), 1.22 (s, 3H), 0.90 – 0.85 (m, 3H).

^{13}C-NMR (125 MHz, $CDCl_3$, 298 K) δ [ppm] = *major diastereomer:* 143.7, 139.5, 132.6, 129.7, 127.9, 123.5, 67.6, 56.3, 50.1, 47.4, 31.9, 30.0, 29.4, 29.3, 29.2, 29.2, 22.7, 21.6, 21.0, 14.1; *minor diastereomer:* 143.7, 137.8, 131.8, 129.7, 128.1, 125.6, 66.8, 58.2, 54.5, 47.6, 31.9, 29.4, 29.3, 29.23, 29.20, 28.1, 22.7, 21.6, 21.0, 14.1.

IR ν_{max} [cm^{-1}] = 3395, 2930, 2860, 1722, 1613, 1387, 1264, 1199, 1152, 1069, 1016, 951, 845.

HRMS (ESI+): m/z calculated for $[M+H]^+$ = 394.2410, found = 394.2411.

Diethyl 3-(hydroxymethyl)-3-methyl-4-nonylidenecyclopentane-1,1-dicarboxylate **30a**

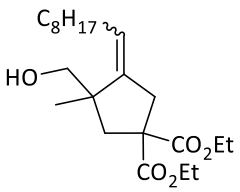

According to **GP-5**, Cp_2TiCl_2 (0.012 g, 0.05 mmol, 0.10 eq.), 2,4,6-collidine hydrochloride (0.236 g, 1.50 mmol, 3.00 eq.), Mn (0.082 g, 1.50 mmol, 3.00 eq.) and diethyl 2-((2-methyloxiran-2-yl)methyl)-2-(undec-2-yn-1-yl)malonate **30** (0.190 g, 0.50 mmol, 1.00 eq.) are reacted in THF (5 mL) for 48 h. After purification via flash column chromatography (SiO_2, ^{n}pentane:Et_2O = 60:40) diethyl 3-(hydroxymethyl)-3-methyl-4-nonylidenecyclopentane-1,1-dicarboxylate **30a** (0.049 g, 0.13 mmol, 26%, *d.r.* = 62:38) is obtained as a colorless oil.

^{1}H-NMR (500 MHz, C_6D_6, 298 K) δ [ppm] = *major diastereomer:* 5.15 (tt, *J* = 7.3, 2.4 Hz, 1H), 4.03 – 3.92 (m, 4H), 3.56 – 3.15 (m, 4H), 2.83 (d, *J* = 13.8 Hz, 1H), 2.41 (d, *J* = 13.9 Hz, 1H), 2.08 – 1.91 (m, 2H), 1.49 – 1.17 (m, 12H), 1.12 (s, 3H), 0.95 – 0.89 (m, 9H); *minor diastereomer:* 5.34 (tt, *J* = 7.6, 2.0 Hz, 1H), 4.03 – 3.92 (m, 4H), 3.56 – 3.15 (m, 4H), 2.94 (d, *J* = 13.7 Hz, 1H), 2.47 (dd, *J* = 13.7, 1.2 Hz, 1H), 2.08 – 1.91 (m, 2H), 1.24 (s, 3H), 1.49 – 1.17 (m, 12H), 0.95 – 0.89 (m, 9H).

^{13}C-NMR (125 MHz, C_6D_6, 298 K) δ [ppm] = *major diastereomer:* 172.5, 172.1, 145.0, 122.7, 70.1, 61.6, 61.4, 58.5, 47.9, 43.7, 38.2, 32.3, 30.6, 29.96, 29.94, 29.75, 29.74, 28.6, 24.7, 23.1, 14.4, 14.03, 14.00; *minor diastereomer:* 172.2, 171.9, 142.8, 125.3, 69.2, 61.5, 61.3, 58.4, 47.6, 46.4, 44.6, 32.3, 30.6, 29.97, 29.94, 29.8, 29.7, 28.6, 24.1, 23.1, 14.4, 14.1, 14.0.

IR ν_{max} [cm^{-1}] = 3472, 2927, 2857, 1729, 1463, 1367, 1284, 1189, 1096, 1062, 859, 423.

HRMS (APCI): m/z calculated for $[M-H]^-$ = 381.2636, found = 381.2634.

(*E*)-(4-(4-fluorobenzylidene)-3-methyl-1-tosylpyrrolidin-3-yl)methanol **24a**

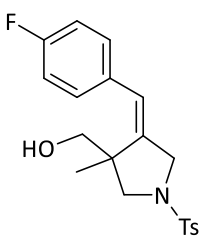

According to **GP-6**, Cp_2TiCl_2 (0.037 g, 0.15 mmol, 0.15 eq.), $CpCr(CO)_3H$ (0.020 g, 0.10 mmol, 0.10 eq.), $LiBH_4$ (0.011 g, 0.50 mmol, 0.5 eq.) and *N*-(3-(4-fluorophenyl)prop-2-yn-1-yl)-4-methyl-*N*-((2-methyloxiran-2-yl)methyl)benzene sulfonamide **24** (0.373 g, 1.00 mmol, 1.0 eq.) are reacted in 1,4-dioxane (2 mL) for 72 h. After purification via flash column chromatography (SiO_2, CH:EA:NEt_3 = 80:19:1) (*E*)-(4-(4-fluorobenzylidene)-3-methyl-1-tosylpyrrolidin-3-yl)methanol **24a** (0.093 g, 0.25 mmol, 25%) is obtained as a white solid.

R_f (^{n}pentane:Et_2O = 50:50) = 0.2

^{1}H-NMR (500 MHz, $CDCl_3$, 298 K) δ [ppm] = 7.76 – 7.70 (m, 2H), 7.36 (d, *J* = 8.0 Hz, 2H), 7.10 (dd, *J* = 8.0, 5.4 Hz, 2H), 7.00 – 6.93 (m, 2H), 6.48 (s, 1H), 3.96 (qd, *J* = 13.8, 2.1 Hz, 2H), 3.42 (d, *J* = 9.4 Hz, 1H), 3.39 (d, *J* = 11.1 Hz, 1H), 3.32 (d, *J* = 11.1 Hz, 1H), 2.92 (d, *J* = 9.4 Hz, 1H), 2.45 (s, 3H), 1.62 (br s, 1H), 1.00 (s, 3H).

^{13}C-NMR (125 MHz, $CDCl_3$, 298 K) δ [ppm] = 162.1 (d, *J* = 246.9 Hz), 144.0, 142.3, 132.5, 132.4 (d, *J* = 3.5 Hz), 130.3 (d, *J* = 7.9 Hz), 129.9, 128.1, 123.6, 115.2 (d, *J* = 21.4 Hz), 66.4, 58.1, 54.6, 48.4, 21.7, 21.6.

^{19}F-NMR (470 MHz $CDCl_3$, 298 K) δ [ppm] = -114.63.

IR ν_{max} [cm^{-1}] = 3559 (br), 2876, 2360, 1596, 1505, 1335, 1220, 1154, 1090, 1037, 819, 782, 708, 603, 584, 548, 518, 486.

HRMS (ESI+): m/z calculated for $[M+H]^+$ = 376.1377, found = 376.1376.

M_p = 133°C

(4-Methylene-3-phenethyl-1-tosylpyrrolidin-3-yl)methanol **25a**

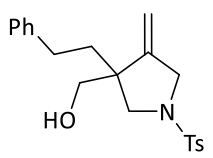

According to **GP-5**, Cp_2TiCl_2 (0.012 g, 0.05 mmol, 0.10 eq.), 2,4,6-collidine hydrochloride (0.195 g, 1.25 mmol, 2.50 eq.), Mn (0.055 g, 1.00 mmol, 2.00 eq.) and 4-methyl-*N*-((2-phenethyloxiran-2-yl)methyl)-*N*-(prop-2-yn-1-yl)benzenesulfonamide **25** (0.185 g, 0.50 mmol, 1.00 eq.) are reacted in THF (5 mL) for 48 h. After purification via flash column chromatography (SiO_2, ^{n}pentane:Et_2O = 50:50) (4-Methylene-3-phenethyl-1-tosylpyrrolidin-3-yl)methanol **25a** (0.087 g, 0.23 mmol, 46%) is obtained as a white solid.

According to **GP-6**, Cp_2TiCl_2 (0.019 g, 0.075 mmol, 0.15 eq.), $CpCr(CO)_3H$ (0.010 g, 0.05 mmol, 0.10 eq.), $LiBH_4$ (0.005 g, 0.25 mmol, 0.50 eq.) and *N*-(3-(4-fluorophenyl)prop-2-yn-1-yl)-4-methyl-*N*-((2-methyloxiran-2-yl)methyl)benzene sulfonamide **25** (0.373 g, 1.00 mmol, 1.00 eq.) are reacted in 1,4-dioxane (2 mL) for 72 h. After purification via flash column chromatography (SiO_2, CH:EA:NEt_3 = 80:19:1) (*E*)-(4-(4-fluorobenzylidene)-3-methyl-1-tosylpyrrolidin-3-yl)methanol **25a** (0.093 g, 0.25 mmol, 25%) is obtained as a white solid.

R_f (^{n}pentane:Et_2O = 50:50) = 0.1

^{1}H-NMR (500 MHz, $CDCl_3$, 298 K) δ [ppm] = 7.74 – 7.68 (m, 2H), 7.34 (d, *J* = 8.1 Hz, 2H), 7.29 – 7.22 (m, 2H), 7.21 – 7.14 (m, 1H), 7.13 – 7.07 (m, 2H), 5.12 (t, *J* = 2.1 Hz, 1H), 4.93 (t, *J* = 2.4 Hz, 1H), 3.95 – 3.81 (m, 2H), 3.58 – 3.51 (m, 1H), 3.46 – 3.41 (m, 1H), 3.35 (d, *J* = 9.7 Hz, 1H), 3.16 (d, *J* = 9.8 Hz, 1H), 2.59 – 2.44 (m, 2H), 2.43 (s, 3H), 1.93 – 1.86 (m, 1H), 1.73 – 1.63 (m, 2H).

^{13}C-NMR (125 MHz, $CDCl_3$, 298 K) δ [ppm] = 148.4, 144.0, 141.9, 132.4, 129.9, 128.6, 128.3, 128.0, 126.1, 108.0, 66.2, 54.8, 53.1, 51.1, 36.5, 30.6, 21.7.

HRMS (ESI+): m/z calculated for $[M+H]^+$ = 372.1628, found = 372.1628.

IR ν_{max} [cm^{-1}] = 3547, 2930, 1663, 1599, 1462, 1331, 1156, 1093, 1050, 1040, 1024, 1017, 920, 810, 702, 661, 584, 544, 522, 489.

(3-Methylene-1-tosyloctahydro-3a*H*-indol-3a-yl)methanol **27a**

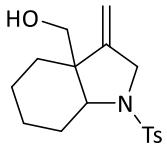

According to **GP-5**, Cp_2TiCl_2 (0.012 g, 0.05 mmol, 0.15 eq.), 2,4,6-collidine hydrochloride (0.195 g, 1.25 mmol, 2.50 eq.), Mn (0.055 g, 1.00 mmol, 2.00 eq.) and 4-methyl-*N*-(prop-2-yn-1-yl)-*N*-(*cis*-1-oxaspiro[2.5]octan-4-yl)benzenesulfonamide **27** (0.160 g, 0.50 mmol, 1.00 eq.) are reacted in THF (5 mL) for 48 h. After purification via flash column chromatography (SiO_2, ^{n}pentane:Et_2O = 50:50) (3-Methylene-1-tosyloctahydro-3a*H*-indol-3a-yl)methanol **27a** (0.151 g, 0.23 mmol, 94%) is obtained as a white solid.

R_f (^{n}pentane:Et_2O = 50:50) = 0.1

^{1}H-NMR (500 MHz, $CDCl_3$, 298 K) δ [ppm] = 7.76 – 7.71 (m, 2H), 7.32 – 7.28 (m, 2H), 5.11 (t, *J* = 2.1 Hz, 1H), 4.94 (t, *J* = 2.5 Hz, 1H), 4.07 – 3.93 (m, 2H), 3.76 (dd, *J* = 10.2, 5.7 Hz, 1H), 3.09 (d, *J* = 11.1 Hz, 1H), 2.95 (d, *J* = 11.1 Hz, 1H), 2.42 (s, 3H), 1.96 – 1.85 (m, 2H), 1.63 – 1.53 (m, 2H), 1.50 – 1.43 (m, 1H), 1.28 – 1.09 (m, 3H).

^{13}C-NMR (125 MHz, $CDCl_3$, 298 K) δ [ppm] = 146.2, 143.5, 136.9, 129.8, 127.2, 108.1, 67.3, 61.0, 51.6, 49.9, 29.7, 27.7, 23.5, 21.7, 21.1.

HRMS (ESI+): m/z calculated for $[M+H]^+$ = 322.1471, found = 322.1472.

IR ν_{max} [cm^{-1}] = 3508, 2925, 2858, 1449, 1330, 1159, 1146, 1096, 1085, 1051, 809, 664, 584, 541, 512, 471, 439, 422.

(*R*)-1-tosylpyrrolidin-3-ol **(*R*)-14a**

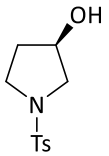

In a flame-dried *Schlenk* flask, D-Kagan-Br_2 **64** (0.046 g, 0.075 mmol, 0.15 eq.) is added and the flask is transferred into a *glovebox* where $CpCr(CO)_3H$ (0.010 g, 0.05 mmol, 0.10 eq.), $LiBH_4$ (0.005 g, 0.25 mmol, 0.50 eq.) and **PhenSulfAm** (0.050 g, 0.075 mmol, 0.15 eq.) are added. Freshly distilled 1,4-dioxane (1 mL) and 3-tosyl-6-oxa-3-azabicyclo[3.1.0]hexane **14** (0.120 g, 0.50 mmol, 1.00 eq.) are added in argon counterflow and the reaction is stirred for 72 h at 45°C. NaOH solution (2 M, 2 mL) is added and the mixture is stirred for 30 min at RT. The layers are separated, the aqueous layer is extracted with Et_2O, the combined organic layers are filtered through a silica plug and the solvent is removed *in vacuo.* After purification via flash column chromatography (SiO_2, DCM:MeOH = 95:5) (*R*)-1-tosylpyrrolidin-3-ol **(*R*)-14a** (0.077 g, 0.32 mmol, 64%, *ee* = 66%) is obtained as a white solid.

R_f (DCM:MeOH = 95:5) = 0.3

^{1}H-NMR (400 MHz, $CDCl_3$, 298 K) δ [ppm] = 7.71 (d, *J* = 8.2 Hz, 2H), 7.32 (d, *J* = 8.2 Hz, 2H), 4.36 (tt, *J* = 4.7, 2.3 Hz, 1H), 3.41 – 3.32 (m, 3H), 3.23 (ddd, *J* = 11.1, 2.2, 1.4 Hz, 1H), 2.42 (s, 3H), 1.96 – 1.78 (m, 3H).

^{13}C-NMR (100 MHz, $CDCl_3$, 298 K) δ [ppm] = 143.7, 133.8, 129.8, 127.7, 70.9, 56.2, 46.1, 34.4, 21.7.

The analytical data is in agreement with the literature.[280]

(*S*)-1-tosylpyrrolidin-3-ol **(*S*)-14a**

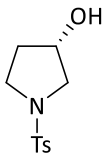

According to **GP-7**, L-Kagan-Cl_2 (0.053 g, 0.10 mmol, 0.10 eq.), $CpCr(CO)_3H$ (0.020 g, 0.10 mmol, 0.10 eq.), $LiBH_4$ (0.011 g, 0.50 mmol, 0.50 eq.) and 3-tosyl-6-oxa-3-azabicyclo[3.1.0]hexane **14** (0.239 g, 1.00 mmol, 1.00 eq.) are reacted for 72 h at RT. After purification via flash column chromatography (SiO_2, DCM:MeOH = 95:5) (*S*)-1-tosylpyrrolidin-3-ol **(*S*)-14a** (0.077 g, 0.32 mmol, 23%, *ee* = 40%) is obtained as a white solid.

R_f (DCM:MeOH = 95:5) = 0.3

^{1}H-NMR (400 MHz, $CDCl_3$, 298 K) δ [ppm] = 7.71 (d, *J* = 8.2 Hz, 2H), 7.32 (d, *J* = 8.2 Hz, 2H), 4.36 (tt, *J* = 4.7, 2.3 Hz, 1H), 3.41 – 3.32 (m, 3H), 3.23 (ddd, *J* = 11.1, 2.2, 1.4 Hz, 1H), 2.42 (s, 3H), 1.96 – 1.78 (m, 3H).

^{13}C-NMR (100 MHz, $CDCl_3$, 298 K) δ [ppm] = 143.7, 133.8, 129.8, 127.7, 70.9, 56.2, 46.1, 34.4, 21.7.

The analytical data is in agreement with the literature.[281]

(*R*)-1,2-diphenylethan-1-ol **(*R*)-39a**

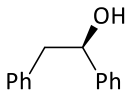

According to **GP-7**, D-Kagan-Cl_2 **63** (0.053 g, 0.10 mmol, 0.10 eq.), $CpCr(CO)_3H$ (0.020 g, 0.10 mmol, 0.10 eq.), $LiBH_4$ (0.011 g, 0.50 mmol, 0.50 eq.) and *cis*-stilbene oxide **39** (0.196 g, 1.00 mmol, 1.00 eq.) are reacted for 72 h at RT. After purification via flash column chromatography (SiO_2, CH:EA = 95:5) (*R*)-1,2-diphenylethan-1-ol **(*R*)-39a** (0.070 g, 0.35 mmol, 35%, *ee* = 46%) is obtained as a white solid.

R_f (CH:EA = 95:5) = 0.1

^{1}H-NMR (400 MHz, $CDCl_3$, 298 K) δ [ppm] = 7.39 – 7.19 (m, 10H), 4.91 (dd, *J* = 8.4, 4.9 Hz, 1H), 3.09 – 2.97 (m, 2H), 1.85 (br s, 1H).

^{13}C-NMR (100 MHz, $CDCl_3$, 298 K) δ [ppm] = 144.0, 138.2, 129.7, 128.7, 128.6, 127.8, 126.8, 126.0, 75.5, 46.2.

The analytical data is in agreement with the literature.[282]

(*S*)-1,2-diphenylethan-1-ol **(*S*)-39a**

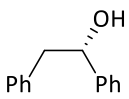

According to **GP-7**, D-Kagan-Cl_2 **63**(0.053 g, 0.10 mmol, 0.10 eq.), $CpCr(CO)_3H$ (0.020 g, 0.10 mmol, 0.10 eq.), $LiBH_4$ (0.011 g, 0.50 mmol, 0.50 eq.) and *cis*-stilbene oxide **39** (0.196 g, 1.00 mmol, 1.00 eq.) are reacted for 72 h at RT. After purification via flash column chromatography (SiO_2, CH:EA = 90:10) (*S*)-1,2-diphenylethan-1-ol **(*S*)-39a** (0.069 g, 0.35 mmol, 35%, *ee* = 50%) is obtained as a white solid.

R_f (CH:EA = 95:5) = 0.1

^{1}H-NMR (400 MHz, $CDCl_3$, 298 K) δ [ppm] = 7.39 – 7.19 (m, 10H), 4.91 (dd, *J* = 8.4, 4.9 Hz, 1H), 3.09 – 2.97 (m, 2H), 1.85 (br s, 1H).

^{13}C-NMR (100 MHz, $CDCl_3$, 298 K) δ [ppm] = 144.0, 138.2, 129.7, 128.7, 128.6, 127.8, 126.8, 126.0, 75.5, 46.2.

The analytical data is in agreement with the literature.[283]

Methyl (9*S*,12*R*)-9,12-dihydroxyoctadecanoate **1,4-34a**

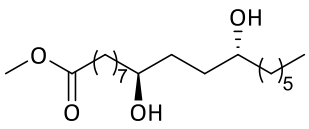

According to **GP-8**, D-Kagan-Br_2 **64** (0.023 g, 0.038 mmol, 0.15 eq.), $CpCr(CO)_3H$ (0.005 g, 0.025 mmol, 0.10 eq.), $LiBH_4$ (0.003 g, 0.125 mmol, 0.50 eq.), sulfonamide **PhenSulfAm** (0.025 g, 0.038 mmol, 0.15 eq.) and methyl 8-((2*S*,3*R*)-3-((*R*)-2-hydroxyoctyl)oxiran-2-yl)octanoate **34** (0.082 g, 0.25 mmol, 1.00 eq.) are reacted for 72 h at 45°C. After purification via flash column chromatography (SiO_2, CH:EA = 80:20 to 50:50) methyl (9*S*,12*R*)-9,12-dihydroxyoctadecanoate **1,4-34a** (0.045 g, 0.14 mmol, 56%, *d.r.* = >99:<1, *r.r.* = >99:<1) is obtained as a white solid.

R_f (CH:EA = 50:50) = 0.2

^{1}H-NMR (500 MHz, $CDCl_3$, 298 K) δ [ppm] = 3.66 (s, 3H), 3.64 (br s, 1H), 2.29 (t, *J* = 7.5 Hz, 2H), 2.20 (br s, 1H), 1.69 – 1.57 (m, 4H), 1.54 – 1.36 (m, 8H), 1.36 – 1.22 (m, 16H), 0.90 – 0.85 (m, 3H).

^{13}C-NMR (125 MHz, $CDCl_3$, 298 K) δ [ppm] = 174.5, 72.1, 72.0, 51.6, 37.7, 37.6, 34.2, 33.39, 33.36, 32.0, 29.6, 29.5, 29.3, 29.2, 25.84, 25.76, 25.0, 22.8, 14.2.

$[\alpha]_D^{20}$ = +7.1° (CH_2Cl_2)

The analytical data is in agreement with the literature.[91]

Methyl (10*S*,12*R*)-10,12-dihydroxyoctadecanoate **1,3-34a**

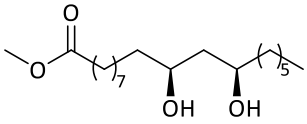

According to **GP-8**, L-Kagan-Br_2 **65** (0.031 g, 0.050 mmol, 0.20 eq.), $CpCr(CO)_3H$ (0.005 g, 0.025 mmol, 0.10 eq.), $LiBH_4$ (0.003 g, 0.125 mmol, 0.50 eq.), sulfonamide **PhenSulfAm** (0.025 g, 0.038 mmol, 0.15 eq.) and methyl 8-((2*S*,3*R*)-3-((*R*)-2-hydroxyoctyl)oxiran-2-yl)octanoate **34** (0.082 g, 0.25 mmol, 1.00 eq.) are reacted for 72 h at 45°C. After purification via flash column chromatography (SiO_2, CH:EA = 80:20 to 50:50) methyl (10*S*,12*R*)-10,12-dihydroxyoctadecanoate **1,3-34a** (0.045 g, 0.14 mmol, 32%, *d.r.* = >99:<1, *r.r.* = >99:<1) is obtained as a white solid.

R_f (CH:EA = 50:50) = 0.4

^{1}H-NMR (500 MHz, $CDCl_3$, 298 K) δ [ppm] = 3.87 – 3.80 (m, 2H), 3.65 (s, 3H), 2.86 (br s, 2H), 2.29 (t, *J* = 7.5 Hz, 2H), 1.64 – 1.56 (m, 3H), 1.51 – 1.22 (m, 23H), 0.90 – 0.84 (m, 3H).

^{13}C-NMR (125 MHz, $CDCl_3$, 298 K) δ [ppm] = 174.48, 73.36, 73.30, 51.58, 42.99, 38.40, 38.34, 34.21, 31.94, 29.65, 29.47, 29.43, 29.27, 29.21, 25.44, 25.42, 25.04, 22.72, 14.19.

$[\alpha]_D^{20}$ = -0.9° (CH_2Cl_2)

The analytical data is in agreement with the literature.[91]

(2*S*,4*R*)-tridecane-2,4-diol **1,3-35a**

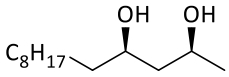

According to **GP-8**, D-Kagan-Br_2 **64** (0.031 g, 0.050 mmol, 0.20 eq.), $CpCr(CO)_3H$ (0.005 g, 0.025 mmol, 0.10 eq.), $LiBH_4$ (0.003 g, 0.125 mmol, 0.50 eq.), sulfonamide **PhenSulfAm** (0.025 g, 0.038 mmol, 0.15 eq.) and (2*S*,4*S*,5*R*)-4,5-epoxy-tridecane-2-ol **35** (0.054 g, 0.25 mmol, 1.00 eq.) are reacted for 72 h at 45°C. After purification via flash column chromatography (SiO_2, CH:EA = 80:20 to 60:40) (2*S*,4*R*)-tridecane-2,4-diol **1,3-35a** (0.010 g, 0.046 mmol, 18%, *d.r.* = >99:<1, *r.r.* = >99:<1) is obtained as a white solid.

R_f (CH:EA = 60:40) = 0.3

^{1}H-NMR (500 MHz, $CDCl_3$, 298 K) δ [ppm] = 4.09 – 4.02 (m, 1H), 3.88 – 3.82 (m, 1H), 2.63 (br s, 1H), 1.61 – 1.22 (m, 18H), 1.21 (d, *J* = 6.1 Hz, 3H), 0.88 (t, *J* = 6.9 Hz, 3H).

^{13}C-NMR (125 MHz, $CDCl_3$, 298 K) δ [ppm] = 73.3, 69.4, 44.8, 38.5, 32.0, 29.76, 29.75, 29.69, 29.5, 25.5, 24.4, 22.8, 14.3.

$[\alpha]_D^{20}$ = +19.2° (CH_2Cl_2)

The analytical data is in agreement with the literature.[210]

(2*S*,5*R*)-tridecane-2,5-diol **1,4-35a**

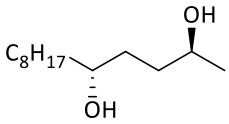

According to **GP-8**, L-Kagan-Br_2 **65** (0.031 g, 0.050 mmol, 0.20 eq.), $CpCr(CO)_3H$ (0.005 g, 0.025 mmol, 0.10 eq.), $LiBH_4$ (0.003 g, 0.125 mmol, 0.50 eq.), sulfonamide **PhenSulfAm** (0.025 g, 0.038 mmol, 0.15 eq.) and (2*S*,4*S*,5*R*)-4,5-epoxy-tridecane-2-ol **35** (0.054 g, 0.25 mmol, 1.00 eq.) are reacted for 72 h at 45°C. After purification via flash column chromatography (SiO_2, CH:EA = 80:20 to 50:50) (2*S*,5*R*)-tridecane-2,5-diol **1,4-35a** (0.013 g, 0.060 mmol, 24%, *d.r.* = >99:<1, *r.r.* = >99:<1) is obtained as a white solid.

^{1}H-NMR (500 MHz, $CDCl_3$, 298 K) δ [ppm] = 3.90 – 3.81 (m, 1H), 3.68 – 3.60 (m, 1H), 2.09 (br s, 1H), 1.66 – 1.22 (m, 18H), 1.21 (d, *J* = 6.1 Hz, 3H), 0.88 (t, *J* = 6.9 Hz, 3H).

^{13}C-NMR (125 MHz, $CDCl_3$, 298 K) δ [ppm] = 72.0, 68.2, 37.7, 35.2, 33.4, 32.0, 29.8, 29.7, 29.4, 25.9, 23.7, 22.8, 14.2.

$[\alpha]_D^{20}$ = +4.9° (CH_2Cl_2)

The analytical data is in agreement with the literature.[210]

4 References

[1] J. Colberg, K. Kuok Hii, S. G. Koenig, *ACS Sustainable Chem. Eng.* **2022**, *10*, 8239–8241.

[2] International Council of Chemical Associations, *The Global Chemical Industry: Catalyzing Growth and Addressing Our World's Sustainability Challenges,* Oxford Economics, **2019**.

[3] International Energy Agency, *Chemicals,* https://www.iea.org/energy-system/industry/chemicals, 25.04.2024.

[4] P. Gabrielli, L. Rosa, M. Gazzani, R. Meys, A. Bardow, M. Mazzotti, G. Sansavini, *One Earth* **2023**, *6*, 682–704.

[5] United Nations, *Sustainable Development Goals,* https://www.un.org/sustainabledevelopment/news/communications-material/, 26.04.2024.

[6] United Nations, *Sustainable Development Goal 12,* https://sdgs.un.org/goals/goal12#targets_and_indicators, 25.04.2024.

[7] P. T. Anastas, J. C. Warner, *Green Chemistry: Theory and Practice*, Oxford University Press, Oxford, **1998**.

[8] P. T. Anastas, J. B. Zimmerman, *Green Chem.* **2019**, *21*, 6545–6566.

[9] B. M. Trost, *Science* **1991**, *254*, 1471–1477.

[10] C. H. Bartholomew, R. J. Farrauto, *Fundamentals of industrial catalytic processes,* 2. ed., Wiley, Hoboken, NJ, **2006**.

[11] J. Humphreys, R. Lan, S. Tao, *Adv. Energy Sustain. Res.* **2021**, *2*, 2000043.

[12] V. Kyriakou, I. Garagounis, A. Vourros, E. Vasileiou, M. Stoukides, *Joule* **2020**, *4*, 142–158.

[13] M. C. Cann, M. Connelly, *Real-world Cases in Green Chemistry*, American Chemical Society, Washington, D. C., **2000**.

[14] M. A. Murphy, *Found. Chem.* **2018**, *20*, 121–165.

[15] G. Rothenberg, *Catalysis*, Wiley-VCH, Weinheim, **2008**.

[16] J. H. Clark, *Green Chem.* **1999**, *1*, 1–8.

[17] K.-H. Hellwich, *Stereochemie*, Springer, Berlin, Heidelberg, **2007**.

[18] K.-G. Fahlbusch, F.-J. Hammerschmidt, J. Panten, W. Pickenhagen, D. Schatkowski, K. Bauer, D. Garbe, H. Surburg in *Ullmann's Encyclopedia of Industrial Chemistry*, Wiley, Weinheim, **2003**.

[19] K. Roth, *Chem. unserer Zeit* **2005**, *39*, 212–217.

[20] T. Eriksson, S. Björkman, B. Roth, P. Höglund, *J. Pharm. Pharmacol* **2000**, *52*, 807–817.

[21] V. Jacques, A. W. Czarnik, T. M. Judge, L. H. T. van der Ploeg, S. H. DeWitt, *Proc. Natl. Acad. Sci. USA* **2015**, *112*, E1471-E1479.

[22] J. F. Larrow, E. N. Jacobsen in *Organometallics in Process Chemistry*, Springer, Berlin, Heidelberg, **2004**, 123–152.

[23] E. N. Jacobsen, A. Pfaltz, H. Yamamoto, *Comprehensive asymmetric catalysis*, Springer, London, **2003**.

[24] M. H. Wu, E. N. Jacobsen, *Tetrahedron Lett.* **1997**, *38*, 1693–1696.

[25] L. E. Martinez, W. A. Nugent, E. N. Jacobsen, *J. Org. Chem.* **1996**, *61*, 7963–7966.

[26] N. T. Patil, V. S. Shinde, B. Gajula, *Org. Biomol. Chem.* **2012**, *10*, 211–224.

[27] H. Pellissier, *Adv. Synth. Catal.* **2020**, *362*, 2289–2325.

[28] S. M. Inamdar, V. S. Shinde, N. T. Patil, *Org. Biomol. Chem.* **2015**, *13*, 8116–8162.

[29] N. P. Mankad, *Chem. Eur. J.* **2016**, *22*, 5822–5829.

[30] C. C. Malakar, L. Dell'Amico, W. Zhang, *Eur. J. Org. Chem.* **2023**, *26*, e202201114.

[31] S. Matsunaga, M. Shibasaki, *Chem. Commun.* **2014**, *50*, 1044–1057.

[32] M. Shibasaki, M. Kanai, S. Matsunaga, N. Kumagai, *Acc. Chem. Res.* **2009**, *42*, 1117–1127.

[33] J. Park, S. Hong, *Chem. Soc. Rev.* **2012**, *41*, 6931–6943.

[34] S. B. Ambegave, Shubham, T. R. More, N. T. Patil, *Chem. Commun.* **2023**, *59*, 8007–8016.

[35] K. Sonogashira, Y. Tohda, N. Hagihara, *Tetrahedron Lett.* **1975**, *16*, 4467–4470.

[36] K. Sonogashira, *J. Organomet. Chem.* **2002**, *653*, 46–49.

[37] M. Sawamura, M. Sudoh, Y. Ito, *J. Am. Chem. Soc.* **1996**, *118*, 3309–3310.

[38] X. Huo, R. He, X. Zhang, W. Zhang, *J. Am. Chem. Soc.* **2016**, *138*, 11093–11096.

[39] B. M. Trost, C.-I. J. Hung, G. Mata, *Angew. Chem. Int. Ed.* **2020**, *59*, 4240–4261; *Angew. Chem.* **2020**, *132*, 4268–4291.

[40] J. F. Teichert, B. L. Feringa, *Angew. Chem. Int. Ed.* **2010**, *49*, 2486–2528; *Angew. Chem.* **2010**, *122*, 2538–2582.

[41] R. He, P. Liu, X. Huo, W. Zhang, *Org. Lett.* **2017**, *19*, 5513–5516.

[42] X. Huo, G. Li, X. Wang, W. Zhang, *Angew. Chem. Int. Ed.* **2022**, *61*, e202210086; *Angew. Chem.* **2022**, *134, e202210086*.

[43] G. J. M. van der Kerk, J. G. Noltes, J. G. A. Luijten, *J. Appl. Chem.* **1957**, *7*, 356–365.

[44] D. H. R. Barton, S. W. McCombie, *J. Chem. Soc., Perkin Trans. 1* **1975**, 1574.

[45] C. Chatgilialoglu, A. Studer, *Encyclopedia of Radicals in Chemistry, Biology and Materials*, Wiley, Chichester, **2012**.

[46] S. Z. Zard, *Radical reactions in organic synthesis,* 1. ed., Oxford University Press, Oxford, **2003**.

[47] A. Studer, D. P. Curran, *Angew. Chem. Int. Ed.* **2016**, *55*, 58–102; *Angew. Chem.* **2016**, *128*, 58–106.

[48] C. P. Jasperse, D. P. Curran, T. L. Fevig, *Chem. Rev.* **1991**, *91*, 1237–1286.

[49] A. Gansäuer, *Radicals in Synthesis I*, Springer, Berlin, Heidelberg, **2006**.

[50] K. J. Romero, M. S. Galliher, D. A. Pratt, C. R. J. Stephenson, *Chem. Soc. Rev.* **2018**, *47*, 7851–7866.

[51] Y.-R. Luo, *Comprehensive handbook of chemical bond energies*, CRC Press, Boca Raton, London, New York, **2007**.

[52] M. B. Smith, J. March, *March's advanced organic chemistry*. *Reactions, mechanisms, and structure,* 6. ed., Wiley, New York, Weinheim, **2007**.

[53] J. P. van Hook, A. V. Tobolsky, *J. Am. Chem. Soc.* **1958**, *80*, 779–782.

[54] S. H. Kyne, G. Lefèvre, C. Ollivier, M. Petit, V.-A. Ramis Cladera, L. Fensterbank, *Chem. Soc. Rev.* **2020**, *49*, 8501–8542.

[55] H.-M. Huang, J. J. W. McDouall, D. J. Procter, *Nat. Catal.* **2019**, *2*, 211–218.

[56] J. Aubé in *Comprehensive Organic Synthesis*. *Volume 1* (Eds.: B. M. Trost, I. Fleming), Pergamon, Oxford, **1991**, 819–834.

[57] K. M. Sadhu, D. S. Matteson, *Tetrahedron Lett.* **1986**, *27*, 795–798.

[58] T. J. Michnick, D. S. Matteson, *Synlett* **1991**, *1991*, 631–632.

[59] N. Prileschajew, *Ber. Dtsch. Chem. Ges.* **1909**, *42*, 4811–4815.

[60] D. A. Singleton, S. R. Merrigan, J. Liu, K. N. Houk, *J. Am. Chem. Soc.* **1997**, *119*, 3385–3386.

[61] B. D. Brandes, E. N. Jacobsen, *J. Org. Chem.* **1994**, *59*, 4378–4380.

[62] Z.-X. Wang, Y. Tu, M. Frohn, J.-R. Zhang, Y. Shi, *J. Am. Chem. Soc.* **1997**, *119*, 11224–11235.

[63] M. Tokunaga, J. F. Larrow, F. Kakiuchi, E. N. Jacobsen, *Science* **1997**, *277*, 936–938.

[64] S. E. Schaus, B. D. Brandes, J. F. Larrow, M. Tokunaga, K. B. Hansen, A. E. Gould, M. E. Furrow, E. N. Jacobsen, *J. Am. Chem. Soc.* **2002**, *124*, 1307–1315.

[65] T. Katsuki, K. B. Sharpless, *J. Am. Chem. Soc.* **1980**, *102*, 5974–5976.

[66] T. Katsuki, V. Martin in *Organic Reactions*, Wiley, **2004**, 1–299.

[67] A. Gansäuer, C.-A. Fan, F. Keller, P. Karbaum, *Chem. Eur. J.* **2007**, *13*, 8084–8090.

[68] T. V. RajanBabu, W. A. Nugent, *J. Am. Chem. Soc.* **1994**, *116*, 986–997.

[69] J. Gorzynski Smith, *Synthesis* **1984**, *1984*, 629–656.

[70] F. Moschona, I. Savvopoulou, M. Tsitopoulou, D. Tataraki, G. Rassias, *Catalysts* **2020**, *10*, 1117.

[71] W. A. Nugent, T. V. RajanBabu, *J. Am. Chem. Soc.* **1988**, *110*, 8561–8562.

[72] T. V. RajanBabu, W. A. Nugent, *J. Am. Chem. Soc.* **1989**, *111*, 4525–4527.

[73] T. V. RajanBabu, W. A. Nugent, M. S. Beattie, *J. Am. Chem. Soc.* **1990**, *112*, 6408–6409.

[74] A. Gansäuer, H. Bluhm, M. Pierobon, *J. Am. Chem. Soc.* **1998**, *120*, 12849–12859.

[75] T. McCallum, X. Wu, S. Lin, *J. Org. Chem.* **2019**, *84*, 14369–14380.

[76] W. M. Haynes, *CRC handbook of chemistry and physics,* 95. ed., CRC Press, Boca Raton, **2014**.

[77] A. Gansäuer, S. Narayan, *Adv. Synth. Catal.* **2002**, *344*, 465–475.

[78] A. Gansäuer, M. Pierobon, H. Bluhm, *Angew. Chem. Int. Ed.* **1998**, *37*, 101–103; *Angew. Chem.* **1998**, *110*, 107–109.

[79] H. C. Brown, S. K. Gupta, *J. Am. Chem. Soc.* **1975**, *97*, 5249–5255.

[80] H. C. Brown, E. F. Knights, C. G. Scouten, *J. Am. Chem. Soc.* **1974**, *96*, 7765–7770.

[81] H. C. Brown, G. Zweifel, *J. Am. Chem. Soc.* **1961**, *83*, 1241–1246.

[82] A. Gansäuer, H. Bluhm, *Chem. Commun.* **1998**, 2143–2144.

[83] A. Gansäuer, M. Behlendorf, D. von Laufenberg, A. Fleckhaus, C. Kube, D. V. Sadasivam, R. A. Flowers, *Angew. Chem. Int. Ed.* **2012**, *51*, 4739–4742; *Angew. Chem.* **2012**, *124*, 4819–4823.

[84] A. Gansäuer, H. Bluhm, T. Lauterbach, *Adv. Synth. Catal.* **2001**, *343*, 785–787.

[85] A. Rosales, J. Muñoz-Bascón, V. Manuel Morales-Alcázar, J. A. Castilla-Alcalá, J. Enrique Oltra, *RSC Adv.* **2012**, *2*, 12922.

[86] J. Y. Cha, J. T. S. Yeoman, S. E. Reisman, *J. Am. Chem. Soc.* **2011**, *133*, 14964–14967.

[87] A. Gansäuer, T. Lauterbach, H. Bluhm, M. Noltemeyer, *Angew. Chem. Int. Ed.* **1999**, *38*, 2909–2910; *Angew. Chem.* **1999**, *111*, 3112–3114.

[88] E. Cesarotti, H. B. Kagan, R. Goddard, C. Krüger, *J. Organomet. Chem.* **1978**, *162*, 297–309.

[89] H. Weißbarth, F. Mühlhaus, A. Gansäuer, *Synthesis* **2020**, *52*, 2940–2947.

[90] A. Gansäuer, C.-A. Fan, F. Keller, J. Keil, *J. Am. Chem. Soc.* **2007**, *129*, 3484–3485.

[91] N. Funken, F. Mühlhaus, A. Gansäuer, *Angew. Chem. Int. Ed.* **2016**, *55*, 12030–12034; *Angew. Chem.* **2016**, *128*, 12209–12213.

[92] R. J. Hamill, *Drugs* **2013**, *73*, 919–934.

[93] I. Paterson, D. J. Berrisford, *Angew. Chem. Int. Ed. Engl.* **1992**, *31*, 1179–1180.

[94] B. D. Brandes, E. N. Jacobsen, *Synlett* **2001**, *2001*, 1013–1015.

[95] C. Schneider, *Synthesis* **2006**, *2006*, 3919–3944.

[96] A. Gansäuer, L. Shi, M. Otte, I. Huth, A. Rosales, I. Sancho-Sanz, N. M. Padial, J. E. Oltra in *Radicals in Synthesis III* (Eds.: M. Heinrich, A. Gansäuer), Springer, Berlin, Heidelberg, **2012**, 93–120.

[97] F. A. Carey, R. J. Sundberg, *Advanced Organic Chemistry*. *Part A: Structure and Mechanisms*, Kluwer Academic Publishers, Boston, **2002**.

[98] D. P. Curran, *Synthesis* **1988**, *1988*, 417–439.

[99] D. P. Curran, *Synthesis* **1988**, *1988*, 489–513.

[100] A. G. Davies, *Organotin Chemistry*, Wiley, Weinheim, **2004**.

[101] P. A. Baguley, J. C. Walton, *Angew. Chem. Int. Ed.* **1998**, *37*, 3072–3082; *Angew. Chem.* **1998**, *110*, 3272–3283.

[102] I. J. Boyer, *Toxicology* **1989**, *55*, 253–298.

[103] B. C. Gilbert, A. F. Parsons, *J. Chem. Soc., Perkin Trans. 2* **2002**, 367–387.

[104] A. Studer, S. Amrein, *Synthesis* **2002**, *2002*, 835–849.

[105] E. Denisov, C. Chatgilialoglu, A. Shestakov, T. Denisova, *Int. J. Chem. Kinet.* **2009**, *41*, 284–293.

[106] C. Chatgilialoglu, M. Newcomb in *Advances in Organometallic Chemistry*, *44* (Eds.: R. West, A. F. Hill), Academic Press, **1999**, 67–112.

[107] M. Newcomb, *Tetrahedron* **1993**, *49*, 1151–1176.

[108] C. Chatgilialoglu, *Chem. Eur. J.* **2008**, *14*, 2310–2320.

[109] J. M. Kanabus-Kaminska, J. A. Hawari, D. Griller, C. Chatgilialoglu, *J. Am. Chem. Soc.* **1987**, *109*, 5267–5268.

[110] J. C. Walton, A. Studer, *Acc. Chem. Res.* **2005**, *38*, 794–802.

[111] A. F. Barrero, J. E. Oltra, J. M. Cuerva, A. Rosales, *J. Org. Chem.* **2002**, *67*, 2566–2571.

[112] A. Gansäuer, M. Behlendorf, A. Cangönül, C. Kube, J. M. Cuerva, J. Friedrich, M. van Gastel, *Angew. Chem. Int. Ed.* **2012**, *51*, 3266–3270; *Angew. Chem.* **2012**, *124*, 3320–3324.

[113] A. Gansäuer, C.-A. Fan, F. Piestert, *J. Am. Chem. Soc.* **2008**, *130*, 6916–6917.

[114] A. Gansäuer, M. Otte, F. Piestert, C.-A. Fan, *Tetrahedron* **2009**, *65*, 4984–4991.

[115] P. N. Rylander in *Ullmann's Encyclopedia of Industrial Chemistry*, Wiley-VCH, Weinheim, **2000**.

[116] A. J. Birch, D. H. Williamson in *Organic Reactions*, Wiley, **2004**, 1–186.

[117] C. Masters, *Homogeneous Transition-metal Catalysis*. *A Gentle Art*, Chapman and Hall, New York, London, **1981**.

[118] T. Ohta, H. Takaya, M. Kitamura, K. Nagai, R. Noyori, *J. Org. Chem.* **1987**, *52*, 3174–3176.

[119] B. D. Vineyard, W. S. Knowles, M. J. Sabacky, G. L. Bachman, D. J. Weinkauff, *J. Am. Chem. Soc.* **1977**, *99*, 5946–5952.

[120] R. Noyori, *Angew. Chem. Int. Ed.* **2002**, *41*, 2008–2022; *Angew. Chem.* **2002**, *114*, 2108–2123.

[121] C. S. G. Seo, R. H. Morris, *Organometallics* **2019**, *38*, 47–65.

[122] W. S. Knowles in *Asymmetric Catalysis on Industrial Scale* (Eds.: H.-U. Blaser, E. Schmidt), Wiley, **2003**, 21–38.

[123] W. S. Knowles, *Angew. Chem. Int. Ed.* **2002**, *41*, 1998–2007; *Angew. Chem.* **2002**, *114*, 2096-2107.

[124] D. Mingos, R. H. Crabtree, *Comprehensive Organometallic Chemistry III*. *Vol. 1*, Elsevier, London, **2007**.

[125] J. A. Roth, M. Orchin, *J. Organomet. Chem.* **1979**, *182*, 299–311.

[126] R. L. Sweany, D. S. Comberrel, M. F. Dombourian, N. A. Peters, *J. Organomet. Chem.* **1981**, *216*, 37–63.

[127] F. Ungváry, L. Markó, *Organometallics* **1982**, *1*, 1120–1125.

[128] J. A. Roth, P. Wiseman, L. Ruszala, *J. Organomet. Chem.* **1982**, *240*, 271–275.

[129] J. W. Connolly, *Organometallics* **1984**, *3*, 1333–1337.

[130] J. F. Garst, T. M. Bockman, R. Batlaw, *J. Am. Chem. Soc.* **1986**, *108*, 1689–1691.

[131] M. J. Thomas, T. A. Shackleton, S. C. Wright, D. J. Gillis, J. P. Colpa, M. C. Baird, *J. Chem. Soc., Chem. Commun.* **1986**, *0*, 312–314.

[132] B. Wassink, M. J. Thomas, S. C. Wright, D. J. Gillis, M. C. Baird, *J. Am. Chem. Soc.* **1987**, *109*, 1995–2002.

[133] J. Choi, L. Tang, J. R. Norton, *J. Am. Chem. Soc.* **2007**, *129*, 234–240.

[134] R. L. Sweany, J. Halpern, *J. Am. Chem. Soc.* **1977**, *99*, 8335–8337.

[135] K. Fujita, T. Nakamura, H. Yorimitsu, K. Oshima, *J. Am. Chem. Soc.* **2001**, *123*, 3137–3138.

[136] L. Tang, E. T. Papish, G. P. Abramo, J. R. Norton, M.-H. Baik, R. A. Friesner, A. Rappé, *J. Am. Chem. Soc.* **2003**, *125*, 10093–10102.

[137] J. Hartung, M. E. Pulling, D. M. Smith, D. X. Yang, J. R. Norton, *Tetrahedron* **2008**, *64*, 11822–11830.

[138] A. L. J. Beckwith, C. J. Easton, A. K. Serelis, *J. Chem. Soc., Chem. Commun.* **1980**, 482–483.

[139] A. L. Beckwith, C. H. Schiesser, *Tetrahedron* **1985**, *41*, 3925–3941.

[140] J. R. Norton, T. Spataru, D. M. Camaioni, S.-J. Lee, G. Li, J. Choi, J. A. Franz, *Organometallics* **2014**, *33*, 2496–2502.

[141] K. B. Capps, A. Bauer, G. Kiss, C. D. Hoff, *J. Organomet. Chem.* **1999**, *586*, 23–30.

[142] J. Halpern, M. Pribanic, *Inorg. Chem.* **1970**, *9*, 2616–2618.

[143] J. Halpern, *Inorg. Chim. Acta* **1983**, *77*, L105-L106.

[144] G. Li, D. P. Estes, J. R. Norton, S. Ruccolo, A. Sattler, W. Sattler, *Inorg. Chem.* **2014**, *53*, 10743–10747.

[145] G. Li, A. Han, M. E. Pulling, D. P. Estes, J. R. Norton, *J. Am. Chem. Soc.* **2012**, *134*, 14662–14665.

[146] B. B. Wayland, S. Ba, A. E. Sherry, *Inorg. Chem.* **1992**, *31*, 148–150.

[147] G. Kiss, K. Zhang, S. L. Mukerjee, C. D. Hoff, G. C. Roper, *J. Am. Chem. Soc.* **1990**, *112*, 5657–5658.

[148] J. Choi, M. E. Pulling, D. M. Smith, J. R. Norton, *J. Am. Chem. Soc.* **2008**, *130*, 4250–4252.

[149] D. P. Estes, D. C. Grills, J. R. Norton, *J. Am. Chem. Soc.* **2014**, *136*, 17362–17365.

[150] J. L. Kuo, *Dissertation*, Columbia University, New York, **2017**.

[151] T. A. Weil, S. Metlin, I. Wender, *J. Organomet. Chem.* **1973**, *49*, 227–232.

[152] P. D. Taylor, M. Orchin, *J. Org. Chem.* **1972**, *37*, 3913–3915.

[153] D. C. Woska, Y. Ni, B. B. Wayland, *Inorg. Chem.* **1999**, *38*, 4135–4138.

[154] W. C. Watkins, T. Jaeger, C. E. Kidd, S. Fortier, M. C. Baird, G. Kiss, G. C. Roper, C. D. Hoff, *J. Am. Chem. Soc.* **1992**, *114*, 907–914.

[155] D. C. Eisenberg, C. J. C. Lawrie, A. E. Moody, J. R. Norton, *J. Am. Chem. Soc.* **1991**, *113*, 4888–4895.

[156] Q. Yao, A. Bakac, J. H. Espenson, *Organometallics* **1993**, *12*, 2010–2012.

[157] D. M. Camaioni, B. Ginovska-Pangovska, G. K. Schenter, S. M. Kathmann, T. Autrey, *J. Phys. Chem. A* **2012**, *116*, 7228–7237.

[158] D. W. Stephan, G. Erker, *Angew. Chem. Int. Ed.* **2010**, *49*, 46–76; *Angew. Chem.* **2010**, *122*, 50–81.

[159] E. S. Wiedner, M. B. Chambers, C. L. Pitman, R. M. Bullock, A. J. M. Miller, A. M. Appel, *Chem. Rev.* **2016**, *116*, 8655–8692.

[160] A. Panfilova, *Dissertation*, Rheinische Friedrich-Wilhelms-Universität, Bonn, **2019**.

[161] C. Yao, T. Dahmen, A. Gansäuer, J. Norton, *Science* **2019**, *364*, 764–767.

[162] R. F. Jordan, J. R. Norton, *J. Am. Chem. Soc.* **1982**, *104*, 1255–1263.

[163] S. Tshepelevitsh, A. Kütt, M. Lõkov, I. Kaljurand, J. Saame, A. Heering, P. G. Plieger, R. Vianello, I. Leito, *Eur. J. Org. Chem.* **2019**, *2019*, 6735–6748.

[164] M. Tilset, V. D. Parker, *J. Am. Chem. Soc.* **1989**, *111*, 6711–6717.

[165] R. B. Richrath, T. Olyschläger, S. Hildebrandt, D. G. Enny, G. D. Fianu, R. A. Flowers, A. Gansäuer, *Chem. Eur. J.* **2018**, *24*, 6371–6379.

[166] T. Hilche, S. L. Younas, A. Gansäuer, J. Streuff, *ChemCatChem* **2022**, *14*, e202200530.

[167] T. Kawamoto, I. Ryu, *Org. Biomol. Chem.* **2014**, *12*, 9733–9742.

[168] L. Banfi, E. Narisano, R. Riva, N. Stiasni, M. Hiersemann, T. Yamada, T. Tsubo in *Encyclopedia of Reagents for Organic Synthesis*, Wiley, Chichester, **2001**, 1–13.

[169] L. Banfi, E. Narisano, R. Riva, E. W. Baxter in *Encyclopedia of Reagents for Organic Synthesis*, Wiley, Chichester, **2001**, 1–4.

[170] F. A. Carey, R. J. Sundberg, *Advanced Organic Chemistry*. *Part B: Reactions and Synthesis*, Springer US, Boston, MA, **1990**.

[171] J. R. M. Giles, B. P. Roberts, *J. Chem. Soc., Perkin Trans. 2* **1983**, 743–755.

[172] A. N. Abeywickrema, A. L. Beckwith, *Tetrahedron Lett.* **1986**, *27*, 109–112.

[173] T. Kawamoto, S. Uehara, H. Hirao, T. Fukuyama, H. Matsubara, I. Ryu, *J. Org. Chem.* **2014**, *79*, 3999–4007.

[174] J. A. Barltrop, D. Bradbury, *J. Am. Chem. Soc.* **1973**, *95*, 5085–5086.

[175] J. T. Groves, K. W. Ma, *J. Am. Chem. Soc.* **1974**, *96*, 6527–6529.

[176] X.-H. Li, X.-H. Ju, *Comput. Theor. Chem.* **2013**, *1025*, 46–51.

[177] C. Han, Y. Dong, B. Wang, C. Zhang, *Russ. J. Phys. Chem.* **2016**, *90*, 1997–2005.

[178] D. W. Hart, J. Schwartz, *J. Am. Chem. Soc.* **1974**, *96*, 8115–8116.

[179] P. Wipf, H. Jahn, *Tetrahedron* **1996**, *52*, 12853–12910.

[180] J. Gordon, S. Hildebrandt, K. R. Dewese, S. Klare, A. Gansäuer, T. V. RajanBabu, W. A. Nugent, *Organometallics* **2018**, *37*, 4801–4809.

[181] G. A. Luinstra, J. H. Teuben, *J. Chem. Soc., Chem. Commun.* **1990**, 1470–1471.

[182] S. Klare, *Dissertation*, Rheinische Friedrich-Wilhelms-Universität, Bonn, **2019**.

[183] S.-Y. Tang, N. J. Rijs, J. Li, M. Schlangen, H. Schwarz, *Chem. Eur. J.* **2015**, *21*, 8483–8490.

[184] T. Hilche, *Dissertation*, Rheinische Friedrich-Wilhelms-Universität, Bonn, **2023**.

[185] G. Shizgal, *Dissertation*, Rheinische Friedrich-Wilhelms-Universität, Bonn, **2022**.

[186] M. Badertscher, P. Bühlmann, E. Pretsch, *Structure Determination of Organic Compounds,* 4. ed., Springer, Berlin, Heidelberg, **2009**.

[187] H. Nöth, R. Hartwimmer, *Chem. Ber.* **1960**, *93*, 2238–2245.

[188] C. R. Lucas, A. Shaver in *Inorganic Syntheses* (Eds.: A. G. MacDiarmid), Wiley, **1977**, 91–94.

[189] K. Burgess, W. A. van der Donk, *J. Am. Chem. Soc.* **1994**, *116*, 6561–6569.

[190] C. L. Cavallaro, J. Schwartz, *J. Org. Chem.* **1996**, *61*, 3863–3864.

[191] G. Weiss, *Bachelor Thesis*, Rheinische Friedrich-Wilhelms-Universität, Bonn, **2018**.

[192] P. Rittmeyer, U. Wietelmann in *Ullmann's Encyclopedia of Industrial Chemistry*, Wiley-VCH, Weinheim, **2000**.

[193] J. Seyden-Penne, *Reductions by the alumino- and borohydrides in organic synthesis,* 2. ed., Wiley-VCH, New York, Weinheim, **1997**.

[194] G. Weiss, *Master Thesis*, Rheinische Friedrich-Wilhelms-Universität, Bonn, **2020**.

[195] H. C. Brown, Y. M. Choi, S. Narasimhan, *Inorg. Chem.* **1981**, *20*, 4454–4456.

[196] J. Strong, T. R. Tuttle Jr, *J. Phys. Chem. A* **1973**, *77*, 533–539.

[197] A. Gansäuer, D. von Laufenberg, C. Kube, T. Dahmen, A. Michelmann, M. Behlendorf, R. Sure, M. Seddiqzai, S. Grimme, D. V. Sadasivam et al., *Chem. Eur. J.* **2015**, *21*, 280–289.

[198] H. Hagemann, R. Cerný, *Dalton Trans.* **2010**, *39*, 6006–6012.

[199] R. Díaz-Torres, S. Alvarez, *Dalton Trans.* **2011**, *40*, 10742–10750.

[200] I. E. Golub, O. A. Filippov, N. V. Belkova, L. M. Epstein, E. S. Shubina, *J. Organomet. Chem.* **2018**, *865*, 247–256.

[201] G. Li, J. R. Norton, *Org. Lett.* **2024**, *26*, 1382–1386.

[202] A. Gansäuer, M. Klatte, G. M. Brändle, J. Friedrich, *Angew. Chem. Int. Ed.* **2012**, *51*, 8891–8894; *Angew. Chem.* **2012**, *124*, 9021–9024.

[203] Y.-Q. Zhang, V. Jakoby, K. Stainer, A. Schmer, S. Klare, M. Bauer, S. Grimme, J. M. Cuerva, A. Gansäuer, *Angew. Chem. Int. Ed.* **2016**, *55*, 1523–1526; *Angew. Chem.* **2016**, *128*, 1546–1550.

[204] S. Höthker, R. Mika, H. Goli, A. Gansäuer, *Chem. Eur. J.* **2023**, *29*, e202301031.

[205] A. Gansäuer, M. Otte, L. Shi, *J. Am. Chem. Soc.* **2011**, *133*, 416–417.

[206] B. Giese, B. Kopping, T. Göbel, J. Dickhaut, G. Thoma, K. J. Kulicke, F. Trach in *Organic Reactions*, Wiley, **2004**, 301–856.

[207] A. N. Hancock, C. H. Schiesser, *Chem. Commun.* **2013**, *49*, 9892–9895.

[208] D. P. Estes, J. R. Norton, S. Jockusch, W. Sattler, *J. Am. Chem. Soc.* **2012**, *134*, 15512–15518.

[209] S. Poyraz, H. A. Döndaş, N. Y. Döndaş, J. M. Sansano, *Front. Pharmacol.* **2023**, *14*, 1239658.

[210] N. Funken, *Dissertation*, Rheinische Friedrich-Wilhelms-Universität, Bonn, **2016**.

[211] J. Meinwald, S. S. Labana, M. S. Chadha, *J. Am. Chem. Soc.* **1963**, *85*, 582–585.

[212] W. Liu, W. Li, A. Spannenberg, K. Junge, M. Beller, *Nat. Catal.* **2019**, *2*, 523–528.

[213] W. Liu, T. Leischner, W. Li, K. Junge, M. Beller, *Angew. Chem. Int. Ed.* **2020**, *59*, 11321–11324; *Angew. Chem.* **2020**, *132*, 11417–11420.

[214] X. Liu, L. Longwitz, B. Spiegelberg, J. Tönjes, T. Beweries, T. Werner, *ACS Catal.* **2020**, *10*, 13659–13667.

[215] L. Tadiello, T. Gandini, B. M. Stadler, S. Tin, H. Jiao, J. G. de Vries, L. Pignataro, C. Gennari, *ACS Catal.* **2022**, *12*, 235–246.

[216] M. Vayer, S. Zhang, J. Moran, D. Lebœuf, *ACS Catal.* **2022**, *12*, 3309–3316.

[217] T. Liedtke, P. Spannring, L. Riccardi, A. Gansäuer, *Angew. Chem. Int. Ed.* **2018**, *57*, 5006–5010; *Angew. Chem.* **2018**, *130*, 5100–5104.

[218] T. Hilche, P. H. Reinsberg, S. Klare, T. Liedtke, L. Schäfer, A. Gansäuer, *Chem. Eur. J.* **2021**, *27*, 4903–4912.

[219] T. Liedtke, T. Hilche, S. Klare, A. Gansäuer, *ChemSusChem* **2019**, *12*, 3166–3171.

[220] Z. Zhang, D. Slak, T. Krebs, M. Leuschner, N. Schmickler, E. Kuchuk, J. Schmidt, L. I. Domenianni, J. B. Kleine Büning, S. Grimme et al., *J. Am. Chem. Soc.* **2023**, *145*, 26667–26677.

[221] A. Gansäuer, C. Kube, K. Daasbjerg, R. Sure, S. Grimme, G. D. Fianu, D. V. Sadasivam, R. A. Flowers, *J. Am. Chem. Soc.* **2014**, *136*, 1663–1671.

[222] D. C. Eisenberg, J. R. Norton, *Isr. J. Chem.* **1991**, *31*, 55–66.

[223] K.-Y. Ye, T. McCallum, S. Lin, *J. Am. Chem. Soc.* **2019**, *141*, 9548–9554.

[224] H. Schiff, *Justus Liebigs Ann. Chem.* **1864**, *131*, 118–119.

[225] C. Ettling, *Justus Liebigs Ann. Chem.* **1840**, *35*, 241–276.

[226] H. Schiff, *Justus Liebigs Ann. Chem.* **1869**, *150*, 193–200.

[227] P. Pfeiffer, E. Buchholz, O. Bauer, *J. Prakt. Chem.* **1931**, *129*, 163–177.

[228] P. Pfeiffer, E. Breith, E. Lübbe, T. Tsumaki, *Justus Liebigs Ann. Chem.* **1933**, *503*, 84–130.

[229] N. P. van Leest, W. Stroek, M. A. Siegler, J. I. van der Vlugt, B. de Bruin, *Inorg. Chem.* **2020**, *59*, 12903–12912.

[230] N. P. van Leest, F. J. de Zwart, M. Zhou, B. de Bruin, *JACS Au* **2021**, *1*, 1101–1115.

[231] R. F. J. Epping, F. J. de Zwart, N. P. van Leest, J. I. van der Vlugt, M. A. Siegler, S. Mathew, J. N. H. Reek, B. de Bruin, *Inorg. Chem.* **2024**, *63*, 1974–1987.

[232] National Institute of Environmental Health Sciences, *Spin Trap Database,* https://tools.niehs.nih.gov/stdb/index.cfm, 22.08.2024.

[233] E. G. Janzen, T. Kasai, K. Kuwata, *Bull. Chem. Soc. Jpn.* **1973**, *46*, 2061–2062.

[234] B. Callebaut, J. Hullaert, K. van Hecke, J. M. Winne, *Org. Lett.* **2019**, *21*, 310–314.

[235] R. A. Fernandes, V. Bethi, *Tetrahedron* **2014**, *70*, 4760–4767.

[236] D. J. Vyas, E. Larionov, C. Besnard, L. Guénée, C. Mazet, *J. Am. Chem. Soc.* **2013**, *135*, 6177–6183.

[237] A. Murphy, A. Pace, T. D. P. Stack, *Org. Lett.* **2004**, *6*, 3119–3122.

[238] Y. Tian, E. Jürgens, D. Kunz, *Chem. Commun.* **2018**, *54*, 11340–11343.

[239] M. Cleij, A. Archelas, R. Furstoss, *J. Org. Chem.* **1999**, *64*, 5029–5035.

[240] J. A. Varela, C. González-Rodríguez, S. G. Rubín, L. Castedo, C. Saá, *J. Am. Chem. Soc.* **2006**, *128*, 9576–9577.

[241] M. G. Unthank, N. Hussain, V. K. Aggarwal, *Angew. Chem. Int. Ed.* **2006**, *45*, 7066–7069; *Angew. Chem.* **2006**, *118*, 7224–7227.

[242] P. Fristrup, B. B. Dideriksen, D. Tanner, P.-O. Norrby, *J. Am. Chem. Soc.* **2005**, *127*, 13672–13679.

[243] E. Mai, C. Schneider, *Chem. Eur. J.* **2007**, *13*, 2729–2741.

[244] P. C. Page, B. R. Buckley, L. F. Appleby, P. A. Alsters, *Synthesis* **2005**, 3405–3411.

[245] M. J. Moran, K. Martina, V. Bieliunas, F. Baricco, S. Tagliapietra, G. Berlier, W. M. de Borggraeve, G. Cravotto, *Adv. Synth. Catal.* **2021**, *363*, 2850–2860.

[246] Z. Zhang, *Dissertation*, Rheinische Friedrich-Wilhelms-Universität, Bonn, **2019**.

[247] Y. Tsuchiya, T. Kumamoto, T. Ishikawa, *J. Org. Chem.* **2004**, *69*, 8504–8505.

[248] A. S. K. Hashmi, J. P. Weyrauch, E. Kurpejović, T. M. Frost, B. Miehlich, W. Frey, J. W. Bats, *Chem. Eur. J.* **2006**, *12*, 5806–5814.

[249] R. Liu, D. Yang, F. Chang, L. Giordano, G. Liu, A. Tenaglia, *Asian J. Org. Chem.* **2019**, *8*, 2011–2016.

[250] P. Gao, X.-B. Yan, T. Tao, F. Yang, T. He, X.-R. Song, X.-Y. Liu, Y.-M. Liang, *Chem. Eur. J.* **2013**, *19*, 14420–14424.

[251] P. Ghosh, P. Saha, S. Bondalapati, K. Indukuri, A. K. Saikia, *J. Org. Chem.* **2014**, *79*, 4119–4124.

[252] P. B. Huleatt, M. L. Khoo, Y. Y. Chua, T. W. Tan, R. S. Liew, B. Balogh, R. Deme, F. Gölöncsér, K. Magyar, D. P. Sheela et al., *J. Med. Chem.* **2015**, *58*, 1400–1419.

[253] C.-H. Luo, P.-L. Wang, C.-C. Chang, *J. Org. Chem.* **2021**, *86*, 15033–15044.

[254] S. Caddick, J. D. Wilden, D. B. Judd, *J. Am. Chem. Soc.* **2004**, *126*, 1024–1025.

[255] M. M. Elenkov, L. Tang, A. Meetsma, B. Hauer, D. B. Janssen, *Org. Lett.* **2008**, *10*, 2417–2420.

[256] B. M. Trost, M. R. Machacek, B. D. Faulk, *J. Am. Chem. Soc.* **2006**, *128*, 6745–6754.

[257] F. Kleinbeck, F. D. Toste, *J. Am. Chem. Soc.* **2009**, *131*, 9178–9179.

[258] J. Cabezas, A. Oehlschlager, *Synthesis* **1999**, *1*, 107–111.

[259] I. Manjón-Mata, M. T. Quirós, E. Buñuel, D. J. Cárdenas, *Adv. Synth. Catal.* **2020**, *362*, 146–151.

[260] M. J. Begley, N. Housden, A. Johns, J. A. Murphy, *Tetrahedron* **1991**, *47*, 8417–8430.

[261] A. Gansäuer, F. Piestert, I. Huth, T. Lauterbach, *Synthesis* **2008**, *2008*, 3509–3515.

[262] A. Gansäuer, M. Pierobon, H. Bluhm, *Synthesis* **2001**, *16*, 2500–2520.

[263] L. M. Urbanczyk-Pearson, F. J. Femia, J. Smith, G. Parigi, J. A. Duimstra, A. L. Eckermann, C. Luchinat, T. J. Meade, *Inorg. Chem.* **2008**, *47*, 56–68.

[264] T. K. Panda, M. T. Gamer, P. W. Roesky, H. Yoo, D. H. Berry in *Inorganic Syntheses*, Wiley, **2014**, 35–37.

[265] R. F. Jordan, J. R. Norton, *J. Am. Chem. Soc.* **1982**, *104*, 1255–1263.

[266] P. Leoni, A. Landi, M. Pasquali, *J. Organomet. Chem.* **1987**, *321*, 365–369.

[267] A. P. Dieskau, J.-M. Begouin, B. Plietker, *Eur. J. Org. Chem.* **2011**, *2011*, 5291–5296.

[268] A. Gansäuer, S. Narayan, N. Schiffer-Ndene, H. Bluhm, J. E. Oltra, J. M. Cuerva, A. Rosales, M. Nieger, *J. Organomet. Chem.* **2006**, *691*, 2327–2331.

[269] R. M. Irfan, D. Jiang, Z. Sun, L. Zhang, S. Cui, P. Du, *J. Catal.* **2017**, *353*, 274–285.

[270] H. Li, D. Xi, Y. Niu, C. Wang, F. Xu, L. Liang, P. Xu, *J. Inorg. Biochem.* **2019**, *195*, 174–181.

[271] Y. Lu, G. W. Coates, *J. Am. Chem. Soc.* **2023**, *145*, 22425–22432.

[272] T. Uchida, T. Katsuki, *Helv. Chim. Acta* **2002**, *85*, 3078–3089.

[273] S. Guduguntla, M. Fañanás-Mastral, B. L. Feringa, *J. Org. Chem.* **2013**, *78*, 8274–8280.

[274] C. Gómez, B. Maciá, V. J. Lillo, M. Yus, *Tetrahedron* **2006**, *62*, 9832–9839.

[275] D. Méndez-Sánchez, J. Mangas-Sánchez, E. Busto, V. Gotor, V. Gotor-Fernández, *Adv. Synth. Catal.* **2016**, *358*, 122–131.

[276] D. S. G. Henriques, K. Zimmer, S. Klare, A. Meyer, E. Rojo-Wiechel, M. Bauer, R. Sure, S. Grimme, O. Schiemann, R. A. Flowers et al., *Angew. Chem. Int. Ed.* **2016**, *55*, 7671–7675; *Angew. Chem.* **2016**, *128*, 7801–7805.

[277] S. Patnaik, A. D. Sadow, *Angew. Chem. Int. Ed.* **2019**, *58*, 2505–2509; *Angew. Chem.* **2019**, *131*, 2527–2531.

[278] K. Kamata, K. Yonehara, Y. Nakagawa, K. Uehara, N. Mizuno, *Nat. Chem.* **2010**, *2*, 478–483.

[279] S. M. A. H. Siddiki, A. S. Touchy, M. A. R. Jamil, T. Toyao, K. Shimizu, *ACS Catal.* **2018**, *8*, 3091–3103.

[280] C. Chen, S. Jin, Z. Zhang, B. Wei, H. Wang, K. Zhang, H. Lv, X.-Q. Dong, X. Zhang, *J. Am. Chem. Soc.* **2016**, *138*, 9017–9020.

[281] S. Li, H. Zhu, L. Li, W. Chen, J. Jiang, Z.-W. Qu, S. Grimme, Y.-Q. Zhang, *Angew. Chem. Int. Ed.* **2023**, *62*, e202309525; *Angew. Chem.* **2023**, *135, e202309525*.

[282] X. Liu, Q. Wang, C. Han, X. Feng, H. Du, *Chin. J. Chem.* **2019**, *37*, 663–666.

[283] W. Miao, J. Zhang, Y. Yang, W. Tang, D. Xue, J. Xiao, H. Sun, C. Wang, *Angew. Chem. Int. Ed.* **2023**, *62*, e202306015; *Angew. Chem.* **2023**, *135, e202306015*.

5 Appendix

5.1 Abbreviations

$[\alpha]_D^{20}$	specific rotation at 20°C
1,4-CHD	1,4-cyclohexadiene
9-BBN	9-borabicyclo[3.3.1]nonane
Å	Ångström (unit)
ac	acetate
acac	acetylacetonate
AIBN	azobisisobutyronitrile
AnisTRAP	2,2'-bis[1-(4-methoxyphenyl)phosphino-ethyl]-1,1'-biferrocene
APCI	atmospheric pressure chemical ionization
aq.	aqueous
Ar	aryl
ARO	asymmetric ring-opening reaction
BDE	bond dissociation energy
Bn	benzyl
BOX	bis(oxazoline)
br s	broad singlet
CH	cyclohexane
COD	1,5-cyclooctadiene
Coll	2,4,6-trimethylpyridine
Cp	cyclopentadienyl
Cp*	1,2,3,4,5-pentamethylcyclopentadienyl
Cy	cyclohexyl
d	doublet
d.r.	diastereomeric ratio
DCE	1,1-dichloroethane
DCM	dichloromethane
DET	diethyl tartrate
DFT	density functional theory
DFTB	density functional based tight binding
DIAD	diisopropyl azodicarboxylate
DIPAMP	1,2-bis-phenyl(*ortho*-tolyl)phosphino) ethane
DMF	*N,N*-dimethylformamide
dmg	dimethylglyoxime
DMPO	5,5-dimethyl-1-pyrroline *N*-oxide
DMSO	dimethyl sulfoxide
DPP	dipyrrin-bis(*ortho*,*para*-di-*tert*-butylphenolato
dppe	1,2-bis(diphenylphosphino) ethane
e.r.	enantiomeric ratio
EA	ethyl acetate
ee	enantiomeric excess
EI	electron ionization
ent	enantiomer

E_{ox}	oxidation potential
EPR	electron paramagnetic resonance
eq.	equivalent
ESI	electrospray ionization
Et	ethyl
et al.	and others
Fc	ferrocene
Fmoc	fluorenylmethoxycarbonyl
FT-IR	fourier-transform infrared spectroscopy
G	gauss (unit of magnetic field)
GDP	gross domestic product
GP	general procedure
HAT	hydrogen atom transfer
HDA	hydride donating ability
hex	hexyl
HKR	hydrolytic kinetic resolution
HPLC	high performance liquid chromatography
HRMS	high-resolution mass spectrometry
hv	radiation with light
^{i}Pr	isopropyl
IR	infrared spectroscopy
J	coupling constant
k_H	rate constant of hydrogen atom transfer
L_n	ligand
Lut	2,6-lutidine
M	molarity
M	metal
m	*meta*
m	multiplet
m/z	mass-to-charge ratio
*m*CPBA	*meta*-chloroperoxybenzoic acid
Me	methyl
mol	amount of substance
mol%	molar fraction
MOM	methoxymethyl ether
M_p	melting point
MS	mass spectrometry
Ms	molecular sieve
^{n}Bu	normal butyl
NMR	nuclear magnetic resonance
NOESY	nuclear Overhauser effect spectroscopy
Nu	nucleophile
o	*ortho*
o/n	overnight
OTf	triflate
p	*para*
PBN	phenyl *N*-*t*-butylnitrone
Ph	phenyl
Phen	phenylene

pK_a	acid dissociation constant
ppm	parts per million
Pro	proline
Py	pyridine
q	quartet
R	substituent
r.r.	regioisomeric ratio
rac.	racemic
Red-Al	sodium bis(2-methoxyethoxy)aluminium hydride
REO	regiodivergent epoxide opening
R_f	retardation factor
RT	room temperature
s	singlet
sept	septet
SET	single electron transfer
sext	sextet
S_H2	homolytic substitution second order
Sia	siamyl
S_N2	nucleophilic substitution second order
t	triplet
TAA	tetraaza[14]annulene
TBAF	Tetra-*n*-butylammonium fluoride
TBDMS	*tert*-butyldimethylsilyl
TBHP	*tert*-butyl hydroperoxide
TBS	*tert*-butyldimethylsilyl
^{t}Bu	tertiary butyl
tert	tertiary
TFA	trifluoroacetate
THF	tetrahydrofuran
TLC	thin-layer chromatography
TMP	2,2,6,6-tetramethylpiperidinato
TMS	trimethylsilyl
TS	transition state
Ts	tosyl
UV	ultraviolet
X	halogen, pseudohalogen, sulfonic acid
Δ	heating
δ	chemical shift
ΔG	*Gibbs* free energy
ν	wavenumber
σ	mirror plane

5.2 List of Figures

Figure 1: The United Nations 17 Sustainable Development Goals.[5] 1
Figure 2: The 12 principles of Green Chemistry. 2
Figure 3: Enantiomers of *ibuprofen*, limonene, and thalidomide. 4
Figure 4: 'Privileged ligands' in asymmetric catalysis. 5
Figure 5: Iridium bound prochiral electrophile and zinc bound prochiral nucleophile. 13
Figure 6: Acidity of pyridine hydrochloride, 2,6-lutidine hydrochloride, and 2,4,6-collidine hydrochloride in water. 20
Figure 7: Enantiomers of the menthol-derived *Kagan* complex. 23
Figure 8: Interactions between the reduced *Kagan* complex and *meso*-epoxides. Different degrees of steric interactions between the epoxide sides cause a regioselective opening of the epoxide.[89] 24
Figure 9: The antifungal drug amphotericin B, which contains multiple diol units. Exemplary, one 1,3- and 1,4-diol unit are marked. 26
Figure 10: Changing FT-IR spectra of a crude reaction mixture before work-up, recorded immediately and after short exposure to air. Reaction conditions: 1.0 eq. epoxide **2**, 0.1 eq. Cp_2TiCl_2, 0.1 eq. $CpCr(CO)_3H$, 0.5 eq. KBH_4, 0.05 eq. LiCl, THF, RT, 48h (performed by *Shizgal)*.[185] 49
Figure 11: Ligand metathesis between Cp_2TiCl_2 and BH_4^- facilitated by a *Lewis* acidic metal cation in the formation of $Cp_2Ti(H)Cl$. 52
Figure 12: Reaction conversion and share of the desired product alcohol in relation to the added amount of LiCl to the reaction with 50 mol% of KBH_4. 56
Figure 13: Comparison of different borohydride and solvent combinations in the reaction with **2**. [a] calculated by multiplication of respective conversion rates and product ratios. 61
Figure 14: Both enantiomers of the *Kagan* complex. 73
Figure 15: Supramolecular *Kagan*-sulfonamide complex during catalyst activation.[220] 79
Figure 16: Anion receptors from the class of sulfonamides. 80
Figure 17: Stabilization of $Cp_2Ti^{III}Cl$ by supramolecular binding of sulfonamide **PhenSulfAm**. Ar = 3,5-$(CF_3)_2C_6H_3$.[218] 80
Figure 18: Cobalt complexes used in HAT catalyst screening. 92
Figure 19: Comparison between some cobalt complexes in the cooperative catalysis with Cp_2TiCl_2 in reaction with **2**. [a] calculated by multiplication of respective conversion rates and product ratios. . 95
Figure 20: EPR spectrum of a sample taken directly from the reaction mixture after 22 h. Reaction conditions: 1.0 eq. **2**, 0.1 eq. **45**, 0.1 eq. Cp_2TiCl_2, 0.5 eq. $LiBH_4$, 4.0 eq. PBN, 1,4-dioxane, RT. 97
Figure 21: $CpCr(CO)_3H$ **1.** 100

5.3 List of Schemes

Scheme 1: Industrial synthesis of *ibuprofen* in the original stoichiometric six-step route by *Boots* (bottom) and the improved *Boots-Hoechst-Calanese* three-step synthesis with all three steps being catalytic (top).[13] 3

Scheme 2: Asymmetric ring opening (ARO) of *meso*-epoxides using an enantiopure (salen)CrCl complex developed by *Jacobsen*..... 6

Scheme 3: Synthetic application of protected 1,2-amino alcohols obtained from ARO in the total synthesis of pharmaceutically active balanol and (–)-carbovir. 7

Scheme 4: General representation of sequential catalysis. 8

Scheme 5: General representation of relay catalysis..... 8

Scheme 6: Schematic representation of cooperative catalysis. 9

Scheme 7: General representation of intra- and intermolecular cooperative catalysis. 9

Scheme 8: Mechanism of the *Sonogashira* cross-coupling. 10

Scheme 9: Enantioselective allylic alkylation of α-cyano esters cooperatively catalyzed by rhodium and palladium. 11

Scheme 10: Iridium and zinc catalyzed enantio- and diastereodivergent allylation of α-hydroxyketones by *Zhang et al*. 12

Scheme 11: Thermal or photochemical decomposition of radical initiator azobisisobutyronitrile (AIBN). 14

Scheme 12: General representation of radical chain reactions. In = initiator. 15

Scheme 13: *Sharpless* epoxidation of allylic alcohols. E = CO_2Et. 16

Scheme 14: Epoxide ring-opening reactions via (a) nucleophilic attack, (b) one-electron reductive C–O bond homolysis and (c) two-electron reduction. 17

Scheme 15: Analogy between the cyclopropyl methyl radical and the σ-complex of an epoxide with a paramagnetic transition metal. 18

Scheme 16: Follow-up reactions of the β-titanoxy radical. [Ti] = Cp_2TiCl. 18

Scheme 17: Regioselectivity of the S_N2 vs. SET reductive epoxide opening. 19

Scheme 18: Mechanism of the titanocene-catalyzed epoxide opening by *Gansäuer*. Reaction conditions: 0.05 eq. Cp_2TiCl_2, 1.5 eq. Coll·HCl, 1.5 eq. Mn, 4.3 eq. 1,4-CHD.[74,77] 20

Scheme 19: *Brown* hydroboration and oxidation of styrene. 21

Scheme 20: Various applications of the titanocene-catalyzed reductive epoxide opening. 22

Scheme 21: Titanocene-catalyzed cyclization in the total synthesis of a furanoditerpenoid naturally occurring in *Spongia officinalis.* 22

Scheme 22: Titanocene-mediated radical acrylate addition and lactonization in the total synthesis of maoecrystal Z. 23

Scheme 23: Exemplary calculation of the enantiomeric enrichment during the REO of enantioenriched epoxides via a double asymmetric process. 26
Scheme 24: General scheme of selectivity in the REO. 27
Scheme 25: Water as hydrogen atom donor in the titanocene-mediated epoxide opening. 30
Scheme 26: Catalytically active titanocene species of water activation in the hydrogen atom transfer and the DFT-calculated BDE. 30
Scheme 27: H_2 as terminal hydrogen atom source in the titanocene-catalyzed epoxide reduction with the *Wilkinson* catalyst. 31
Scheme 28: Mechanism of the titanocene-catalyzed epoxide opening coupled with rhodium-catalyzed HAT. 31
Scheme 29: Asymmetric hydrogenation in the synthesis of L-DOPA by *Knowles*. 32
Scheme 30: Radical olefin hydrogenation mediated by transition metal hydrides via two sequential hydrogen atom transfers. 33
Scheme 31: Radical cyclization mediated by the *Schwartz* reagent. 33
Scheme 32: Radical cyclization catalyzed by *Schwartz* reagent with Red-Al. 34
Scheme 33: Radical cyclization catalyzed by $CpCr(CO)_3H$. 34
Scheme 34: Formation of the cyclization major product and the isomerization and hydrogenation by-products during the catalytic radical cyclization. [Cr] = $CpCr(CO)_3$. 35
Scheme 35: Activated radical acceptor olefins promote the desired cyclization pathway. 35
Scheme 36: Equilibrium of metal radicals with hydrogen. 36
Scheme 37: Two possible mechanisms of hydrogen activation via homolytic and heterolytic H_2 bond cleavage. 38
Scheme 38: Possible modes of M–H bond cleavage in transition metal hydrides. 39
Scheme 39: $CpCr(CO)_3H$ as HAT catalyst with H_2 as terminal reductant in the titanocene-catalyzed epoxide opening. 39
Scheme 40: Protonation of a titanocene alkoxide by $CpCr(CO)_3H$ (top) and reduction of $Cp_2Ti^{IV}(TFA)_2$ by $CpCr(CO)_3^-$ with possible subsequent regeneration of $CpCr(CO)_3H$ (bottom). 41
Scheme 41: Cooperative catalysis between chromium and titanium for the activation of H_2 in the selective reduction of epoxides yielding *anti-Markovnikov* alcohols. 41
Scheme 42: Proposed catalytic cycle of the titanoce-catalyzed epoxide opening with $CpCr(CO)_3H/NaCpCr(CO)_3$. H_2 is transferred sequentially as hydrogen atom, proton, and electron. [Ti] = Cp_2Ti, X = OMs. 42
Scheme 43: Two functions of borohydride reagents. 44
Scheme 44: Generation of the borane radical anion via hydrogen atom abstraction and subsequent halogen atom abstraction. 45

Scheme 45: Rate constants for HAT by the borohydride and cyanoborohydride anion to aryl and alkyl radicals, determined via radical clock experiments. 45
Scheme 46: Photo-induced reduction of halobenzenes using $NaBH_4$ as hydrogen atom source. 46
Scheme 47: Radical reduction of 7,7-dibromonorcarane using $NaBH_4$. 46
Scheme 48: Proposed cooperative catalytic 'globe' of the titanocene and chromium hydride catalyzed epoxide opening with borohydrides. 47
Scheme 49: Two competing processes: Decomposition of $Cp_2Ti(H)Cl$ under formation of H_2 (left) and HAT from $Cp_2Ti(H)Cl$ to $CpCr(CO)_3$• as part of the relay hydrogen atom transfer from BH_4^-, generating both active catalysts (right). 48
Scheme 50: DFTB calculated free enthalpy for the plausible activation of $Cp_2Ti^{III}Cl$ and $CpCr(CO)_3H$ with BH_4^- through relay hydride transfer via $Cp_2Ti^{IV}(H)Cl$. Geometry optimization: PBE0-D4[CPCM-(THF)]/def2-TZVP; single-point energies: PWPB95-D4/def2-QZVP; solvation free energies: COSMO-RS; thermostatistical correction: GFN2-xTB[GBSA].[184] 50
Scheme 51: Competing possible reactions of titanocene dichloride with borohydrides. 51
Scheme 52: Formation of the allylic alcohol side product by β-hydrogen abstraction either by Cp_2TiCl• (top) or $CpCr(CO)_3$• (bottom). 53
Scheme 53: *Lewis* acid assisted reduction of epoxides to the *Markovnikov* alcohol side product via a S_N2-like reaction by hydride donating reducing agents. 54
Scheme 54: Formation of the *Markovnikov* alcohol **2c** by reaction of **2** with $LiBH_4$ in THF. 54
Scheme 55: Synthesis of $LiBH_4$ from $NaBH_4$ and KBH_4 by metathesis with LiCl. 54
Scheme 56: Equilibria of titanocene(III) species in solution. In presences of Coll·HCl formation of a *resting state* occurs. 56
Scheme 57: Proposed *resting state* of active $Cp_2Ti^{III}Cl$ with LiCl. 57
Scheme 58: Reprogramming of the typical borohydride reactivity by cooperative catalysis. 61
Scheme 59: 5-*exo* vs. 6-*endo* cyclization of the 5-hexenyl radical. 65
Scheme 60: Kinetic competition in radical cyclization reactions. [Cr]-H = $CpCr(CO)_3H$, [Ti] = Cp_2TiCl.. 65
Scheme 61: Undesired hydrogenation of multiple bonds by $CpCr(CO)_3H$ leading to catalyst consumption. Double bonds generally react faster in this reaction than triple bonds. [Cr]-H = $CpCr(CO)_3H$. 66
Scheme 62: Intermolecular radical addition to *tert*-butyl acrylate (top) in comparison to intermolecular radical addition to ethyl propiolate (bottom). 72
Scheme 63: Control experiment with $(^nBu_4N)BH_4$ without catalysts. 76
Scheme 64: *Meinwald* rearrangement followed by carbonyl reduction leading to loss of the epoxide configuration and a mixture of regioisomers. R^1 and R^2 are electronically and sterically similar. 76
Scheme 65: Desymmetrization of *meso*-**14** under the cooperative conditions of the REO. 86

Scheme 66: Epoxide opening of **5** using Cp*Cr(CO)$_3$H and Cp$_2$TiCl$_2$ vs. Cp$_2$TiCl$_2$ alone. [a] isolated as mixture of 78:22 **5a** and allylic alcohol **5b**. 89
Scheme 67: Radical cyclization of **18** using Cp*Cr(CO)$_3$H. 90
Scheme 68: Opening of **5** by cooperative cobalt and titanium catalysis. 97
Scheme 69: Persistent radical species formed by HAT to PBN, that was identified from the characteristic EPR spectrum shown in Figure 20. 98
Scheme 70: Synthesis of CpCr(CO)$_3$H **1**. 99
Scheme 71: Synthesis of NaCp **52**. 100
Scheme 72: Synthesis of Cp*Cr(CO)$_3$H **53**. 100
Scheme 73: One-step synthesis of **47**. 103
Scheme 74: Synthesis of L-neomenthol **60**. 104
Scheme 75: Synthesis of D-menthylcyclopentadiene **62**. 104
Scheme 76: Metalation of D-*Kagan*-Cl$_2$ **63**..... 104
Scheme 77: Synthesis of D-*Kagan*-Br$_2$ **64.**..... 105
Scheme 78: Synthesis of **7** by modified *Corey-Chaykovsky* epoxidation. 106
Scheme 79: Synthesis of ketone **67** (performed by *Plato*)..... 106
Scheme 80: Synthesis of epoxide **13**. 106
Scheme 81: Synthesis of olefins **69** and **71**. 107
Scheme 82: *Matteson* epoxidation of acetophenone..... 108
Scheme 83: Synthesis of precursor olefin **75**. 108
Scheme 84: Derivatizations of **75**. [a] performed by *Schmickler*. 108
Scheme 85: *Prilezhaev* epoxidation of the olefin precursors. [a] performed by *Schmickler*. 109
Scheme 86: Alternative synthetic route to **24** from **18**. 109
Scheme 87: Synthesis of **25**..... 109
Scheme 88: Synthesis of **27**..... 110
Scheme 89: Synthesis of **85**..... 110
Scheme 90: Synthesis of **88**..... 111
Scheme 91: Synthesis of substituted propargyl alcohols and propargyl bromides. [a] performed by *Heinrichs*. 111
Scheme 92: Synthesis of epoxide **94** (performed by *Heinrichs*)..... 111
Scheme 93: Synthesis of **29**, **30**, and **31**. 112
Scheme 94: Synthesis of **28**..... 112
Scheme 95: Synthesis of (*Z*)-β-hydroxy alkene **99**. 113

5.4 List of Tables

Table 1: Comparison of bond dissociation energies of several single bonds. 14

Table 2: Enantioselective reduction of *meso*-epoxides catalyzed by the *Kagan* complex. 24

Table 3: Regiodivergent epoxide opening of racemic and enantioenriched epoxides with different *Kagan* enantiomers. 25

Table 4: Synthesis of *syn* and *anti* 1,3- and 1,4-difunctionalized molecules via REO. 27

Table 5: BDE values of several hydrogen atom donors and rate constants for the hydrogen atom abstraction by primary alkyl radicals.[51,105–107] 29

Table 6: Bond dissociation energies of various transition metal hydrides.[124,136,148–150] 36

Table 7: Comparison of BDE values of transition metal hydrides to the rate constants k_H of the HAT to the tris(*p-tert*-butylphenyl) methyl radical at 25°C in toluene.[155] 37

Table 8: Conditions and scope of the titanocene-catalyzed epoxide opening with $CpCr(CO)_3H$ as HAT catalyst and H_2 as terminal reductant improved by *Panfilova*. 40

Table 9: Scope of the $CpCr(CO)_3H$/$NaCpCr(CO)_3$ and H_2 cooperative system. Yield of the inseparable allylic alcohol by-product is shown in parentheses. 43

Table 10: Previous reaction condition development.[191] 51

Table 11: $LiBH_4$ as sole reductant and as additive together with $NaBH_4$ in THF.[194] 53

Table 12: LiCl as additive in the reaction with KBH_4 and $NaBH_4$.[194] 55

Table 13: Substrate scope of the cooperative catalytic epoxide opening with KBH_4 and LiCl.[194] 57

Table 14: Application of $LiBH_4$ in 1,4-dioxane. 59

Table 15: Catalyst loading influence and control experiments. 60

Table 16: Substrate scope of the cooperative catalytic epoxide opening with $LiBH_4$ in 1,4-dioxane 62

Table 17: Adjustments of the reaction conditions for cyclization reactions. 66

Table 18: Scope of cyclization reactions by cooperative catalysis yielding *N*-tosylated pyrrolidine derivatives. 67

Table 19: Cyclization reactions by cooperative catalysis of other substrates. 69

Table 20: Cyclizations of previously uncharacterized products using classic conditions of titanocene catalysis. 70

Table 21: Diastereoselective Ir-catalyzed hydrogenations of cyclization products. 72

Table 22: Regiodivergent epoxide opening with previously identified conditions of the reductive epoxide opening. 74

Table 23: Influence of the *Kagan* complex's anionic ligands in the reaction with $LiBH_4$ in THF. 75

Table 24: REO reactions using $(^nBu_4N)BH_4$ in THF. 75

Table 25: REO reactions using $NaBH_3CN$ in THF. 77

Table 26: REO reactions using $LiBH_4$ in 1,4-dioxane. 78

Table 27: Influence of the catalyst loadings..... 78
Table 28: Screening of different sulfonamides as additives for the REO..... 81
Table 29: REO reactions using **PhenSulfAm** in combination with different catalyst loadings and reaction temperatures..... 82
Table 30: REO reactions under optimized conditions using the L-*Kagan*-Br_2..... 82
Table 31: REO reactions under cooperative conditions..... 83
Table 32: REO reactions under cooperative conditions..... 85
Table 33: Desymmetrization of *meso*-epoxides under cooperative conditions at room temperature.86
Table 34: BDE values of $(C_5R_5)Cr(CO)_3H$ complexes and their rate constants k_H of the HAT to methyl methacrylate at 35°C.[136] 88
Table 35: Test reaction of the cooperative system with $Cp^*Cr(CO)_3H$ and Cp_2TiCl_2. 89
Table 36: Bond dissociation energies of cobalt hydrides in comparison to chromium hydrides. 90
Table 37: Screening reaction of cooperative systems with several cobalt complexes..... 93
Table 38: Screening reaction using cobalt salophen **46** in combination with different borohydrides and solvents..... 95
Table 39: Influence of the cobalt catalyst loading. 96
Table 40: Cooperative cobalt and titanium catalysis for H_2 activation..... 98
Table 41: Synthesis of ligands **54** and **(*S*)-55**..... 101
Table 42: Synthesis of cobalt complexes by metalation with $Co(OAc)_2 \cdot 4H_2O$..... 102
Table 43: *Corey-Chaykovsky* epoxidation of ketones..... 105
Table 44: *Prilezhaev* epoxidation of olefins. 107
Table 45: Synthesis of **38** and **34** by *syn*-selective epoxidation of β-hydroxy alkenes catalyzed by $VO(acac)_2$..... 113

5.5 Abstract

Cooperative catalysis can enable reactivity and selectivity not achievable with a single catalyst, making it a key strategy for developing sustainable reactions. In this work, the unique reactivities of two earth-abundant metals, titanium and chromium, were coupled in a reactive network, allowing the use of readily available, affordable, and reasonably safe borohydrides as hydrogen atom and electron donors in the cooperative catalysis of radical reactions. The system synergizes titanocene catalysts, efficient in radical epoxide opening reactions, and a chromium hydride complex, a well-established radical hydrogenation catalyst.

The reprogramming of the borohydride reactivity is achieved by an unprecedented relay hydrogen atom transfer, from the borohydride via a titanocene hydride species to chromium, simultaneously activating both catalysts. This process completely outcompetes the usual nucleophilic reduction character of the BH_4^- anion. The mechanistic details of the system have been investigated through both computational and experimental studies, leading to the successful experimental realization of the proposed catalytic 'globe'. Pairing the strongly reducing and *Lewis* acidic $LiBH_4$ with 1,4-dioxane enables precise reagent delivery by controlling the reactivity of the borohydride through solubility.

The system facilitated reductive epoxide openings for preparation of various *anti-Markovnikov* alcohols with a broad functional group tolerance, and as well C–C bond-forming cyclization. Moreover, the integration of regiodivergent epoxide openings into cooperative catalysis was realized using enantiopure titanocenes in combination with sulfonamide additives. This method allows the synthesis of enantiopure 1,3- and 1,4-difunctionalized units from common starting materials. Particularly attractive is the possibility to directly obtain unprotected 1,3- and 1,4-diols, avoiding the need for additional protection group introduction and removal. Such reactions were unattainable through previous radical cooperative catalysis or epoxide reductions involving *Meinwald* rearrangement and carbonyl reduction.

The advantage of these systems over previous titanocene-catalyzed epoxide openings is the elimination of the need for stoichiometric acids and toxic hydrogen atom donors. The only stoichiometric reagent required is the borohydride, thus improving atom economy and sustainability. Additionally, the use of pressurized, flammable hydrogen gas is avoided by providing borohydrides as a safer and more manageable alternative for research laboratories.